Analyse de performances en traitement d'antenne : bornes inférieures de l'erreur quadratique moyenne et seuil de résolution limite

Mohammed Nabil El Korso

N° d'ordre :

THESE DE DOCTORAT

DE L'UNIVERSITÉ PARIS-SUD 11

Spécialité : Physique

Présentée par

Mohammed Nabil EL KORSO

pour obtenir le grade de

DOCTEUR DE L'UNIVERSITÉ PARIS-SUD 11

Sujet de la thèse :

Analyse de performances en traitement d'antenne. Bornes inférieures de l'erreur quadratique moyenne et seuil de résolution limite

Thèse présentée et soutenue le 07 Juillet 2011 devant le jury composé de :

Mr.	Pascal LARZABAL	Université Paris-Sud XI	Président
Mr.	Jean-Marc BROSSIER	Inst. Polytechnique de Grenoble	Rapporteur
Mr.	Jean-Yves TOURNERET	Inst. Nat. Polytechnique de Toulouse	Rapporteur
Mr.	Gérard FAVIER	Université Nice	Examinateur
Mr.	Karim ABED EL MERAIM	TELECOM PARIS TECH	Examinateur
Mme.	Sylvie MARCOS	Université Paris-Sud XI	Directeur de thèse
Mr.	Rémy BOYER	Université Paris-Sud XI	Directeur de thèse
Mr.	Alexandre RENAUX	Université Paris-Sud XI	Directeur de thèse

Laboratoire des Signaux et Systèmes
Université Paris-Sud / SUPELEC / CNRS / UMR 8506
3 rue Joliot Curie,Plateau du Moulon, 91192 Gif sur Yvette, France

à mes parents

Remerciements

Et voilà la fin. 3 ans après voilà la fin. Déjà !

Ce qui à été le plus dur pour moi est sans aucun doute l'écriture de ces quelques lignes de remerciements. Ceci est d'autant plus dur que j'ai passé 3 merveilleuses années et que ça m'est difficile de remercier à la hauteur, les gens que j'ai cotoyé et qui ont fait de moi un "Docteur".

La richesse de la vie se mesure par la valeur de ses expériences. Ces 3 années de thèse m'ont permi de vivre, sans aucun doute, l'expérience la plus riche tant sur le plan humain, que sur le plan scientifique. J'ai fait la connaissance d'un certain nombre de personnes. Des personnes sur lesquelles j'ai pu compter tout au long de ces 3 dernières années, mais aussi dans les années à avenir. De plus, j'ai été formé par une équipe de choc, je n'aurai jamais pu espérer mieux : Rémy, Alex et Sylvie. Merci à vous, du fond du coeur. Plus que mes encadrants, vous étiez une seconde famille pour moi. Vous étiez et vous êtes toujours un exemple pour moi et j'espère que je vous ferai honneur en formant des étudiants comme vous l'aviez si bien fait avec moi.

Mes remerciements s'adressent également aux membres du jury pour l'intérêt qu'ils ont porté à mes travaux ainsi que pour leurs remarques très pertinentes sur mon manuscrit. Je remercie tous particulièrement Jean-Marc Brossier et Jean-Yves Tourneret qui ont accepté de rapporter sur ce travail. J'ai été aussi très sensible à la présence dans ce jury de Pascal Larzabal et de Karim abed Meraim, dont les articles m'ont toujours grandement intéressé. Enfin, je tiens à remercier Gérard Favier d'avoir fait le voyage jusqu'à Gif et de m'avoir fait l'honneur de participer à mon jury de thèse.

Cette thèse n'aurait pas eu le même goût sans l'exceptionnelle ambiance qui règne au L2S, plus particulièrement dans la division Signaux tenu, d'une main de maître, par "Monsieur" Pascal Bondon.

Merci Alex. Merci à toi pour tes conseils scientifiques et personnels. Sache que j'ai été et je suis toujours admiratif de ta vision de la recherche. Merci de m'avoir apporté ta rigueur scientifique. Merci pour ton soutien lors de mes nombreux moments de doute, tu as été comme un grand frère durant ces 3 ans.

Merci Rémy. Merci à toi de m'avoir poussé tout le temps aussi loin, travailler plus pour gagner plus (en terme de papiers bien sûr !). Merci pour ta disponibilité et ta générosité. Tu as toujours eu le flaire "for the right way to take".

Merci Sylvie. Merci à vous pour vos conseils scientifiques très subtiles que vous m'avez prodigués, pour vos encouragements, votre soutient indéfectible pendant ces trois années de travail commun. Et enfin de merci de m'avoir accueilli au sien votre équipe.

Merci à Thang et Duy, de m'avoir supporté durant ces 3 ans au sein de la cellule C4.03b. Partager ce bureau avec vous a été un énorme plaisir. Merci à Fred pour tes discussions scientifiques ou pas mais toujours accompagnées d'humour. Merci à toi d'avoir organisé et maintenu le petit moment de bonheur de la semaine, le football. Merci à Ziad, Amadou, Sofiane, Vero et Hachem pour votre sagesse et surtout votre bonne humeur permanente. Merci à Laurie pour tes bonnes blagues, ta "PANDA" me manquera ! Merci à Mael, Sofiane, Amadou, Elsa et Stephan pour les séances de piscine à Massy. Merci à Aurélia pour ta bonne humeur et ta disponibilité. Merci à José pour tes conseils sportifs ainsi que pour ta gaité permanente. Merci à Claude, Thomas, Jean-Phi, Guillaume, Samson, Pierre et Eric pour votre bonne humeur. Merci à Lana, Jean-Francois, Adrian, Chengfang, Samir, Fransceca, Zeina, Adel, Benjamin, François, Alper, Sophie, Alessendro, merci à tous pour votre gentillesse, votre bonne humeur, merci d'avoir fait de ces trois ans un moments de bonheur et de gaité. Et enfin, merci à toute l'équipe du Football en particulier Fredou (mon passeur favori !), Rayen, Benji, Julien, Momo et Karim. Sans oublier le personnel du L2S sans lequel le laboratoire tomberait en ruine : Merci à Franck, Frederic, Maryvonne, Daniel, Celine, Helena, Myriam et Jack.

J'aimerais également remercier tous les enseignants qui m'ont accompagné du primaire à l'université, qui ont grandement contribué à ma formation. Plus particulièrement, mes enseignants de maths du Lycée, de l'ENPEI, de l'ENP-Alger et de l'université Paris-sud, sans oublier le Prof A. Belouchrani.

Je tiens aussi à remercier ma petite soeur Douja et mon grand frère Abdel-Hamid qui m'ont toujours encouragé et soutenu. Merci à mon petit frère Djamel, qui a bien voulu partager l'appartement avec moi, supportant mon humeur qui n'a pas toujours été joyeuse et me préparant des repas délicieux qui me rappelaient la cuisine de ma mère !

Bien-sûr, cette thèse n'aurait eu aucun sens si elle n'était pas partagée avec une personne qui m'est chère, Fatima. Merci d'avoir était à mes cotés à chaque fois que j'en avais besoin tant sur le plan humain que sur le plan scientifique.

Cependant, mon plus profond remerciement va à mes parents. Ils ont sacrifié toute leur vie à l'éducation et au bien être de leurs enfants. Merci pour vos conseils très précieux. Vous m'aviez toujours guidé dans la bonne direction, sans jamais m'imposer vos choix. Merci pour votre confiance. Ce travail vous est dédié.

Mohammed Nabil EL KORSO
15 Juillet 2011

CLEAR EYES, FULL HEARTS, CAN'T LOSE !
Peter Berg

Résumé

Ce manuscrit est dédié à l'analyse de performances en traitement d'antenne pour l'estimation des paramètres d'intérêt à l'aide d'un réseau de capteurs. Il est divisé en deux parties :

- Tout d'abord, nous présentons l'étude de certaines bornes inférieures de l'erreur quadratique moyenne liées à la localisation de sources dans le contexte champ proche. Nous utilisons la borne de Cramér-Rao pour l'étude de la zone asymptotique (notamment en terme de rapport signal à bruit avec un nombre fini d'observations). Puis, nous étudions d'autres bornes inférieures de l'erreur quadratique moyenne qui permettent de prévoir le phénomène de décrochement de l'erreur quadratique moyenne des estimateurs (on cite, par exemple, la borne de McAulay-Seidman, la borne de Hammersley-Chapman-Robbins et la borne de Fourier Cramér-Rao).
- Deuxièmement, nous nous concentrons sur le concept du seuil statistique de résolution limite, c'est-à-dire, la distance minimale entre deux signaux noyés dans un bruit additif qui permet une "correcte" estimation des paramètres. Nous présentons quelques applications bien connues en traitement d'antenne avant d'étendre les concepts existants au cas de signaux multidimensionnels. Par la suite, nous étudions la validité de notre extension en utilisant un test d'hypothèses binaire. Enfin, nous appliquons notre extension à certains modèles d'observation multidimensionnels.

Mots clés : Traitement d'antenne, théorie de l'estimation, théorie de la détection, seuil statistique de résolution limite, étude des performances asymptotiques et non-asymptotiques des estimateurs, estimation de direction d'arrivée en champ proche, bornes inférieures de l'erreur quadratique moyenne, signaux multidimensionnels.

Abstract

This manuscript concerns the performance analysis in array signal processing. It can be divided into two parts :

- First, we present the study of some lower bounds on the mean square error related to the source localization in the near field context. Using the Cramér-Rao bound, we investigate the mean square error of the maximum likelihood estimator *w.r.t.* the direction of arrivals in the so-called asymptotic area (*i.e.,* for a high signal to noise ratio with a finite number of observations.) Then, using other bounds than the Cramér-Rao bound, we predict the threshold phenomena.
- Secondly, we focus on the concept of the statistical resolution limit (*i.e.,* the minimum distance between two closely spaced signals embedded in an additive noise that allows a correct resolvability/parameter estimation.) We define and derive the statistical resolution limit using the Cramér-Rao bound and the hypothesis test approaches for the mono-dimensional case. Then, we extend this concept to the multidimensional case. Finally, a generalized likelihood ratio test based framework for the multidimensional statistical resolution limit is given to assess the validity of the proposed extension.

Keywords : Array processing, estimation theory, detection theory, statistical resolution limit, asymptotic and non-asymptotic performance analysis, near field, lower bounds on the mean square error, multidimensional signals.

Table des matières

Table des figures

Liste des tableaux

Notations

Acronymes

- **ALU** : Antenne Linéaire Uniforme.
- **ALNU** : Antenne Linéaire Non Uniforme.
- **BCR** : Borne de Cramér-Rao.
- **BFCR** : Borne de Fourier Cramér-Rao.
- **BHCR** : Borne de Hammersley-Chapman-Robbins.
- **BMH** : Borne de McAulay-Hofstetter.
- **BMS** : Borne de McAulay-Seidman.
- **CIA** : Critère d'Information d'Akaike.
- **EQM** : Erreur Quadratique Moyenne.
- **MIF** : Matrice d'Information de Fisher.
- **MV** : Maxmimum de Vraisemblance.
- **RSB** : Rapport Signal sur Bruit.
- **RSBI** : rapport signal sur bruit plus interférences.
- **SDI** : Sources D'Intérêt.
- **SI** : Sous-espace des Interférences.
- **SRL** : Seuil de Résolution Limite.
- **SRLM** : Seuil de Résolution Limite pour des signaux Multidimensionnels.

Symboles mathématiques généraux

- $\mathbb{C}$ indique le corps des complexes.
- $\mathbb{R}$ indique le corps des réels.
- $\Re\{z\}$ indique la partie réelle d'un nombre complexe z.
- $\Im\{z\}$ indique la partie imaginaire d'un nombre complexe z.
- Le symbole * indique l'opérateur de conjugaison.
- $abs(.)$ indique la valeur absolue.
- $O(\beta)$ regroupe les termes d'ordre supérieurs ou égales à β.

Symboles et opérateurs matriciels

- a, A, les lettres en italiques représentent une quantité scalaire.

- $\mathbf{a}$, les lettres minuscules en gras représentent une quantité vectorielle (vecteur colonne).
- $\mathbf{A}$, les lettre majuscules en gras représentent une quantité matricielle.
- $\mathcal{A}$, les lettre majuscules calligraphiques en gras représentent une quantité tensorielle.
- $\mathbf{A}^T$, le symbole ^{T} indique l'opérateur transposé.
- $\mathbf{A}^H$, le symbole ^{H} indique l'opérateur Hermitien (transposé conjugué).
- $\mathbf{A}^\dagger$, le symbole † indique l'opérateur pseudo-inverse tel que $\mathbf{A}^\dagger = \left(\mathbf{A}^H\mathbf{A}\right)^{-1}\mathbf{A}^H$ où $\mathbf{A}$ est de rang plein colonne.
- $\mathbf{I}_N$ indique la matrice identité de taille $N \times N$.
- $|\mathbf{A}|$ indique le déterminant de la matrice $\mathbf{A}$.
- $\|.\|$ indique la norme L^2.
- $[\mathbf{a}]_i$ est l'élément correspondant à la $i^{\text{ème}}$ ligne du vecteur $\mathbf{a}$.
- $[\mathbf{A}]_{i,j}$ est l'élément correspondant à la $i^{\text{ème}}$ ligne et $j^{\text{ème}}$ colonne de la matrice $\mathbf{A}$.
- $[\mathcal{A}]_{i_1,\ldots,i_I}$ est l'élément se trouvant à la position $i_1, \ldots, i_I$ du $\mathcal{A}$.
- $tr\left(\mathbf{A}\right)$ est la trace de la matrice carrée $\mathbf{A}$.
- $\langle\mathbf{A}\rangle$ indique le sous espace engendré par les colonnes de la matrice $\mathbf{A}$.
- diag(.) est l'opérateur de diagonalisation.
- bdiag(.) est l'opérateur de diagonalisation par bloc.
- $\otimes$ est l'opérateur de Kronecker.
- $\odot$ est l'opérateur de Hadamard.
- $vec\left(.\right)$ est l'opérateur qui vectorise une matrice en concaténant ses colonnes.
- $sgn\left(.\right)$ est la fonction signe.
- Soient deux matrices réelles $\mathbf{A}$ et $\mathbf{B}$ de taille $N \times N$, alors la relation d'ordre

$$\mathbf{A} \succeq \mathbf{B},$$

  signifie que la matrice $\mathbf{A} - \mathbf{B}$ est définie non-négative.

Symboles relatifs aux probabilités

- $\mathcal{N}_{\mathbb{K}}\left(\mathbf{m}, \mathbf{C}\right)$ indique une loi gaussienne multivariée sur le corps $\mathbb{K}$ (circulaire si $\mathbb{K} = \mathbb{C}$) de moyenne $\mathbf{m}$ et de matrice de covariance $\mathbf{C}$.
- $\chi^2\left(N\right)$ indique une loi du chi2 réelle à N degrés de libertés basée sur une somme au carré de N variables aléatoires indépendantes suivant une loi gaussienne de moyenne nulle et de variance 1.
- $\Pr\left(.\right)$ indique une probabilité.
- $p\left(x\right)$ indique une densité de probabilité.
- $p\left(x|\,y\right)$ indique une densité de probabilité conditionnelle ou une vraisemblance et sera précisée selon le contexte.
- $E\left\{.\right\}$ indique l'opérateur d'espérance mathématique.

Chapitre 1

Introduction

L'extraction d'information pertinente cachée dans des observations bruitées est l'un des objectifs du traitement du signal. Une telle information est généralement décrite par un ou plusieurs paramètres d'intérêt [Van68, Rendf] (par exemple : une fréquence, une phase, une direction d'arrivée etc..) La théorie de l'estimation a pour but de présenter un cadre formel pour résoudre ce type de problème [Sch91, Leh83]. Plus particulièrement, l'estimation paramétrique, consiste à estimer les paramètres d'intérêt en se basant sur un modèle d'observation. En traitement du signal, le modèle d'observation est pré-défini grâce à des connaissances *a priori* du processus physique et dépend, non seulement des paramètres d'intérêt, mais aussi des paramètres de nuisance (dont la variance du bruit) incorporant ainsi un modèle statistique [Kay93, Van01].

Le problème de l'estimation de paramètres d'intérêt a fait l'objet de nombreuses recherches en traitement d'antennes. Plus particulièrement, le traitement d'antennes utilise l'information mesurée par un réseau de capteurs afin d'estimer les directions d'arrivées d'un nombre fini d'émetteurs [BK83, Böh86, SN90a, SN90b, Mar98, OVSN93, VO91, VOK91, VSO97]. Ce dernier a donné lieu à l'élaboration d'une pléthore d'algorithmes de l'estimation à haute résolution [KV96] (par exemple, MUSIC [Sch81], ESPRIT [RPK86, YF98], root-MUSIC [RH89], ZF-MUSIC [EBBM09], PCM-MUSIC [EBM09] etc..) Par contre, il existe moins de travaux étudiant les performances optimales associées aux différents modèles paramétriques.

L'erreur quadratique moyenne est l'indicateur de performance le plus utilisé [SN89, Sch91, Kay93, Bel95, VON95, Mar98, BFL04, SM05b, Ath05, Rendf, EBRM10a]. On constate (pour des problèmes non linéaires) que l'erreur quadratique moyenne de l'estimateur du maximum de vraisemblance est répartie en trois régions bien distinctes selon la valeur du rapport signal sur bruit (voir, figure 1.1 [Van68, RB74, Rendf]) :

- la zone dite *asymptotique* où la valeur estimée du paramètre est proche de la vraie valeur,
- la zone dite *de décrochement* due à un accroissement brusque de l'erreur quadratique moyenne (dont la cause est l'apparition d'observations aberrantes),
- et enfin, la zone dite *de non-information* où l'observation se réduit principalement à la composante du bruit, d'où la distribution des estimées quasi uniforme de l'erreur quadratique moyenne.

Ainsi, la zone de décrochement d'un estimateur délimite sa zone de fonctionnement optimal. D'où l'importance de l'analyse de performance afin de déterminer

- le comportement asymptotique des estimateurs,
- la prédiction du décrochement.

Par ailleurs, le *seuil de résolution limite*, appelé aussi *pouvoir séparateur*, est un autre indicateur de performance moins utilisé mais d'une importance croissante dans tout problème d'estimation paramétrique. Ce dernier traduit la capacité d'un algorithme à séparer deux sources

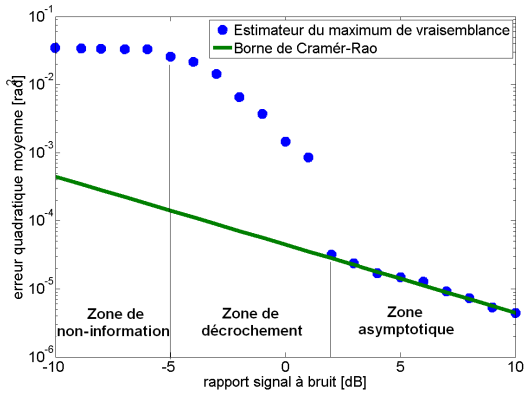

FIGURE 1.1 – Illustration de la zone asymptotique, la zone de décrochement et la zone de non-information pour un problème de localisation de source en champ lointain [ML99].

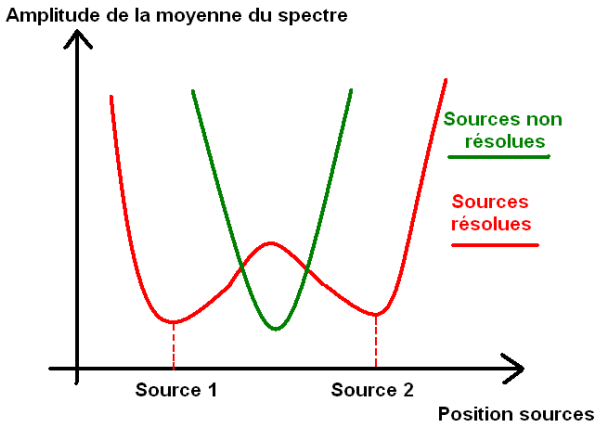

FIGURE 1.2 – Illustration du cas *sources résolues* et *sources non résolues* en probléme d'estimation paramétrique à l'aide d'une allure générale d'un pseudo-spectre d'algorithme [Mar98].

proches [Mar98]. Plus précisément, il représente la distance minimale entre deux signaux permettant une séparation/estimation correcte des paramètres d'intérêt (voir, figure 1.2).

Les travaux présentés dans ce document s'inscrivent dans cette thématique.

1.1 Objectif de la thèse

Initialement, nous nous sommes intéressés au problème de la localisation de sources en champ proche qui fait l'objet de peu de travaux dans la littérature (par rapport à la localisation en champ lointain) bien que présentant un intérêt certain. Lors d'une localisation de sources en champ proche à l'aide d'un réseau de capteurs passif, on fait l'hypothèse que l'amplitude et la phase des sources varient au cours du temps, et que les sources sont situées prés de l'antenne. Dans ce cas, la formulation sources lointaines (fronts d'ondes plans) n'est plus valable et de ce fait, on doit prendre en compte un modèle paramétré non seulement par l'azimut (le même que dans le cas du champ lointain), mais aussi par la distance entre la source et un capteur de référence. Dans la littérature, on trouve une pléthore de méthodes d'estimation pour ce type

de problèmes [HB91, YF98, GAMH05, ZC07, BP08], cependant les performances ultimes de tels estimateurs n'ont pas complètement été étudiées en détails.

Ainsi, nos objectifs initiaux étaient les suivants :

- Caractériser les performances asymptotiques ultimes de l'estimateur du maximum de vraisemblance en terme d'erreur quadratique moyenne à l'aide de la borne de Cramér-Rao [Fis22, Dug37, Fre43, Rao45, Cra46],
- Prédire le décrochement de ce même estimateur à l'aide d'autres bornes inférieures de l'erreur quadratique moyenne plus précises que la borne de Cramér-Rao [Gla72, FL02, CGQL08, TT10],
- Caractériser les performances asymptotiques ultimes en terme de seuil statistique de résolution limite [Cox73, SD95, Lee92, Lee94, Smi98, Mar98, SM04, LN07, AW08, EBRM10b, KBRM11b, KBRM11a].

1.2 Résultats de la thèse

Dans ce manuscrit, nous calculons et analysons différentes bornes inférieures de l'erreur quadratique moyenne dans le cadre de la localisation passive d'une source située en champ proche à savoir la borne la plus connue, c'est-à-dire, la borne de Cramér-Rao [Cra46], mais aussi la borne de McAulay-Seidman [MS69], la borne de Hammersley-Chapman-Robbins [Ham50], la borne de McAulay-Hofstetter [MH71] et, plus particulièrement, une borne récemment introduite dans la littérature dénommée borne de Fourier Cramér-Rao [TT10]. Lors de cette étude nous avons caractérisé les performances optimales asymptotiques et non-asymptotiques des estimateurs et, en particulier, de l'estimateur du maximum de vraisemblance. Nous nous sommes intéressés à la prédiction du phénomène de décrochement pour lequel ces bornes sont utiles. Cette analyse est pertinente, d'autant plus, qu'à notre connaissance, aucun résultat concernant des bornes inférieures autres que la borne de Cramér-Rao, n'est disponible dans la littérature. A cet effet, nous rappelons que la borne de Cramér-Rao est une borne optimiste (et même non valable) dans les zones dites non-asymptotiques (lorsque le rapport signal sur bruit ou le nombre d'observations décroît), et donc non utilisable dans ces zones.

Cette étude nous a permis d'avoir une analyse des performances asymptotiques mais aussi une bonne prédiction du phénomène de décrochement. De plus, nous avons démontré que la borne de Fourier Cramér-Rao, récemment proposée, demeure moins performante que certaines de ses prédécesseurs, on cite en particulier la borne de McAulay-Hofstetter. Et ceci, contrairement aux résultats proposés dans [TT10].

Pour compléter notre analyse, il nous fallait caractériser les performances asymptotiques ultimes de l'estimateur du maximum de vraisemblance en terme du seuil statistique de résolution limite. Nous nous sommes basés principalement sur deux approches : l'approche basée sur la borne de Cramér-Rao [Lee92, LL93, Lee94, Smi05] et l'approche basée sur un test d'hypothèses [LN07]. Or, nous avons constaté que le seuil de résolution limite basé sur l'approche par la borne de Cramér-Rao n'était introduit que dans le cas monodimensionnel (nous rappelons qu'une source située dans le champ proche est paramétrée par deux paramètres d'intérêt : l'azimut et la distance. Nous étions donc en face d'un problème multidimensionnel.) Ceci nous a poussé à introduire et à étendre les résultats de Smith sur le seuil de résolution limite pour des signaux monodimensionnels au cas multidimensionnel. Dès lors, nous avons aussi étendu nos objectifs initiaux et nous nous sommes intéressés en détails au seuil de résolution limite pour un modèle multidimensionnel plus général à P paramètres d'intérêt par signal. Ainsi, nous avons étudié le seuil de résolution limite pour un modèle harmonique multidimensionnel (en utilisant l'approche basée sur la borne de Cramér-Rao), pour la localisation de sources se situant en champ proche (en

utilisant l'approche basée sur un test d'hypothèses) mais aussi pour le radar MIMO en présence d'interférences (en utilisant les projecteurs obliques [BS94] et l'approche dite *matched subspace filter* [SF94,KS99,KSM01,JF05]).

1.3 Structure du manuscrit

Nous avons choisi de présenter ce manuscrit en nous appuyant sur les publications citées ci-dessous. Ainsi, nous ne présenterons que les principaux résultats et quelques résultats de simulations. Les détails calculatoires, les simulations et des analyses plus approfondies sont présentés dans les publications citées ci-dessous. Le manuscrit de thèse est organisé comme suit :

- **le chapitre** 2 est dédié aux bornes inférieures de l'erreur quadratique moyenne pour la localisation de sources en champ proche. La première partie de ce chapitre est consacrée à l'étude de la borne de Cramér-Rao. Dans la seconde partie, nous nous intéressons à la prédiction du décrochement à l'aide de bornes plus précises.
- **le chapitre** 3 est dédié au seuil de résolution limite. Nous commencerons par l'étude du seuil de résolution limite pour des signaux monodimensionnels (en nous basant sur différentes approches.) Ensuite, nous introduirons l'extension au cas multidimensionnel. Une analyse sur la pertinence de cette extension est aussi fournie. De plus, nous traitons, en exemple, le modèle harmonique à P paramètres d'intérêt par signal (rappelons que ce modèle est plus général que le modèle de localisation de sources en champ proche.) Enfin, nous fournissons aussi, une autre approche pour le calcul du seuil de résolution limite dans le cas multidimensionnel (où nous traiterons aussi le cas du champ proche.)

Enfin, notons que par souci d'uniformisation, nous avons choisi de ne pas inclure nos travaux concernant l'estimation paramétrique dans le contexte du champ lointain et du champ proche qui ont donné lieu aux publications suivantes **[J5]**, **[C2]**, **[C4]** et **[C5]**.

1.4 Publications

Les travaux reportés dans ce document ont donné lieu aux articles et communications suivants :

Revues internationales (papiers acceptés ou publiés)

[J1] M. N. El Korso, R. Boyer, A. Renaux and S. Marcos, "Conditional and unconditional Cramér-Rao bounds for near-field source localization", *IEEE* Transactions on Signal Processing, Volume : 58, Issue : 5, May 2010, pp. 2901-2907.

[J2] M. N. El Korso, R. Boyer, A. Renaux and S. Marcos, "Statistical Resolution Limit of the Uniform Linear Cocentered Orthogonal Loop and Dipole Array", *IEEE* Transactions on Signal Processing, Volume : 59, Issue : 1, Jan 2011, pp. 425-431.

[J3] M. N. El Korso, R. Boyer, A. Renaux and S. Marcos, "Statistical Resolution Limit for the Multidimensional Harmonic Retrieval Model : Hypothesis Test and Cramer-Rao Bound Approaches", *EURASIP* Journal on Advances in Signal Processing, special issue on "Advances in Angle-of-Arrival and Multidimensional Signal Processing for Localization and Communications", Jun 2011, p. 1-14, doi :10.1186/1687-6180-2011-12.

[J4] M. N. El Korso, R. Boyer, A. Renaux and S. Marcos, "A Statistical Analysis of Achievable Resolution Limit in the Near Field Context Using Nonuniform and Lacunar Array", accepté à Signal Processing, *Elsevier*.

Revues internationales (papiers soumis)

[J5] M. N. El Korso, R. Boyer and S. Marcos, "Fast Sequential Direction Of Arrival Finding Using the Projected Companion Matrix", soumis à *Digital Signal Processing*, Novembre 2010.

[J6] M. N. El Korso, R. Boyer, A. Renaux and S. Marcos, "On the Statistical Resolvability Of Point Sources in Subspace Interference Using a GLRT-Based Framework", soumis à Signal Processing, *Elsevier*, Avril 2011.

[J7] M. N. El Korso, R. Boyer, A. Renaux and S. Marcos, "Statistical Resolution Limit for Source Localization With Clutter Interference in a MIMO radar Context", soumis à *IEEE* Transactions on Signal Processing, Avril 2011.

Congrés avec comité de lecture et actes

[C1] M. N. El Korso, R. Boyer, A. Renaux and S. Marcos, "Non-matrix closed form expressions of the Cramér-Rao bounds for near-field localization parameters", in Proc. *of IEEE International Conference on Acoustics, Speech, and Signal Processing, ICASSP-09*, Taipei, Taiwan.

[C2] M. N. El Korso, G. Bouleux, B. Boyer and S. Marcos, "Sequential estimation of the range and the bearing using the zero-forcing MUSIC approach", in Proc. of *the 17th European Signal Processing Conference, EUSIPCO-09*, Glasgow, Scotland.

[C3] M. N. El Korso, R. Boyer, A. Renaux and S. Marcos, "Expressions non-matricielles des bornes de Cramér-Rao pour la localisation de source en champ proche", in Proc. of *Colloque GRETSI* 2009, Dijon, France.

[C4] M. N. El Korso, B. Boyer and S. Marcos, "Fast Sequential Source Localization Using the Projected Companion Matrix Approach", in Proc. of *IEEE Workshop on Computational Advances in Multi-Sensor Adaptive Processing, CAMSAP-09*, Aruba, Dutch Antilles.

[C5] M. N. El Korso, G. Bouleux, B. Boyer and S. Marcos, " Estimation séquentielle des paramètres de localisation en champ proche à l'aide de l'approche Zero-Forcing", in Proc. of *Colloque GRETSI* 2009, Dijon, France.

[C6] M. N. El Korso, R. Boyer, A. Renaux and S. Marcos, "Statistical resolution limits for multiple parameters of interest and for multiple signals", in Proc. of *IEEE International Conference on Acoustics, Speech, and Signal Processing, ICASSP-10*, Dallas, TX, USA.

[C7] M. N. El Korso, R. Boyer, A. Renaux and S. Marcos, "Statistical Resolution Limit : Application to Passive Polarized Source Localization", in Proc. of Detection, Architecture and Technology *Workshop DAT-2011*, Algiers, Algeria.

[C8] M. N. El Korso, R. Boyer, A. Renaux and S. Marcos, "Statistical resolution limit for source localization in a MIMO context", in Proc. of *IEEE International Conference on Acoustics, Speech, and Signal Processing, ICASSP-11*, Prague, Czech Republic.

[C9] M. N. El Korso, R. Boyer, A. Renaux and S. Marcos, " A GLRT-based framework for the multidimensional statistical resolution limit", *IEEE Workshop on Statistical Signal Processing SSP-11*, Nice, France.

[C10] T. D. Vu, **M. N. El Korso**, R. Boyer, A. Renaux and S. Marcos, "Angular Resolution Limit for Vector Sensor Arrays : Detection and Information Theory Approaches", *IEEE Workshop on Statistical Signal Processing SSP-11*, session spéciale : *Polarized Signal Processing*, Nice, France.

[C11] T. D. Vu, **M. N. El Korso**, R. Boyer, A. Renaux and S. Marcos, " Résolution limite angulaire Appoches basées sur la théorie de l'information et sur la théorie de la détection", *GRETSI-11*, Bordeaux, France.

[C12] M. N. El Korso, A. Renaux, R. Boyer and S. Marcos, "Bornes inférieures de l'erreur quadratique moyenne pour la localisation de sources en champ proche", *GRETSI-11*, Bordeaux, France.

Séminaires

[S1] "On Performance Analysis in Array Signal Processing : Lower Bounds and Statistical Resolution Limit", Avril 2011, Institute of Telecommunications, Darmstadt University of Technology, Germany.

[S2] "Multidimensional Resolution Limit : A Survey and Applications", Signal Processing Summer School, Juin 2010, Peyresq, France.

[S3] "Statistical resolution limits for multiple parameters of interest and for multiple signals", The Ph.D. students day of the Laboratory of Signals and Systems, Juin 2010, Les Loges-en-Josas, France.

[S4] "On Statistical Resolution Limit and its Application in Array Signal Processing : Overview and Survey", Laboratory of Signals and Systems, Juillet 2009, Gif-Sur-Yvette, France.

[S5] "Asymptotic estimators performance in the near field context", The Ph.D. students day of the Laboratory of signals and systems, Juin 2009, Gif-Sur-Yvette, France.

Chapitre 2

Bornes inférieures de l'erreur quadratique moyenne pour la localisation de sources en champ proche

2.1 Introduction

La localisation passive de sources à l'aide d'une antenne composée d'un réseau de capteurs est un sujet d'une importance croissante avec plusieurs applications à la clef : radar, sismologie, communication numériques, etc. Le cas de la localisation de sources en champ lointain a été largement traité et une pléthore d'algorithmes d'estimation a été proposée dans la littérature [Kie52, Cap69, Leh83, KT83, LVT89, Van95, CM97, KV96, Mar98, Van02, SM05b]. Dans cette configuration, on peut faire l'hypothèse que les fronts d'ondes sont plans. Cependant, si les sources sont localisées dans le champ proche, la courbure des fronts d'ondes incidentes sur les capteurs ne peut plus être négligée. Par conséquent, chaque source doit être caractérisée par son azimut et sa distance (la distance entre la source et un point de référence sur l'antenne considérée.) Il existe différents algorithmes d'estimation adaptés à ce problème [HB91, YF98, GAMH05, ZC07, EBBM09], mais il existe très peu de travaux étudiant les performances optimales associées à ce modèle.

En traitement d'antenne on peut distinguer deux types de modèles concernant les signaux issus de sources [Van68, SN89, Kay93, OVSN93] : 1) le modèle déterministe (ou conditionnel), c'est-à-dire, où l'on suppose que les signaux sont déterministes mais inconnus, et 2) le modèle stochastique (ou inconditionnel), c'est-à-dire, où l'on suppose que les signaux émis suivent une loi Gaussienne complexe circulaire de moyenne nulle et de matrice de covariance $\mathbf{\Sigma}$ inconnue. La validité du modèle dépend de l'application en question. En effet, l'hypothèse du modèle stochastique n'est pas valable pour des applications telles que le radar avec des formes d'onde connues à l'émission [Van01, BT06, NS09] ou la communication radio [LC03] par exemple. Dans ce cas, le choix légitime serait alors de considérer un modèle déterministe. Cependant, d'autres applications sont mieux décrites par le modèle stochastique, comme, le traitement sismique [Van02] ou la tomographie [Hay85].

Pour caractériser les performances des estimateurs, la borne de Cramér-Rao (BCR) est un outil mathématique très utilisé en traitement du signal. Cette dernière exprime une borne inférieur de la matrice de covariance d'erreur de tout estimateur non biaisé [Cra46]. Bien entendu, la BCR dépend du modèle considéré. De ce fait, dans le cas de l'estimation de direction d'arrivée d'une source située en champ proche nous allons étudier les deux BCRs ; la BCR pour le modèle déterministe, dénommée la BCR déterministe (BCRD) et la BCR pour le modèle aléatoire, dénommée la BCR stochastique (BCRS). Il faut noter qu'asymptotiquement, la BCRS

est atteinte en terme de nombre d'observations par l'estimateur du maximum de vraisemblance stochastique (MVS) [SN89, OVSN93]. La BCRD est, quant à elle, atteinte asymptotiquement en terme de rapport signal à bruit (RSB) (ou en nombre de capteurs) par l'estimateur du maximum de vraisemblance déterministe (MVD) [RFCL06].

La plupart des résultats existants dans la littérature sur la BCRS et la BCRD concerne la localisation de sources en champ lointain. De plus, il est important de dire que la majeure partie de ces résultats donnent seulement des expressions matricielles de la matrice d'information de Fisher (MIF) qui est l'inverse de la BCR. De ce fait, le coût calculatoire associé à la BCR est très important pour un grand nombre des observations (en ce qui concerne la BCRD) ou un grand nombre de capteurs (en ce qui concerne la BCRS), d'où la nécessité d'avoir des expressions non matricielles pour le calcul de la BCR. Dans [SN90b], la BCRS a été indirectement calculée dans le cas asymptotique (en terme de nombre des observations) comme étant équivalente à la matrice de covariance du MVS. Dix ans après, Stoica *et al.* [SLG01], Pesavento et Gershman [PG01] et Gershman *et al.* [GSPL02] ont recalculé la BCRS sous forme matricielle (avant inversion de la MIF qui est simplement donnée par la formule de Slepian Bang [SM05b]) dans le cas d'un bruit blanc, coloré et de matrice de covariance inconnue. D'autre part, la BCRD pour le contexte champ lointain a été calculée par Stoica *et al.* dans [SN89].

Contrairement au champ lointain, la BCR pour les problèmes de localisation de source en champ proche a été peu étudiée. On peut trouver des expressions matricielles pour la BCRS dans [WF93]. Récemment, Grosicki *et al.* [GAMH05] ont étendu les formules matricielles de la BCRS dans le contexte du champ lointain au champ proche. A notre connaissance, aucune expression analytique non matricielle de la BCRS ou de la BCRD n'est disponible dans la littérature. Un des buts de ce chapitre est de combler ce manque. En particulier, nous calculons et analysons des expressions non matricielles compactes de la BCRD et de la BCRS dans le cas d'une source à bande étroite située en champ proche. Nous calculons analytiquement la BCRS et la BCRD par rapport aux paramètres physiques du problème, à savoir, l'azimut, la distance, l'amplitude et la phase de la source. Nous analysons aussi, le comportement de la BCR par rapport à certains de ces paramètres, à savoir, la fréquence porteuse du signal, la distance, l'azimut et le nombre de capteurs. De plus, nous validons nos différentes expressions théoriques par des simulations numériques et nous comparons les deux BCRs.

Nous rappelons que la BCR est une borne non utilisable dans les zones non-asymptotiques, et donc non utilisable dans ces zones. De ce fait, nous complétons cette analyse par la prédiction du décrochement. La zone dite de décrochement est un accroissement brusque de l'erreur quadratique moyenne (dont la cause est l'apparition des observations aberrantes). Ainsi, la zone de décrochement d'un estimateur délimite sa zone de fonctionnement optimal. Nous calculons et analysons différentes bornes déterministes inférieures de l'erreur quadratique moyenne dans le cadre de la localisation passive d'une source en champ proche : la borne de McAulay-Seidman (BMS) [MS69], la borne de Hammersley-Chapman-Robbins (BHCR) [Ham50], la borne de McAulay-Hofstetter (BMH) [MH71] et, plus particulièrement, une borne récemment introduite dans la littérature dénommée la borne de Fourier Cramér-Rao (BFCR) [TT10]. Le but de cette étude est de caractériser les performances optimales non-asymptotiques des estimateurs dans le contexte champ proche. Plus particulièrement, on s'intéresse à la prédiction du phénomène de décrochement pour lequel ces bornes sont utiles. Cette analyse est pertinente, d'autant plus, qu'à notre connaissance, aucun résultat concernant des bornes inférieures autres que la BCR (par rapport à la localisation en champ proche), n'est disponible dans la littérature.

Dans ce qui suit, nous ne citerons que les principaux résultats, les détails calculatoires sont détaillés dans l'article associé à ce chapitre qui se trouve à l'**Annexe A.1** (M. N. El Korso, R. Boyer, A. Renaux and S. Marcos, "*Conditional and unconditional Cramér-Rao bounds for near-*

field source localization", IEEE Transactions on Signal Processing, Volume : 58, Issue : 5, May 2010, pp. 2901-2907) et l'**Annexe A.2** (M. N. El Korso, A. Renaux, R. Boyer and S. Marcos, "*Deterministic Lower Bounds on the Mean Square Error for Near Field Source Localization*", en préparation pour IEEE Transactions on Signal Processing).

2.2 Modèle des observations

Considérons une Antenne Linéaire Uniforme (ALU) composée de N ($N > 1$) capteurs avec une distance entre capteurs notée d. L'ALU reçoit un signal émis par une source à bande étroite située dans le champ proche. Par conséquent, le modèle d'observation peut s'écrire comme suit

$$y_n(t) = s(t)e^{j\tau_n} + v_n(t),$$

avec $t = 1, \ldots, T$ et $n = 0, \ldots, N-1$. $y_n(t)$ et $s(t)$ représentent le signal observé à la sortie du $n^{ème}$ capteur et le signal source, respectivement. Le processus aléatoire $v_n(t)$ est un bruit additif et T est le nombre d'observations. Puisque la source est supposée dans le champ proche de l'antenne, le retard temporel τ_n qui représente le temps de propagation du signal de la source au $n^{ème}$ capteur est donné par [GAMH05]

$$\tau_n = \frac{2\pi r}{\lambda}\left(\sqrt{1 + \frac{n^2 d^2}{r^2} - \frac{2nd\sin\theta}{r}} - 1\right),$$

où λ est la longueur d'onde et $r, \theta \in [0, \pi/2[$ représentent la distance et l'azimut du signal source, respectivement. Si la distance appartient à la région de Fresnel [HB91], c'est-à-dire, si

$$0.62(d^3(N-1)^3/\lambda)^{1/2} < r < 2d^2(N-1)^2/\lambda, \tag{2.1}$$

alors le temps de propagation τ_n peut être approximé par

$$\tau_n = \omega n + \phi n^2 + O\left(\frac{d^2}{r^2}\right), \tag{2.2}$$

où ω et ϕ sont généralement appelées les angles électriques. Ils s'expriment en fonction des paramètres physiques du problème à l'aide de $\omega = -2\pi\frac{d}{\lambda}\sin(\theta)$ et de $\phi = \pi\frac{d^2}{\lambda r}\cos^2(\theta)$.
Par conséquent, en utilisant (2.2), le modèle des observations peut s'écrire comme suit

$$y_n(t) = s(t)e^{j\left(\omega n + \phi n^2\right)} + v_n(t). \tag{2.3}$$

De ce fait, le vecteur d'observation peut être exprimé comme suit

$$\mathbf{y}(t) = [y_1(t) \ldots y_N(t)]^T = \mathbf{a}(\omega, \phi)s(t) + \mathbf{v}(t), \tag{2.4}$$

où $\mathbf{v}(t) = [v_1(t) \ldots v_N(t)]^T$ et où le $n^{ème}$ élément du vecteur directionnel $\mathbf{a}(\omega, \phi)$ est donné par $[\mathbf{a}(\omega, \phi)]_n = e^{j(\omega n + \phi n^2)}$ (notons que pour le champ lointant ϕ est supposé égal à zero).

2.3 Les bornes de Cramér-Rao

Dans ce qui suit, nous utiliserons les hypothèses suivantes :
- On admet que le bruit est un processus complexe circulaire blanc Gaussien aléatoire avec une moyenne nulle et une variance inconnue σ^2,

– Le bruit est supposé décorélé temporellement et spatialement,

La fonction de densité de probabilité conjointe des observations $\boldsymbol{\chi} = [\mathbf{y}^T(1)\dots\mathbf{y}^T(T)]^T$ pour un vecteur de paramètres inconnus $\boldsymbol{\xi}$ donné peut s'écrire comme suit :

$$p(\boldsymbol{\chi}|\,\boldsymbol{\xi}) = \frac{1}{\pi^{NT}\det(\boldsymbol{\Sigma})} e^{-(\boldsymbol{\chi}-\boldsymbol{\mu})^H\boldsymbol{\Sigma}^{-1}(\boldsymbol{\chi}-\boldsymbol{\mu})}, \tag{2.5}$$

où $\boldsymbol{\Sigma}$ et $\boldsymbol{\mu}$ représentent la matrice de covariance et la moyenne de $\boldsymbol{\chi}$, respectivement.

Le but de cette section est l'obtention de la BCRD et de la BCRS pour le modèle donné en (2.4) en fonction de la distance r et de l'azimut θ.

2.3.1 Expressions analytiques

Notons $E\left\{(\hat{\boldsymbol{\xi}}-\boldsymbol{\xi})(\hat{\boldsymbol{\xi}}-\boldsymbol{\xi})^T\right\}$ la matrice de covariance d'un estimateur non biaisé de $\boldsymbol{\xi}$, noté par $\hat{\boldsymbol{\xi}}$. Le principe d'inégalité de covariance stipule que [Cra46] $\mathrm{MSE}([\hat{\boldsymbol{\xi}}]_i) = E\left\{\left([\hat{\boldsymbol{\xi}}]_i - [\boldsymbol{\xi}]_i\right)^2\right\} \geq \mathrm{BCR}([\boldsymbol{\xi}]_i)$, où $\mathrm{BCR}([\boldsymbol{\xi}]_i) = [\mathbf{MIF}^{-1}(\boldsymbol{\xi})]_{i,i}$ et où $\mathbf{MIF}(\boldsymbol{\xi})$ représente la MIF. Par conséquent, nous donnerons une inversion analytique de la MIF qui nous conduit à des expressions non matricielles compactes de la BCR. Enfin, en utilisant la formule de changement de variable [Kay93], nous fournirons des expressions (non matricielles) de la BCR en fonction des paramètres physiques du problème qui sont la distance et l'azimut.
Du fait que nous travaillons avec un modèle des observations Gaussien (2.5) (pour un modèle déterministe, c'est-à-dire, à moyenne paramétrée ou pour un modèle stochastique, c'est-à-dire, à covariance paramétrée), le $i^{ème}, k^{ème}$ élément de la MIF correspondant au vecteur de paramètre $\boldsymbol{\xi}$ peut être écrit sous cette forme [SM05b] (formule dite de Slepian-Bang)

$$[\mathbf{MIF}(\boldsymbol{\xi})]_{i,k} = tr\left\{\boldsymbol{\Sigma}^{-1}\frac{\partial\boldsymbol{\Sigma}}{\partial[\boldsymbol{\xi}]_i}\boldsymbol{\Sigma}^{-1}\frac{\partial\boldsymbol{\Sigma}}{\partial[\boldsymbol{\xi}]_k}\right\} + 2\Re\left\{\frac{\partial\boldsymbol{\mu}^H}{\partial[\boldsymbol{\xi}]_i}\boldsymbol{\Sigma}^{-1}\frac{\partial\boldsymbol{\mu}}{\partial[\boldsymbol{\xi}]_k}\right\}. \tag{2.6}$$

Dans ce qui suit nous noterons **BCRD** et **MIFD**, respectivement, la matrice de Cramér-Rao et la matrice d'information de Fisher déterministes. De même **BCRS** et **MIFS** représentent, respectivement, la matrice Cramér-Rao et la matrice d'information de Fisher stochastiques.

BCR pour le modèle déterministe

Premièrement, nous considérons le modèle déterministe avec $s(t) = \alpha(t)e^{j(2\pi f_0 t+\psi(t))}$ représente le signal émis pour une fréquence porteuse valant f_0 et $\alpha(t)$, $\psi(t)$ représentent l'amplitude réelle et la phase de la source, respectivement. Notons $\boldsymbol{\psi} = [\psi(1)\dots\psi(T)]^T$ et $\boldsymbol{\alpha} = [\alpha(1)\dots\alpha(T)]^T$ où les vecteurs de paramètres inconnus sont $\boldsymbol{\xi} = [\omega\ \phi\ \boldsymbol{\psi}^T\ \boldsymbol{\alpha}^T\ \sigma^2]^T$ (si on s'intéresse aux angles électriques) ou $\boldsymbol{\kappa} = [\theta\ r\ \boldsymbol{\psi}^T\ \boldsymbol{\alpha}^T\ \sigma^2]^T$ (si on s'intéresse aux paramètres physiques). Ainsi, dans (2.6), on aura $\boldsymbol{\Sigma} = \sigma^2\mathbf{I}_{NT}$ et $\boldsymbol{\mu} = [s(1)\mathbf{a}^T(\omega,\phi)\dots s(T)\mathbf{a}^T(\omega,\phi)]^T$. Nous commencerons par calculer $\mathbf{BCRD}(\boldsymbol{\xi})$, puis, nous en déduirons $\mathbf{BCRD}(\boldsymbol{\kappa})$ grâce à un changement de variables. Notons que $\boldsymbol{\kappa}$ et $\boldsymbol{\xi}$ sont supposés déterministes et de ce fait, leur taille croît avec le nombre d'observations (dans ce cas là, la BRCD est atteinte à fort RSB [RFCL06].)

En utilisant (2.6), on obtient

$$[\mathbf{MIFD}(\boldsymbol{\xi})]_{i,k} = \frac{NT}{\sigma^4}\frac{\partial\sigma^2}{\partial[\boldsymbol{\xi}]_i}\frac{\partial\sigma^2}{\partial[\boldsymbol{\xi}]_k} + \frac{2}{\sigma^2}\Re\left\{\frac{\partial\boldsymbol{\mu}^H}{\partial[\boldsymbol{\xi}]_i}\frac{\partial\boldsymbol{\mu}}{\partial[\boldsymbol{\xi}]_k}\right\}. \tag{2.7}$$

Structure bloc diagonale de l'information de Fisher : En utilisant (2.7) et après quelques calculs algébriques on obtient le lemme suivant :

Lemme 1 *La structure bloc diagonale de la matrice* $\mathbf{MIFD}(\boldsymbol{\xi})$ *pour une source située dans le champ proche est donnée par*

$$\mathbf{MIFD}(\boldsymbol{\xi}) = bdiag\left(\boldsymbol{Q}, \boldsymbol{Y}\right), \tag{2.8}$$

où

$$\boldsymbol{Q} = \left[\begin{array}{cc|c} f_{\omega\omega} & f_{\omega\phi} & \mathbf{f}_{\omega\boldsymbol{\psi}} \\ f_{\phi\omega} & f_{\phi\phi} & \mathbf{f}_{\phi\boldsymbol{\psi}} \\ \hline \mathbf{f}_{\boldsymbol{\psi}\omega} & \mathbf{f}_{\boldsymbol{\psi}\phi} & \mathbf{F}_{\boldsymbol{\psi}\boldsymbol{\psi}} \end{array}\right], \tag{2.9}$$

et $\boldsymbol{Y} = bdiag\left(\frac{2N}{\sigma^2}\mathbf{I}_T, \frac{NT}{\sigma^4}\right)$. *On notera le RSB "déterministe"* $D_{RSB} = ||\boldsymbol{\alpha}||^2/\sigma^2$. *Les élements de la matrice* $\boldsymbol{Q}$ *sont donnés par*

$$f_{\omega\omega} = D_{RSB}\ T\frac{N(N-1)(2N-1)}{3},$$

$$f_{\phi\phi} = D_{RSB}\ T\frac{N(N-1)(2N-1)(3N^2-3N-1)}{15},$$

et

$$f_{\omega\phi} = f_{\phi\omega} = D_{RSB}\ T\frac{N^2(N-1)^2}{2}.$$

De plus, les vecteurs, de taille $T \times 1$, $\mathbf{f}_{\boldsymbol{\psi}\omega}$, $\mathbf{f}^T_{\omega\boldsymbol{\psi}}$, $\mathbf{f}_{\boldsymbol{\psi}\phi}$ *et* $\mathbf{f}^T_{\phi\boldsymbol{\psi}}$ *sont donnés par*

$$\mathbf{f}_{\boldsymbol{\psi}\omega} = \mathbf{f}^T_{\omega\boldsymbol{\psi}} = \frac{1}{\sigma^2}N(N-1)(\boldsymbol{\alpha}\odot\boldsymbol{\alpha}),$$

et

$$\mathbf{f}_{\boldsymbol{\psi}\phi} = \mathbf{f}^T_{\phi\boldsymbol{\psi}} = \frac{1}{\sigma^2}\frac{N(N-1)(2N-1)}{3}(\boldsymbol{\alpha}\odot\boldsymbol{\alpha}).$$

Enfin, la matrice $\mathbf{F}_{\boldsymbol{\psi}\boldsymbol{\psi}}$, *de taille* $T \times T$, *est donnée par*

$$\mathbf{F}_{\boldsymbol{\psi}\boldsymbol{\psi}} = \frac{2N}{\sigma^2}diag(\boldsymbol{\alpha}\odot\boldsymbol{\alpha}). \tag{2.10}$$

Notons que, grâce à la diversité temporelle de la source, $\mathbf{F}_{\boldsymbol{\alpha}\boldsymbol{\psi}} = \mathbf{F}^T_{\boldsymbol{\psi}\boldsymbol{\alpha}}$ sont des matrices nulles (c'est-à-dire que les paramètres $\boldsymbol{\psi}$ et $\boldsymbol{\alpha}$ sont découplés.) Nous remarquons une propriété bien connue, à savoir que la variance du bruit est bien découplée par rapport aux autres paramètres [Kay93, SM05b]. Les termes nuls restants sont la conséquence de l'application de la partie réelle dans (2.7) à des termes purement imaginaires.

Inversion analytique : La taille de la MIF donnée en (2.8) dépend du nombre des observations. C'est pourquoi son inversion numérique peut être une opération très coûteuse pour un grand nombre des observations. C'est l'une des raisons pour laquelle nous avons proposé une inversion analytique. En utilisant la partition dans (2.8) et après l'écriture analytique de l'expression de l'inverse du complément de Schur de $\mathbf{F}_{\psi,\psi}$ [GL89], l'expression compacte non matricielle de la BCRD par rapport à $\boldsymbol{\xi}$ associée au modèle (2.3) s'exprime suivant le théorème :

Théorème 1 *Les expressions non matricielles de la matrice* $\boldsymbol{BCRD}(\boldsymbol{\xi})$ *correspondant aux angles électriques, pour* $N \geq 3$*, sont données par*

$$BCRD(\omega) = \frac{6(2N-1)(8N-11)}{D_{RSB}(N^2-1)N(N^2-4)}, \tag{2.11}$$

$$BCRD(\phi) = \frac{90}{D_{RSB}(N^2-1)N(N^2-4)}, \tag{2.12}$$

$$BCRD(\psi(t)) = \frac{1}{2\alpha^2(t)D_{RSB}} \frac{N^4-31N^3+48N^2-26N+2}{N^2(N+1)(N^2-4)}, \quad \forall t \tag{2.13}$$

$$BCRD(\alpha(t)) = \frac{\sigma^2}{2N} \quad \forall t, \tag{2.14}$$

et

$$BCRD\left(\sigma^2\right) = \frac{\sigma^4}{NT}. \tag{2.15}$$

Et les termes croisés sont donnés par $BCRD(\omega,\phi) = BCRD(\phi,\omega) = -\frac{90}{D_{RSB}N(N^2-4)(N+1)}$.

Changement de vecteur de paramètres : Même si le modèle (2.3) est fréquemment utilisé en traitement d'antenne, sa BCRD par rapport à $\boldsymbol{\xi}$ ne nous apporte aucune information concernant les paramètres physiques réels du problème. De ce fait, il est intéressant d'analyser la BCRD par rapport à la distance et à l'azimut directement. En partant de $\mathbf{BCRD}(\boldsymbol{\xi})$, nous pouvons facilement obtenir $\mathbf{BCRD}(\boldsymbol{\kappa})$ en utilisant la propriété suivante (voir [Kay93] p. 45)

$$\mathbf{BCRD}(\boldsymbol{\kappa}) = \frac{\partial \mathbf{g}(\boldsymbol{\xi})}{\partial \boldsymbol{\xi}} \mathbf{BCRD}(\boldsymbol{\xi}) \frac{\partial \mathbf{g}^T(\boldsymbol{\xi})}{\partial \boldsymbol{\xi}}, \tag{2.16}$$

où

$$\boldsymbol{\kappa} = \mathbf{g}(\boldsymbol{\xi}) = [-\arcsin(\frac{\omega\lambda}{2\pi d}) \quad \frac{\pi d^2}{\lambda\phi}\cos^2\left(\arcsin(\frac{\omega\lambda}{2\pi d})\right) \quad \boldsymbol{\psi}^T \ \boldsymbol{\alpha}^T \ \sigma^2]^T,$$

et où la matrice Jacobienne, $\frac{\partial \mathbf{g}(\boldsymbol{\xi})}{\partial \boldsymbol{\xi}}$, est donnée par

$$\frac{\partial \mathbf{g}(\boldsymbol{\xi})}{\partial \boldsymbol{\xi}} = \begin{bmatrix} \frac{\partial g_1(\boldsymbol{\xi})}{\partial \xi_1} & 0 & 0 & \cdots & 0 \\ \frac{\partial g_2(\boldsymbol{\xi})}{\partial \xi_1} & \frac{\partial g_2(\boldsymbol{\xi})}{\partial \xi_2} & 0 & \cdots & 0 \\ 0 & 0 & 1 & \cdots & 0 \\ \vdots & \vdots & & \ddots & \\ 0 & 0 & 0 & & 1 \end{bmatrix}, \tag{2.17}$$

avec

$$\frac{\partial g_1(\boldsymbol{\xi})}{\partial \xi_1} = -\frac{\lambda}{2\pi d\sqrt{1-\frac{\omega^2\pi^2d^4}{\lambda^2}}}, \tag{2.18}$$

$$\frac{\partial g_2(\boldsymbol{\xi})}{\partial \xi_1} = -\frac{\lambda\omega}{2\pi\phi}\cos\left(\arcsin(\frac{\lambda\omega}{2\pi d})\right)\frac{1}{\sqrt{1-\left(\frac{\lambda\omega}{2\pi d}\right)^2}}, \tag{2.19}$$

et

$$\frac{\partial g_2(\boldsymbol{\xi})}{\partial \xi_2} = -\frac{\pi d^2}{\lambda\phi^2}\cos^2\left(\arcsin(\frac{\lambda\omega}{2\pi d})\right). \tag{2.20}$$

En utilisant (2.16), l'expression de la matrice Jacobienne ci-dessus et après quelques efforts calculatoires nous obtenons

Théorème 2 *Les expressions non matricielles de la BCRD pour une source située dans le champ proche, avec $N \geq 3$ et $\theta \neq \frac{\pi}{2}$, sont données par*

$$\begin{aligned} BCRD(\theta) &= \frac{3\lambda^2}{2D_{RSB}d^2\pi^2\cos^2(\theta)}\frac{(8N-11)(2N-1)}{(N^2-1)N(N^2-4)}, \\ BCRD(r) &= \frac{6r^2\lambda^2}{D_{RSB}\pi^2 d^4} \times \frac{15r^2 + 30drp_1(N)\sin(\theta) + d^2p_2(N)\sin^2(\theta)}{p_3(N)\cos^4(\theta)}, \end{aligned} \tag{2.21}$$

où $p_1(N) = N-1$, $p_2(N) = (8N-11)(2N-1)$ et $p_3(N) = N(N^2-1)(N^2-4)$.

Notons que, bien sûr, $\mathbf{BCRD}(\psi)$, $\mathbf{BCRD}(\alpha)$ *et* $BCRD\left(\sigma^2\right)$ *restent inchangées. Et les termes croisés entre θ et r s'expriment désormais comme suit*

$$BCRD(\theta, r) = BCRD(r, \theta) = -\frac{3\lambda^2 r}{D_{RSB}\pi^2 d^3}\frac{15rp_1(N) + dp_2(N)\sin(\theta)}{p_3(N)\cos^3(\theta)}. \tag{2.22}$$

BCR pour le modèle aléatoire

Maintenant, nous allons nous intéresser au calcul de la BCRS pour des signaux sources supposés complexes circulaires Gaussiens (de moyenne nulle et de variance σ_s^2) indépendants du bruit. Dans cette configuration les vecteurs de paramètres inconnus sont donnés par $\boldsymbol{\rho} = [\omega\ \phi\ \sigma_s^2\ \sigma^2]^T$ (si on s'intéresse aux angles électriques) ou $\boldsymbol{\vartheta} = [\theta\ r\ \sigma_s^2\ \sigma^2]^T$ (si on s'intéresse aux paramètres physiques). De ce fait, $\boldsymbol{y}(t)|\boldsymbol{\rho} \sim \mathcal{CN}(\mathbf{0}, \boldsymbol{\Sigma})\ \forall t = 1, \ldots, T$, où la matrice de covariance est donnée par $\boldsymbol{\Sigma} = \sigma_s^2\mathbf{a}(\omega,\phi)\mathbf{a}^H(\omega,\phi) + \sigma^2\mathbf{I}_N$. Par conséquent, la MIF donnée par (2.6) s'exprime ainsi

$$[\mathbf{MIFS}(\boldsymbol{\rho})]_{i,k} = T\ tr\left\{\boldsymbol{\Sigma}^{-1}\frac{\partial\boldsymbol{\Sigma}}{\partial[\boldsymbol{\rho}]_i}\boldsymbol{\Sigma}^{-1}\frac{\partial\boldsymbol{\Sigma}}{\partial[\boldsymbol{\rho}]_k}\right\}. \tag{2.23}$$

En utilisant les résultats de [SLG01] pour deux paramètres d'intérêt, nous obtenons

$$[\mathbf{BCRS}(\boldsymbol{\rho})]_{1:2,1:2} = \frac{1}{2S_{RSB}\ \sigma_s^2 T}\left(\Re\left\{\left(\mathbf{D}^H\boldsymbol{\Pi}^{\perp}_{\mathbf{a}(\omega,\phi)}\mathbf{D}\right) \odot \left(\mathbf{J} \otimes \mathbf{a}^H(\omega,\phi)\boldsymbol{\Sigma}^{-1}\mathbf{a}(\omega,\phi)\right)^T\right\}\right)^{-1}, \tag{2.24}$$

où $S_{RSB} = \frac{\sigma_s^2}{\sigma^2}$ est le RSB associé au modèle aléatoire, où $\mathbf{J} = \mathbf{1}_2\mathbf{1}_2^T$ avec $\mathbf{1}_2 = [1\ 1]^T$, $\mathbf{D} = \left[\frac{\partial\mathbf{a}(\omega,\phi)}{\partial\omega}\ \frac{\partial\mathbf{a}(\omega,\phi)}{\partial\phi}\right]$ et $\boldsymbol{\Pi}^{\perp}_{\mathbf{a}(\omega,\phi)} = \mathbf{I}_N - \frac{1}{N}\mathbf{a}(\omega,\phi)\mathbf{a}^H(\omega,\phi)$. Dans ce qui suit, nous allons utiliser (2.24) pour obtenir des expressions non matricielles de $\mathbf{BCRS}(\boldsymbol{\rho})$.

Inversion analytique

Théorème 3 *Les expressions non matricielles de* $\mathbf{BCRS}(\boldsymbol{\rho})$ *correspondant aux angles électriques, pour $N \geq 3$, sont données par*

$$BCRS(\omega) = \left(1 + \frac{1}{S_{RSB}\ N}\right)\frac{6(2N-1)(8N-11)}{S_{RSB}\ T(N^2-1)N(N^2-4)}, \tag{2.25}$$

$$BCRS(\phi) = \left(1 + \frac{1}{S_{RSB}\ N}\right)\frac{90}{S_{RSB}\ T(N^2-1)N(N^2-4)}. \tag{2.26}$$

De plus, les termes croisés sont donnés par

$$[\mathbf{BCRS}(\boldsymbol{\rho})]_{1,2} = [\mathbf{BCRS}(\boldsymbol{\rho})]_{2,1} = -\left(1 + \frac{1}{S_{RSB}\ N}\right)\frac{90}{S_{RSB}\ TN(N^2-4)(N+1)}.$$

Changement de variables : En utilisant le même changement de variable donné par (2.16)-(2.20), on peut facilement obtenir le résultat suivant

Théorème 4 *Les expressions non matricielles de* $\mathbf{BCRS}(\boldsymbol{\vartheta})$ *pour une source située dans le champ proche, avec* $N \geq 3$ *et* $\theta \neq \frac{\pi}{2}$*, sont données par*

$$BCRS(\theta) = \left(1 + \frac{1}{S_{RSB}\ N}\right) \frac{3\lambda^2}{2S_{RSB}\ T d^2 \pi^2 \cos^2(\theta)} \frac{(8N-11)(2N-1)}{N(N^2-1)(N^2-4)}, \tag{2.27}$$

$$BCRS(r) = \left(1 + \frac{1}{S_{RSB}\ N}\right) \frac{6r^2\lambda^2}{S_{RSB}\ T\pi^2 d^4} \frac{15r^2 + 30dr(N-1)\sin(\theta) + d^2(8N-11)(2N-1)\sin^2(\theta)}{N^2(N^2-1)(N^2-4)\cos^4(\theta)}. \tag{2.28}$$

Les termes croisés entre θ *et* r *sont donnés par*

$$\begin{aligned}[\mathbf{BCRS}(\boldsymbol{\vartheta})]_{1,2} &= [\mathbf{BCRS}(\boldsymbol{\vartheta})]_{2,1} \\ &= -\left(1 + \frac{1}{S_{RSB}\ N}\right) \frac{3\lambda^2 r}{S_{RSB}\ T\pi^2 d^3} \frac{15r(N-1) + d(8N-11)(2N-1)\sin(\theta)}{N(N^2-1)(N^2-4)\cos^3(\theta)}.\end{aligned} \tag{2.29}$$

2.3.2 Résultats de simulation et analyse

Le but de cette section est de valider et d'analyser les expressions non matricielles compactes données dans les sections précédentes.

Comportement de la BCRD et de le BCRS

Pour ces simulations, nous avons considéré une ALU de 10 capteurs avec une distance entre capteurs $d = \frac{\lambda}{2}$. Le nombre d'observations est égal à $T = 20$ et la source est repérée par les coordonnées suivantes $(\theta, r) = (30^o, 6\lambda)$ (qui appartient à la région de Fresnel selon (2.1)). Dans les Fig. 2.1 et Fig. 2.2, nous avons superposé les BCRD/BCRS analytiques, obtenues par (2.21), (2.22), (2.27) et (2.28), avec les BCRS/BCRD exactes calculées par inversion numérique de la MIF. De plus nous avons fait varier la variance du bruit de 0.1 à 1 pour différentes valeurs de la fréquence porteuse ($\lambda = \frac{c}{f_0}$, où c représente la vitesse de la lumière). On observe que ces figures valident bien nos expressions analytiques. De plus, à l'aide des expressions non matricielles données par (2.21), (2.22), (2.27) et (2.28), nous remarquons que

- La BCRD et la BCRS sont invariantes par rapport à la phase du signal source.
- Comme dans le cas du champ lointain, BCRD(θ) et BCRS(θ) ne dépendent que de l'azimut selon $1/\cos^2(\theta)$. De ce fait, l'ALU n'est pas une antenne isotrope pour une source située en champ proche.
- BCRD(r) et BCRS(r) dépendent à la fois de l'azimut et de la distance. Pour $\lambda, r \propto d$, la dépendance par rapport à la distance est quant à elle de $O(r^2)$, ce qui veut dire que l'estimation s'améliore quand la source se rapproche de l'antenne (cependant il faut respecter la contrainte de la région de Fresnel 2.1). La dépendance en la distance par rapport à l'azimut est $1/\cos^4(\theta)$. Si θ est proche de $\pi/2$, BCR(r) tend vers l'infini et cette convergence est plus rapide que celle de BCR(θ).
- Pour un nombre suffisant de capteurs, BCRD(θ), BCRD(r), BCRS(θ) et BCRS(r) sont de l'ordre de $O(1/N^3)$.

- Pour $\lambda \propto d$, BCRD(θ) et BCRS(θ) sont indépendantes de la fréquence porteuse f_0. Ce qui n'est pas le cas de BCRD(r) et de BCRS(r). La Fig. 2.1 montre que, pour différentes valeurs de l'azimut et pour une variance de bruit fixée ($\sigma^2 = 0.5$), plus grande est la fréquence porteuse, plus bas sont BCRD(r) et BCRS(r).
- Pour un grand nombre de capteurs et une distance entre capteurs fixée, BCRD(θ) et BCRS(θ) exprimées dans le champ proche tendent vers les BCR exprimées dans le champ lointain [SN90a]. Cette dernière remarque est en adéquation avec l'intuition car, du fait de la contrainte (2.1) un grand nombre de capteurs implique une grande distance entre la source et l'antenne (tout en restant dans le région de Fresnel.)
- Les expressions de la BCRD montrent que les paramètres physiques d'intérêt sont fortement couplés vu que BCRD (θ, r) est $O(1/N^3)$ comme BCRD(θ) et BCRD(r). Les même remarques s'appliquent pour la BCRS.

Comparaison entre la BCRD et la BCRS

Comme le modèle déterministe ne requiert aucune hypothèse sur le signal de la source, nous supposerons alors que la phase et l'amplitude du signal source sont une réalisation donnée d'un processus complexe circulaire blanc Gaussien aléatoire avec une moyenne nulle est une variance σ_s^2. Ceci nous permettra de faire une comparaison entre la BCRD et la BCRS. Nous considérons ici les deux quantités D_{RSB} et S_{RSB} égales que nous noterons simplement par RSB.

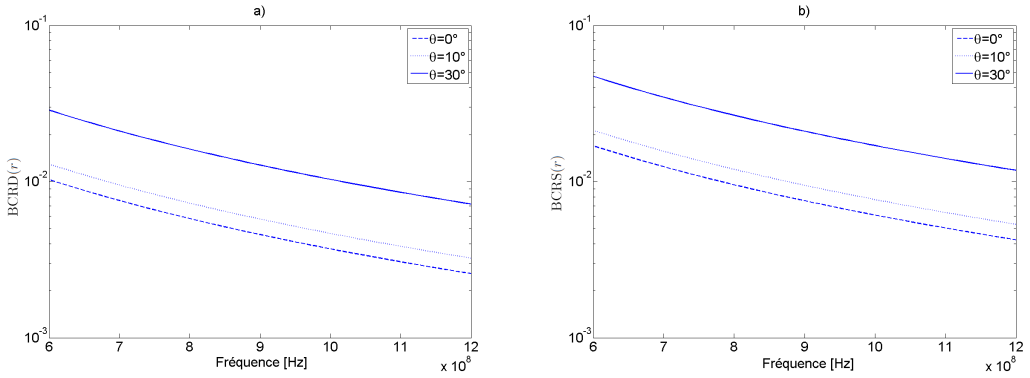

FIGURE 2.1 – BCR(r) en fonction de f_0 pour $\sigma^2 = 0.5$ et pour différentes valeurs de $\theta = 10^o, 30^o, 50^o$: a) BCRD(r), b) BCRS(r).

Corollaire 1 *En utilisant (2.11), (2.12), (2.25) et (2.26), on obtient :* $\frac{BCRS(\omega)}{BCRD(\omega)} = \left(1 + \frac{1}{RSB \quad N}\right)$, *et* $\frac{BCRS(\phi)}{BCRD(\phi)} = \left(1 + \frac{1}{RSB \quad N}\right)$.

De même, grâce à (2.21), (2.22), (2.27) et (2.28), on obtient : $\frac{BCRS(\theta)}{BCRD(\theta)} = \left(1 + \frac{1}{RSB \quad N}\right)$, *et* $\frac{BCRS(r)}{BCRD(r)} = \left(1 + \frac{1}{RSB \quad N}\right)$, *c'est-à-dire,* $BCRS(\omega) \geq BCRD(\omega)$, $BCRS(\phi) \geq BCRD(\phi)$, $BCRS(\theta) \geq BCRD(\theta)$ *et* $BCRS(r) \geq BCRD(r)$ *(voir Fig. 2.2). Le lecteur pourra trouver des résultats similaires dans [SN90b] pour le contexte du champ lointain.*

De plus,

- Pour un nombre de capteurs fixé :

$$\text{BCRD}(\theta) \overset{\text{RSB}\to\infty}{\to} \text{BCRS}(\theta),$$

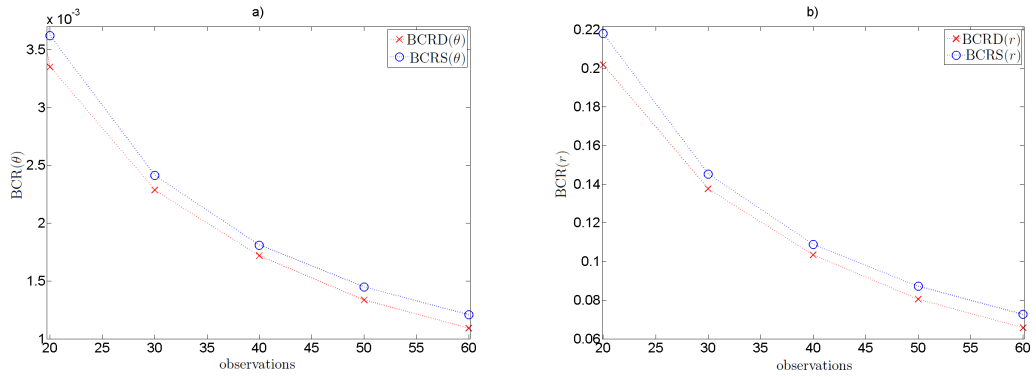

FIGURE 2.2 – BCR en fonction du nombre d'observations et pour $N = 10$ capteurs : *a*) BCRD(θ) et BCRS(θ), *b*) BCRD(r) et BCRS(r).

et

$$\text{BCRD}(r) \overset{\text{RSB}\to\infty}{\to} \text{BCRS}(r).$$

– Pour un RSB fixé :

$$\text{BCRD}(\theta) \overset{N\to\infty}{\to} \text{BCRS}(\theta),$$

et

$$\text{BCRD}(r) \overset{N\to\infty}{\to} \text{BCRS}(r).$$

– Et enfin, pour $\frac{1}{\text{RSB}\ \ \text{N}} \ll 1$:

$$\text{BCRD}(\theta) \approx \text{BCRS}(\theta),$$

et

$$\text{BCRD}(r) \approx \text{BCRS}(r).$$

Nous rappelons que la BCR est une borne optimiste (et même non valable) dans les zones non-asymptotiques, et donc non utilisable dans ces zones. Le but de la section suivante est de montrer l'apport des autres bornes plus précises que la BCR pour prédire le phénomène de décrochement.

Dans la section suivante nous ne citerons que les principaux résultats, les détails calculatoires sont explicités dans l'**Annexe A.2** (M. N. El Korso, A. Renaux, R. Boyer and S. Marcos, "Deterministic Performance Bounds on the Mean Square Error for Near Field Source Localization", en préparation pour *IEEE Transactions on Signal Processing.*).

2.4 Autres bornes inférieures de l'erreur quadratique moyenne

Dans ce qui suit, nous utiliserons les hypothèses suivantes :

– On admet que le bruit suit une loi normale complexe circulaire multidimensionnelle, de moyenne nulle et de matrice de covariance $\mathbf{\Sigma}_{\text{bruit}}$ connue et supposée de rang plein.

– Le vecteur de paramètres inconnus est défini par $\boldsymbol{\xi} = [\omega\ \phi]^T$ [LC93, Ren07].

La fonction de vraisemblance relative au vecteur des observations $\boldsymbol{\chi} = [\mathbf{y}^T(1)\dots\mathbf{y}^T(T)]^T \sim \mathcal{CN}(\boldsymbol{\mu}(\boldsymbol{\xi}_0), \mathbf{\Sigma}(\boldsymbol{\xi}_0))$ pour un $\boldsymbol{\xi}_0$ donné, s'écrit simplement par :

$$p(\boldsymbol{\chi}|\boldsymbol{\xi}_0) = \frac{1}{\pi^{NT}\det\{\mathbf{\Sigma}(\boldsymbol{\xi}_0)\}} e^{-(\boldsymbol{\chi}-\boldsymbol{\mu}(\boldsymbol{\xi}_0))^H \mathbf{\Sigma}(\boldsymbol{\xi}_0)^{-1}(\boldsymbol{\chi}-\boldsymbol{\mu}(\boldsymbol{\xi}_0))},$$

où $\boldsymbol{\xi}_0, \omega_0, \phi_0$ représentent les vraies valeurs des paramètres candidats $\boldsymbol{\xi}, \omega$ et ϕ, respectivement. Les valeurs de $\boldsymbol{\mu}(\boldsymbol{\xi}_0)$ et $\boldsymbol{\Sigma}(\boldsymbol{\xi}_0)$ seront spécifiées par la suite (selon le modéle déterminisite ou aléatoire).

2.4.1 Expressions Analytiques

Dans [Gla72, FL02, CGQL08, TT10] les auteurs ont proposé une unification de différentes bornes sur l'erreur quadratique moyenne. Plus précisément, s'appuyant sur un problème d'optimisation sous contraintes, Forster et Larzabal [FL02], ont présenté une unification de bornes sur l'erreur quadratique moyenne en imposant des contraintes sur le biais. Ils ont montré, par un choix judicieux de ces contraintes, qu'on pouvait ainsi donner une expression explicite de la borne de Cramér-Rao, la borne de Barankin ou la borne de Battacharya. Notons que l'on peut trouver l'extension des travaux de Forster et Larzabal [FL02] dans le cas de plusieurs paramètres inconnus déterministes dans [CGQL08]. Dans [TT10], Todros et Tabrikian ont proposé une nouvelle classe de bornes sur l'erreur quadratique moyenne en utilisant la transformation intégrale généralisée appliquée à la fonction de vraisemblance. Ainsi, ils ont montré que certaines bornes sur l'erreur quadratique moyenne (par exemple, la borne de Cramér-Rao, la borne de McAulay-Seidman et la borne de Battacharya) sont obtenues par un choix approprié du noyau de la transformation intégrale de la fonction de rapport de vraisemblance.

En utilisant l'une des deux approches, on constate que l'unification s'exprime à l'aide d'une matrice $\boldsymbol{K}$ inversible et d'une matrice $\boldsymbol{\Gamma}$ à valeurs complexes, comme suit :

$$\mathrm{MSE}(\hat{\boldsymbol{\xi}}) = \int_{\mathbb{C}^{NT}} \left(\hat{\boldsymbol{\xi}} - \boldsymbol{\xi}_0\right)\left(\hat{\boldsymbol{\xi}} - \boldsymbol{\xi}_0\right)^T p(\boldsymbol{\chi}|\boldsymbol{\xi}_0) d\boldsymbol{\chi} \succcurlyeq \boldsymbol{C} = \boldsymbol{\Gamma}\boldsymbol{K}^{-1}\boldsymbol{\Gamma}^H \tag{2.30}$$

où $\boldsymbol{K}$ peut être décompsée à l'aide de $\boldsymbol{\gamma}$ comme suit $\boldsymbol{K} = \int_{\mathbb{C}^{NT}} \boldsymbol{\gamma}\boldsymbol{\gamma}^H p(\boldsymbol{\chi}|\boldsymbol{\xi}_0) d\boldsymbol{\chi}$ et où $\hat{\boldsymbol{\xi}}$ est un estimateur du vrai paramètre déterministe $\boldsymbol{\xi}_0$ et où $\boldsymbol{A} \succcurlyeq \boldsymbol{B}$ signifie que la matrice $\boldsymbol{A} - \boldsymbol{B}$ est définie non négative. Par consequent, pour différentes valeurs de $\boldsymbol{\Gamma}$ et de $\boldsymbol{\gamma}$, on aura différentes bornes inférieures de l'erreur quadratique moyenne. La BCR (notée dans cette section $\boldsymbol{C}_{\mathrm{BCR}}$ par souci d'uniformisation) est donnée par le couple :

$$\begin{cases} \boldsymbol{\Gamma}_{\mathrm{BCR}} & = \mathbf{1}_2, \\ \boldsymbol{\gamma}_{\mathrm{BCR}} & = \frac{\partial \ln p(\boldsymbol{x}|\boldsymbol{\xi})}{\partial \boldsymbol{\xi}}|_{\boldsymbol{\xi}=\boldsymbol{\xi}_0}, \end{cases}$$

où $\mathbf{1}_l$ représente le vecteur de dimension $l \in \{1, \ldots, L\}$ rempli de 1. La borne de McAulay-Seidman (BMS) [MS69] peut être définie par le couple suivant :

$$\begin{cases} \boldsymbol{\Gamma}_{\mathrm{BMS}} & = \boldsymbol{\Phi}, \\ \boldsymbol{\gamma}_{\mathrm{BMS}} & = [\nu(\boldsymbol{x}|\boldsymbol{\xi}_1) \ \ldots \ \nu(\boldsymbol{x}|\boldsymbol{\xi}_L)]^T, \end{cases}$$

où $\nu(\boldsymbol{x}|\boldsymbol{\xi}_l) = \frac{p(\boldsymbol{x}|\boldsymbol{\xi}_l)}{p(\boldsymbol{x}|\boldsymbol{\xi}_0)}$, $\boldsymbol{\Phi} = [\boldsymbol{\xi}_1 - \boldsymbol{\xi}_0 \ \ldots \ \boldsymbol{\xi}_L - \boldsymbol{\xi}_0]^T$ avec $\{\boldsymbol{\xi}_1, \ldots, \boldsymbol{\xi}_L\}$ qui représente un ensemble de points test appartenant à $\boldsymbol{\Theta}$. La borne de Hammersley-Chapman-Robbins (BHCR) [Ham50] est, quant à elle, donnée par :

$$\begin{cases} \boldsymbol{\Gamma}_{\mathrm{BHCR}} & = [\mathbf{0}_2 \ \boldsymbol{\Phi}], \\ \boldsymbol{\gamma}_{\mathrm{BHCR}} & = [1 \ \boldsymbol{\gamma}_{\mathrm{BMS}}]^T, \end{cases}$$

où $\mathbf{0}_l$ représente le vecteur de dimension $l \in \{1, \ldots, L\}$ rempli de 0 et enfin la borne de McAulay-Hofstetter (BMH) [MH71] peut être exprimée par :

$$\begin{cases} \boldsymbol{\Gamma}_{\mathrm{BMH}} & = [\boldsymbol{I}_2 \ \boldsymbol{\Phi}], \\ \boldsymbol{\gamma}_{\mathrm{BMH}} & = [\boldsymbol{\gamma}_{\mathrm{BCR}} \ \boldsymbol{\gamma}_{\mathrm{BMS}}]^T, \end{cases}$$

où $\boldsymbol{I}_2$ est la matrice identité d'ordre 2. La borne de Fourier Cramér-Rao (BFCR), récemment proposée [TT10], peut également être écrite sous la forme (2.30). Pour avoir un gain en temps de calcul, cette dernière utilise la transformée de Fourier discrète (TFD) des vecteurs $\boldsymbol{\Phi}$ et $\boldsymbol{\gamma}_{\text{BMS}}$. La TFD peut être obtenue grâce à une multiplication matricielle notée $\boldsymbol{W}$. Ainsi, le couple $(\boldsymbol{\Gamma}, \boldsymbol{\gamma})$ adéquat pour la BFCR est donné par :

$$\begin{cases} \boldsymbol{\Gamma}_{\text{BFCR}} & = [\boldsymbol{I}_2 \ \boldsymbol{\Phi}\boldsymbol{W}^H] \\ \boldsymbol{\gamma}_{\text{BFCR}} & = [\boldsymbol{\gamma}_{\text{BCR}} \ \boldsymbol{\gamma}_{\text{BMS}}\boldsymbol{W}^T]^T. \end{cases} \tag{2.31}$$

où

$$[\boldsymbol{W}]_{p,l} = \exp(-i\boldsymbol{\Omega}_p^T\boldsymbol{\xi}_l) \tag{2.32}$$

représente la matrice de transformation relative à la TFD bi-dimensionelle et $\boldsymbol{\Omega}_p$ s'exprime à l'aide du $p^{ème}$ point test frequentiel $\boldsymbol{f}_p = [f_p \ f'_p]^T$ comme suit : $\boldsymbol{\Omega}_p = \left[\frac{2\pi f_p}{\delta([\boldsymbol{\xi}]_1)L_1} \ \frac{2\pi f'_p}{\delta([\boldsymbol{\xi}]_2)L_2}\right]^T$, avec $L = L_1L_2$, tel que $f_p \in \{1, \ldots, L_1\}$, $f'_p \in \{1, \ldots, L_2\}$, L_i est le nombre de points test associé à la variable $[\boldsymbol{\xi}]_i$ et $\delta([\boldsymbol{\xi}]_i)$ est la distance (constante) entre deux points test associée à la variable $[\boldsymbol{\xi}]_i$, $i = 1, 2$.

Après calcul, on peut montrer que les bornes précitées peuvent être écrites comme suit pour le modèle d'observation sus-mentionné

$$\boldsymbol{C}^{(L)}_{\text{BMS}} = \boldsymbol{\Phi}\boldsymbol{\Psi}^{-1}\boldsymbol{\Phi}^T, \tag{2.33}$$

$$\boldsymbol{C}^{(L)}_{\text{BHCR}} = \boldsymbol{\Phi}\left(\boldsymbol{\Psi} - \mathbf{1}\mathbf{1}^T\right)^{-1}\boldsymbol{\Phi}^T, \tag{2.34}$$

$$\boldsymbol{C}^{(L)}_{\text{BMH}} = \boldsymbol{C}_{\text{BCR}} + \boldsymbol{Q}\boldsymbol{R}^{-1}\boldsymbol{Q}^T, \tag{2.35}$$

$$\boldsymbol{C}^{(L,P)}_{\text{BFCR}} = \boldsymbol{C}_{\text{BCR}} + \boldsymbol{Q}\boldsymbol{W}^H\left(\boldsymbol{W}\boldsymbol{R}\boldsymbol{W}^H\right)^{-1}\boldsymbol{W}\boldsymbol{Q}^T, \tag{2.36}$$

où nous avons introduit la dépendance de ces bornes par rapport aux points test [1] (symboles L et P). Notons $\text{DKL}\left(p(\boldsymbol{x}|\boldsymbol{\xi}_l)||p(\boldsymbol{x}|\boldsymbol{\xi}_0)\right)$, la distance de Kullback-Leibler [Sch91] entre $p(\boldsymbol{x}|\boldsymbol{\xi}_l)$ et $p(\boldsymbol{x}|\boldsymbol{\xi}_0)$. On peut alors définir tous les éléments apparaissant dans (2.33)-(2.36) comme suit :

$$\boldsymbol{Q} = \boldsymbol{C}_{\text{BCR}}\boldsymbol{D} - \boldsymbol{\Phi}, \tag{2.37}$$

tel que

$$\boldsymbol{D} = \left[\boldsymbol{d}(\boldsymbol{\xi}_1) \quad \ldots \quad \boldsymbol{d}(\boldsymbol{\xi}_L)\right],$$

et

$$\boldsymbol{d}(\boldsymbol{\xi}_l) = -\left(\frac{\partial \text{DKL}\left(p(\boldsymbol{x}|\boldsymbol{\xi}_l)||p(\boldsymbol{x}|\boldsymbol{\xi})\right)}{\partial\boldsymbol{\xi}}\right)^T|_{\boldsymbol{\xi}=\boldsymbol{\xi}_0} \tag{2.38}$$

où la dérivée vectorielle est donnée par $\left[\dot{\boldsymbol{\mu}}(\boldsymbol{\xi}_0)\right]_{i,j} = \frac{\partial[\boldsymbol{\mu}(\boldsymbol{\xi})]_i}{\partial[\boldsymbol{\xi}]_j}|_{\boldsymbol{\xi}=\boldsymbol{\xi}_0}$. De plus, la matrice $\boldsymbol{R}$ est donnée par

$$\boldsymbol{R} = \boldsymbol{\Psi} - \boldsymbol{D}^T\boldsymbol{C}_{\text{BCR}}\boldsymbol{D}, \tag{2.39}$$

et les éléments de la matrice $\boldsymbol{\Psi}$ sont définis par

$$[\boldsymbol{\Psi}]_{m,n} = E_{\boldsymbol{\chi}|\boldsymbol{\xi}_0}\left\{v(\boldsymbol{x}, \boldsymbol{\xi}_m)v(\boldsymbol{x}, \boldsymbol{\xi}_n)\right\}, \tag{2.40}$$

1. Notons par ailleurs que les valeurs des points tests qui maximisent les bornes (dites bornes optimales) sont celles où la fonction d'ambiguïté exhibe des maxima locaux [Rendf, RM95, XBR04, RM97, TK99, Xu01, RAFL07]. Cela étant dit, il a été montré que, dans le cas où, les points tests couvrent les extrémités de $\boldsymbol{\Theta}$ et aussi la vraie valeur du paramètre $\boldsymbol{\xi}_0$, alors même si on obtient des bornes en dessous des bornes optimales, la différence est suffisamment faible pour que leur utilisation reste pertinente [Rendf].

où $E_{\boldsymbol{\chi}|\boldsymbol{\xi}_l}\{.\}$ indique l'opérateur d'espérance mathématique relatif à $p(\boldsymbol{\chi}|\boldsymbol{\xi}_l)$.

Sachant que, pour un modèle Gaussien (circulaire) à moyenne paramétrée ou à covariance paramétrée, $\boldsymbol{C}_{\text{BCR}}$ est donné par l'inverse de la MIF (2.6), alors dans la suite nous ne donnerons que l'expression de $\boldsymbol{D}$ et $\boldsymbol{\Psi}$. Ainsi, en utilisant la valeur de $\boldsymbol{D}$ et de $\boldsymbol{\Psi}$ et (2.37) et (2.39), nous obtiendrons $\boldsymbol{C}^{(L)}_{\text{BMS}}$, $\boldsymbol{C}^{(L)}_{\text{BHCR}}$, $\boldsymbol{C}^{(L)}_{\text{BMH}}$ et $\boldsymbol{C}^{(L,P)}_{\text{BFCR}}$ (voir (2.33), (2.34), (2.35) et (2.36).)

Expressions analytiques pour le modèle déterministe

Pour le modèle déterministe, nous avons $\boldsymbol{\chi} \sim \mathcal{CN}(\boldsymbol{\mu}(\boldsymbol{\xi}_0), \boldsymbol{\Sigma}_{\text{bruit}})$ avec

$$\boldsymbol{\mu}(\boldsymbol{\xi}_0) = [s(1)\mathbf{a}^T(\omega_0,\phi_0)\dots s(L)\mathbf{a}^T(\omega_0,\phi_0)]^T,$$

et

$$[\mathbf{FIM}]_{i,k} = 2\Re\left\{\frac{\partial\boldsymbol{\mu}(\boldsymbol{\xi}_0)^H}{\partial[\boldsymbol{\xi}_\mathbf{0}]_i}\boldsymbol{\Sigma}^{-1}_{\text{bruit}}\frac{\partial\boldsymbol{\mu}(\boldsymbol{\xi}_0)}{\partial[\boldsymbol{\xi}_\mathbf{0}]_k}\right\},\ i=1,2,\ k=1,2. \tag{2.41}$$

Notons que :

$$\begin{aligned}
&\text{KLD}\left(p(\boldsymbol{\chi}|\boldsymbol{\xi}_n)||p(\boldsymbol{\chi}|\boldsymbol{\xi})\right) = \int_{\mathbb{C}^{NT}} p(\boldsymbol{\chi}|\boldsymbol{\xi}_n)\text{Ln}\frac{p(\boldsymbol{\chi}|\boldsymbol{\xi}_n)}{p(\boldsymbol{\chi}|\boldsymbol{\xi})}d\boldsymbol{\chi}\\
&= \int_{\mathbb{C}^{NT}}\left[(\boldsymbol{\chi}-\boldsymbol{\mu}(\boldsymbol{\xi}))^H\boldsymbol{\Sigma}^{-1}_{\text{bruit}}(\boldsymbol{\chi}-\boldsymbol{\mu}(\boldsymbol{\xi})) - (\boldsymbol{\chi}-\boldsymbol{\mu}(\boldsymbol{\xi}_n))^H\boldsymbol{\Sigma}^{-1}_{\text{bruit}}(\boldsymbol{\chi}-\boldsymbol{\mu}(\boldsymbol{\xi}_n))\right]p(\boldsymbol{\chi}|\boldsymbol{\xi}_n)d\boldsymbol{\chi}\\
&= \int_{\mathbb{C}^{NT}}\left[\boldsymbol{\chi}^H\boldsymbol{\Sigma}^{-1}_{\text{bruit}}(\boldsymbol{\mu}(\boldsymbol{\xi}_n)-\boldsymbol{\mu}(\boldsymbol{\xi})) - \boldsymbol{\mu}(\boldsymbol{\xi})^H\boldsymbol{\Sigma}^{-1}_{\text{bruit}}(\boldsymbol{\chi}-\boldsymbol{\mu}(\boldsymbol{\xi}))\right]f(\boldsymbol{\chi}|\boldsymbol{\xi}_n)d\boldsymbol{\chi}\\
&= (\boldsymbol{\mu}(\boldsymbol{\xi}_n)-\boldsymbol{\mu}(\boldsymbol{\xi}))^H\boldsymbol{\Sigma}^{-1}_{\text{bruit}}(\boldsymbol{\mu}(\boldsymbol{\xi}_n)-\boldsymbol{\mu}(\boldsymbol{\xi}))\,.
\end{aligned} \tag{2.42}$$

De plus, les éléments de la matrice $\boldsymbol{\Psi}$ peuvent être donnés par :

$$\begin{aligned}
&[\boldsymbol{\Psi}]_{m,n} = \int_{\mathbb{C}^{NT}}\frac{1}{\pi\left|\boldsymbol{\Sigma}_{\text{bruit}}\right|}\exp\left((\boldsymbol{\chi}-\boldsymbol{\mu}(\boldsymbol{\xi}_0))^H\boldsymbol{\Sigma}^{-1}_{\text{bruit}}(\boldsymbol{\chi}-\boldsymbol{\mu}(\boldsymbol{\xi}_0))\right)\times\\
&\exp\left(-(\boldsymbol{\chi}-\boldsymbol{\mu}(\boldsymbol{\xi}_m))^H\boldsymbol{\Sigma}^{-1}_{\text{bruit}}(\boldsymbol{\chi}-\boldsymbol{\mu}(\boldsymbol{\xi}_m)) - (\boldsymbol{\chi}-\boldsymbol{\mu}(\boldsymbol{\xi}_n))^H\boldsymbol{\Sigma}^{-1}_{\text{bruit}}(\boldsymbol{\chi}-\boldsymbol{\mu}(\boldsymbol{\xi}_n))\right)d\boldsymbol{\chi}\\
&= \frac{\alpha(\boldsymbol{\xi}_m,\boldsymbol{\xi}_n)}{\pi\left|\boldsymbol{\Sigma}_{\text{bruit}}\right|}\underbrace{\int_{\mathbb{C}^{NT}}\exp-(\boldsymbol{\chi}-\boldsymbol{\mu}(\boldsymbol{\xi}_m)-\boldsymbol{\mu}(\boldsymbol{\xi}_n)+\boldsymbol{\mu}(\boldsymbol{\xi}_0))^H\boldsymbol{\Sigma}^{-1}_{\text{bruit}}(\boldsymbol{\chi}-\boldsymbol{\mu}(\boldsymbol{\xi}_m)-\boldsymbol{\mu}(\boldsymbol{\xi}_n)+\boldsymbol{\mu}(\boldsymbol{\xi}_0))\,d\boldsymbol{\chi}}_{\pi|\boldsymbol{\Sigma}_{\text{bruit}}|}\\
&= \alpha(\boldsymbol{\xi}_m,\boldsymbol{\xi}_n),
\end{aligned}$$

où

$$\begin{aligned}
\alpha(\boldsymbol{\xi}_m,\boldsymbol{\xi}_n) =& \exp(-2\boldsymbol{\mu}(\boldsymbol{\xi}_0)^H\boldsymbol{\Sigma}^{-1}_{\text{bruit}}\boldsymbol{\mu}(\boldsymbol{\xi}_0) - \boldsymbol{\mu}(\boldsymbol{\xi}_0)^H\boldsymbol{\Sigma}^{-1}_{\text{bruit}}(\boldsymbol{\mu}(\boldsymbol{\xi}_m)+\boldsymbol{\mu}(\boldsymbol{\xi}_n))\\
&+\boldsymbol{\mu}(\boldsymbol{\xi}_m)^H\boldsymbol{\Sigma}^{-1}_{\text{bruit}}(\boldsymbol{\mu}(\boldsymbol{\xi}_n)-\boldsymbol{\mu}(\boldsymbol{\xi}_0)) + \boldsymbol{\mu}(\boldsymbol{\xi}_m)^H\boldsymbol{\Sigma}^{-1}_{\text{bruit}}(\boldsymbol{\mu}(\boldsymbol{\xi}_n)-\boldsymbol{\mu}(\boldsymbol{\xi}_0))).
\end{aligned} \tag{2.43}$$

De ce fait, en utilisant (2.35), (2.34), (2.33) et (2.36), $\boldsymbol{C}^{(L)}_{\text{BMH}}$, $\boldsymbol{C}^{(L)}_{\text{BHCR}}$, $\boldsymbol{C}^{(L)}_{\text{BMS}}$ et $\boldsymbol{C}^{(L,P)}_{\text{BCRF}}$ sont données en remplaçant (2.41), (2.42) et (2.43) dans (2.37) et (2.39).

Expressions analytiques pour le modèle stochastique

Pour le modèle stochastique nous avons $\boldsymbol{\chi} \sim \mathcal{CN}(\mathbf{0}, \boldsymbol{\Sigma}(\boldsymbol{\xi}_0))$ où $\boldsymbol{\Sigma}(\boldsymbol{\xi}_0) = \sigma_s^2\boldsymbol{I}_T\otimes\mathbf{a}(\omega_0,\phi_0)\mathbf{a}^H(\omega_0,\phi_0)+\boldsymbol{\Sigma}_{\text{bruit}}$, avec

$$[\mathbf{FIM}]_{i,k} = T\ \text{tr}\left\{\boldsymbol{\Sigma}(\boldsymbol{\xi}_0)^{-1}\frac{\partial\boldsymbol{\Sigma}(\boldsymbol{\xi}_0)}{\partial[\boldsymbol{\xi}_\mathbf{0}]_i}\boldsymbol{\Sigma}(\boldsymbol{\xi}_0)^{-1}\frac{\partial\boldsymbol{\Sigma}(\boldsymbol{\xi}_0)}{\partial[\boldsymbol{\xi}_\mathbf{0}]_k}\right\},\ i=1,2,\ k=1,2. \tag{2.44}$$

Notons que :

$$\begin{aligned}
&\mathrm{KLD}\left(p(\boldsymbol{\chi}|\boldsymbol{\xi}_n)||p(\boldsymbol{\chi}|\boldsymbol{\xi})\right) = \int_{\mathbb{C}^{NT}} p(\boldsymbol{\chi}|\boldsymbol{\xi}_n)\mathrm{Ln}\frac{p(\boldsymbol{\chi}|\boldsymbol{\xi}_n)}{p(\boldsymbol{\chi}|\boldsymbol{\xi})}d\boldsymbol{\chi} \\
&= \int_{\mathbb{C}^{NT}} \frac{1}{\pi^{NT}\left|\boldsymbol{\Sigma}(\boldsymbol{\xi}_n)\right|}\left(\boldsymbol{\chi}^H\left(\boldsymbol{\Sigma}(\boldsymbol{\xi}_n)^{-1} - \boldsymbol{\Sigma}(\boldsymbol{\xi})^{-1}\right)\boldsymbol{\chi}\right)\exp\left(-\boldsymbol{\chi}^H\boldsymbol{\Sigma}(\boldsymbol{\xi}_n)^{-1}\boldsymbol{\chi}\right)d\boldsymbol{\chi} + \mathrm{Ln}\frac{\left|\boldsymbol{\Sigma}(\boldsymbol{\xi})\right|}{\left|\boldsymbol{\Sigma}(\boldsymbol{\xi}_n)\right|} \\
&= E_{\boldsymbol{\chi}|\boldsymbol{\xi}_n}\left\{\boldsymbol{\chi}^H\boldsymbol{\Sigma}(\boldsymbol{\xi})\boldsymbol{\chi}\right\} + E_{\boldsymbol{\chi}|\boldsymbol{\xi}_n}\left\{\boldsymbol{\chi}^H\boldsymbol{\Sigma}(\boldsymbol{\xi}_n)\boldsymbol{\chi}\right\} + \mathrm{Ln}\frac{\left|\boldsymbol{\Sigma}(\boldsymbol{\xi})\right|}{\left|\boldsymbol{\Sigma}(\boldsymbol{\xi}_n)\right|}. \qquad (2.45)
\end{aligned}$$

Comme

$$E_{\boldsymbol{\chi}|\boldsymbol{\xi}_n}\left\{\boldsymbol{\chi}^H\boldsymbol{\Sigma}(\boldsymbol{\xi})\boldsymbol{\chi}\right\} = \sum_{i=1}^{NT}\sum_{j=1}^{NT} E_{\boldsymbol{\chi}|\boldsymbol{\xi}_n}\left\{[\boldsymbol{\chi}]_i^*[\boldsymbol{\chi}]_j\left[\boldsymbol{\Sigma}(\boldsymbol{\xi})^{-1}\right]_{i,j}\right\} = \mathrm{tr}\left(\boldsymbol{\Sigma}(\boldsymbol{\xi}_n)\boldsymbol{\Sigma}(\boldsymbol{\xi})^{-1}\right) \qquad (2.46)$$

et

$$E_{\boldsymbol{\chi}|\boldsymbol{\xi}_n}\left\{\boldsymbol{\chi}^H\boldsymbol{\Sigma}(\boldsymbol{\xi}_0)^{-1}\boldsymbol{\chi}\right\} = NT. \qquad (2.47)$$

Alors, en remplaçant (2.46) et (2.47) dans (2.45) nous obtenons :

$$\mathrm{KLD}\left(p(\boldsymbol{\chi}|\boldsymbol{\xi}_n)||f(\boldsymbol{\chi}|\boldsymbol{\xi})\right) = \mathrm{Ln}\frac{\left|\boldsymbol{\Sigma}\right|}{\left|\boldsymbol{\Sigma}(\boldsymbol{\xi}_n)\right|} + \mathrm{tr}\left(\boldsymbol{\Sigma}(\boldsymbol{\xi}_n)\boldsymbol{\Sigma}(\boldsymbol{\xi})^{-1}\right) + NT. \qquad (2.48)$$

De plus, on notera que :

$$[\boldsymbol{\Psi}]_{n,m} = \frac{\left|\boldsymbol{\Sigma}(\boldsymbol{\xi}_0)\right|}{\pi^{NT}\left|\boldsymbol{\Sigma}(\boldsymbol{\xi}_m)\right|\left|\boldsymbol{\Sigma}(\boldsymbol{\xi}_n)\right|}\underbrace{\int_{\mathbb{C}^{NT}}\exp\left(-\boldsymbol{\chi}^H\left(\boldsymbol{\Sigma}(\boldsymbol{\xi}_m)^{-1} + \boldsymbol{\Sigma}(\boldsymbol{\xi}_n)^{-1} - \boldsymbol{\Sigma}(\boldsymbol{\xi}_0)^{-1}\right)\boldsymbol{\chi}\right)d\boldsymbol{\chi}}_{\pi^{NT}\left|(\boldsymbol{\Sigma}(\boldsymbol{\xi}_m)^{-1}+\boldsymbol{\Sigma}(\boldsymbol{\xi}_n)^{-1}-\boldsymbol{\Sigma}(\boldsymbol{\xi}_0)^{-1})^{-1}\right|} \qquad (2.49)$$

$$= \frac{\left|\boldsymbol{\Sigma}(\boldsymbol{\xi}_0)\right|}{\left|\boldsymbol{\Sigma}(\boldsymbol{\xi}_m)\right|\left|\boldsymbol{\Sigma}(\boldsymbol{\xi}_n)\right|\left|\boldsymbol{\Sigma}(\boldsymbol{\xi}_m)^{-1} + \boldsymbol{\Sigma}(\boldsymbol{\xi}_n)^{-1} - \boldsymbol{\Sigma}(\boldsymbol{\xi}_0)^{-1}\right|} \qquad (2.50)$$

De ce fait, en utilisant (2.35), (2.34), (2.33),(2.36) et $\frac{\partial \mathrm{Ln}\left|\boldsymbol{\Sigma}(\boldsymbol{\xi})\right|}{\partial \boldsymbol{\xi}} = \mathrm{tr}\left\{\boldsymbol{\Sigma}(\boldsymbol{\xi})^{-1}\frac{\partial\boldsymbol{\Sigma}(\boldsymbol{\xi})}{\partial\boldsymbol{\xi}}\right\}$ [PP06], $\boldsymbol{C}_{\mathrm{BMH}}^{(L)}$, $\boldsymbol{C}_{\mathrm{BHCR}}^{(L)}$, $\boldsymbol{C}_{\mathrm{BMS}}^{(L)}$ et $\boldsymbol{C}_{\mathrm{BCRF}}^{(L,P)}$ sont données en remplaçant (2.41), (2.42) et (2.43) dans (2.37) et (2.39).

2.4.2 Analyse numérique

Pour ces simulations, nous avons considéré une antenne composée de $N = 10$ capteurs avec une distance inter-capteurs $d = \frac{\lambda}{2}$. La source, située dans la région de Fresnel, est repérée par les coordonnées suivantes $(\theta, r) = (30^\circ, 6\lambda)$. On supposera également que $\boldsymbol{\Sigma}_{\mathrm{bruit}} = \sigma^2\boldsymbol{I}$.

Il est à noter que les EQM empiriques de l'estimateur du MVD représentées dans les Fig. 2.3 et 2.4, ont été obtenues avec 1000 tirages de type Monte-Carlo. L'ensemble des points tests utilisés pour la BMS, la BHCR, la BMH et la BFCR est égal à $L = 2^{14}$ (plus précisément, l'ensemble des points test suivant le paramètre ω est fixé à $L_1 = 2^7$, de même que celui par rapport à ϕ qui est donné par $L_2 = 2^7$). La BFCR se calcule aussi en choisissant un ensemble de points de test fréquentiels. A cet effet, et pour garder une complexité de calcul sensiblement égale à la BMS, la BHCR et la BMH, on a choisi deux points tests fréquentiels parmi les 2^{14} maximisant la BFCR.

Pour le modèle déterministe, les Fig. 2.3 et Fig. 2.4 nous montrent les différentes bornes de l'EQM des deux paramètres d'intérêt ω et ϕ. On constate tout d'abord que l'EQM sur ϕ est inférieure à celle sur ω, ce qui était prévisible vue la plage de variation des deux paramètres.

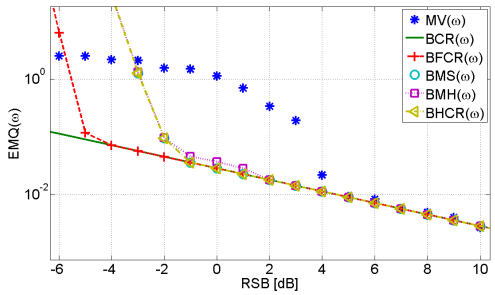

FIGURE 2.3 – Bornes inférieures de l'erreur quadratique moyenne pour le modèle déterministe en fonction de ω pour $(\theta, r) = (30^\circ, 6\lambda)$ et $T = 15$.

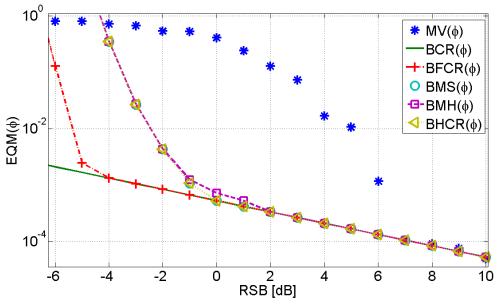

FIGURE 2.4 – Bornes inférieures de l'erreur quadratique moyenne pour le modèle déterministe en fonction de ϕ pour $(\theta, r) = (30^\circ, 6\lambda)$ et $T = 15$.

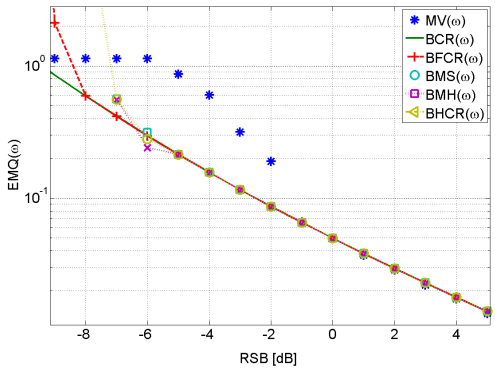

FIGURE 2.5 – Bornes inférieures de l'erreur quadratique moyenne pour le modèle aléatoire en fonction de ω pour $(\theta, r) = (30^\circ, 6\lambda)$ et $T = 100$.

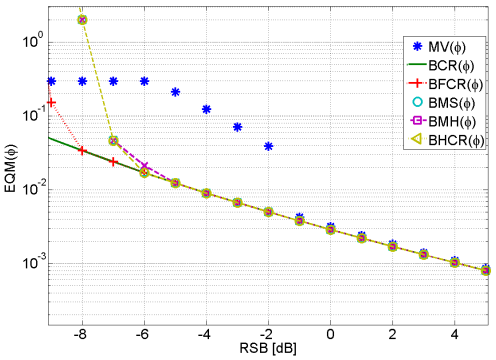

FIGURE 2.6 – Bornes inférieures de l'erreur quadratique moyenne pour le modèle aléatoire en fonction de ϕ pour $(\theta, r) = (30^\circ, 6\lambda)$ et $T = 100$.

De plus, la BMS, la BHCR, la BMH et la BFCR décrivent bien le décrochement du MV. Cela étant dit, on remarque que la BMH est la plus pertinente (prédiction du décrochement à moins de 4 dB), vient ensuite la BHCR et la BMS (prédiction du décrochement à moins de 7 dB). Enfin, la BFCR nous fournit une prédiction du décrochement avoisinant les 10 dBs. Les mêmes conclusions peuvent être déduites pour le modèle aléatoire (voir les Fig. 2.5 et Fig. 2.6.)

De façon générale on constate que la BFCR demeure moins performante que toutes les bornes présentées dans cette contribution. Ceci est dû au fait que la BFCR "comprime" les contraintes en appliquant la TFD. Cette compression de contraintes est à l'origine de la dégradation de cette borne. Ce point n'a pas été mentionné dans [TT10] où la BFCR apparaît comme une borne plus pertinente par rapport à la BMS, BHCR et la BMH dans le cas particulier de l'analyse spectrale. Cela étant dit, il faut noter que la BFCR a été calculée à partir de 2^9 points tests, or les autres bornes (BMS, BHCR et la BMH) ont étés calculées en maximisant seulement 1 point test parmi 2^9. Ceci explique, pourquoi dans [TT10] la BFCR apparaît comme étant plus précise que les autres bornes contrairement à l'exemple traité ici.

Chapitre 3

Seuil de résolution limite en traitement d'antenne

3.1 Introduction

Le seuil statistique de résolution limite (SRL), aussi nommé pouvoir séparateur, c'est-à-dire, la distance minimale entre deux signaux [1] permettant une correcte séparation/estimation des paramètres d'intérêt, est un sujet d'une importance croissante et qui vise diverses applications comme le radar, le sonar, le traitement d'images, analyse spectrale, etc. Pour la formation de voies, le seuil de résolution ne dépend que de l'ouverture de l'antenne [Ste76]. Ainsi, on peut citer la résolution de Fourier et de Rayleigh données respectivement par la largeur du lobe principal de la fonction de directivité et sa largeur à 3 dB [Mar98, Abe06], respectivement. Avec la venue des méthodes à haute résolution, les seuils de la résolution définis par Fourier et Rayleigh ont été repoussés, d'où la nécessité d'introduire de nouveaux critères du seuil statistique de résolution limite.

Dans la littérature on définit/calcule le SRL principalement selon trois familles de critères [Cox73, KB86, Lee92, Lee94, SD95, Dil98, Smi98, SM05a, Smi05, DA06, LN07, FLV08, AW08, AD08, KG09, KBRM11b, KBRM11a, VEB$^+$11, EBRM11a, EBRM11b] :

1. La première famille est basée sur le pseudo-spectre des algorithmes d'estimation (voir figure 3.1.) Si nous supposons, par exemple, que deux signaux sont paramétrés par les directions d'arrivée (DDA) θ_1 et θ_2, alors, le critère de Cox [Cox73] stipule que *les deux signaux sont résolus si les moyennes des valeurs du pseudo-spectre aux points θ_1 et θ_2 sont inférieures à la moyenne de la valeur du pseudo-spectre au point $\frac{\theta_1+\theta_2}{2}$*. Un second critère, basé lui aussi sur le pseudo-spectre, a été proposé par Sharman et Durrani [SD95] et stipule que *les deux signaux sont résolus si la dérivée seconde de la moyenne du pseudo-spectre au point $\frac{\theta_1+\theta_2}{2}$ est négative.*

   A noter qu'il existe une approche dite stochastique pour laquelle on définira une probabilité de résolution. Celle-ci a été peu étudiée en raison de sa difficulté [LW90].

   On remarque bien que cette famille de critères est spécifique aux algorithmes utilisés. Pour plus d'exemples, le lecteur pourra se référer aux références suivantes [Cox73, KB86, SD95, AD08]. Dans la suite, nous présenterons deux autres familles de critères valables pour tout type d'algorithme.

1. Dans la suite, la notion de distance entre deux signaux correspond à la métrique (d, C), tel que $d : C \times C \to \mathbb{R}$ où d et C représentent la distance de Minkowski et l'espace des paramètres d'intérêt des signaux (par exemple, distance entre deux fréquences en analyse spectrale, distance entre deux directions d'arrivées en localisation de sources, etc ...), respectivement.

2. La seconde famille est basée sur un test d'hypothèses binaire [SM05a, LN07, AW08]. L'idée principale consiste à utiliser ces tests d'hypothèses pour décider si un ou deux signaux sont présents. Le but est alors de relier la distance minimale (entre les deux signaux pour un rapport signal à bruit donné) à la probabilité de fausse alarme P_{fa} et/ou à la probabilité de détection P_d. Ainsi, dans [SM05a], Sharman et Milanfar ont considéré le problème du calcul du SRL en analyse spectrale en utilisant le test du rapport de vraisemblance (TRV). Par conséquent, les auteurs ont calculé l'expression du SRL pour une P_{fa} et une P_d données. Dans [LN07], Liu et Nehorai ont défini le seuil de résolution limite angulaire (c'est-à-dire, le SRL par rapport aux DDA) en utilisant le TRV dans sa forme asymptotique en terme de nombre d'observations. A cet effet, les auteurs ont relié l'expression du SRL à la borne de Cramér-Rao. Enfin, on peut trouver dans [AW08] le calcul du SRL par rapport aux fréquences pour des sinusoïdes complexes en utilisant, cette fois ci, l'approche Bayésienne.
3. La troisième famille est basée sur la précision d'estimation des paramètres en terme de variance [Lee92, LL93, Lee94, Smi98, Dil98, Smi05, EBRM10b, KBRM11b, KBRM11a]. Puisque la BCR est une borne inférieure de l'erreur quadratique moyenne, elle exprime ainsi les performances ultimes en terme d'estimation paramétrique. Par conséquent, elle peut être utilisée pour définir/obtenir le SRL. De ce fait, on distingue deux critères *intuitifs* du SRL basés sur la BCR :

   i) Le premier critère a été introduit par Lee en 1992 [Lee92]. Dans un contexte de traitement d'antenne, il stipule que *deux signaux sont correctement résolus par rapport aux DDA, si l'écart type maximale est inférieure à au moins deux fois la différence entre* θ_1 *et* θ_2. Ainsi, et sous certaines conditions de régularité [Leh83], les écarts types $\sigma_{\hat{\theta}_1}$ et $\sigma_{\hat{\theta}_2}$, d'un estimateur non biaisé $\hat{\boldsymbol{\theta}} = [\hat{\theta}_1\ \hat{\theta}_2]^T$ peuvent être approximées par $\sqrt{\mathrm{BCR}(\theta_1)}$ et $\sqrt{\mathrm{BCR}(\theta_2)}$, respectivement. Par conséquent, le SRL est, selon le critère de Lee, égal à $2\max\left\{\sqrt{\mathrm{BCR}(\theta_1)}, \sqrt{\mathrm{BCR}(\theta_2)}\right\}$. Pour des applications se basant sur le critère de Lee, le lecteur pourra se référer à [Lee92, Lee94, Dil98].

   ii) On peut noter que le couplage entre les paramètres est ignoré par ce dernier critère (c'est-à-dire, absence du terme croisé dans la matrice de Cramèr-Rao $\mathrm{BCR}(\theta_1, \theta_2)$). C'est pour cela que Smith [Smi98, Smi05] a introduit un critère qui tient compte de ce couplage entre les paramètres d'intérêt. Ce critère est donné comme suit : *deux signaux sont résolus par rapport aux DDA si la différence entre les DDA,* δ*, est plus grande que l'écart type de la différence de ces DDA*. L'écart type peut être approximée par la BCR (sous certaines conditions de régularité.) Par conséquent, le SRL au sens de Smith peut être défini comme étant $\delta = |\theta_1 - \theta_2|$ pour lequel l'inégalité suivante

   $$\delta < \sqrt{\mathrm{BCR}\,(\delta)}$$

   est atteinte. Par conséquent, le SRL est donné par la solution de l'équation suivante

   $$\delta^2 = \mathrm{BCR}\,(\delta)\,.$$

   Dans [Smi98, Smi05], Smith a calculé le SRL (en terme des DDA) pour deux signaux modélisés par des pôles complexes. Dans [DA06], Delmas et Abeida ont calculé le SRL en terme de DDA suivant le critère de Smith pour des signaux sources discrets modulés en BPSK (*binary phase-shift keying*), QPSK (*quadrature phase-shift keying*) et MSK (*minimum-shift keying.*)

On notera que le SRL basé sur la précision de l'estimation (c'est-à-dire, basé sur la BCR) est un concept intuitif. Dans [LN07], les auteurs ont relié le SRL basé sur un test d'hypothèses à

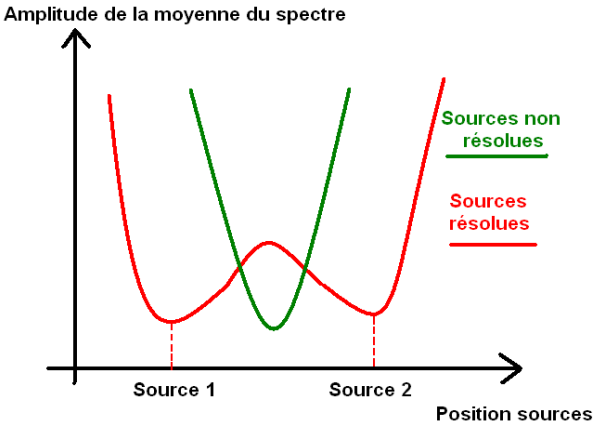

FIGURE 3.1 – Illustration du cas *sources résolues* et *sources non résolues* à l'aide d'un pseudo-spectre d'algorithme d'estimation.

celui basé sur la BCR (plus particulièrement celui basé sur le critère de Smith). Ainsi, et pour un grand nombre d'observations, les auteurs ont montré que le SRL basé sur un test d'hypothèses binaire peut être écrit comme la solution de l'équation suivante [LN07, eq. 9]

$$\delta^2 = \lambda \, \mathrm{BCR}\left(\delta\right),$$

où λ est un facteur de translation exprimé en fonction de P_{fa} et P_d.

A noter qu'il existe deux autres critères moins utilisés dans la littérature. Le premier est basé sur le critère d'information d'Akaike (CIA). Dans [SSS95] les auteurs ont relié la fonction relative au CIA à la séparation δ. Un autre critère est basé sur l'application du lemme de Stein permettant ainsi de relier la distance de Kullback-Leibler à la séparation δ [VEB+11]

La première partie de ce chapitre est consacrée au calcul du SRL pour la localisation de sources polarisées (voir, section 3.2.1) et pour la localisation de sources en présence des interférences (voir, section 3.2.2) qui sont des applications pour lesquelles aucun résultat n'était disponible dans la littérature. Notre but initial était de continuer l'étude des performances proposée au chaptire 2, à savoir la localisation de sources en champs proche. Lors du calcul du SRL dans le contexte champ proche (c'est-à-dire, deux paramètres d'intérêt par source qui sont la distance et la DDA), nous avons constaté que tous les critères susmentionnés ont été introduits dans le cas d'un seul paramètre d'intérêt par signal. Toutefois, dans de nombreux problèmes d'estimation, les signaux sont paramétrés par plus d'un paramètre d'intérêt par signal. On peut citer les problèmes liés au cas Multiple-Input Multiple-Output (MIMO) [God97, THL+01, GS05, STWT06, NS09] ou dans le cadre général des problèmes d'harmoniques multidimensionnelles [JStB01, MSPM04], etc. A cet effet, dans la section 3.3 nous avons proposé un critère du SRL pour des signaux multidimensionnels, nommé SRLM. Ainsi que le calcul du SRLM pour les modèles suivants : modèle harmonique multidimensionnel, le radar MIMO mais aussi la localisation de sources en champ proche.

3.2 Seuil de résolution limite pour des signaux monodimensionnels

Dans cette section, nous présenterons deux exemples applicatifs du calcul du SRL pour des signaux monodimensionels, c'est-à-dire, des signaux comportant un seul paramètre d'intérêt par source. Dans la section 3.2.1, nous allons tout d'abord étudier le problème de localisation de sources polarisées situées dans le champ lointain. Puis, dans la section 3.2.2, nous présenterons un résultat du calcul du SRL pour le problème de localisation de sources en champ lointain en présence d'interférences structurées.

Dans ce qui suit, nous ne citerons que les principaux résultats. Le lecteur trouvera les détails calculatoires ainsi qu'une analyse théorique et numérique plus approfondie dans l'**Annexe B.1** (M. N. El Korso, R. Boyer, A. Renaux and S. Marcos, *"Statistical Resolution Limit of the Uniform Linear Cocentered Orthogonal Loop and Dipole Array"*, *IEEE* Transactions on Signal Processing, Volume : 59, Issue : 1, Jan 2011, pp. 425-431) et l'**Annexe B.2** (M. N. El Korso, R. Boyer, A. Renaux and S. Marcos, *"On the Statistical Resolvability Of Point Sources in Subspace Interference Using a GLRT-Based Framework"*, soumis à *Elsevier* Signal Processing).

3.2.1 Seuil de résolution limite pour la localisation de sources polarisées

Modèle des observations

Considérons une antenne linéaire uniforme de type COLD (cocentered orthogonal loop and dipole array) notée ALU-COLD composée de N capteurs ; où chaque capteur est formé d'une boucle et d'un dipôle. Cette ALU-COLD reçoit deux signaux provenant de deux sources émettrices. Le signal observé par le $\ell^{ème}$ capteur à la $t^{ème}$ observation est donnée par [LC91, LSZ96]

$$\boldsymbol{y}_\ell(t) = \begin{bmatrix} y_{\mathrm{b}}(t) & y_{\mathrm{d}}(t) \end{bmatrix}^T = \sum_{m=1}^{2} \alpha_m(t)\mathbf{u}_m e^{j\ell\omega_m} + \boldsymbol{v}_\ell(t), \tag{3.1}$$

où $\ell = 0 \dots N-1$ et $t = 1 \dots T$ avec T représentant le nombre d'observations. Notons $\omega_m = \frac{2\pi}{\lambda} d \sin(\theta_m)$ l'angle électrique où θ_m, d et λ représentent l'azimut de la $m^{ème}$ source, l'espacement inter-capteur et la longueur d'onde, respectivement. Les deux signaux sources sont modélisés par $\alpha_m(t) = a_m e^{j(2\pi f_0 t + \phi_m(t))}$ où a_m est l'amplitude du signal (non nulle), $\phi_m(t)$ la phase du signal et f_0 la fréquence porteuse du signal. Le bruit additif sera noté $\boldsymbol{v}_\ell(t) = \begin{bmatrix} v_{\mathrm{b}}(t) & v_{\mathrm{d}}(t) \end{bmatrix}^T$. Le vecteur de polarisation $\mathbf{u}_m$ est donné par

$$\mathbf{u}_m = \begin{bmatrix} \frac{2j\pi A_{sl}}{\lambda} \cos(\rho_m) \\ -L_{sd} \sin(\rho_m) e^{j\psi_m} \end{bmatrix}, \tag{3.2}$$

où $\rho_m \in [0, \pi/2]$ et $\psi_m \in [-\pi, \pi]$ sont les paramètres de polarisation.

Par conséquent, la forme vectorielle du modèle des observations à la $t^{ème}$ observation est donné par :

$$\boldsymbol{y}(t) = \begin{bmatrix} \boldsymbol{y}_0^T(t) & \dots & \boldsymbol{y}_{N-1}^T(t) \end{bmatrix}^T = \sum_{m=1}^{2} \mathbf{A}_m(t)\mathbf{a}_m + \begin{bmatrix} \boldsymbol{v}_0^T(t) & \dots & \boldsymbol{v}_{N-1}^T(t) \end{bmatrix}^T, \tag{3.3}$$

où $\mathbf{A}_m(t) = \mathbf{I}_L \otimes (\alpha_m(t)\mathbf{u}_m)$. Le vecteur directionnel est défini par $\mathbf{a}_m = \begin{bmatrix} 1 & e^{j\omega_m} & \dots & e^{j(N-1)\omega_m} \end{bmatrix}^T$. Dans la suite de cette section, nous ferons les hypothèses suivantes :

- Le bruit est supposé complexe circulaire blanc Gaussien de moyenne nulle et de variance inconnue σ^2.

– Les signaux sources sont supposés connus [2] et déterministes [LC93,LHSV95,CM97,Ren07]. Le vecteur de paramètres inconnus est alors donné par $\boldsymbol{\xi} = [\omega_1\ \omega_2\ \sigma^2]^T$.
– Afin de simplifier les calculs, et sans perte de généralité, on supposera $L_{sd} = \frac{2\pi A_{sl}}{\lambda} = 1$ [LSZ96] et $w_1 > w_2$.

Après calcul (application de (2.6) puis inversion de la MIF), on trouve :

$$\mathrm{BCR}(\omega_1) = \frac{\sigma^2}{2N}\frac{a_2^2\alpha}{a_1^2a_2^2\alpha^2 - \Re^2\{r_T\mathbf{u}_1^H\mathbf{u}_2\eta\}}, \tag{3.4}$$

$$\mathrm{BCR}(\omega_2) = \frac{\sigma^2}{2N}\frac{a_1^2\alpha}{a_1^2a_2^2\alpha^2 - \Re^2\{r_T\mathbf{u}_1^H\mathbf{u}_2\eta\}}, \tag{3.5}$$

$$\mathrm{BCR}(\omega_1,\omega_2) = -\frac{\sigma^2}{2N}\frac{\Re\{r_T\mathbf{u}_1^H\mathbf{u}_2\eta\}}{a_1^2a_2^2\alpha^2 - \Re^2\{r_T\mathbf{u}_1^H\mathbf{u}_2\eta\}}. \tag{3.6}$$

où $\alpha = \frac{1}{6}(N-1)N(2N-1)$, $r_T = \frac{1}{T}\sum_{t=1}^{T}\alpha_1^*(t)\alpha_2(t)$ et

$$\eta = \sum_{\ell=0}^{L-1}\ell^2 e^{-j(\omega_1-\omega_2)\ell} = \sum_{\ell=0}^{L-1}\ell^2 e^{-j\mathrm{sgn}(\omega_1-\omega_2)\delta_\omega^{(\mathrm{COLD})}\ell},$$

avec $\delta_\omega^{(\mathrm{COLD})} = \omega_1 - \omega_2$.

Calcul du SRL

Notons $\delta_\omega^{(\mathrm{COLD})}$ le SRL associé au modèle (3.3) qui est donné par le critère de Smith [Smi05] comme suit :

$$\delta_\omega^{(\mathrm{COLD})} = \sqrt{\mathrm{BCR}(\delta_\omega^{(\mathrm{COLD})})} \Longleftrightarrow f(\delta_\omega^{(\mathrm{COLD})}) = \left(a_1^2 + a_2^2\right)\alpha, \tag{3.7}$$

où dans notre cas $f(\delta_\omega^{(\mathrm{COLD})}) = \frac{2}{\sigma^2T^2}\left(a_1^2a_2^2\alpha^2 - \Re^2\{r_T\mathbf{u}_1^H\mathbf{u}_2\eta\}\right)\left(\left(\delta_\omega^{(\mathrm{COLD})}\right)^2 + 2\mathrm{BCR}(\omega_1,\omega_2)\right)$ et

$$\mathrm{BCR}(\delta_\omega^{(\mathrm{COLD})}) = \mathrm{BCR}(\omega_1) + \mathrm{BCR}(\omega_2) - 2\mathrm{BCR}(\omega_1,\omega_2). \tag{3.8}$$

Par conséquent, en utilisant (3.4-3.6) et après calcul on obtient :

i) Le SRL, solution de l'équation implicite (3.7), pour des signaux sources orthogonaux (c'est-à-dire, $r_T = \frac{1}{T}\sum_{t=1}^{T}\alpha_1^*(t)\alpha_2(t) = 0$ [LC93]), est donné par

$$\delta_\omega^{(\mathrm{COLD-O})} = \frac{\sigma}{\sqrt{2T\alpha}}\sqrt{\frac{a_1^2 + a_2^2}{a_1^2a_2^2}}. \tag{3.9}$$

Enfin, dans le cas de deux signaux sources ayant la même puissance (c'est-à-dire, $a_1 = a_2 = a$), on obtient

$$\delta_\omega^{(\mathrm{COLD-O})} = \frac{1}{\sqrt{T\alpha\mathrm{RSB}}}, \tag{3.10}$$

où $\mathrm{RSB} = a^2/\sigma^2$. Ce résultat est qualitativement équivalent à celui trouvé dans [DA06, AW08] pour des sources non polarisées.

2. Le lecteur notera que le SRL pour des signaux sources connus est sensiblement égal à celui des signaux sources inconnues, pour plus de détails voir l'**Annexe B.1**.

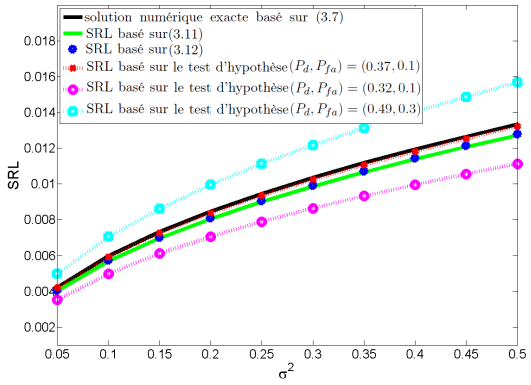

FIGURE 3.2 – Le SRL en fonction de σ^2 pour $T = 100$ observations : Le SRL basé sur l'équation (3.11) et (3.12) est sensiblement égal à la solution numérique exacte basée sur (3.7). Ceci valide nos expressions du SRL. De plus, on note que, par exemple, pour $P_d = 0.37$ et $P_{fa} = 0.1$, le SRL basé sur le critère de Smith est sensiblement égal au SRL calculé en utilisant le test d'hypothèse (voir **Annexe B.1**). Les courbes correspondant à $(P_d, P_{fa}) = (0.49, 0.3)$ et $(P_d, P_{fa}) = (0.32, 0.1)$, nous montrent l'influence du facteur de translation sur le SRL.

ii) Le SRL, solution implicite de l'équation (3.7) pour des signaux sources non-orthogonaux (c'est-à-dire, $r_T \neq 0$), est donné par :

$$\delta_\omega^{(\mathrm{COLD})} = \alpha \sqrt{\frac{a_1^2 a_2^2 - \Re^2\{r_T \mathbf{u}_1^H \mathbf{u}_2\}}{2\beta \Im\{r_T \mathbf{u}_1^H \mathbf{u}_2\}} \left(1 - \sqrt{1 - \frac{2\sigma^2 \beta \Im\{r_T \mathbf{u}_1^H \mathbf{u}_2\}}{\alpha T} \frac{\left((a_1^2 + a_2^2) + 2\Re\{r_T \mathbf{u}_1^H \mathbf{u}_2\}\right)}{(\Re^2\{r_T \mathbf{u}_1^H \mathbf{u}_2\} - a_1^2 a_2^2)^2}}\right)}, \tag{3.11}$$

où $\beta = \sum_{\ell=0}^{N-1} \ell^3 = \frac{1}{4}(N-1)^2 N^2$. Pour un grand nombre d'observations (voir, Fig. 3.2), on peut exprimer le SRL par

$$\delta_\omega^{(\mathrm{COLD})} = \frac{\sigma}{\sqrt{2T\alpha}} \sqrt{\frac{a_1^2 + a_2^2 + 2\Re\{r_T \mathbf{u}_1^H \mathbf{u}_2\}}{a_1^2 a_2^2 - \Re^2\{r_T \mathbf{u}_1^H \mathbf{u}_2\}}}. \tag{3.12}$$

Remarquons, que dans ce cas, le SRL est fonction des paramètres de polarisation. De plus, dans le cas de signaux sources ayant la même puissance, on obtient :

$$\delta_\omega^{(\mathrm{COLD})} = \frac{1}{\sqrt{T\alpha \mathrm{RSB}}} \sqrt{\frac{1 + \Re\{\tilde{r}_T \mathbf{u}_1^H \mathbf{u}_2\}}{1 - \Re^2\{\tilde{r}_T \mathbf{u}_1^H \mathbf{u}_2\}}}, \tag{3.13}$$

où $\tilde{r}_T = \frac{1}{T} \sum_{t=1}^{T} e^{j(\phi_2(t) - \phi_1(t))}$.

Analyses numériques

Dans ce qui suit, nous allons comparer le SRL pour des sources polarisées à celui des sources non-polarisées. Par un calcul analogue à celui de la section 3.2.1, on obtient le SRL pour des

sources non-polarisées :

$$\delta_\omega^{(\mathrm{ALU})} = \frac{\sigma}{\sqrt{2T\alpha}}\sqrt{\frac{a_1^2+a_2^2+2\Re\{r_T\}}{a_1^2a_2^2-\Re^2\{r_T\}}}. \tag{3.14}$$

i) On remarque d'après (3.9) et (3.14) que le SRL pour des signaux sources orthogonaux (c'est-à-dire $r_T = 0$ [LC93]) et polarisées est égale au SRL pour des signaux sources orthogonaux non-polarisées. Par conséquent, la polarisation n'apporte aucune amélioration du SRL pour des signaux sources orthogonaux.

ii) Intéressons nous maintenant aux signaux sources non orthogonaux. De (3.12) et (3.14), on peut vérifier que

$$\delta_\omega^{(\mathrm{COLD})} \leq \delta_\omega^{(\mathrm{ALU})} \quad \text{ssi} \quad \Re\{r_T\} \geq \Re\{r_T\mathbf{u}_1^H\mathbf{u}_2\}. \tag{3.15}$$

De plus, comme $\Re\{r_T\mathbf{u}_1^H\mathbf{u}_2\} = \Re\{r_T\}\Re\{\mathbf{u}_1^H\mathbf{u}_2\} - \Im\{r_T\}\Im\{\mathbf{u}_1^H\mathbf{u}_2\}$ et $\Re\{\mathbf{u}_1^H\mathbf{u}_2\} \leq 1$, la condition (3.15) est satisfaite pour $\Im\{r_T\} = 0$ et/ou pour $\Im\{\mathbf{u}_1^H\mathbf{u}_2\} = 0$. Par conséquent, $\delta_\omega^{(\mathrm{COLD})} < \delta_\omega^{(\mathrm{ALU})}$ pour les trois cas suivants :

C1. si les signaux sources sont réels et positifs, c'est-à-dire, $\Im\{r_T\} = 0$ ou à phase commune, c'est-à-dire, $\phi_1(t) = \phi_2(t), \forall t$.

C2. si $\psi_1 = \psi_2$, c'est-à-dire, $\Im\{\mathbf{u}_1^H\mathbf{u}_2\} = 0$.

C3. si $\rho_1 = 0$ ou $\rho_2 = 0$, c'est-à-dire, $\Im\{\mathbf{u}_1^H\mathbf{u}_2\} = 0$.

Les conditions **C1.**, **C2.** et **C3.** sont des conditions suffisantes pour avoir $\delta_\omega^{(\mathrm{COLD})} < \delta_\omega^{(\mathrm{ALU})}$. Afin d'étudier les autres cas, on a tracé dans la Fig. 3.3 la variable $D(r_L, \mathbf{u}_1^H\mathbf{u}_2) = \Re\{r_T\} - \Re\{r_T\mathbf{u}_1^H\mathbf{u}_2\}$ en fonction des paramètres de polarisation ρ et ψ. On constate que si $D > 0$ alors $\delta_\omega^{(\mathrm{COLD})} < \delta_\omega^{(\mathrm{ALU})}$. La Fig. 3.3 montre qu'en général $\delta_\omega^{(\mathrm{COLD})} < \delta_\omega^{(\mathrm{ALU})}$ et que $\delta_\omega^{(\mathrm{COLD})} > \delta_\omega^{(\mathrm{ALU})}$ seulement pour une petite région (celle qui correspond à la partie inférieure délimitée par le plan horizontal.) Cela signifie, que généralement, le SRL est amélioré grâce aux paramètres de polarisation pour des signaux sources non-orthogonaux.

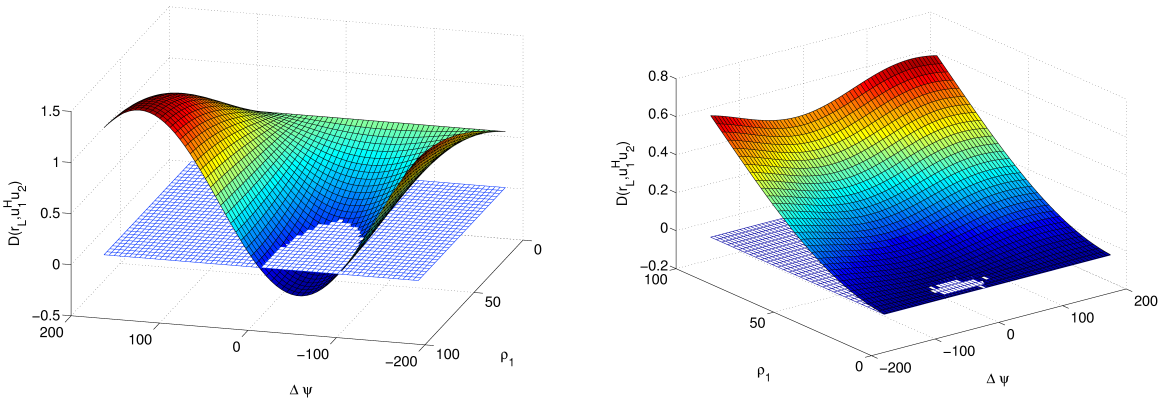

FIGURE 3.3 – $D(r_L, \mathbf{u}_1^H\mathbf{u}_2)$ en fonction des paramètres de polarisation ρ et ψ ; $a_1 = 2$, $a_2 = 3$, $r_T = \frac{1+i}{20}$ avec $N = 20$. (à gauche) $\rho_2 = 85$ deg et (à droite) $\rho_2 = 5$ deg.

3.2.2 Seuil de résolution limite pour des sources en présence d'interférences

Dans cette section, nous allons calculer le SRL pour des sources en champ lointain. Contrairement aux précédents travaux sur le SRL [SM04, SM05a, LN07, AW08], dans ce contexte nous

considérons un modèle plus riche incluant la présence de sources interférences. En effet, nous considérons le problème du calcul du SRL pour deux sources d'intérêt (notées $\boldsymbol{s}_1$ et $\boldsymbol{s}_2$) noyées dans un sous-espace des interférences engendré par des sources de nuisance (voir, Fig. 3.4).

Modèle des observations

Considérons une antenne linéaire non uniforme (ALNU) avec N capteurs, qui reçoit un signal émis par M sources se situant dans le champ lointain $\{s_1(t), \ldots, s_M(t)\}$ (M étant supposé connu ou précédemment estimé [Van68]). Le signal observé à la $t^{ème}$ observation par rapport au $n^{ème}$ capteur est donné par [KV96]

$$y_n(t) = \sum_{m=1}^{M} s_m(t) \exp(j\omega_m d_n) + v_n(t), \quad t = 1, \ldots, T, \quad n = 0, \ldots, N-1, \tag{3.16}$$

où T représente le nombre d'observations, $\omega_m = -2\pi \sin(\theta_m)/\nu$ le paramètre d'intérêt de la $m^{ème}$ source avec θ_m et ν qui représentent l'angle d'arrivée et la longueur d'onde. Dans la suite, on notera d_n la distance entre le premier capteur et le $n^{ème}$ capteur. Le bruit additif $v_n(t)$ est supposé complexe circulaire Gaussien de moyenne nulle et de variance σ^2. La forme vectorielle des observations à la $t^{ème}$ observation est donnée par

$$\boldsymbol{y}(t) = \begin{bmatrix} y_0(t) & \ldots & y_{N-1}(t) \end{bmatrix}^T = \begin{bmatrix} \boldsymbol{a}_1 & \ldots & \boldsymbol{a}_M \end{bmatrix} \breve{\boldsymbol{s}}(t) + \boldsymbol{v}(t), \tag{3.17}$$

où $\boldsymbol{v}(t) = [v_0(t) \ldots v_{N-1}(t)]^T$, $\breve{\boldsymbol{s}}(t) = [s_1(t) \ \ldots \ s_M(t)]^T$ et $[\boldsymbol{a}_m]_{n+1} = \exp(j\omega_m d_n)$, $m = 1, 2, \ldots, M$. Par conséquent, le vecteur des observations complet est donné par

$$\boldsymbol{y} \triangleq \begin{bmatrix} \boldsymbol{y}^T(1) & \boldsymbol{y}^T(2) & \ldots & \boldsymbol{y}^T(T) \end{bmatrix}^T. \tag{3.18}$$

Dans la suite nous nous proposons de calculer le SRL, δ, dans le contexte de la localisation de sources en présence des interférences (voir, Fig. 3.4). A cet effet, nous supposons que :

- Les deux sources d'intérêt (SDI) sont notées $\boldsymbol{s}_1$ et $\boldsymbol{s}_2$ (avec $\boldsymbol{s}_1 \neq \boldsymbol{s}_2$). Par conséquent, le SRL (c'est-à-dire, la séparation) est défini par $\delta \triangleq \omega_2 - \omega_1$.
- Le sous-espace des interférences (SI) [BS94] est représenté par les $M-2$ sources restantes $\{\boldsymbol{s}_3, \ldots, \boldsymbol{s}_M\}$. Chaque paire de sources est considérée comme largement espacée. Une condition suffisante est que la séparation minimale sur l'ensemble de la combinaison des paires de sources des interférences, notée Δ_ω, doit vérifier $\Delta_\omega > \delta$.

Pour calculer le SRL nous utilisons le critère basé sur le test d'hypothèses. L'hypothèse $\mathcal{H}_0$ représente le cas où les deux SDI sont combinées en un seul signal, alors que l'hypothèse $\mathcal{H}_1$ incarne la situation où les deux SDI sont résolues.

$$\begin{cases} \mathcal{H}_0 : & \delta = 0, \\ \mathcal{H}_1 : & \delta \neq 0. \end{cases} \tag{3.19}$$

La séparation δ est un paramètre inconnu, donc, il est impossible de concevoir un test de détection du type Neyman-Pearson. L'alternative la plus utilisée en traitement du signal est alors l'utilisation du test du rapport de vraisemblance gènéralisé (TRV) [Kay98] dont la statistique est donnée par :

$$G(\boldsymbol{y}) = \frac{\max_{\delta, \boldsymbol{\rho}_1} p(\boldsymbol{y}|\delta, \boldsymbol{\rho}_1, \mathcal{H}_1)}{\max_{\boldsymbol{\rho}_0} p(\boldsymbol{y}|\boldsymbol{\rho}_0, \mathcal{H}_0)} = \frac{p(\boldsymbol{y}|\hat{\delta}, \hat{\boldsymbol{\rho}}_1, \mathcal{H}_1)}{p(\boldsymbol{y}|\hat{\boldsymbol{\rho}}_0, \mathcal{H}_0)} \underset{\mathcal{H}_0}{\overset{\mathcal{H}_1}{\gtrless}} \eta', \tag{3.20}$$

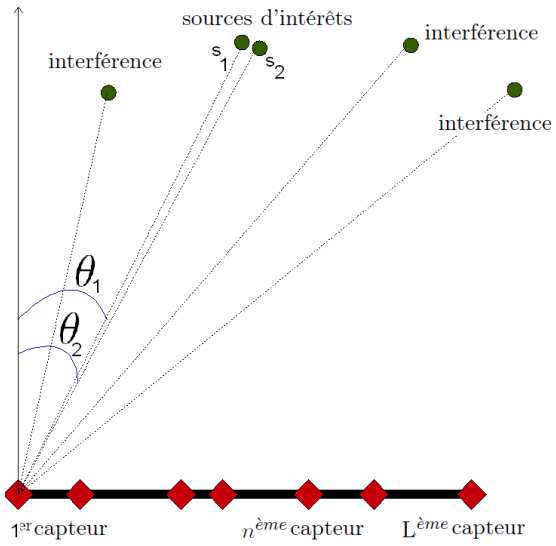

FIGURE 3.4 – Deux SDI proches noyées dans les interférences formées par 3 sources de nuisance.

où $p(\boldsymbol{y}|\boldsymbol{\rho}_0, \mathcal{H}_0)$ et $p(\boldsymbol{y}|\delta, \boldsymbol{\rho}_1, \mathcal{H}_1)$ représentent la densité de probabilité des observations sous $\mathcal{H}_0$ et $\mathcal{H}_1$, respectivement, et où η', $\hat{\delta}$ et $\hat{\boldsymbol{\rho}}_i$ sont le seuil de détection, l'estimation du maximum de vraisemblance de δ sous $\mathcal{H}_1$ et le l'estimation du maximum de vraisemblance du vecteur $\boldsymbol{\rho}_i$ (qui contient tous les paramètres de nuisance) sous $\mathcal{H}_i, i = 0, 1$. Malheureusement, la solution analytique relative au test (3.20) par rapport à δ n'existe pas à cause de la non-linéarité du modèle des observations [SM04, Van68, Van02, OVSN93]. De ce fait, nous proposons d'approximer le modèle d'observation en nous basant sur l'hypothèse que δ est proche de zéro (cette hypothèse est soutenue par le fait que les algorithmes à haute résolution ont, asymptotiquement, un pouvoir de résolution infini [Van02].) Par conséquent, le modèle approché (à l'aide d'un développement limité à l'ordre 1 en $\delta = 0$, tel que $\omega_1 = \omega_c - \frac{\delta}{2}$ et $\omega_2 = \omega_c + \frac{\delta}{2}$) s'écrit :

$$\boldsymbol{y} = \boldsymbol{A}\boldsymbol{s}_+ + \delta \boldsymbol{B}\boldsymbol{s}_- + \boldsymbol{e} + \boldsymbol{v}, \tag{3.21}$$

où $\boldsymbol{e} = \boldsymbol{C}\boldsymbol{s}$. La matrice $\boldsymbol{C}$ supposée connue ou précédemment estimée [Beh90] est donnée par $\boldsymbol{C} = [\boldsymbol{A}_3 \ \ldots \ \boldsymbol{A}_M]$, $\boldsymbol{s} = [\boldsymbol{s}_3^T \ \ldots \ \boldsymbol{s}_M^T]^T$, et

$$\boldsymbol{s}_+ = \boldsymbol{s}_1 + \boldsymbol{s}_2, \tag{3.22}$$

$$\boldsymbol{s}_- = \boldsymbol{s}_2 - \boldsymbol{s}_1, \tag{3.23}$$

avec $\boldsymbol{s}_i = [s_i(1) \ \ldots \ s_i(T)]^T$. $\boldsymbol{d} = [d_0 \ d_1 \ \ldots \ d_{N-1}]^T$ et $\boldsymbol{a}$ représente le vecteur directionnel par rapport au paramètre $\omega_c = \frac{\omega_1 + \omega_2}{2}$ supposé connu [LN07] ou précédemment estimé [SM05a] (c'est-à-dire, $[\boldsymbol{a}]_{n+1} \triangleq \exp(j\omega_c d_n)$, $n = 0, \ldots, N-1$). On définit aussi

$$\boldsymbol{A} \triangleq \begin{bmatrix} \boldsymbol{a} & & \boldsymbol{0} \\ & \ddots & \\ \boldsymbol{0} & & \boldsymbol{a} \end{bmatrix}_{(NT)\times T} = \boldsymbol{I}_T \otimes \boldsymbol{a}, \tag{3.24}$$

$$\boldsymbol{B} \triangleq \frac{j}{2}\boldsymbol{I}_T \otimes \dot{\boldsymbol{a}}, \quad \text{avec} \quad \dot{\boldsymbol{a}} \triangleq \boldsymbol{a} \odot \boldsymbol{d}, \tag{3.25}$$

$$\boldsymbol{A}_m \triangleq \boldsymbol{I}_T \otimes \boldsymbol{a}_m, \quad \text{pour } m = 3, \ldots, M. \tag{3.26}$$

Le modèle (3.21) étant linéaire en δ, nous pouvons alors calculer le SRL.

Calcul du SRL

La relation entre le SRL et le RSBI-RSB requis pour résoudre deux SDI pour différents cas (SDI connue ou inconnue, SI connu ou inconnu avec variance du bruit connue ou inconnue) est représenté dans le tableau 3.1 où on a défini $\boldsymbol{w} = \boldsymbol{B}\boldsymbol{s}_-$ et $\boldsymbol{D} = [\boldsymbol{A}\ \boldsymbol{C}]$ avec le rapport signal à bruit et le rapport signal à bruit plus les interférences défini par RSB $\triangleq \frac{\sum_{m=1}^{2}||\boldsymbol{s}_m||^2}{\sigma^2}$ et RSBI $\triangleq \frac{\sum_{m=1}^{2}||\boldsymbol{s}_m||^2}{\|\boldsymbol{s}\|^2+\sigma^2}$, respectivement. δ_i et λ_i, $i = 1, \ldots, 4$, représentent le SRL et le facteur de translation pour le $i^{ème}$ cas, respectivement. La loi du chi2 centré avec i degrés de liberté est désignée par χ_i^2 et la loi du F centrée avec i_1 et i_2 degrés de liberté est notée F_{i_1,i_2}. Le paramètre de translation λ_1 est estimé numériquement comme solution de $Q^{-1}_{\chi_1^2}(P_{fa}) = Q^{-1}_{\chi_1^2(\lambda_1)}(P_d)$, où $Q^{-1}_{\chi_1^2}(.)$ est la fonction inverse de $Q_{\chi_1^2}(.)$ qui désigne la surface de la queue de distribution à droite de la loi χ_1^2. De même on définit λ_2, λ_3 et λ_4 comme solution de $Q^{-1}_{\chi_1^2}(P_{fa}) = Q^{-1}_{\chi_1^2(\lambda_2)}(P_d)$, $Q^{-1}_{\chi_{2T}^2}(P_{fa}) = Q^{-1}_{\chi_{2T}^2(\lambda_3)}(P_d)$, et $Q^{-1}_{F_{2L,2(N-M)T}}(P_{fa}) = Q^{-1}_{2L,2(N-M)T(\lambda_4)}(P_d)$, respectivement. Le lecteur trouvera les détails calculatoires dans l'**Annexe B.2**, ainsi que certaines expressions du SRL pour des cas particuliers (par exemple, sources orthogonales, sans présence des interférences, relations avec les BCRs adéquates, etc.)

	SDI	SI	Variance du bruit	RSBI pour $M \geq 2$	RSB pour $M = 2$
Cas 1	connue	connu	connue	$\frac{\|\boldsymbol{s}_1\|^2+\|\boldsymbol{s}_2\|^2}{\|\boldsymbol{s}\|^2+\frac{2}{\lambda_1}\delta_1^2\|\boldsymbol{w}\|^2}$	$\lambda_1\frac{\|\boldsymbol{s}_1\|^2+\|\boldsymbol{s}_2\|^2}{2\delta_1^2\|\boldsymbol{w}\|^2}$
Cas 2	connue	inconnu	connue	$\frac{\|\boldsymbol{s}_1\|^2+\|\boldsymbol{s}_2\|^2}{\|\boldsymbol{s}\|^2+\frac{2}{\lambda_2}\delta_2^2\|\boldsymbol{P}_{\boldsymbol{C}}^{\perp}\boldsymbol{w}\|^2}$	$\lambda_2\frac{\|\boldsymbol{s}_1\|^2+\|\boldsymbol{s}_2\|^2}{2\delta_2^2\|\boldsymbol{w}\|^2}$
Cas 3	inconnue	inconnu	connue	$\frac{\|\boldsymbol{s}_1\|^2+\|\boldsymbol{s}_2\|^2}{\|\boldsymbol{s}\|^2+\frac{2}{\lambda_3}\delta_3^2\|\boldsymbol{P}_{\boldsymbol{D}}^{\perp}\boldsymbol{w}\|^2}$	$\lambda_3\frac{\|\boldsymbol{s}_1\|^2+\|\boldsymbol{s}_2\|^2}{2\delta_3^2\|\boldsymbol{P}_{\boldsymbol{A}}^{\perp}\boldsymbol{w}\|^2}$
Cas 4	inconnue	inconnu	inconnue	$\frac{\|\boldsymbol{s}_1\|^2+\|\boldsymbol{s}_2\|^2}{\|\boldsymbol{s}\|^2+\frac{2}{\lambda_4}\delta_4^2\|\boldsymbol{P}_{\boldsymbol{D}}^{\perp}\boldsymbol{w}\|^2}$	$\lambda_4\frac{\|\boldsymbol{s}_1\|^2+\|\boldsymbol{s}_2\|^2}{2\delta_4^2\|\boldsymbol{P}_{\boldsymbol{A}}^{\perp}\boldsymbol{w}\|^2}$

TABLE 3.1 – La relation entre le SRL et le RSBI/RSB requis pour résoudre deux SDI.

La Fig. 3.5 représente le RSBI en fonction du SRL pour les différents cas (avec $T = 100$ observations, $\nu = 0.5m$ et $(P_{fa}, P_d) = (0.01, 0.99)$.) Nous remarquons que la différence entre le cas 1 et le cas 2 (10 dB) est due au projecteur orthogonal sur l'espace des interférences $\boldsymbol{P}_{\boldsymbol{C}}^{\perp}$. De même la différence entre le cas 2 et le cas 3 (25 dB) est due principalement au projecteur orthogonal sur l'espace engendré par la direction centrale ω_c et les interférences présente dans $\boldsymbol{P}_{\boldsymbol{D}}^{\perp}$. Enfin, la différence entre le cas 3 et le cas 4 est minime (0.5 dB) et est seulement due au paramètre de translation λ_4. En conclusion, les différences des RSBIs et donc des SRLs sont principalement dues

- à l'effet des sous espaces des interférences ($\langle\boldsymbol{C}\rangle$ et $\langle\boldsymbol{D}\rangle$),
- et, avec un degré moindre, au facteur de translation λ_i.

De plus, dans l'**Annexe B.2**, le lecteur trouvera la démonstration permettant de comparer les 4 cas cités dans le tableau 3.1, c'est-à-dire, pour le même SRL, nous avons démontré que

$$\text{RSBI}_1 \leq \text{RSBI}_2 \leq \text{RSBI}_3 \leq \text{RSBI}_4.$$

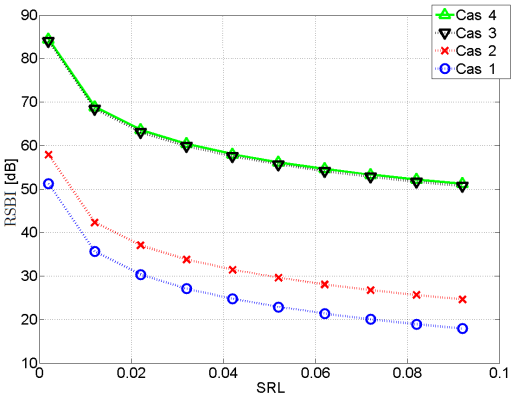

FIGURE 3.5 – RSBI en fonction du SRL pour des sources en champ lointain en présence d'interférences.

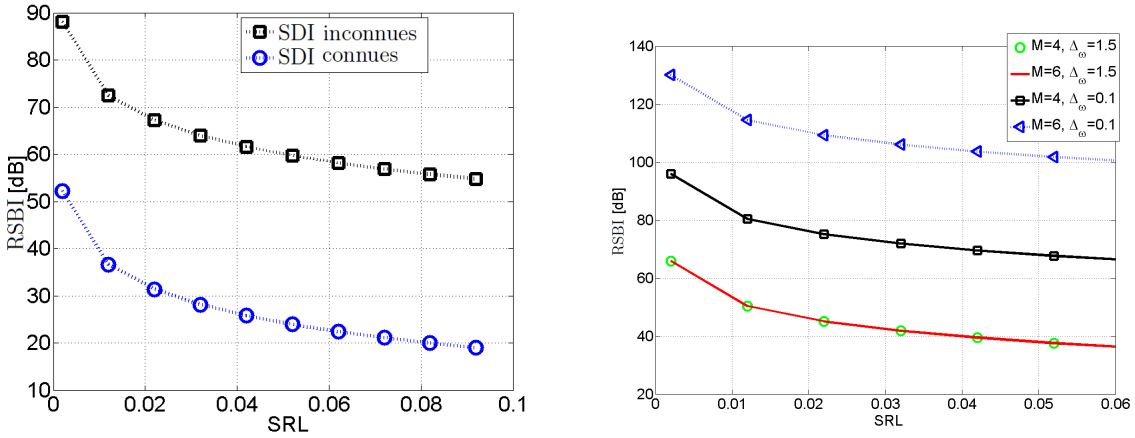

FIGURE 3.6 – *(à gauche)* Le RSBI requis pour résoudre deux SDI connues/inconnues pour une ALU avec $N = 10$ capteurs, $d = \frac{\nu}{2}$ et $M = 4$ avec $\Delta_\omega = 0.75$. *(à droite)* Le RSBI requis pour résoudre deux SDI inconnues pour une ALU avec $N = 10$ capteurs, $d = \frac{\nu}{2}$ et pour différentes valeurs de M et de Δ_ω.

Simulations numériques

Cette section est consacrée à l'analyse numérique du RBSI en fonction du SRL. Le nombre d'observations est fixé à $T = 100$ avec $\nu = 0.5m$ et $(P_{fa}, P_d) = (0.01, 0.99)$. Nous constatons que le RSBI (ou par équivalence le SRL) est affecté par :

- *la connaissance a priori des signaux sources :* en effet, on constate que la connaissance a priori des sources a un fort impact sur le SRL évalué approximativement à 40 dB (voir, Fig. 3.6*(à gauche)*),
- *les sources des interférences :* de la Fig. 3.6*(à droite)* nous constatons que les sources des interférences additionnelles n'ont aucun effet si elles sont bien espacées, c'est-à-dire, si $\Delta_\omega \gg \delta$. Par contre si Δ_ω est de l'ordre de δ alors la dégradation du SRL est évalué à 30 dB.
- *L'orthogonalité des sources* améliore aussi le SRL. De la Fig. 3.7 nous constatons que le gain apporté par l'orthogonalité est approximativement égal à 3 dB,

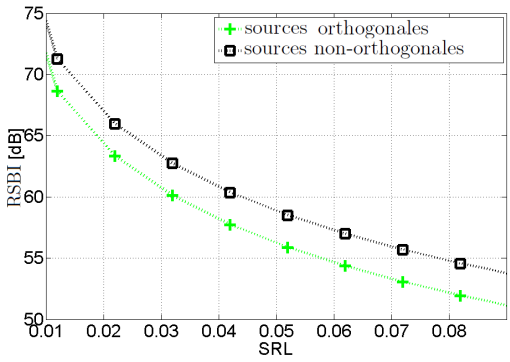

FIGURE 3.7 – Le RSBI requis pour résoudre deux sources du type BPSK inconnues orthogonales/non-orthogonales pour une ALU avec $N = 10$ capteurs, $d = \frac{\nu}{2}$ et $M = 4$.

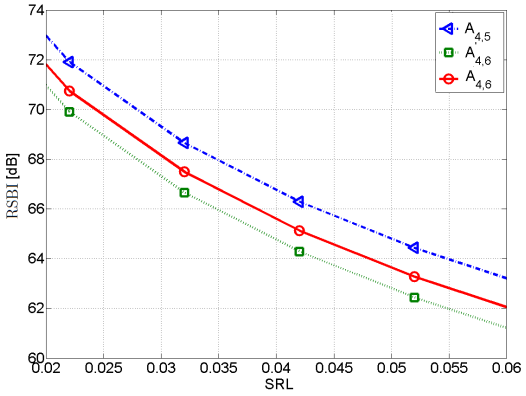

FIGURE 3.8 – Le RSBI requis pour résoudre deux sources connues à l'aide d'une antenne parfaite $A_{4,6}$, une antenne quelconque $A'_{4,6}$ et une antenne à minimum de redondance $A_{4,5}$ décrites au tableau 3.2.

– *la géométrie d'antenne :* dans le tableau 3.2, nous avons présenté certaines géométries d'antenne linéaire pour $N = 4$ capteurs. D'après les simulations de la Fig. 3.8, nous remarquons que l'ouverture d'antenne (c'est-à-dire, l'ajout d'une distance d) produit un gain de 2 dB par rapport au SRL. D'un autre côté, nous constatons que le SRL est sensiblement le même pour différentes géométries d'antennes avec le même nombre de capteur et la même ouverture d'antenne (une différence de seulement 1 dB).

3.3 Seuil de résolution limite pour des signaux multidimensionnels

Après avoir traité dans les sections 3.2.1 et 3.2.2 le SRL dans le cas monodimensionnel, dans cette section, nous nous intéressons au seuil statistique de résolution limite pour des signaux multidimensionnels (SRLM). Nous rappelons que le seuil de résolution limite basé sur l'approche par la borne de Cramér-Rao n'était introduit que dans le cas monodimensionnel. Pour ce faire, nous allons tout d'abord introduire un critère du SRLM basé sur l'extension du critère de Smith. En deuxième lieu, nous montrerons que le critère proposé est asymptotiquement équivalent (à

Configuration	Position des capteurs	ouverture	distance redondante	Écart manquant
Antenne parfaite $A_{4,6}$	$[0,1,4,6]$	$6d$	$R=\{\}$	$G=\{\}$
Antenne quelconque $A'_{4,6}$	$[0,1,2,6]$	$6d$	$R=\{1\}$	$G=\{3\}$
Antenne à minimum de redondance $A_{4,5}$	$[0,1,2,5]$	$5d$	$R=\{1\}$	$G=\{\}$

TABLE 3.2 – Caractéristique des différentes géométries d'antennes avec le même nombre de capteurs et des ouvertures différentes. L'antenne parfaite ne contient pas de redondance et aucun écart n'est manquant. La position des capteurs traduit leur coordonnées sur l'axe des abscisses. L'unité, d, correspond à l'écart minimal entre deux capteurs successifs. L'écart entre deux capteurs est donc un multiple de d qui doit être compris entre d et $(L-1)d$. Une distance redondante se traduit par la répétition d'un écart [VH86]. Un écart manquant est dû à l'absence d'un écart entre d et $(L-1)d$ [Mof68]. Une antenne est dite parfaite, si aucun écart n'est manquant et si aucune distance n'est redondante [AGGS96, ASG99, MD01].

un facteur de translation près) à un test UPP (uniformément le plus puissant). Enfin, nous donnerons quelques exemples applicatifs (modèle harmonique multidimensionnel, radar MIMO mais aussi le SRLM dans le contexte de la localisation de sources en champ proche).

Dans ce qui suit, nous ne citerons que les principaux résultats. Le lecteur trouvera le détail calculatoire, ainsi qu'une analyse théorique et numérique plus approfondie dans l'**Annexe C.1** concernant le critère du SRLM (M. N. El Korso, R. Boyer, A. Renaux and S. Marcos, "Statistical resolution limits for multiple parameters of interest and for multiple signals", in Proc. of *IEEE International Conference on Acoustics, Speech, and Signal Processing, ICASSP-10*, Dallas, TX, USA), dans l'**Annexe C.2** concernant l'analyse du critère du SRLM (M. N. El Korso, R. Boyer, A. Renaux and S. Marcos, " A GLRT-based framework for the multidimensional statistical resolution limit", Proc. in Workshop on Statistical Signal Processing *SSP-11*, Nice, France), dans les **Annexes C.3** à **C.5** pour quelques applications du SRLM (M. N. El Korso, R. Boyer, A. Renaux and S. Marcos, "Statistical Resolution Limit for the Multidimensional Harmonic Retrieval Model : Hypothesis Test and Cramer-Rao Bound Approaches", accepté, *EURASIP* Journal on Advances in Signal Processing, special issue on "Advances in Angle-of-Arrival and Multidimensional Signal Processing for Localization and Communications"),(M. N. El Korso, R. Boyer, A. Renaux and S. Marcos, "Statistical Resolution Limit for Source Localization With Clutter Interference in a MIMO radar Context", soumis à *IEEE* Transactions on Signal Processing),(M. N. El Korso, R. Boyer, A. Renaux and S. Marcos, "A Statistical Analysis of Achievable Resolution Limit in the Near Field Context Using Nonuniform and Lacunar Array", soumis à *IEEE* Transactions on Signal Processing).

3.3.1 Modèle d'observation

Dans ce qui suit nous allons utiliser un modèle d'observation généré par deux signaux sources avec P paramètres d'intérêt par signal. Le modèle d'observation est structuré sous forme vectorielle comme suit :

$$\mathbf{y} = \boldsymbol{f}(\boldsymbol{\xi}_1) + \boldsymbol{f}(\boldsymbol{\xi}_2) + \mathbf{v}, \tag{3.27}$$

où $\mathbf{y} \in \mathbb{R}^N$ et $\mathbf{v} \in \mathbb{R}^N$ représentent respectivement le vecteur d'observation[3] et le vecteur bruit avec une densité de probabilité connue. Le vecteur de paramètres inconnu est donné par $\boldsymbol{\xi}_m \subseteq \mathbb{R}^{P+q_m}$, $m = 1, 2$ avec $q_1 + q_2 = Q$ où q_m représente la dimension des paramètres de nuisance par signal. Nous supposerons aussi que le modèle (3.27) est identifiable et que la matrice d'information de Fisher existe et est inversible. Nous pouvons rassembler tous les paramètres dans un vecteur $\tilde{\boldsymbol{\xi}} = \left[\boldsymbol{\xi}_1^T \boldsymbol{\xi}_2^T\right]^T \in \mathbb{R}^{2P+Q}$. En réarrangeant les élements du vecteur $\tilde{\boldsymbol{\xi}}$, nous obtenons $\boldsymbol{\xi} = \left[\boldsymbol{\omega}^T \ \boldsymbol{\rho}^T\right]^T$ où $\boldsymbol{\omega} \in \mathbb{R}^{2P}$ et $\boldsymbol{\rho} \in \mathbb{R}^Q$ représentent, respectivement, le vecteur des paramètres d'intérêt, et le vecteur des paramètres de nuisance.

3.3.2 Extension du seuil de résolution limite au cas multidimensionnel

Critère du SRLM

Dans ce qui suit nous allons considérer les hypothèses suivantes :

- **A1.** Les éléments du vecteur $\boldsymbol{\omega}$ sont de la même nature, c'est-à-dire, les paramètres d'intérêt ont la même unité de mesure (par exemple des fréquences).
- **A2.** Chaque $p^{ème}$ paramètre, noté $\omega_1^{(p)}$, correspondant à la première source, peut être aussi proche que possible du $p^{ème}$ paramètre, $\omega_2^{(p)}$, correspondant à la deuxième source, mais jamais égal. Cette hypothèse est fréquemment utilisée pour les signaux multidimensionnels, car l'événement $\omega_1^{(p)} = \omega_2^{(p)}$ est considéré comme ayant une probabilité quasi-nulle [GS05, p74].

Sous ces hypothèses (à noter que ces hypothèses peuvent être relaxées, pour plus de détails voir l'**Appendice C.1**), nous proposons le critère du SRLM comme suit

Le SRLM, noté δ, pour le modèle (3.27) est donné comme la solution implicite de l'équation suivante

$$\delta^2 = BCR\left(\delta\right) \tag{3.28}$$

avec

$$\delta = \sum_{p=1}^{P} \delta_p, \tag{3.29}$$

où δ_p représente le SRL dit "local" qui est donné par $\delta_p \triangleq \left|\omega_2^{(p)} - \omega_1^{(p)}\right|$.

Après calcul, nous obtenons le résultat suivant :

Théorème 5 *Le SRLM pour le modèle (3.27) à P paramètres d'intérêt par signal est donné par δ, qui représente la solution implicite de l'équation suivante :*

$$\delta^2 - A_{\text{direct}} - A_{\text{croisé}} = 0, \tag{3.30}$$

où A_{direct} représente la contribution des termes directs (c'est-à-dire, par rapport au même paramètre p)

$$A_{\text{direct}} = \sum_{p=1}^{P} \left[BCR(\omega_1^{(p)}) + BCR(\omega_2^{(p)}) - 2BCR(\omega_1^{(p)}, \omega_2^{(p)})\right], \tag{3.31}$$

3. Si les observations sont complexes, alors le vecteur d'observation (3.27) sera formé par la concaténation de la partie réelle et de la partie imaginaire des observations complexes. De ce fait, l'étude proposée dans la suite de la section reste valide.

et où $A_{\text{croisé}}$ *représente la contribution des termes croisés (entre le* $p^{éme}$ *paramétre et le* $p'^{éme}$ *paramétre) qui est donnée par*

$$A_{\text{croisé}} = \sum_{p=1}^{P} \sum_{\substack{p'=1 \\ p' \neq p}}^{P} g_p g_{p'} \left(BCR(\omega_1^{(p)}, \omega_1^{(p')}) + BCR(\omega_2^{(p)}, \omega_2^{(p')}) - 2BCR(\omega_1^{(p)}, \omega_2^{(p')}) \right), \quad (3.32)$$

avec $g_p = sgn\left(\omega_1^{(p)} - \omega_2^{(p)}\right)$.

Le critère précédemment introduit est un critère intuitif car il est basé sur le critère de Smith. Dans la section suivante, nous allons l'analyser et prouver que ce dernier est asymptotiquement équivalent (à un facteur de translation près) à un test d'hypothèses UPP (uniformément le plus puissant.)

Analyse du critère du SRLM

Pour analyser le SRLM nous nous replaçons dans le cadre d'un test d'hypothèses [SM05a, LN07, AW08]. Plus précisément, l'hypothèse $\mathcal{H}_0$ représente le cas où les deux sources d'intérêt (SDI) sont combinées en un seul signal (c'est-à-dire, $\forall p \in [1 \dots P]$, $\omega_1^{(p)} = \omega_2^{(p)}$), alors que l'hypothèse $\mathcal{H}_1$ incarne la situation où les deux SDI sont résolues (c'est-à-dire, $\exists p \in [1 \dots P]$, $\omega_1^{(p)} \neq \omega_2^{(p)}$) :

$$\begin{cases} \mathcal{H}_0 : & \delta_{\text{detection}} = 0, \\ \mathcal{H}_1 : & \delta_{\text{detection}} > 0, \end{cases} \quad (3.33)$$

où $\delta_{\text{detection}}$ représente la distance entre C_1 et C_2 avec $C_q = \left\{\omega_q^{(1)}, \omega_q^{(2)}, \dots, \omega_q^{(P)}\right\}$, $q = 1, 2$. Par conséquent, la mesure naturelle est celle de Minkowski à l'ordre 1 qui est donnée comme suit :

$$\delta_{\text{detection}} \triangleq \sum_{p=1}^{P} \left| \omega_2^{(p)} - \omega_1^{(p)} \right|. \quad (3.34)$$

Comme dans le cas monodimensionnel, la distance $\delta_{\text{detection}}$ est un paramètre inconnu, donc, il est impossible de concevoir un test de détection du type Neyman-Pearson. L'alternative la plus utilisée en traitement du signal est alors l'utilisation du test du rapport de vraisemblance (TRV) [Kay98] dont la statistique est donnée par :

$$\begin{aligned} L_G(\mathbf{y}) &= \frac{\max_{\delta_{\text{detection}}, \boldsymbol{\rho}_1} \; p(\mathbf{y}|\delta_{\text{detection}}, \boldsymbol{\rho}_1, \mathcal{H}_1)}{\max_{\boldsymbol{\rho}_0} \; p(\mathbf{y}|\boldsymbol{\rho}_0, \mathcal{H}_0)} \\ &= \frac{p(\mathbf{y}|\hat{\delta}_{\text{detection}}, \hat{\boldsymbol{\rho}}_1, \mathcal{H}_1)}{p(\mathbf{y}|\hat{\boldsymbol{\rho}}_0, \mathcal{H}_0)} \underset{\mathcal{H}_0}{\overset{\mathcal{H}_1}{\gtrless}} \varsigma', \end{aligned} \quad (3.35)$$

où $p(\mathbf{y}|\boldsymbol{\rho}_0, \mathcal{H}_0)$ et $p(\mathbf{y}|\delta, \boldsymbol{\rho}_1, \mathcal{H}_1)$ représentent la densité de probabilité des observations sous $\mathcal{H}_0$ et $\mathcal{H}_1$, respectivement, et où ς', $\hat{\delta}_{\text{detection}}$ et $\hat{\boldsymbol{\rho}}_i$ sont le seuil de détection, l'estimation du maximum de vraisemblance de $\delta_{\text{detection}}$ sous $\mathcal{H}_1$ et l'estimation du maximum de vraisemblance du vecteur $\boldsymbol{\rho}_i$ (qui contient tous les paramètres de nuisance) sous $\mathcal{H}_i, i = 0, 1$. Pour simplifier les calculs, nous considérons la statistique équivalente à (3.35) :

$$T_G(\mathbf{y}) = \text{Ln } L_G(\mathbf{y}) \underset{\mathcal{H}_0}{\overset{\mathcal{H}_1}{\gtrless}} \varsigma = \text{Ln}\varsigma'. \quad (3.36)$$

Malheureusement, la solution analytique relative au test (3.36) n'existe généralement pas [SM04, Van68, Van02, OVSN93]. Par conséquent, nous considérerons le cas asymptotique (en terme d'observations [LN07]). Dans [Kay98, eq (6C.1)], l'auteur a démontré (pour un grand nombre d'observations) que la statistique $T_G(\mathbf{y})$ suivait les lois de probabilité suivantes :

$$T_G(\mathbf{y}) \sim \begin{cases} \chi_1^2 & \text{sous } \mathcal{H}_0 \\ \chi_1^2(\kappa'(P_{fa}, P_d)) & \text{sous } \mathcal{H}_1 \end{cases} \tag{3.37}$$

où P_{fa} et P_d représentent, respectivement, la probabilité de fausse alarme et la probabilité de détection par rapport au test (3.33). Supposons que $\mathrm{BCR}(\delta_{\text{detection}})$ existe (voir les hypothèses **A.1** et **A.2**), le paramètre de décentrage $\kappa'(P_{fa}, P_d)$ [Kay98, p.239] est alors donné par

$$\kappa'(P_{fa}, P_d) = \delta^2_{\text{detection}} \left(\mathrm{BCR}(\delta_{\text{detection}})\right)^{-1}. \tag{3.38}$$

D'un autre côté, le paramètre de décentrage peut être évalué à l'aide de P_{fa} et P_d [Sch91,LN07] comme solution de l'équation suivante :

$$Q^{-1}_{\chi_1^2}(P_{fa}) = Q^{-1}_{\chi_1^2(\kappa'(P_{fa},P_d))}(P_d), \tag{3.39}$$

où $Q^{-1}_{\chi_1^2}(P_{fa})$ et $Q^{-1}_{\chi_1^2(\kappa'(P_{fa},P_d))}(P_d)$ sont, respectivement, les fonctions inverses de $Q_{\chi_1^2}(.)$ et $Q_{\chi_1^2(\kappa'(P_{fa},P_d))}(.)$ qui désignent la surface de la queue de distribution à droite des lois χ_1^2 et $\chi_1^2(\kappa'(P_{fa}, P_d))$.

En combinant, (3.38) et (3.39) nous obtenons

$$\delta_{\text{detection}} = \kappa(P_{fa}, P_d)\sqrt{\mathrm{BCR}(\delta_{\text{detection}})}, \tag{3.40}$$

où le facteur de translation est donné par $\kappa(P_{fa}, P_d) = \sqrt{\kappa'(P_{fa}, P_d)}$ (voir, Fig. 3.9).

Il est intéressant de noter que le test d'hypothèses (3.33) est un test binaire unilatéral et que l'estimateur du MV utilisé est sans contrainte. Ainsi, on peut en déduire que le TRV, utilisé pour déterminer le SRLM, est [Leh83, Sch91, Kay98] : *i*) asymptotiquement UPP, et *ii*) a un taux de fausse alarme asymptotiquement constant.

Par conséquent, de (3.28) et (3.40), nous tirons le résultat suivant :

Théorème 6 *Le SRLM, donné en (3.28), basé sur l'extension du critère de Smith est asymptotiquement équivalent (à un facteur de translation près) à un test d'hypothèses UPP (3.33).*

Enfin, de (3.40) on note que le SRLM basé sur l'extension de Smith est exactement égal au SRLM basé sur le test d'hypothèses (3.33) pour toute valeur de P_{fa} et P_d vérifiant $\kappa(P_{fa}, P_d) = 1$ (voir, Fig. 3.9)

3.3.3 Applications aux modèles harmoniques multidimensionnels

Modèle d'observation

Dans cette section, nous appliquons le critère énoncé dans la section précédente au calcul du SRLM pour le modèle multidimensionnel harmonique, à deux sources et à P paramètres d'intérêt par source. Ce modèle très général peut être ainsi utilisé dans plusieurs applications, par exemple, la localisation de sources sous marines acoustiques [WZ97], le sondage de canal sans fil [MSPM04, STWT06], la localisation de sources en champ proche [EBRM09], la localisation

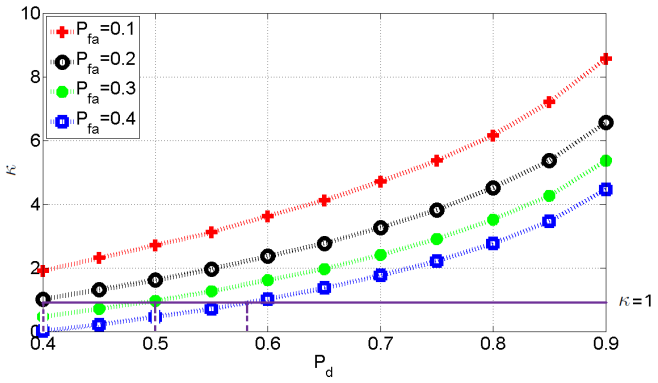

FIGURE 3.9 – Le facteur de translation κ en fonction de la probabilité de fausse alarme P_{fa} et la probabilité de détection P_d. On peut remarquer qu'augmenter P_d ou diminuer P_{fa} a pour effet d'augmenter la valeur du facteur de translation κ (ce qui est normal, puisque ceci correspond à un test d'hypothèses plus sélectif [Sch91, Kay98].

des cibles multiples dans un système radar MIMO [NS09] etc. Le modèle multidimensionnel harmonique est donné par [HN98, PMB04, GS05, RHG07, Boy08, NS10] :

$$[\boldsymbol{\mathcal{Y}}(t)]_{n_1,\ldots,n_P} = [\boldsymbol{\mathcal{X}}(t)]_{n_1,\ldots,n_P} + [\boldsymbol{\mathcal{V}}(t)]_{n_1,\ldots,n_P}, \quad t = 1,\ldots,T, \quad \text{et} \quad n_p = 0,\ldots,N_p-1, \quad (3.41)$$

où les tenseurs $\boldsymbol{\mathcal{Y}}(t)$, $\boldsymbol{\mathcal{X}}(t)$ et $\boldsymbol{\mathcal{V}}(t)$ représentent les observations bruitées, les observations non bruitées et le bruit additif. Le nombre d'observations et le nombre de capteurs dans chaque vecteur sont notés T et $(N_1,\ldots,N_P)$, respectivement. Plus précisément, les observations pour le modèle multidimensionnel harmonique non bruitées sont données par [PMB04, HN98, RHG07, Boy08] :

$$[\boldsymbol{\mathcal{X}}(t)]_{n_1,\ldots,n_P} = \sum_{m=1}^{2} s_m(t) \prod_{p=1}^{P} e^{j\omega_m^{(p)} n_p}, \quad (3.42)$$

où $\omega_m^{(p)}$ et $s_m(t)$ sont la $m^{ème}$ fréquence le long de la $p^{ème}$ dimension et le $m^{ème}$ signal source, respectivement. Le signal source est supposé de la forme $s_m(t) = \alpha_m(t)e^{j\phi_m(t)}$ où $\alpha_m(t)$ et $\phi_m(t)$ représentent l'amplitude réelle et la phase du $m^{ème}$ signal source à la $t^{ème}$ observation, respectivement. Afin de simplifier les expressions, nous supposerons que le bruit est un processus aléatoire blanc, complexe circulaire, Gaussien de moyenne nulle et de variance inconnue σ^2. De plus, les signaux sources sont supposés connus et orthogonaux [LC93, NS09].

Le calcul du SRLM

En utilisant les hypothèses énoncées à la section 3.3.3, le vecteur de paramètres inconnus est alors donné par

$$\boldsymbol{\xi} = \begin{bmatrix} \boldsymbol{\omega}^T & \sigma^2 \end{bmatrix}^T, \quad (3.43)$$

où

$$\boldsymbol{\omega} = \begin{bmatrix} \left(\boldsymbol{\omega}^{(1)}\right)^T & \ldots & \left(\boldsymbol{\omega}^{(P)}\right)^T \end{bmatrix}^T,$$

avec

$$\boldsymbol{\omega}^{(p)} = \begin{bmatrix} \omega_1^{(p)} & \omega_2^{(p)} \end{bmatrix}^T. \quad (3.44)$$

Afin d'appliquer (3.40) nous commençons par calculer la BCR. Rappelons, qu'à notre connaissance, aucune expression analytique non matricielle de la BCR pour le modèle (3.41) n'est disponible dans la littérature. Après calculs, nous obtenons le résultat énoncé dans le théorème suivant :

Théorème 7 *La BCR pour le modèle harmonique multidimensionnel à P paramètres d'intérêt par source, sous l'hypothèse d'orthogonalité des signaux sources, pour le paramètre $\omega_m^{(p)}$ est donné par*

$$BCR(\omega_m^{(p)}) = \frac{6}{TNRSB_m} C_p, \quad m \in \{1, 2\}, \tag{3.45}$$

où $N = \prod_{p=1}^{P} N_p$, $RSB_m = \frac{\|\boldsymbol{\alpha}_m\|^2}{\sigma^2}$ représente le rapport signal à bruit de la $m^{ème}$ source et où

$$C_p = \frac{N_p(1 - 3V_P) + 3V_P + 1}{(N_p + 1)(N_p^2 - 1)} \quad avec \quad V_P = \frac{1}{1 + 3\sum_{p=1}^{P} \frac{N_p - 1}{N_p + 1}}.$$

De plus, les termes croisés sont donnés par

$$BCR(\omega_m^{(p)}, \omega_{m'}^{(p')}) = \begin{cases} 0 & pour\ m \neq m', \\ \frac{-6}{TNRSB_m} \tilde{C}_{p,p'} & pour\ m = m'\ et\ p \neq p', \end{cases} \tag{3.46}$$

où

$$\tilde{C}_{p,p'} = \frac{3V_P}{(N_p + 1)(N_{p'} + 1)}.$$

En remplaçant (3.45) et (3.46) dans (3.30), nous obtenons le SRLM pour le modèle (3.41)

Théorème 8 *Le SRLM pour le modèle harmonique multidimensionnel à P paramètres d'intérêt par source, sous l'hypothèse d'orthogonalité des signaux sources, est donné par*

$$\delta = \sqrt{\frac{6}{TNRSB_E} \left(\sum_{p=1}^{P} C_p - \sum_{\substack{p,\, p' = 1 \\ p \neq p'}}^{P} g_p g_{p'} \tilde{C}_{p,p'} \right)}, \tag{3.47}$$

où le RSB étendu est donné par $RSB_E = \frac{RSB_1 RSB_2}{RSB_1 + RSB_2}$ avec $g_p = sgn\left(\omega_1^{(p)} - \omega_2^{(p)}\right)$.

Analyse numérique du SRLM

- Tout d'abord, de la Fig. 3.10 notons que la solution numérique du SRLM basée sur (3.47) est en bon accord avec le critère donné en (3.30). Ceci valide nos expressions analytiques. De plus, nous remarquons que pour $P_d = 0.37$ et $P_{fa} = 0.1$, le SRLM basé sur la BCR est exactement égal au SRLM basé sur le test d'hypothèses. Dans le cas $P_d = 0.49$ et $P_{fa} = 0.3$ et/ou $P_d = 0.32$ et $P_{fa} = 0.1$, on peut noter l'influence du facteur de translation, $\kappa(P_{fa}, P_d)$ sur le SRLM.
- Le SRLM est $O\left(\sqrt{\frac{1}{\mathrm{RSB}_E}}\right)$ ce qui est conforme avec les résultats antérieurs pour le cas $P = 1$ [SM05a, DA06, AW08].

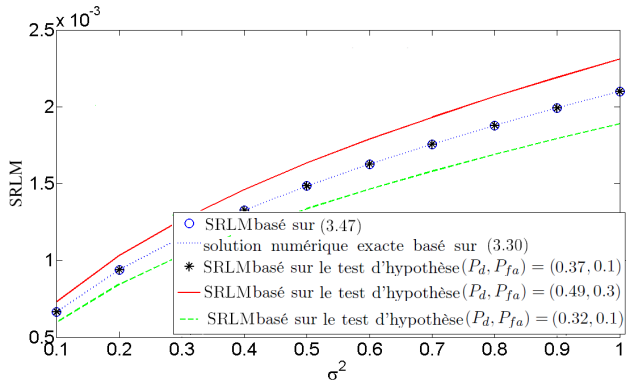

FIGURE 3.10 – SRLM en fonction de σ^2 pour $T = 100$.

– De (3.47) et pour un grand nombre de capteurs $N_1 = N_2 = \cdots = N_P = N \gg 1$, nous obtenons une expression plus compacte :

$$\delta = \sqrt{\frac{12}{TN^{P+1}\mathrm{RSB}_E}\frac{P}{1+3P}}.$$

Par conséquent, le SRLM est, dans ce cas, de l'ordre de $O\left(\sqrt{\frac{1}{N^{P+1}}}\right)$.

– De plus, pour $P \geq 1$, nous avons $\frac{(P+1)(3P+1)}{P(3P+4)} < 1$, par conséquent, le rapport entre le SRLM pour P paramètres d'intérêt, noté δ_P, et le SRLM pour $P+1$ paramètres d'intérêt, noté δ_{P+1}, est donné par

$$\frac{\delta_{P+1}}{\delta_P} = \sqrt{\frac{(P+1)(3P+1)}{NP(3P+4)}}, \tag{3.48}$$

ce qui signifie que le SRLM pour $P+1$ paramètres d'intérêt est inférieur à celui pour P paramètres d'intérêt (voir Fig. 3.11). Cela peut s'expliquer par le rajout d'observations dû à la $(P+1)^{ème}$ dimension supplémentaire. Il convient de noter que cette propriété est prouvée théoriquement, grâce à (3.48) en supposant un nombre important de capteurs. Cependant, de la Fig. 3.11 nous remarquons que, dans la pratique, $\delta_p > \delta_{p+1}$ peut être vérifié même pour un petit nombre de capteurs (par exemple, dans Fig. 3.11 nous avons utilisé $3 \leq N_p \leq 5$ pour $p = 3, \ldots, 6$).

– En utilisant le fait que

$$\sqrt{\frac{4}{TN^{P+1}\mathrm{RSB}_E}} \leq \delta_P < \delta_{P-1} < \cdots < \delta_1$$

nous pouvons alors noter que le SRLM est borné inférieurement par $\sqrt{\frac{4}{TN^{P+1}\mathrm{RSB}_E}}$.

3.3.4 Autre approche pour le calcul du SRLM

Afin de clore cette section consacrée au SRLM, nous présentons une autre approche pour le calcul du SRLM en traitant brièvement deux exemples assez connus en traitement d'antenne qui sont : la localisation de sources en champ proche et la localisation de cibles à l'aide d'un radar MIMO en présence d'interférences. Cette approche alternative diffère de la précédente (celle présentée à la section 3.3.2) dans le sens où le SRLM sera considéré comme un vecteur

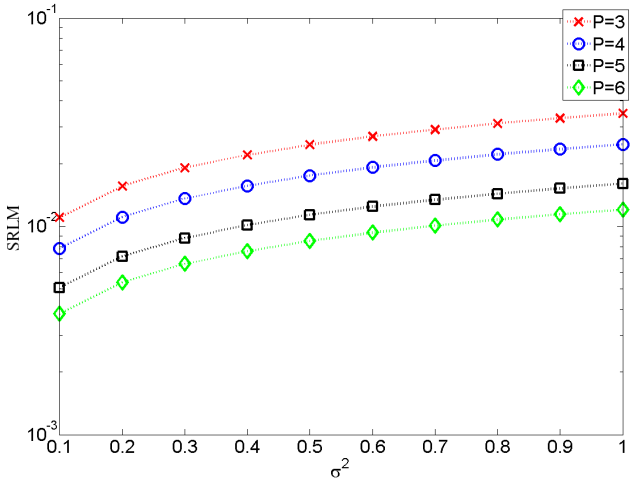

FIGURE 3.11 – Le SRLM pour le modèle harmonique avec M sources, avec $P = 3, 4, 5, 6$, $T = 100$, et $N_1 = 3$, $N_2 = 5$, $N_3 = 4$, $N_4 = 4$, $N_5 = 4$ et $N_6 = 3$.

comportant tous les écarts des paramètres d'intérêt. Dés lors, le test d'hypothèses adéquat est le suivant :

$$\begin{cases} \mathcal{H}_0 : & \boldsymbol{\delta} \triangleq \left[\omega_1^{(1)} - \omega_2^{(1)} \quad \dots \quad \omega_1^{(P)} - \omega_2^{(P)}\right]^T = \mathbf{0}, \\ \mathcal{H}_1 : & \boldsymbol{\delta} \neq \mathbf{0}, \end{cases} \tag{3.49}$$

où l'hypothèse $\mathcal{H}_0$ représente le cas où les deux sources sont combinées en une seule source, alors que l'hypothèse $\mathcal{H}_1$ incarne la situation où les deux sources sont résolues.

SRLM pour la localisation de sources en champ proche

Dans cette section nous présentons le résultat du calcul du SRLM pour la localisation de sources en champ proche. Les détails calculatoires, des simulations et une analyse plus approfondie sont présentés dans l'**Annexe C.4** (M. N. El Korso, R. Boyer, A. Renaux and S. Marcos, "A Statistical Analysis of Achievable Resolution Limit in the Near Field Context Using Nonuniform and Lacunar Array", soumis à *IEEE* Transactions on Signal Processing.)

Dans ce qui suit, nous utiliserons le modèle déterministe d'observations défini à la section 2.2 pour la localisation de sources en champ proche avec deux sources émettrices. De plus nous supposerons que les signaux sources sont connus. Nous avons montré dans l'**Annexe C.4**, pour un nombre d'observations très grand, que le SRLM s'exprime comme suit :

Théorème 9 *La relation entre le SRLM et le rapport signal à bruit (RSB) requis pour résoudre deux sources connues se situant dans le champ proche est donnée par*

$$RSB \triangleq \frac{\|\boldsymbol{s}_1\|^2 + \|\boldsymbol{s}_2\|^2}{\sigma^2} = \lambda(P_{fa}, P_d) \frac{\|\boldsymbol{s}_1\|^2 + \|\boldsymbol{s}_2\|^2}{2\,\|\boldsymbol{s}_-\|^2\, \boldsymbol{\delta}^T \boldsymbol{F} \boldsymbol{\delta}} \tag{3.50}$$

où $\boldsymbol{\delta} = [\delta_\rho \ \delta_\kappa]^T = [\rho_2 - \rho_1 \ \kappa_2 - \kappa_1]^T$ *avec* $\rho_m = \frac{-2\pi}{\nu} \sin(\theta_m)$ *et* $\kappa_m = \frac{\pi}{\nu r_m} \cos^2(\theta_m)$. *Avec*

$$\boldsymbol{F} = \begin{bmatrix} f_2 & f_3 \\ f_3 & f_4 \end{bmatrix} \tag{3.51}$$

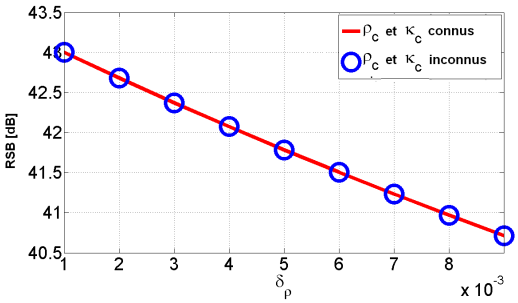

FIGURE 3.12 – Le RSB requis pour résoudre deux sources situées en champ proche en fonction de δ_ρ pour $\delta_\kappa = 0.003$. On remarque le même comportement du RSB en fonction de δ_κ pour δ_ρ fixe.

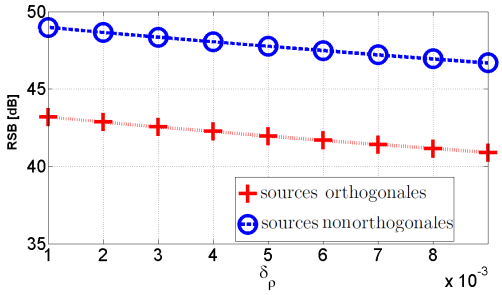

FIGURE 3.13 – Le RSB requis pour résoudre deux sources situées en champ proche en fonction de δ_ρ pour $\delta_\kappa = 0.003$ dans le cas de signaux sources orthogonaux et signaux sources non orthogonaux. On remarque le même comportement du RSB en fonction de δ_κ pour δ_ρ fixe.

et $f_i = \sum_{n=0}^{N-1} (d_n)^i$ *où* d_n *représente la distance entre le premier capteur et le* $n^{ème}$ *capteur où* $\lambda(P_{fa}, P_d)$ *est solution de* $Q^{-1}_{(\lambda(P_{fa},P_d))}(P_d) = Q^{-1}(P_{fa})$.

Le lecteur notera que (3.50) a été calculé sous l'hypothèse de connaissance des variables $\rho_c = \frac{\rho_1+\rho_2}{2}$ et $\kappa_c = \frac{\kappa_1+\kappa_2}{2}$. Toutefois, dans l'**Annexe C.4** nous avons montré par simulation que cette hypothèse n'affecte pas la valeur du SRLM (voir, figure 3.12). Pour des sources orthogonales (c'est-à-dire, $\boldsymbol{s}_1^H \boldsymbol{s}_2 = 0$) nous obtenons le résultat suivant (voir, figure 3.13) :

Théorème 10 *La relation entre le SRLM et le rapport signal à bruit requis pour résoudre deux sources orthogonales connues,* RSB_0*, se situant dans le champ proche est donnée par*

$$RSB_o = \frac{\lambda(P_{fa}, P_d)}{2\boldsymbol{\delta}^T \boldsymbol{F}\boldsymbol{\delta}}. \tag{3.52}$$

SRLM pour le MIMO radar en présence des interférences

Dans cette section, nous présentons le résultat du calcul du SRLM pour la localisation de sources à l'aide d'un radar MIMO. Les détails calculatoires, les simulations et une analyse plus approfondie sont présentés dans l'**Annexe C.5** (M. N. El Korso, R. Boyer, A. Renaux and S. Marcos, "Statistical Resolution Limit for Source Localization With Clutter Interference in a MIMO radar Context", soumis à *IEEE* Transactions on Signal Processing).

Les observations issues d'un radar MIMO (dans le cas d'antennes réceptrice et émettrice espacées entre elles [JLL09]) qui reçoit un signal réfléchi sur M cibles sont données pour la $\ell^{ème}$ impulsion par

$$\boldsymbol{Y}_\ell = \sum_{m=1}^{M} \rho_m e^{2i\pi f_m \ell} \boldsymbol{a}_{\mathcal{R}}(\omega_m^{(\mathcal{R})}) \boldsymbol{a}_{\mathcal{T}}(\omega_m^{(\mathcal{T})})^T \boldsymbol{S} + \boldsymbol{V}_\ell, \quad \ell \in [0 : L-1] \tag{3.53}$$

où L, ρ_m et f_m représentent le nombre d'échantillons par période d'impulsion, un coefficient proportionnel à la section efficace du radar et la fréquence Doppler normalisée de la $m^{ème}$ cible, respectivement. T, $N_{\mathcal{T}}$ et $N_{\mathcal{R}}$ sont, respectivement, le nombre d'observations, le nombre de capteurs émetteurs et le nombre de capteurs à la réception. Dans la suite, les symboles $\mathcal{T}$ et $\mathcal{R}$ représenteront la partie émettrice et la partie réceptrice du radar MIMO.

De plus, la matrice sources de taille $N_{\mathcal{T}} \times T$ est donnée par $\boldsymbol{S} = \begin{bmatrix} \boldsymbol{s}_0 & \dots & \boldsymbol{s}_{N_{\mathcal{T}}-1} \end{bmatrix}^T$ où $\boldsymbol{s}_{N_t} = \begin{bmatrix} s_{N_t}(1) & \dots & s_{N_t}(T) \end{bmatrix}^T$, et $\boldsymbol{V}_\ell$ (de taille $N_{\mathcal{R}} \times T$) représente la matrice du bruit. Les vecteurs directionnels de transmission et de réception sont donnés par $\boldsymbol{a}_{\mathcal{T}}(.)$ et $\boldsymbol{a}_{\mathcal{R}}(.)$. Le $i^{ème}$ élément de chaque vecteur directionnel est donné par $[\boldsymbol{a}_{\mathcal{T}}(\omega_m^{(\mathcal{T})})]_i = e^{j\omega_m^{(\mathcal{T})} d_i^{(\mathcal{T})}}$ et $[\boldsymbol{a}_R(\omega_m^{(\mathcal{R})})]_i = e^{j\omega_m^{(\mathcal{R})} d_i^{(\mathcal{R})}}$ où $\omega_m^{(\mathcal{T})} = \frac{2\pi}{\nu}\sin(\psi_m)$, $\omega_m^{(\mathcal{R})} = \frac{2\pi}{\nu}\sin(\theta_m)$ et ψ_m est l'angle de la cible vu de l'antenne émettrice, θ_m est l'angle de la cible vu de l'antenne réceptrice, ν est la longueur d'onde. La distance entre le premier capteur et le $i^{ème}$ capteur est noté $d_i^{(\mathcal{T})}$ et $d_i^{(\mathcal{R})}$ pour l'antenne de transmission et pour l'antenne de réception, respectivement. Avant de présenter les résultats, commençons par introduire les quantités suivantes : $\omega_c^{(\mathcal{T})} = \frac{\omega_1^{(\mathcal{T})}+\omega_2^{(\mathcal{T})}}{2}$ et $\omega_c^{(\mathcal{R})} = \frac{\omega_1^{(\mathcal{R})}+\omega_2^{(\mathcal{R})}}{2}$ qui représentent les paramètres centraux. $\dot{\boldsymbol{a}}_{\mathcal{T}}(.) \triangleq \boldsymbol{a}_{\mathcal{T}}(.) \odot \boldsymbol{d}_{\mathcal{T}}$, et $\dot{\boldsymbol{a}}_{\mathcal{R}}(.) \triangleq \boldsymbol{a}_{\mathcal{R}}(.) \odot \boldsymbol{d}_{\mathcal{R}}$ avec $\boldsymbol{d}_T = [d_0^{(\mathcal{T})}\ d_1^{(\mathcal{T})}\ \dots\ d_{N_{\mathcal{T}}-1}^{(\mathcal{T})}]^T$ et $\boldsymbol{d}_R = [d_0^{(\mathcal{R})}\ d_1^{(\mathcal{R})}\ \dots\ d_{N_{\mathcal{R}}-1}^{(\mathcal{R})}]^T$.

A l'instar de la section 3.3.4, nous appliquons un test d'hypothèses binaire

$$\begin{cases} \mathcal{H}_0 : & (\delta_{\mathcal{R}}, \delta_{\mathcal{T}}) = (0,0), \\ \mathcal{H}_1 : & (\delta_{\mathcal{R}}, \delta_{\mathcal{T}}) \neq (0,0), \end{cases} \tag{3.54}$$

où $\delta_{\mathcal{T}} \triangleq \omega_2^{(\mathcal{T})} - \omega_1^{(\mathcal{T})}$ et $\delta_{\mathcal{R}} \triangleq \omega_2^{(\mathcal{R})} - \omega_1^{(\mathcal{R})}$.

Le tableau 3.3 (voir aussi figure 3.14) résume le lien entre le rapport signal à bruit (défini comme RSB $\triangleq \frac{tr\{\boldsymbol{S}\boldsymbol{S}^H\}}{T\sigma^2}$) et le SRLM pour le modèle (3.53) sous les hypothèses suivantes :

	Avec interférences	Sans interférences $M=2$	Sans interférences et antennes symétriques
Variance connue	$\frac{N_{\mathcal{T}}\lambda_{\mathrm{K}}(P_{fa},P_d)}{2\boldsymbol{\zeta}^H\boldsymbol{G}^H\boldsymbol{P}_{\boldsymbol{P}_{\bar{\boldsymbol{D}}}^{\perp}\boldsymbol{G}}\boldsymbol{G}\boldsymbol{\zeta}}$	$\frac{\lambda_{\mathrm{K}}(P_{fa},P_d)}{2L\boldsymbol{\zeta}^H\boldsymbol{K}\boldsymbol{\zeta}}$	$\frac{2N_{\mathcal{T}}\lambda_{\mathrm{K}}(P_{fa},P_d)}{L\left(\left(\delta_{\mathcal{R}}^2+\delta_{\mathcal{T}}^2\right)(\alpha_2-\alpha_1)^2+\delta_{\mathcal{R}}^2\delta_{\mathcal{T}}^2(\alpha_2+\alpha_1)^2\right)}$
Variance inconnue	$\frac{N_{\mathcal{T}}\lambda_{\mathrm{U}}(P_{fa},P_d)}{2\boldsymbol{\zeta}^H\boldsymbol{G}^H\boldsymbol{P}_{\boldsymbol{P}_{\bar{\boldsymbol{D}}}^{\perp}\boldsymbol{G}}\boldsymbol{G}\boldsymbol{\zeta}}$	$\frac{\lambda_{\mathrm{U}}(P_{fa},P_d)}{2L\boldsymbol{\zeta}^H\boldsymbol{K}\boldsymbol{\zeta}}$	$\frac{2N_{\mathcal{T}}\lambda_{\mathrm{U}}(P_{fa},P_d)}{L\left(\left(\delta_{\mathcal{R}}^2+\delta_{\mathcal{T}}^2\right)(\alpha_2-\alpha_1)^2+\delta_{\mathcal{R}}^2\delta_{\mathcal{T}}^2(\alpha_2+\alpha_1)^2\right)}$

TABLE 3.3 – Le RSB requis pour résoudre deux cibles.

- Le sous-espace des interférences (engendré par les $M-2$ sources restantes) est connu,
- Les paramètres centraux, $\omega_c^{(\mathcal{T})}$ et $\omega_c^{(\mathcal{R})}$ sont supposés connus ou préalablement estimés.
- Les α_m, $i = 1 \dots M$ sont considérés déterministes inconnus.
- le bruit est Gaussien complexe blanc circulaire de moyenne nulle et de variance σ^2.

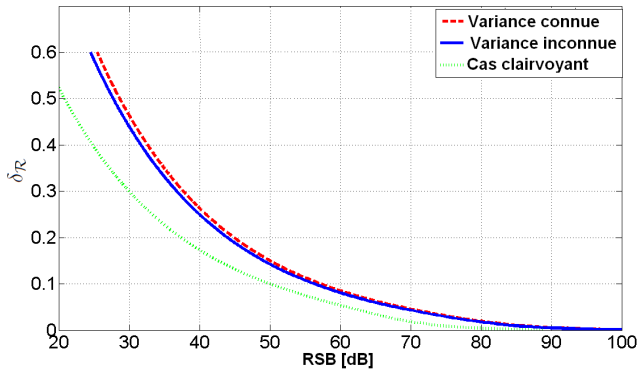

FIGURE 3.14 – $\delta_{\mathcal{R}}$ en fonction du RSB requis pour résoudre deux sources en présence d'une source interfèrente avec une ALU en émission et réception avec $N_{\mathcal{R}} = N_{\mathcal{T}} = 4$ capteurs, $L = 4$ et $T = 100$ observations. Le cas dit *clairvoyant* correspond au cas idéal où tous les paramètres sont connus y compris $\delta_{\mathcal{R}}$.

Les différentes variables données dans le tableau 3.3 sont explicitées comme suit : $\boldsymbol{G} = \begin{bmatrix}\boldsymbol{\varrho}_2 & \boldsymbol{\varrho}_3 & \boldsymbol{\varrho}_4\end{bmatrix}$, la matrice des interférences $\boldsymbol{D} = \begin{bmatrix}\boldsymbol{\varrho}_1 & \boldsymbol{g}_3 & \dots & \boldsymbol{g}_M\end{bmatrix}$, $\boldsymbol{\alpha} = \begin{bmatrix}\alpha_1 + \alpha_2 & \alpha_3 & \dots & \alpha_M\end{bmatrix}^T$ avec

$$\boldsymbol{\zeta} = \frac{j}{2}\begin{bmatrix}\delta_{\mathcal{R}}(\alpha_2 - \alpha_1) \\ \delta_{\mathcal{T}}(\alpha_2 - \alpha_1) \\ \frac{j}{2}\delta_{\mathcal{R}}\delta_{\mathcal{T}}(\alpha_1 + \alpha_2)\end{bmatrix}, \tag{3.55}$$

et où $\boldsymbol{\varrho}_1 = \boldsymbol{c}(f)\otimes\boldsymbol{a}_{\mathcal{T}}(\omega_c^{(\mathcal{T})})\otimes\boldsymbol{a}_{\mathcal{R}}(\omega_c^{(\mathcal{R})})$, $\boldsymbol{\varrho}_2 = \boldsymbol{c}(f)\otimes\boldsymbol{a}_{\mathcal{T}}(\omega_c^{(\mathcal{T})})\otimes\dot{\boldsymbol{a}}_{\mathcal{R}}(\omega_c^{(\mathcal{R})})$, $\boldsymbol{\varrho}_3 = \boldsymbol{c}(f)\otimes\dot{\boldsymbol{a}}_{\mathcal{T}}(\omega_c^{(\mathcal{T})})\otimes\boldsymbol{a}_{\mathcal{R}}(\omega_c^{(\mathcal{R})})$, $\boldsymbol{\varrho}_4 = \boldsymbol{c}(f)\otimes\dot{\boldsymbol{a}}_{\mathcal{T}}(\omega_c^{(\mathcal{T})})\otimes\dot{\boldsymbol{a}}_{\mathcal{R}}(\omega_c^{(\mathcal{R})})$ et $\boldsymbol{c}(f) = [1\dots e^{i2\pi f(L-1)}]^T$. De plus, $\boldsymbol{P}_{\boldsymbol{P}_{\boldsymbol{D}}^{\perp}\boldsymbol{G}} = \boldsymbol{P}_{\boldsymbol{D}}^{\perp} - \boldsymbol{P}_{[\boldsymbol{G}\boldsymbol{D}]}^{\perp}$. $\lambda_{\mathrm{K}}(P_{fa}, P_d)$ et $\lambda_{\mathrm{U}}(P_{fa}, P_d)$ sont solutions de $Q^{-1}_{\chi^2_{2r}}(P_{fa}) = Q^{-1}_{\chi^2_{2r}(\lambda_3(P_{fa},P_d))}(P_d)$ et $Q^{-1}_{F_{2r,2r'}}(P_{fa}) = Q^{-1}_{F_{2r,2r'}(\lambda_{\mathrm{U}}(P_{fa},P_d))}(P_d)$, respectivement, avec $r = T\mathcal{N}_T\mathcal{N}_R - M + 1$ et $r' = T\mathcal{N}_T\mathcal{N}_R - (M+2)$.

3.3.5 Choix du critère du seuil de résolution limite multidimensionnel

Dans les sections 3.3.2 et 3.3.4, nous avons proposé quelques critères pour le seuil de résolution limite multidimensionnel dont voici un récapitulatif :

◇ *Critère basé sur la borne de Cramér-Rao :* Plus précisément, dans la section 3.3.2, nous avons proposé un critère pour le SRLM basé sur la BCR en utilisant la distance l_1 (3.29). Nous avons montré que ce critère est équivalent à un test UPP (à un facteur multiplicateur près.) Cette extension peut être naturellement faite pour une distance l_k avec k entier supérieur à zéro (voir, l'**Appendice C.1**.) Suivant la même démarche que celle dans la section 3.3.2, on peut montrer que le critère du SRLM basé sur la BCR en utilisant la distancel_k est lui aussi équivalent à un test UPP (à un facteur multiplicateur près). Ce critère s'exprimera comme suit :

Théorème 11 *Le SRLM pour le modèle (3.27) à P paramètres d'intérêt par signal en utilisant la distance l_k est donné par* $\delta = \left(\sum_{p=1}^{P}\left|\omega_1^{(p)} - \omega_2^{(p)}\right|^k\right)^{1/k}$, *qui représente la solution implicite de l'équation suivante :*

$$\delta^{2k} - A_{\text{direct}} - A_{\text{croisé}} = 0, \tag{3.56}$$

où

$$A_{\text{directe}} = \sum_{p=1}^{P} \delta_p^{2(k-1)} \left(BCR(\omega_1^{(p)}) + BCR(\omega_2^{(p)}) - 2BCR(\omega_1^{(p)}, \omega_2^{(p)}) \right), \tag{3.57}$$

et

$$A_{\text{croisé}} = \sum_{p=1}^{P} \sum_{\substack{p'=1 \\ p' \neq p}}^{P} \delta_p^{k-1} \delta_{p'}^{k-1} g_p g_{p'} \left(BCR(\omega_1^{(p)}, \omega_1^{(p')}) + BCR(\omega_2^{(p)}, \omega_2^{(p')}) - 2BCR(\omega_1^{(p)}, \omega_2^{(p')}) \right), \tag{3.58}$$

avec $\delta_p = \left| \omega_1^{(p)} - \omega_2^{(p)} \right|$ *et* $g_p = sgn\left(\omega_1^{(p)} - \omega_2^{(p)} \right)$.

◇ *Critère basé sur le test d'hypothèses :* Ce critère utilise un test d'hypothèses binaire qui décrit bien la situation de la figure 3.1. L'hypothèse $\mathcal{H}_0$ représente le cas où les deux sources sont combinées en une seule source, alors que l'hypothèse $\mathcal{H}_1$ représente la situation où les deux sources sont résolues. Dès lors, le test d'hypothèses adéquat est donné par

$$\begin{cases} \mathcal{H}_0 : & \boldsymbol{\delta} \triangleq \left[\omega_1^{(1)} - \omega_2^{(1)} \quad \dots \quad \omega_1^{(P)} - \omega_2^{(P)} \right]^T = \mathbf{0}, \\ \mathcal{H}_1 : & \boldsymbol{\delta} \neq \mathbf{0}, \end{cases} \tag{3.59}$$

Ainsi, dans cette section nous avons proposé plusieurs approches pour le calcul du SRLM. La question naturelle qui se pose est alors *quel critère choisir ?*

Pour répondre à cette question, notons tout d'abord que :

- Le SRLM est un concept récent. Les critères que nous avons proposés dépendent de la mesure du SRLM proposé (SRLM sous forme scalaire en utilisant une distance l_k ou SRLM vectoriel en utilisant un test d'hypothèses binaire.) Dans ce qui suit, nous donnerons les inconvénients de chaque critère. Cela étant dit, tous les critères proposés ont un sens puisqu'ils reflètent bien la situation présentée dans la figure 3.1.
- A titre de comparaison, l'analyse de performance en terme d'erreur d'estimation se fait en se basant sur l'erreur quadratique moyenne. L'erreur quadratique moyenne est une mesure qui a été *arbitrairement* et *naturellement* choisie pour l'analyse de performances. Cependant, rien ne nous empêche d'analyser les performances en terme de la valeur absolue de l'erreur moyenne, ou même, en terme de la valeur absolue de l'erreur cubique moyenne.

Ainsi, le but de cette section a été, en premier lieu, de présenter les différents critères possibles. Dans ce qui suit nous présenterons aussi leurs inconvénients et leurs avantages et ce sera à l'utilisateur de choisir le critère le plus adapté à son application :

◦ *Critère basé sur le test binaire :* Ce critère ne requiert aucune supposition, mis à part, que le modèle des observations soit identifiable. Cependant, l'inconvénient principal de cette approche est que le test (3.59) est difficilement traitable et devient rapidement impossible pour $P > 2$ (sauf pour certains modèles triviaux.)

◦ *Critère basé sur la borne de Cramèr-Rao :* Ce critère suppose que principalement les éléments du vecteur $\boldsymbol{\omega}$ sont de la même nature, c'est-à-dire, que les paramètres d'intérêt ont la même unité de mesure. Dans le cas contraire, nous serons obligés de faire un changement de variable pour obtenir des paramètres ayant la même unité de mesure (par exemple, dans le contexte de la localisation de sources en champ proche, nous pourrons utiliser les angles électriques (paramètres non physiques) au lieu de l'élévation θ et de la distance r (paramètres physiques), voir section 2.2). En ce qui concerne le choix de la norme, c'est-à-dire, la valeur de l'entier k :

- ⋆ Si $k = 1$, le SRLM est facilement calculable en résolvant (3.56). Par contre, on imposera la condition suivante : $\forall p, \omega_1^{(p)} \neq \omega_2^{(p)}$. Cette condition est dûe à la non dérivabilité de δ_p^k par rapport à $\omega_1^{(p)}$ et $\omega_2^{(p)}$ pour $k = 1$.
- ⋆ Pour $k > 1$, le calcul du SRLM devient très compliqué, voir impraticable analytiquement dans de nombreuses situations. Cela étant dit, il est facilement calculable numériquement. De plus, pour des valeurs de k pair, la condition $\forall p, \omega_1^{(p)} \neq \omega_2^{(p)}$ est relaxée.

Chapitre 4

Conclusion et perspectives

Dans ce manuscrit nous nous sommes intéressés à l'analyse de performances en traitement d'antenne. Nous avons essayé de traiter plusieurs aspects de l'analyse de performances, c'est-à-dire,

- l'étude asymptotique de l'erreur quadratique moyenne, qui nous permet de caractériser les performances ultimes d'estimation qu'un algorithme peut espérer atteindre,
- l'étude du décrochement de l'erreur quadratique moyenne, qui délimite la zone de fonctionnement optimal de l'estimateur du maximum de vraisemblance, et enfin,
- l'étude du seuil statistique de résolution limite, appelé aussi pouvoir séparateur. Ce dernier est un autre indicateur de performance moins utilisé mais d'une importance croissante dans tout problème d'estimation paramétrique. Il traduit la capacité d'un algorithme à séparer deux sources proches. Plus précisément, il représente la distance minimale entre deux signaux permettant une correcte séparation/estimation des paramètres d'intérêt.

Plus particulièrement, nous nous sommes initialement intéressés à l'analyse de performances pour la localisation de sources en champ proche. Dans le cas de sources proches de l'antenne, les fronts d'ondes ne sont plus plans et il faut prendre en compte un modèle d'observations paramétré par l'azimut de chaque source, d'une part, mais aussi par la distance entre les sources et un référentiel vis-à-vis de l'antenne. Ainsi, dans ce manuscrit :

- nous avons calculé et analysé les bornes de Cramér-Rao dans le cas d'une source située en champ proche. Notre approche comporte deux avantages : (1) le coût calculatoire des bornes de Cramér-Rao, pour un grand nombre d'observations, sous forme matricielle peut être très coûteux, ce qui n'est pas le cas de nos expressions non-matricielles et (2) des informations pertinentes concernant les performances du système peuvent être facilement déduites,
- nous avons continué notre analyse afin de prédire la zone de décrochement. Ainsi, nous avons calculé et analysé différentes bornes inférieures de l'erreur quadratique moyenne : la borne de McAulay-Seidman, la borne de Hammersley-Chapman-Robbins, la borne de McAulay-Hofstetter et, plus particulièrement, une borne récemment introduite dans la littérature dénommée la borne de Fourier Cramér-Rao. Le but de cette étude est de caractériser les performances optimales non-asymptotiques des estimateurs, dans le contexte champ proche. Plus particulièrement, nous nous sommes intéressés à la prédiction du phénomène de décrochement pour lequel ces bornes sont utiles. Cette analyse est pertinente, d'autant plus, qu'à notre connaissance, aucun résultat concernant des bornes inférieures autres que la borne de Cramér-Rao, n'est disponible dans la littérature. Cette analyse nous a permis d'avoir une bonne prédiction du phénomène de décrochement. Et ceci, pour un modèle d'observation corrompu par un bruit spatialement coloré. De plus, nous avons

démontré, lors de cette étude, que la borne de Fourier Cramér-Rao, récemment proposée, demeure moins performante que certaines de ses prédécesseurs, on cite la borne de McAulay-Hofstetter comme exemple.

– En voulant étudier l'analyse de performances en terme du seuil statistique de résolution limite, nous nous sommes rendus compte que cet aspect est très peu étudié par la communauté du traitement d'antenne. A cet effet, nous avons tout d'abord caractérisé le seuil de résolution limite pour des problèmes fréquents en traitement d'antenne dans le contexte de la localisation de sources en champ lointain. Plus particulièrement, nous avons traité le cas de sources polarisées et le cas de sources en présence d'interférences, qui sont des applications pour lesquelles aucun résultat n'était disponible dans la littérature.
Lorsque nous nous sommes intéressés au seuil de résolution limite pour la localisation de sources en champ proche qui était notre sujet initial, nous avons constaté que tous les critères concertant le seuil de résolution limite ont été introduits dans le cas d'un seul paramètre d'intérêt par signal. Toutefois, dans de nombreux problèmes d'estimation, les signaux sont paramétrés par plus d'un paramètre d'intérêt par signal. A cet effet, nous avons étendu le critère du seuil de résolution limite au cas multidimensionnel. Cette extension, initialement intuitive, est validée par une étude se basant sur un test d'hypothèses. Ainsi, nous avons montré que notre extension est asymptotiquement équivalente (à un facteur de translation près) à un test d'hypothèses uniformément le plus puissant. Enfin, nous avons appliqué notre extension à plusieurs applications de traitement d'antenne (modèle harmonique multidimensionnel, modèle du champ proche et le modèle du MIMO radar).

Les perspectives de ce travail peuvent être séparées en deux groupes

- *Concernant les bornes inférieures de l'erreur quadratique moyenne pour la localisation de sources en champ proche,* il convient aussi d'étendre cette étude
  – dans le cas le plus général (par exemple, un bruit non Gaussien avec une matrice de covariance inconnue mais aussi pour un vecteur de paramètres inconnu contenant tous les paramètres d'intérêt et de nuisance),
  – pour un modèle d'observations multi-sources en présence d'interférences,
  – d'inclure les erreurs de modèle dans l'analyse des bornes inférieures de l'erreur quadratique moyenne.

  Ainsi, on pourra étudier l'influence des interférences, de la statistique du bruit et des erreurs du modèle sur les performances asymptotiques et/ou sur le décrochement.
- *Concernant le seuil de résolution limite en traitement d'antenne,* des perspectives intéressantes seraient de :
  – appliquer le seuil de résolution limite pour d'autres problèmes d'estimation, en particulier dans un contexte multi-paramètres,
  – trouver la configuration optimale pour avoir le seuil de résolution limite le plus bas en utilisant les degrés de liberté du problème (par exemple, minimiser le seuil de résolution limite par rapport aux paramètres de polarisation, par rapport à la géométrie d'antenne ou par rapport à la sélection de forme d'onde), et enfin,
  – étudier l'influence d'erreur de modèle sur le seuil de résolution limite.

Annexe A

Articles sur les bornes inférieures de l'erreur quadratique moyenne pour la localisation de sources en champ proche

A.1 IEEE-SP-2010

M. N. El Korso, R. Boyer, A. Renaux and S. Marcos, "Conditional and unconditional Cramér-Rao bounds for near-field source localization", *IEEE Transactions on Signal Processing*, Volume : 58, Issue : 5, May 2010, pp. 2901-2907.

Conditional and Unconditional Cramér–Rao Bounds for Near-Field Source Localization

Mohammed Nabil El Korso, Rémy Boyer, Alexandre Renaux, and Sylvie Marcos

***Abstract*—Near-field source localization problem by a passive antenna array makes the assumption that the time-varying sources are located near the antenna. In this context, the far-field assumption (i.e., planar wavefront) is, of course, no longer valid and one has to consider a more complicated model parameterized by the bearing (as in the far-field case) and by the distance, named range, between the source and a reference coordinate system. One can find a plethora of estimation schemes in the literature, but their ultimate performance in terms of mean square error (MSE) have not been fully investigated. To characterize these performance, the Cramér–Rao bound (CRB) is a popular mathematical tool in signal processing. The main cause for this is that the MSE of several high-resolution direction of arrival algorithms are known to achieve the CRB under quite general/weak conditions. In this correspondence, we derive and analyze the so-called conditional and unconditional CRBs for a single time-varying near-field source. In each case, we obtain non-matrix closed-form expressions. Our approach has two advantages: i) due to the fact that one has to inverse the Fisher information matrix, the computational cost for a large number of snapshots (in the case of the conditional CRB) and/or for a large number of sensors (in the case of the unconditional CRB), of a matrix-based CRB can be high while our approach is low and ii) some useful information can be deduced from the behavior of the bound. In particular, an explicit relationship between the conditional and the unconditional CRBs is provided and one shows that closer is the source from the array and/or higher is the signal carrier frequency, better is the range estimation.**

***Index Terms*—Bearing and range estimation, Cramér–Rao bound, near field, performance analysis, performance bound, source localization.**

I. Introduction

Passive sources localization by an array of sensors is an important topic with a large number of applications, such as sonar, seismology, digital communications, etc. Particularly, the context of far-field sources has been widely investigated in the literature and several algorithms to estimate the localization parameters have been proposed [2]. In this case, the sources are assumed to be far from the array of sensors. Consequently, the propagating waves are assumed to have planar wavefronts when they reach the array. However, when the sources are located in the so-called near-field region, the curvature of the waves impinging on the sensors can no longer be neglected. Therefore, in this scenario, each source is characterized by its bearing and its range.

In array processing, there exist two different models depending on the assumptions about the signal sources: 1) the so-called conditional model, i.e., when the signals are assumed to be deterministic but unknown and 2) the so-called unconditional model, i.e., when the signals are assumed to be driven by a Gaussian random process. Each model is appropriate for a given situation. For example, the assumption of Gaussian source signal is not realistic for several applications (for example, in radar [3] or radio communication applications [4]). A legitimate choice is then to assume that the emitted signals are deterministic and unknown. On the other hand, in some applications it is appropriate to model the sources as stationary Gaussian processes (for examples in seismology and tomography, see [5]). One can find many estimation schemes adapted to near-field source localization (e.g., [6]–[8]), but only a few number of works studying the optimal performance associated with this model have been proposed. To characterize the performance of an estimator in terms of mean square error (MSE), the Cramér–Rao bound (CRB) is certainly the most popular tool [9].

Since, in array processing, two signals models are generally used, it exists two distinct CRB named the Unconditional CRB (UCRB) and the Conditional CRB (CCRB). More precisely, the UCRB is achieved asymptotically, i.e., for a large number of snapshots, by the Unconditional Maximum Likelihood (UML) estimator [10], whereas the CCRB is achieved asymptotically, i.e., at high signal-to-noise ratio, by the Conditional Maximum Likelihood (CML) estimator [11].

Most of the results concerning the UCRB and the CCRB available in the literature deal with the far-field case. Moreover, in some works, only closed-form expressions of the Fisher information matrix are given. We call these cases *matrix expression* of the CRB since the inversion of the FIM is not presented. On the other hand, we will refer to a *non-matrix* expression of the CRB when the inversion of the FIM is proposed. Note that, in the conditional signal model case, this distinction is fundamental since the size of the parameter vector grows with the number of snapshots.

In [12], the UCRB was indirectly derived as the asymptotic, in terms of number of snapshots, covariance matrix of the UML estimator. Ten years after, Stoica *et al.* [13], Pesavento and Gershman [14] and Gershman *et al.* [15] provided a direct (but similar) matrix-based derivation of this bound using the extended Slepian–Bangs formula for a uniform, a nonuniform, and an unknown noise field, respectively. On the other hand, a matrix-based expression of the CCRB for the far-field case was derived by Stoica *et al.* in [16].

Unlike the far-field case, the CRB for the near-field localization problem has been less studied. One can find in [17] matrix-based expressions of the UCRB for range and bearing estimation. Ottersten *et al.* derived a general matrix-based expressions of the UCRB for unknown parameters associated with the emitted signal [10]. Recently, Grosicki *et al.* [6] extended, to the near-field case, the matrix-form expression for the UCRB similar to that given in [12] in the far-field case. Again, one should note that all the closed-form expressions, given in the literature and above concerning the near-field case, are matrix-based expressions stopped before the inversion of the Fisher information matrix. To the best of our knowledge, no non-matrix expressions are available concerning the CCRB and UCRB for range and bearing estimation in the near-field context. The goal of this correspondence is to fill this lack. Particularly, non-matrix closed-form expressions of the CRB in the case of a single deterministic (but unknown) and stochastic time-varying narrowband source in the near-field region are derived and analyzed. Consequently, this approach avoids the costly computational cost of the matrix-based CRB expressions particularly for a large number of snapshots (for the CCRB) and/or for a large number of sensors (for the UCRB). However, it is not the only reason concerning the usefulness of these non-matrix expressions. Deriving non-matrix expressions of the CRB enables us

Manuscript received October 02, 2009; accepted January 21, 2010. Date of publication February 17, 2010; date of current version April 14, 2010. The associate editor coordinating the review of this manuscript and approving it for publication was Dr. Sergiy A. Vorobyov. This work was presented in part during the International Conference on Acoustics, Speech and Signal Processing (ICASSP), Taipei, Taiwan, R.O.C., 2009 [1]. This project was funded by both region Île de France and Digiteo Research Park.

The authors are with Laboratoire des Signaux et Systémes (L2S), Université Paris-Sud XI, CNRS, SUPELEC, Gif-Sur-Yvette, 91192, France (e-mail: elkorso@lss.supelec.fr; remy.boyer@lss.supelec.fr; alexandre.renaux@lss.supelec.fr; marcos@lss.supelec.fr).

Color versions of one or more of the figures in this paper are available online at http://ieeexplore.ieee.org.

Digital Object Identifier 10.1109/TSP.2010.2043128

to characterize the performance of any unbiased estimator and to use it to deduce some useful information describing the behavior of the MLE variance as a function of the physical parameters.

This correspondence is organized as follows. Section II formulates the problem and basic assumptions. In Section III we present our derivation of the CCRB and the UCRB in the near-field region. Section IV is devoted to the analytical and numerical analysis of the CRB where we provide a discussion on the CRB's behavior. Furthermore, simulation results are provided to validate this theoretical analysis. Finally, conclusions are given in Section V.

Glossary of Notation: The following notations are used through the correspondence. Matrices and vectors are represented by bold uppercase and bold lowercase characters, respectively. Vectors are, by default, in column orientation, whereas $\mathbf{Z}^T, \mathbf{Z}^*, \mathbf{Z}^H, \mathrm{tr}\{\mathbf{Z}\}$ and $\det\{\mathbf{Z}\}$ denote the transpose, the conjugate, the conjugate transpose, the trace and the determinant of the matrix $\mathbf{Z}$, respectively. $[\mathbf{z}]_i$ and $[\mathbf{Z}]_{i,k}$ denote the ith element of the vector $\mathbf{z}$ and the ith row and the kth column element of the matrix $\mathbf{Z}$, respectively. Furthermore, $\Re\{\cdot\}, E\{\cdot\}, \odot, \otimes, \mathrm{diag}(.), \mathrm{bdiag}(.), \mathrm{vec}(.), \delta(.)$ and $\mathrm{mod}(.)$ stand for the real part, the expectation, the Hadamard product, the Kronecker product, the diagonal operator, the block diagonal operator, the vec-operator, the Kronecker symbol and the modulo operator, respectively. $\mathbf{1}_L$ and $\boldsymbol{I}_L$ denote the vector of dimension $L \times 1$ filled by ones and the identity matrix of size $L \times L$, respectively. Finally $j, O(\nu)$ and $\|\boldsymbol{\alpha_i}\|^2 = (1/L)\sum_{t=1}^{L} \alpha_i^2(t)$ denote the complex number $\sqrt{-1}$, the terms of order larger or equal to ν and the normalized norm of the vector $\boldsymbol{\alpha_i}$.

II. Problem Setup and Assumptions

Consider an uniform linear array (ULA) of N sensors with inter-element spacing d that receives a signal emitted by a single near-field and narrowband source. Consequently, the observation model is as follows:

$$x_n(t) = s(t)e^{j2\pi\tau_n} + v_n(t), \quad t = 1, \ldots, L, \quad n = 0, \ldots, N-1$$

where $x_n(t)$ is the observed signal at the output of the $(n+1)$th sensor. In the conditional case, $s(t) = \alpha(t)e^{j(2\pi f_0 t + \psi(t))}$ is the source signal with a carrier frequency equals to f_0 where $\alpha(t)$ and $\psi(t)$ are the real amplitude and the shift phase, respectively. The random process $v_n(t)$ is an additive noise and L is the number of snapshots. The time delay τ_n associated with the signal propagation time from the first sensor to the $(n+1)$th sensor is given by [6]

$$\tau_n = \frac{r}{2\pi\lambda}\left(\sqrt{1 + \frac{n^2d^2}{r^2} - \frac{2nd\sin\theta}{r}} - 1\right)$$

where λ is the signal wavelength and where r and $\theta \in [0, \pi/2]$ denote the range and the bearing of the source, respectively. It is well known that, if the source range is inside of the so-called Fresnel region [7], i.e.,

$$0.62\left(d^3\frac{(N-1)^3}{\lambda}\right)^{1/2} < r < 2d^2\frac{(N-1)^2}{\lambda}, \tag{1}$$

then the time delay τ_n can be approximated by $\tau_n = (\omega n + \phi n^2)/(2\pi) + O(d^2/r^2)$. ω and ϕ are the so-called electric angles which are connected to the physical parameters of the problem by: $\omega = -2\pi d\sin(\theta)/\lambda$ and $\phi = \pi d^2\cos^2(\theta)/(\lambda r)$. Then, neglecting $O(d^2/r^2)$ in the time delay expression [7], the observation model becomes $x_n(t) = s(t)e^{j(\omega n + \phi n^2)} + v_n(t)$. Consequently, the observation vector can be expressed as

$$\boldsymbol{x}(t) = \mathbf{a}(\omega, \phi)s(t) + \mathbf{v}(t) \tag{2}$$

where $\boldsymbol{x}(t) = [x_0(t) \ldots x_{N-1}(t)]^T, \mathbf{v}(t) = [v_0(t) \ldots v_{N-1}(t)]^T$ and where the $(n+1)$th element of the steering vector $\mathbf{a}(\omega, \phi)$ is given by $[\mathbf{a}(\omega, \phi)]_{n+1} = e^{j(\omega n + \phi n^2)}$. The noise will be assumed to be a complex circular white Gaussian random process with zero-mean and unknown variance σ^2, uncorrelated both temporally and spatially. Consequently, the joint probability density function of the observations $\boldsymbol{\chi} = [\boldsymbol{x}^T(1) \cdots \boldsymbol{x}^T(L)]^T$ given a parameter vector $\boldsymbol{\eta}$ is given by

$$p(\boldsymbol{\chi}|\boldsymbol{\eta}) = \prod_{t=1}^{L} p(\boldsymbol{x}(t)|\boldsymbol{\eta}) = \frac{1}{\pi^{NL}\det\{\mathbf{R}\}}e^{-(\boldsymbol{\chi}-\boldsymbol{\mu})^H\mathbf{R}^{-1}(\boldsymbol{\chi}-\boldsymbol{\mu})}$$

where $\mathbf{R}$ and $\boldsymbol{\mu}$ denote the covariance matrix and the average of $\boldsymbol{\chi}$, respectively.

III. Cramér–Rao Bounds Derivation

The goal of this section is to derive the CCRB and the UCRB with respect to the bearing and the range. Let $E\{(\hat{\boldsymbol{\eta}} - \boldsymbol{\eta})(\hat{\boldsymbol{\eta}} - \boldsymbol{\eta})^T\}$ be the covariance matrix of an unbiased estimator, $\hat{\boldsymbol{\eta}}$, of a deterministic parameter vector $\boldsymbol{\eta}$. The covariance inequality principle states that, under quite general/weak conditions, the variance satisfies $\mathrm{MSE}([\hat{\boldsymbol{\eta}}]_i) = E\{([\hat{\boldsymbol{\eta}}]_i - [\boldsymbol{\eta}]_i)^2\} \geq [\mathbf{CRB}(\boldsymbol{\eta})]_{i,i}$ where $\mathbf{CRB}(\boldsymbol{\eta}) = \mathbf{FIM}^{-1}(\boldsymbol{\eta})$. In the following, for sake of simplicity the notation, $\mathrm{CRB}([\boldsymbol{\eta}]_i)$ will be used instead of $[\mathbf{CRB}(\boldsymbol{\eta})]_{i,i}$. Since we are working with a complex circular Gaussian observation model, the (ith, kth) element of the Fisher information matrix (FIM) for the parameter vector $\boldsymbol{\eta}$ is well known and can be written as [18]

$$[\mathbf{FIM}(\boldsymbol{\eta})]_{i,k} = \mathrm{tr}\left\{\mathbf{R}^{-1}\frac{\partial\mathbf{R}}{\partial[\boldsymbol{\eta}]_i}\mathbf{R}^{-1}\frac{\partial\mathbf{R}}{\partial[\boldsymbol{\eta}]_k}\right\} + 2\Re\left\{\frac{\partial\boldsymbol{\mu}^H}{\partial[\boldsymbol{\eta}]_i}\mathbf{R}^{-1}\frac{\partial\boldsymbol{\mu}}{\partial[\boldsymbol{\eta}]_k}\right\}. \tag{3}$$

Note that (3) depends on the assumptions on the parameters of the model (equivalently, on the parameter vector $\boldsymbol{\eta}$) via the probability density function $p(\boldsymbol{\chi}|\boldsymbol{\eta})$. The remaining of the section is dedicated to the study of two source models: i) the conditional model for which $\mathbf{CFIM}(\boldsymbol{\eta})$ and $\mathbf{CCRB}(\boldsymbol{\eta})$ will denote the conditional FIM and the conditional CRB w.r.t. the parameter vector $\boldsymbol{\eta}$, respectively; ii) the unconditional model for which $\mathbf{UFIM}(\boldsymbol{\eta})$ and $\mathbf{UCRB}(\boldsymbol{\eta})$ will denote the unconditional FIM and the unconditional CRB w.r.t. the parameter vector $\boldsymbol{\eta}$, respectively. For each case we provide an analytical inversion of the FIM which leads to a non-matrix closed-form expression of the CRB according to the electrical angles. Finally, by using a simple change of variables, we obtain the (non-matrix) expression of CRB according to the physical parameters (bearing and range) for a single source.

A. The Conditional Model

First, let us consider the conditional model. Let us define $\boldsymbol{\psi} = [\psi(1) \cdots \psi(L)]^T$ and $\boldsymbol{\alpha} = [\alpha(1) \cdots \alpha(L)]^T$. The unknown parameter vectors are $\boldsymbol{\xi} = [\omega\, \phi\, \boldsymbol{\psi}^T\ \boldsymbol{\alpha}^T\ \sigma^2]^T$ or $\boldsymbol{\kappa} = [\theta\, r\, \boldsymbol{\psi}^T\ \boldsymbol{\alpha}^T\ \sigma^2]^T$ depending if we are working on the electrical angles or on the physical parameters of interest. First, we derive $\mathbf{CCRB}(\boldsymbol{\xi})$. Second, by using an appropriate change of variables we will deduce $\mathbf{CCRB}(\boldsymbol{\kappa})$. Note that $\boldsymbol{\kappa}$ and $\boldsymbol{\xi}$ are assumed to be deterministic and that their size grows with the number of snapshots. First, let us focus on the derivation of $\mathbf{CCRB}(\boldsymbol{\xi})$. Due to the conditional model assumption we have

$\mathbf{R} = \sigma^2\mathbf{I}_{NL}$ and $\boldsymbol{\mu} = [s(1)\mathbf{a}^T(\omega,\phi)\cdots s(L)\mathbf{a}^T(\omega,\phi)]^T$. Consequently, by applying (3) one obtains

$$[\mathbf{CFIM}(\boldsymbol{\xi})]_{i,k} = \frac{NL}{\sigma^4}\frac{\partial\sigma^2}{\partial[\boldsymbol{\xi}]_i}\frac{\partial\sigma^2}{\partial[\boldsymbol{\xi}]_k} + \frac{2}{\sigma^2}\Re\left\{\frac{\partial\boldsymbol{\mu}^H}{\partial[\boldsymbol{\xi}]_i}\frac{\partial\boldsymbol{\mu}}{\partial[\boldsymbol{\xi}]_k}\right\}. \quad (4)$$

1) Block-Diagonal Structure of the Fisher Information Matrix: Using (4) and after some tedious, but straightforward, algebraic calculations, one can easily prove the following lemma:

Lemma 1: The structure of $\mathbf{CFIM}(\boldsymbol{\xi})$ for a single near-field source is given by

$$\mathbf{CFIM}(\boldsymbol{\xi}) = \mathrm{bdiag}(\boldsymbol{Q},\boldsymbol{Y}), \quad (5)$$

in which

$$\boldsymbol{Q} = \left[\begin{array}{cc|c} f_{\omega\omega} & f_{\omega\phi} & \mathbf{f}_{\omega\boldsymbol{\psi}} \\ f_{\phi\omega} & f_{\phi\phi} & \mathbf{f}_{\phi\boldsymbol{\psi}} \\ \hline \mathbf{f}_{\boldsymbol{\psi}\omega} & \mathbf{f}_{\boldsymbol{\psi}\phi} & \mathbf{F}_{\boldsymbol{\psi}\boldsymbol{\psi}} \end{array}\right], \quad (6)$$

and $\boldsymbol{Y} = \mathrm{bdiag}((2N/\sigma^2)\mathbf{I}_L, NL/\sigma^4)$, where the conditional SNR is denoted by $\mathrm{C_{SNR}} = \|\boldsymbol{\alpha}\|^2/\sigma^2$, $f_{\omega\omega} = \mathrm{C_{SNR}}LN(N-1)(2N-1)/3$, $f_{\phi\phi} = \mathrm{C_{SNR}}\ LN(N-1)(2N-1)(3N^2-3N-1)/15$, and $f_{\omega\phi} = f_{\phi\omega} = \mathrm{C_{SNR}}\ LN^2(N-1)^2/2$. Furthermore, the $L\times 1$ vectors $\mathbf{f}_{\boldsymbol{\psi}\omega}, (\mathbf{f}_{\omega\boldsymbol{\psi}})^T, \mathbf{f}_{\boldsymbol{\psi}\phi}$ and $(\mathbf{f}_{\phi\boldsymbol{\psi}})^T$ are given by $\mathbf{f}_{\boldsymbol{\psi}\omega} = (\mathbf{f}_{\omega\boldsymbol{\psi}})^T = N(N-1)(\boldsymbol{\alpha}\odot\boldsymbol{\alpha})/\sigma^2$ and $\mathbf{f}_{\boldsymbol{\psi}\phi} = (\mathbf{f}_{\phi\boldsymbol{\psi}})^T = N(N-1)(2N-1)(\boldsymbol{\alpha}\odot\boldsymbol{\alpha})/(3\sigma^2)$. The $L\times L$ matrix $\mathbf{F}_{\boldsymbol{\psi}\boldsymbol{\psi}}$ is given by $\mathbf{F}_{\boldsymbol{\psi}\boldsymbol{\psi}} = 2N\mathrm{diag}(\boldsymbol{\alpha}\odot\boldsymbol{\alpha})/\sigma^2$.

We notice that, thanks to the time-diversity of the source signal, $\mathbf{F}_{\boldsymbol{\alpha}\boldsymbol{\psi}} = (\mathbf{F}_{\boldsymbol{\psi}\boldsymbol{\alpha}})^T$ are null matrices. We also note the well-known property that the signal parameters (i.e., $\omega,\phi,\boldsymbol{\psi},\boldsymbol{\alpha}$) are decoupled from the noise variance [19]. The other zero terms are due to the consideration on the real part which appears in (4) applied to purely imaginary quantities and imply that the amplitude of the signal source $\boldsymbol{\alpha}$ is decoupled from the other model signal parameters (i.e., ω,ϕ and $\boldsymbol{\psi}$).

a) Analytical Inversion: Since the size of $\mathbf{CFIM}(\boldsymbol{\xi})$ proposed in (5) is equal to $(2L+3)\times(2L+3)$, it depends on the number of snapshots. A brute-force numerical inversion to obtain $\mathbf{CCRB}(\boldsymbol{\xi})$ can consequently be a costly operation. Using an appropriate partition of $\mathbf{CFIM}(\boldsymbol{\xi})$ and after writing analytically the expression of the inverse of the Schur complement of the square matrix $\mathbf{F}_{\boldsymbol{\psi}\boldsymbol{\psi}}$ in the upper-left block matrix of $\mathbf{CFIM}(\boldsymbol{\xi})$, we can state the following theorem.

Theorem 1: Non-matrix closed-form expressions of $\mathbf{CCRB}(\boldsymbol{\xi})$ corresponding to the electrical angles, the amplitudes and the shift phases relatively to the model (2) exist *iff* $N \geq 3$ and $\alpha(t)\neq 0\ \forall t = 1\cdots L$. They are expressed as follows:

$$\mathrm{CCRB}(\omega) = \frac{6(2N-1)(8N-11)}{\mathrm{C_{SNR}}\ L(N^2-1)N(N^2-4)}, \quad (7)$$

$$\mathrm{CCRB}(\phi) = \frac{90}{\mathrm{C_{SNR}}\ L(N^2-1)N(N^2-4)}, \quad (8)$$

$$\mathrm{CCRB}(\psi(t)) = \frac{8N^2-12N+4+L\|\boldsymbol{\alpha}\|^2(N^3+3N^2+2N)}{\mathrm{C_{SNR}}\ \alpha^2(t)N^2(N+1)(N+2)},$$

and

$$\mathrm{CCRB}(\alpha(t)) = \frac{\sigma^2}{2N}.$$

Furthermore, the cross terms are given by

$$[\mathbf{CCRB}(\boldsymbol{\xi})]_{1,2} = [\mathbf{CCRB}(\boldsymbol{\xi})]_{2,1} = \frac{-90}{\mathrm{C_{SNR}}\ LN(N^2-4)(N+1)},$$

$$[\mathbf{CCRB}(\boldsymbol{\xi})]_{1,3:3+L} = [\mathbf{CCRB}(\boldsymbol{\xi})]_{3:3+L,1} = \frac{-9(2N-1)}{\mathrm{C_{SNR}}\ LN(N+1)(N+2)}\mathbf{1}_L^T,$$

and

$$[\mathbf{CCRB}(\boldsymbol{\xi})]_{2,3:3+L} = [\mathbf{CCRB}(\boldsymbol{\xi})]_{3:3+L,2} = \frac{15}{\mathrm{C_{SNR}}\ LN(N+1)(N+2)}\mathbf{1}_L^T.$$

Proof: See Appendix A. □

b) Change of Variables: Even if the model (2) is widely used in array signal processing, its CRB relating to $\boldsymbol{\xi}$ does not bring us physical information. Then, it is interesting to analyze the CRB regarding the bearing θ and the range r which are the real physical parameters of the problem. From $\mathbf{CCRB}(\boldsymbol{\xi})$, one can easily obtain $\mathbf{CCRB}(\boldsymbol{\kappa})$ by using a change of variables formula (see [19, p. 45]):

$$\mathbf{CCRB}(\boldsymbol{\kappa}) = \frac{\partial\mathbf{g}(\boldsymbol{\xi})}{\partial\boldsymbol{\xi}^T}\mathbf{CCRB}(\boldsymbol{\xi})\frac{\partial\mathbf{g}^T(\boldsymbol{\xi})}{\partial\boldsymbol{\xi}}$$

where

$$\begin{aligned}\boldsymbol{\kappa} &= \mathbf{g}(\boldsymbol{\xi}) \\ &= [\,-\arcsin(\tfrac{\omega\lambda}{2\pi d}) \quad \tfrac{\pi d^2}{\lambda\phi}\cos^2(\arcsin(\tfrac{\omega\lambda}{2\pi d})) \quad \boldsymbol{\psi}^T \quad \boldsymbol{\alpha}^T\sigma^2\,]^T.\end{aligned}$$

Note that the function $\mathbf{g}(\boldsymbol{\xi})$ is well-defined *iff* $\phi \neq 0 \bmod(\pi)$ which implies $\theta \neq \pi/2 \bmod(\pi)$. This condition is intuitive since it corresponds to the ULA ambiguity situation. Then, if $\phi \neq 0 \bmod(\pi)$, the Jacobian matrix is given by $\partial\mathbf{g}(\boldsymbol{\xi})/\partial\boldsymbol{\xi}^T = \mathrm{bdiag}(\boldsymbol{A}, \boldsymbol{I}_{2L+1})$, where

$$\boldsymbol{A} = \frac{-\lambda}{2\pi d\cos(\theta)}\begin{bmatrix} 1 & 0 \\ -2r\tan(\theta) & \frac{2r^2}{d\cos(\theta)}\end{bmatrix}. \quad (9)$$

Consequently, one obtains the following theorem:

Theorem 2: Non-matrix closed-form expressions of $\mathbf{CCRB}(\boldsymbol{\kappa})$ corresponding to the bearing, the range, the amplitude and the shift phases relatively to the model (2) exist *iff* $N \geq 3$ and $\theta \neq \pi/2 \bmod(\pi)$ and $\alpha(t) \neq 0,\ \forall t = 1\cdots L$ and they are given by (10) and (11), shown at the bottom of the page. Furthermore, the cross terms between θ and r are as follows:

$$[\mathbf{CCRB}(\boldsymbol{\kappa})]_{1,2} = [\mathbf{CCRB}(\boldsymbol{\kappa})]_{2,1} = \frac{-3\lambda^2 r}{\mathrm{C_{SNR}}\ L\pi^2 d^3} \times \frac{15r(N-1)+d(8N-11)(2N-1)\sin(\theta)}{N(N^2-1)(N^2-4)\cos^3(\theta)}.$$

$$\mathrm{CCRB}(\theta) = \frac{3\lambda^2}{2\mathrm{C_{SNR}}\ Ld^2\pi^2\cos^2(\theta)}\frac{(8N-11)(2N-1)}{N(N^2-1)(N^2-4)}, \quad (10)$$

$$\mathrm{CCRB}(r) = \frac{6r^2\lambda^2}{\mathrm{C_{SNR}}\ L\pi^2 d^4}\frac{15r^2+30dr(N-1)\sin(\theta)+d^2(8N-11)(2N-1)\sin^2(\theta)}{N(N^2-1)(N^2-4)\cos^4(\theta)}. \quad (11)$$

B. The Unconditional Model

Let us consider now the unconditional model, i.e., when the signals are assumed to be Gaussian (with zero mean and variance σ_s^2) independent of the noise. The unknown parameter vectors are $\boldsymbol{\rho} = [\omega\ \phi\ \sigma_s^2\ \sigma^2]^T$ or $\boldsymbol{\vartheta} = [\theta\ r\ \sigma_s^2\ \sigma^2]^T$ depending if we are working on the electrical angles or on the physical parameters of interest. We first focus on the derivation of $\mathbf{UCRB}(\boldsymbol{\rho})$.

Under the unconditional model assumption, $\boldsymbol{x}(t)|\boldsymbol{\rho} \sim \mathcal{CN}(\mathbf{0}, \mathbf{R})\ \forall t = 1, \ldots, L$, where the covariance matrix $\mathbf{R} = \sigma_s^2 \mathbf{a}(\omega, \phi)\mathbf{a}^H(\omega, \phi) + \sigma^2 \mathbf{I}_N$. Consequently, the FIM in (3) becomes $[\mathbf{UFIM}(\boldsymbol{\rho})]_{i,k} = L\ \mathrm{tr}\{\mathbf{R}^{-1}(\partial \mathbf{R}/\partial[\boldsymbol{\rho}]_i)\mathbf{R}^{-1}(\partial \mathbf{R}/\partial[\boldsymbol{\rho}]_k)\}$. The matrix expression of $[\mathbf{UCRB}(\boldsymbol{\rho})]_{1:2,1:2}$ can be readily established (we omit the proof since it is obtained in the same way as in [13]) according to

$$[\mathbf{UCRB}(\boldsymbol{\rho})]_{1:2,1:2} = \frac{1}{2\mathrm{U}_{\mathrm{SNR}}\ \sigma_s^2 L}\left(\Re\left\{\left(\mathbf{D}^H \boldsymbol{\Pi}^{\perp}_{\mathbf{a}(\omega,\phi)}\mathbf{D}\right) \odot \left(\mathbf{J} \otimes \mathbf{a}^H(\omega,\phi)\mathbf{R}^{-1}\mathbf{a}(\omega,\phi)\right)^T\right\}\right)^{-1} \quad (12)$$

where $\mathrm{U}_{\mathrm{SNR}} = \sigma_s^2/\sigma^2$ denotes the unconditional SNR, $\mathbf{J} = \mathbf{1}_2\mathbf{1}_2^T, \mathbf{D} = [(\partial \mathbf{a}(\omega,\phi)/\partial\omega)(\partial \mathbf{a}(\omega,\phi)/\partial\phi)]$ and $\boldsymbol{\Pi}^{\perp}_{\mathbf{a}(\omega,\phi)} = \mathbf{I}_N - \mathbf{a}(\omega,\phi)(\mathbf{a}^H(\omega,\phi)\mathbf{a}(\omega,\phi))^{-1}\mathbf{a}^H(\omega,\phi)$. In the following we use (12) to derive non-matrix expressions of $\mathbf{UCRB}(\boldsymbol{\rho})$.

1) Analytical Inversion:

Theorem 3: Non-matrix expressions of $\mathbf{UCRB}(\boldsymbol{\rho})$ corresponding to the electrical angles are, well-defined *iff* $N \geq 3$, and are given by

$$\mathrm{UCRB}(\omega) = \left(1 + \frac{1}{\mathrm{U}_{\mathrm{SNR}}\ N}\right)\frac{6(2N-1)(8N-11)}{\mathrm{U}_{\mathrm{SNR}}\ L(N^2-1)N(N^2-4)}, \quad (13)$$

$$\mathrm{UCRB}(\phi) = \left(1 + \frac{1}{\mathrm{U}_{\mathrm{SNR}}\ N}\right)\frac{90}{\mathrm{U}_{\mathrm{SNR}}\ L(N^2-1)N(N^2-4)}. \quad (14)$$

Furthermore, the cross terms are given by

$$[\mathbf{UCRB}(\boldsymbol{\rho})]_{1,2} = [\mathbf{UCRB}(\boldsymbol{\rho})]_{2,1} = -\left(1 + \frac{1}{\mathrm{U}_{\mathrm{SNR}}\ N}\right)\frac{90}{\mathrm{U}_{\mathrm{SNR}}\ LN(N^2-4)(N+1)}.$$

Proof: See Appendix B. □

2) Change of Variables: using the same change of variables formula as for Theorem 2 one can easily prove.

Theorem 4: Non-matrix closed-form expressions of $\mathbf{UCRB}(\boldsymbol{\vartheta})$ corresponding to the range and bearing for a single narrowband near-field source are well-defined *iff* $N \geq 3$ and $\theta \neq \pi/2 \mathrm{mod}(\pi)$ and they are expressed in (15) and (16), shown at the bottom of the page. Furthermore, the cross terms between θ and r are given by

$$[\mathbf{UCRB}(\boldsymbol{\vartheta})]_{1,2} = [\mathbf{UCRB}(\boldsymbol{\vartheta})]_{2,1} = -\left(1 + \frac{1}{\mathrm{U}_{\mathrm{SNR}}\ N}\right)\frac{3\lambda^2 r}{\mathrm{U}_{\mathrm{SNR}}\ L\pi^2 d^3} \times \frac{15r(N-1) + d(8N-11)(2N-1)\sin(\theta)}{N(N^2-1)(N^2-4)\cos^3(\theta)}.$$

IV. Analysis of the CRB

The goal of this Section is to validate and analyze the proposed closed-form expressions. The behaviors of the CRB are detailed with respect to physical parameters of the problem.

A. Conditional and Unconditional CRB's Behavior

The scenario used in these simulations is an ULA of $N = 6$ sensors spaced by $d = 0.125$ m. The number of snapshots is equal to $L = 100$ and the location of the source is set as $r = 1.25$ m (which belongs to the Fresnel region according to (1) for $f_0 \in [600, 1200]$ MHz). In Fig. 1, we superimpose the CRBs, obtained from (11) and (16) to the computed CRBs. For these simulations, the signal source is a sample of a complex random Gaussian process with variance $\sigma_s^2 = 10$. The variance of the noise varies from 0.1 to 1.

Moreover, Fig. 1 shows the dependence of the $\mathrm{CCRB}(r)$ and $\mathrm{UCRB}(r)$ w.r.t. the carrier frequency f_0 and suggests that higher is the carrier frequency, lower is the bound. Furthermore, from the closed-form expressions given in (10), (11), (15) and (16), we notice the following.

- UCRB and CCRB are phase-invariant.
- $\mathrm{CCRB}(\theta)$ and $\mathrm{UCRB}(\theta)$ are just bearing-dependent as in the far-field scenario w.r.t. $O(1/\cos^2(\theta))$. It means that the ULA in the near-field case is not isotropic.
- For large N and fixed inter-spacing sensor, $\mathrm{CCRB}(\theta)$ and $\mathrm{UCRB}(\theta)$ in the near-field case tend to the asymptotic CRBs in the far-field case which are given by $(3\lambda^2)/(\mathrm{SNR}2d^2\pi^2\cos^2(\theta)N^3)$. This is consistent with the intuition since, due to the Fresnel constraint, large N implies large range, which corresponds to the far-field scenario.
- $\mathrm{CCRB}(r)$ and $\mathrm{UCRB}(r)$ are bearing-dependent and range-dependent. For r proportional to d, the dependence w.r.t. the range is $O(r^2)$, meaning that nearer is the source better is the range estimation (keeping in mind the Fresnel constraints).
- The dependence of the range w.r.t. the bearing is $O(1/\cos^4(\theta))$. For θ close to $\pi/2$ (i.e., close to the ambiguity situation), we observe that $\mathrm{CCRB}(r)$ and $\mathrm{UCRB}(r)$ go to infinity but faster than $\mathrm{CCRB}(\theta)$ and $\mathrm{UCRB}(\theta)$, respectively.
- For a sufficient number of sensors, $\mathrm{CCRB}(\theta), \mathrm{UCRB}(\theta)$, $\mathrm{CCRB}(r)$ and the $\mathrm{UCRB}(r)$ are $O(1/N^3)$.
- For λ proportional to $d, \mathrm{CCRB}(\theta)$ and $\mathrm{UCRB}(\theta)$ are independent of the carrier frequency f_0. This is not the case for $\mathrm{CCRB}(r)$ and $\mathrm{UCRB}(r)$. Furthermore, note that higher is the carrier frequency, better is the estimation of the range (cf. Fig. 1).
- Note that the expressions of $[\mathbf{CCRB}(\boldsymbol{\kappa})]_{1,2}, [\mathbf{CCRB}(\boldsymbol{\kappa})]_{2,1}$, $[\mathbf{UCRB}(\boldsymbol{\vartheta})]_{1,2}$ and $[\mathbf{UCRB}(\boldsymbol{\vartheta})]_{2,1}$ show that the physical parameters of interest are strongly coupled since $[\mathbf{CCRB}(\boldsymbol{\kappa})]_{1,2}$ and $[\mathbf{UCRB}(\boldsymbol{\vartheta})]_{1,2}$ are $O(1/N^3)$ as $\mathrm{CCRB}(\theta), \mathrm{CCRB}(r), \mathrm{UCRB}(\theta)$ and $\mathrm{UCRB}(r)$.
- Finally, since $\mathrm{UCRB}(\omega)$ is $O(1/N^3)$ and $\mathrm{UCRB}(\phi)$ is $O(1/N^5)$, thus, for a sufficient number of sensors the estimation of the so-called second electrical angle ϕ is more accurate than estimating the first electrical angle ω.

$$\mathrm{UCRB}(\theta) = \left(1 + \frac{1}{\mathrm{U}_{\mathrm{SNR}}\ N}\right)\frac{3\lambda^2}{2\mathrm{U}_{\mathrm{SNR}}\ Ld^2\pi^2\cos^2(\theta)}\frac{(8N-11)(2N-1)}{N(N^2-1)(N^2-4)}, \quad (15)$$

$$\mathrm{UCRB}(r) = \left(1 + \frac{1}{\mathrm{U}_{\mathrm{SNR}}\ N}\right)\frac{6r^2\lambda^2}{\mathrm{U}_{\mathrm{SNR}}\ L\pi^2 d^4}\frac{15r^2 + 30dr(N-1)\sin(\theta) + d^2(8N-11)(2N-1)\sin^2(\theta)}{N^2(N^2-1)(N^2-4)\cos^4(\theta)}. \quad (16)$$

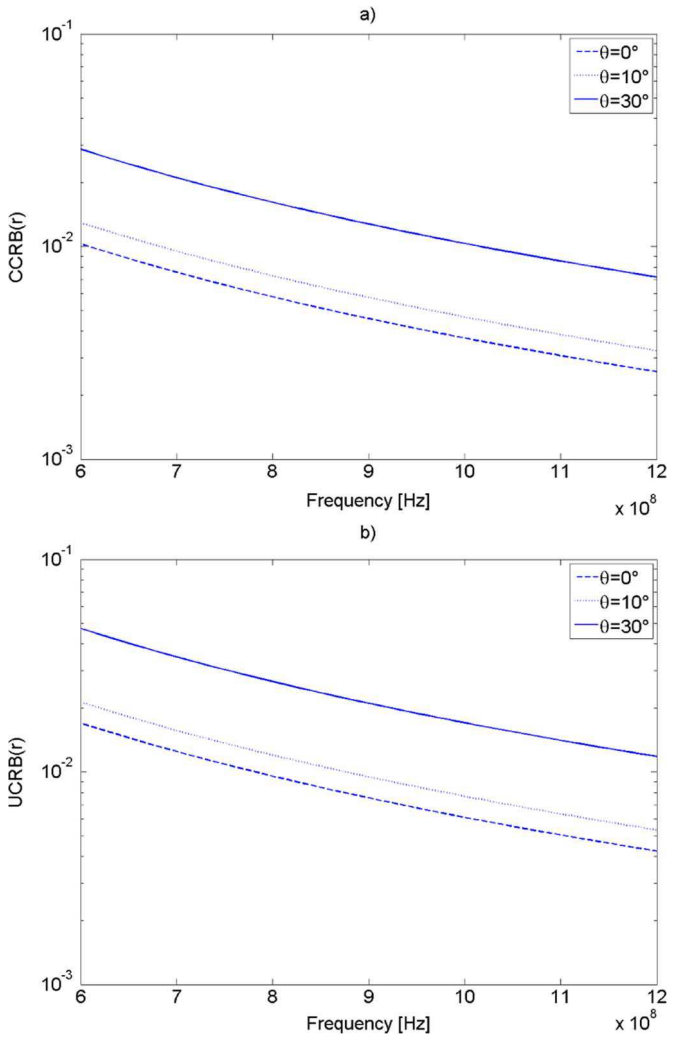

Fig. 1. $\mathrm{CRB}(r)$ versus f_0 for $\sigma^2 = 0.5$ and different values of $\theta = 10°, 30°, 50°$: (a) $\mathrm{CCRB}(r)$ and (b) $\mathrm{UCRB}(r)$.

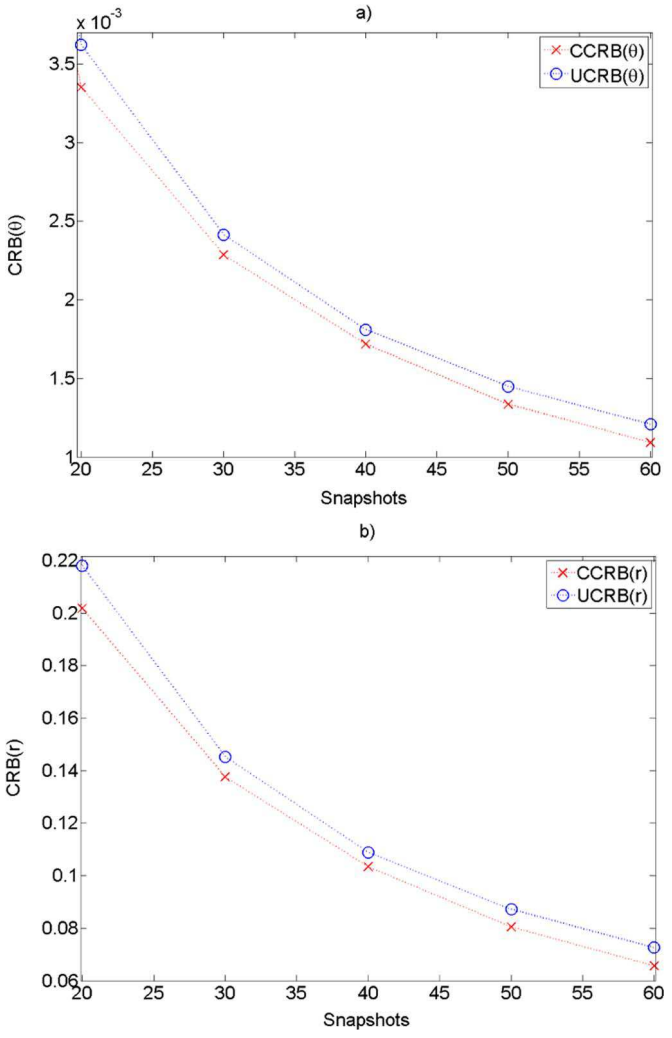

Fig. 2. CRBs versus the number of snaphots for $N = 10$: (a) $\mathrm{CCRB}(\theta)$ and $\mathrm{UCRB}(\theta)$, (b) $\mathrm{CCRB}(r)$ and $\mathrm{UCRB}(r)$.

B. Analytical and Numerical Comparison Between the CCRB and the UCRB

Since the conditional model does not make any assumptions on the source, we can chose the phase and the amplitude of the source as samples of a random process. In this case, we can study an analytical and numerical comparison between the conditional and the unconditional CRB. Furthermore, we assume that the two physical quantities $\mathrm{C_{SNR}}$ and $\mathrm{U_{SNR}}$ are equals to the same quantity denoted by SNR.

Corollary 1: From (7) and (13), one obtains the following: $\mathrm{UCRB}(\omega)/\mathrm{CCRB}(\omega) = 1 + (1/(\mathrm{SNR}\ N))$, and $\mathrm{UCRB}(\phi)/\mathrm{CCRB}(\phi) = 1 + (1/(\mathrm{SNR}\ N))$. In the same way, from (10) and (15), one obtains the following: $\mathrm{UCRB}(\theta)/\mathrm{CCRB}(\theta) = 1 + (1/(\mathrm{SNR}\ N))$, and $\mathrm{UCRB}(r)/\mathrm{CCRB}(r) = 1 + (1/(\mathrm{SNR}\ N))$, i.e., $\mathrm{UCRB}(\omega) \geq \mathrm{CCRB}(\omega), \mathrm{UCRB}(\phi) \geq \mathrm{CCRB}(\phi)$ and $\mathrm{UCRB}(\theta) \geq \mathrm{CCRB}(\theta)$, $\mathrm{UCRB}(r) \geq \mathrm{CCRB}(r)$ (cf. Fig. 2). Note that, a similar result has been shown in the far-field case in [12].

Furthermore,

- for a fixed N: $\mathrm{CCRB}(\theta) \overset{\mathrm{SNR}\to\infty}{\to} \mathrm{UCRB}(\theta)$, and $\mathrm{CCRB}(r) \overset{\mathrm{SNR}\to\infty}{\to} \mathrm{UCRB}(r)$.
- for a fixed SNR: $\mathrm{CCRB}(\theta) \overset{N\to\infty}{\to} \mathrm{UCRB}(\theta)$ and $\mathrm{CCRB}(r) \overset{N\to\infty}{\to} \mathrm{UCRB}(r)$.
- and finally, for $1/(\mathrm{SNR}\ N) \ll 1$: $\mathrm{CCRB}(\theta) \approx \mathrm{UCRB}(\theta)$ and $\mathrm{CCRB}(r) \approx \mathrm{UCRB}(r)$.

V. Conclusion

In this correspondence, the conditional and the unconditional Cramér–Rao bounds are derived in a closed-form expressions for a single near-field time-varying narrowband source in terms of range and bearing. These expressions are given in non-matrix forms which are important in order to avoid a costly Fisher information matrix numerical inversion. Moreover these expressions provide useful information concerning the behavior of the bounds. In this way, the proposed expressions have been analyzed with respect to the physical parameters of the problem. In particular, we provided an explicit link between the conditional and the unconditional CRB and we shown that higher is the carrier frequency and/or closer is the source from the array, better is the estimation of the range.

Appendix A

In this Appendix, we highlight the major steps leading to Theorem 1. From (5) one has,

$$\begin{aligned}\det\{\mathbf{CFIM}(\boldsymbol{\xi})\} &= \det\{\boldsymbol{Q}\}\det\{\boldsymbol{Y}\} \\ &= \det\left\{\boldsymbol{\Lambda}_{\mathbf{F}_{\psi\psi}}\right\}\det\{\mathbf{F}_{\psi\psi}\}\det\{\boldsymbol{Y}\} \qquad (17)\end{aligned}$$

$$\mathbf{D}^H\mathbf{\Pi}_{\mathbf{a}}^{\perp}\mathbf{D} = \mathbf{D}^H\mathbf{D} - \frac{1}{N}(\mathbf{a}^H\mathbf{D})^H(\mathbf{a}^H\mathbf{D})$$
$$= \begin{bmatrix} \sum_{n=0}^{N-1} n^2 - \frac{1}{N}\left(\sum_{n=0}^{N-1} n\right)^2 & \sum_{n=0}^{N-1} n^3 - \frac{1}{N}\left(\sum_{n=0}^{N-1} n\right)\left(\sum_{n=0}^{N-1} n^2\right) \\ \sum_{n=0}^{N-1} n^3 - \frac{1}{N}\left(\sum_{n=0}^{N-1} n\right)\left(\sum_{n=0}^{N-1} n^2\right) & \sum_{n=0}^{N-1} n^4 - \frac{1}{N}\left(\sum_{n=0}^{N-1} n^2\right)^2 \end{bmatrix}.$$

where $\mathbf{\Lambda}_{\mathbf{F}_{\boldsymbol{\psi}\boldsymbol{\psi}}}$ denotes the Schur complement w.r.t. the matrix $\mathbf{F}_{\boldsymbol{\psi}\boldsymbol{\psi}}$. Assuming that $\alpha(t) \neq 0,\ \forall t = 1\cdots L$, $\mathbf{F}_{\boldsymbol{\psi}\boldsymbol{\psi}}$ is invertible and the Schur complement is expressed as follows:

$$\mathbf{\Lambda}_{\mathbf{F}_{\boldsymbol{\psi}\boldsymbol{\psi}}} = \begin{bmatrix} f_{\omega\omega} & f_{\omega\phi} \\ f_{\phi\omega} & f_{\phi\phi} \end{bmatrix} - \begin{bmatrix} \mathbf{f}_{\omega\boldsymbol{\psi}} \\ \mathbf{f}_{\phi\boldsymbol{\psi}} \end{bmatrix} \mathbf{F}_{\boldsymbol{\psi}\boldsymbol{\psi}}^{-1} [\, \mathbf{f}_{\boldsymbol{\psi}\omega} \quad \mathbf{f}_{\boldsymbol{\psi}\phi}\,]$$
$$= \boldsymbol{B} - \frac{\sigma^2}{2N}\boldsymbol{W}\,\mathrm{diag}(\boldsymbol{\alpha}\odot\boldsymbol{\alpha})^{-1}\boldsymbol{W}^T \tag{18}$$

where

$$\boldsymbol{B} = \mathrm{C_{SNR}}\, LN(N-1)\begin{bmatrix} \frac{(2N-1)}{3} & \frac{N(N-1)}{2} \\ \frac{N(N-1)}{2} & \frac{(2N-1)(3N^2-3N-1)}{15} \end{bmatrix},$$

and

$$\boldsymbol{W} = \frac{1}{\sigma^2}\begin{bmatrix} N(N-1) \\ \frac{N(N-1)(2N-1)}{3} \end{bmatrix} \otimes (\boldsymbol{\alpha}\odot\boldsymbol{\alpha})^T.$$

Thus, by replacing (18) in (17) one obtains

$$\det\{\mathbf{CFIM}(\boldsymbol{\xi})\} = \frac{1}{540}\left(\frac{2N}{\sigma^2}\right)^{2L} N^2(N^2-4)(N-1)^2(N+1)^2\|\boldsymbol{\alpha}\|^2\prod_{t=1}^{L}\alpha^2(t).$$

Consequently, $\det\{\mathbf{CFIM}(\boldsymbol{\xi})\} \neq 0$ *iff* $N \geq 3$ and $\alpha(t) \neq 0\ \forall t = 1\ldots L$. Assuming $N \geq 3$ and $\alpha(t) \neq 0\ \forall t = 1\ldots L$, one has

$$\mathbf{CFIM}^{-1}(\boldsymbol{\xi}) = \mathrm{bdiag}(\boldsymbol{Q}^{-1}, \boldsymbol{Y}^{-1})$$

where

$$\boldsymbol{Y}^{-1} = \mathrm{bdiag}\left(\frac{\sigma^2}{2N}\mathbf{I}_L, \frac{\sigma^4}{NL}\right).$$

In order to derive $\boldsymbol{Q}^{-1}$, we use the Schur complement $\mathbf{\Lambda}_{\mathbf{F}_{\boldsymbol{\psi}\boldsymbol{\psi}}}$ given in (18). Thus,

$$[\mathbf{CCRB}(\boldsymbol{\xi})]_{1:2,1:2} = \mathbf{\Lambda}_{\mathbf{F}_{\boldsymbol{\psi}\boldsymbol{\psi}}}^{-1}.$$

Since the Schur complement $\mathbf{\Lambda}_{\mathbf{F}_{\boldsymbol{\psi}\boldsymbol{\psi}}}$ is a 2×2 matrix, its inverse is easily derivable and leads to (7), (8). The other terms are directly derived from the following calculation, where

$$\mathbf{CCRB}(\boldsymbol{\psi}) = \frac{\sigma^2}{2N}\mathrm{diag}(\boldsymbol{\alpha}\odot\boldsymbol{\alpha})^{-1} \times \left(\mathbf{I}_L + \frac{\sigma^2}{2N}\boldsymbol{W}^T\mathbf{\Lambda}_{\mathbf{F}_{\boldsymbol{\psi}\boldsymbol{\psi}}}^{-1}\boldsymbol{W}\,\mathrm{diag}(\boldsymbol{\alpha}\odot\boldsymbol{\alpha})^{-1}\right),$$
$$[\mathbf{CCRB}(\boldsymbol{\xi})]_{1:2,3:L+2} = ([\mathbf{CCRB}(\boldsymbol{\xi})]_{3:L+2,1:2})^H = \frac{-\sigma^2}{2N^2}\mathbf{\Lambda}_{\mathbf{F}_{\boldsymbol{\psi}\boldsymbol{\psi}}}^{-1}\boldsymbol{W}\,\mathrm{diag}(\boldsymbol{\alpha}\odot\boldsymbol{\alpha})^{-1}.$$

APPENDIX B

In this Appendix, the dependence on (ω,ϕ) of $\boldsymbol{a}(\omega,\phi)$ is omitted for sake of simplicity. Applying the matrix inversion lemma [18] to $\mathbf{R}$, one obtains

$$\mathbf{R}^{-1} = \frac{1}{\sigma_s^2}\left(\mathbf{a}\mathbf{a}^H + \frac{1}{\mathrm{U_{SNR}}}\mathbf{I}_N\right)^{-1} = \frac{\mathrm{U_{SNR}}}{\sigma_s^2}\left(\mathbf{I}_N - \mathrm{U_{SNR}}\frac{\mathbf{a}\mathbf{a}^H}{1+\mathrm{U_{SNR}}N}\right).$$

Thus, using the above equation one has

$$\mathbf{J}\otimes\left(\sigma_s^2\mathbf{a}^H\mathbf{R}^{-1}\mathbf{a}\sigma_s^2\right)^T = \sigma_s^2\mathrm{U_{SNR}}\left(N - \frac{\mathrm{U_{SNR}}\,N^2}{1+\mathrm{U_{SNR}}\,N}\right)\mathbf{J}. \tag{19}$$

On the other hand, the derivation of $\boldsymbol{a}$ w.r.t. ω and ϕ leads to

$$[\mathbf{D}]_{i,k} = j((i-1)\delta(k-1) + (i-1)^2\delta(k-2))e^{j(\omega n+\phi n^2)} \quad \forall i = 1\cdots N \text{ and } \forall k = 1,2.$$

Consequently [see the equation shown at the top of the page]. Thus, using the above expression and (19) and after some simplifications, we obtain

$$\Re\left\{\sigma_s^4\left(\mathbf{D}^H\mathbf{\Pi}_{\mathbf{a}}^{\perp}\mathbf{D}\right)\odot(\mathbf{J}\otimes\mathbf{a}^H\mathbf{R}^{-1}\mathbf{a})^T\right\} = \frac{\mathrm{U_{SNR}^2}\,LN(N^2-4)}{6\mathrm{U_{SNR}}\,N+6}\begin{bmatrix} \frac{15}{(N^2-1)} & \frac{15}{(N+1)} \\ \frac{15}{(N+1)} & \frac{(2N-1)(8N-11)}{(N^2-1)} \end{bmatrix} \tag{20}$$

which leads to

$$\det\left\{\sigma_s^4\Re\left\{\left(\mathbf{D}^H\mathbf{\Pi}_{\mathbf{a}}^{\perp}\mathbf{D}\right)\odot(\mathbf{J}\otimes\mathbf{a}^H\mathbf{R}^{-1}\mathbf{a})^T\right\}\right\} = \frac{1}{540}\mathrm{U_{SNR}}\left(1+\frac{\mathrm{U_{SNR}}}{N}\right)N^2(N^2-4)(N-1)^2(N+1)^2.$$

Consequently,

$$\det\left\{\sigma_s^4\Re\left\{\left(\mathbf{D}^H\mathbf{\Pi}_{\mathbf{a}}^{\perp}\mathbf{D}\right)\odot(\mathbf{J}\otimes\mathbf{a}^H\mathbf{R}^{-1}\mathbf{a})^T\right\}\right\} \neq 0 \Leftrightarrow N \geq 3.$$

Then, assuming that $N \geq 3$ and replacing (20) in (12), we obtain

$$[\mathbf{UCRB}(\boldsymbol{\rho})]_{1:2,1:2} = \left(1+\frac{1}{\mathrm{U_{SNR}}\,N}\right)\frac{6}{\mathrm{U_{SNR}}\,L(N^2-4)} \times \begin{bmatrix} \frac{(2N-1)(8N-11)}{(N^2-1)} & -\frac{15}{(N+1)} \\ -\frac{15}{(N+1)} & \frac{15}{(N^2-1)} \end{bmatrix}.$$

REFERENCES

[1] M. N. El. Korso, R. Boyer, A. Renaux, and S. Marcos, "Nonmatrix closed-form expressions of the Cramér-Rao bounds for near-field localization parameters," in *Proc. IEEE Int. Conf. Acoust., Speech, Signal Processing*, Taipei, Taiwan, 2009, pp. 3277–3280.

[2] H. Krim and M. Viberg, "Two decades of array signal processing research: The parametric approach," *IEEE Signal Process. Mag.*, vol. 13, no. 4, pp. 67–94, 1996.

[3] I. Bekkerman and J. Tabrikian, "Target detection and localization using MIMO radars and sonars," *IEEE Trans. Signal Process.*, vol. 54, no. 11, pp. 3873–3883, Oct. 2006.

[4] J. Lebrun and P. Comon, "An algebraic approach to blind identification of communication channels," in *Proc. IEEE ISSPA*, Paris, France, Jul. 2003, pp. 1–4.

[5] S. Haykin, *Array Signal Processing*. Englewood Cliffs, NJ: Prentice-Hall, 1985.

[6] E. Grosicki, K. Abed-Meraim, and Y. Hua, "A weighted linear prediction method for near-field source localization," *IEEE Trans. Signal Process.*, vol. 53, no. 10, pp. 3651–3660, Oct. 2005.

[7] W. Zhi and M. Chia, "Near-field source localization via symmetric subarrays," *IEEE Signal Process. Lett.*, vol. 14, no. 6, pp. 409–412, 2007.
[8] M. N. El. Korso, G. Bouleux, R. Boyer, and S. Marcos, "Sequential estimation of the range and the bearing using the zero-forcing MUSIC approach," in *Proc. EUSIPCO*, Glasgow, Scotland, Aug. 2009, pp. 1404–1408.
[9] H. Cramér, *Mathematical Methods of Statistics*. New York: Princeton Univ. Press, 1946.
[10] B. Ottersten, M. Viberg, P. Stoica, and A. Nehorai, "Exact and large sample maximum likelihood techniques for parameter estimation and detection in array processing," in *Radar Array Processing*, S. Haykin, J. Litva, and T. J. Shepherd, Eds. Berlin, Germany: Springer-Verlag, 1993, ch. 4, pp. 99–151.
[11] A. Renaux, P. Forster, E. Chaumette, and P. Larzabal, "On the high SNR conditional maximum-likelihood estimator full statistical characterization," *IEEE Trans. Signal Process.*, vol. 54, no. 12, pp. 4840–4843, Dec. 2006.
[12] P. Stoica and A. Nehorai, "Performances study of conditional and unconditional direction of arrival estimation," *IEEE Trans. Acoust., Speech, Signal Process.*, vol. 38, pp. 1783–1795, Oct. 1990.
[13] P. Stoica, E. Larsson, and A. Gershman, "The stochastic CRB for array processing: A textbook derivation," *IEEE Signal Process. Lett.*, vol. 8, pp. 148–150, May 2001.
[14] M. Pesavento and A. Gershman, "Maximum-likelihood direction-of-arrival estimation in the presence of unknown nonuniform noise," *IEEE Trans. Signal Process.*, vol. 49, no. 7, pp. 1310–1324, Jul. 2001.
[15] A. Gershman, P. Stoica, M. Pesavento, and E. Larsson, "Stochastic Cramér–Rao bound for direction estimation in unknown noise fields," *Proc. Inst. Electr. Eng.—Radar, Sonar, Navigat.*, vol. 149, pp. 2–8, Jan. 2002.
[16] P. Stoica and A. Nehorai, "MUSIC, maximum likelihood and the Cramér Rao bound," *IEEE Trans. Acoust., Speech, Signal Process.*, vol. 37, pp. 720–741, May 1989.
[17] A. J. Weiss and B. Friedlander, "Range and bearing estimation using polynomial rooting," *IEEE J. Ocean. Eng.*, vol. 18, pp. 130–137, Jul. 1993.
[18] P. Stoica and R. Moses, *Spectral Analysis of Signals*. Englewood Cliffs, NJ: Prentice-Hall, 2005.
[19] S. M. Kay, *Fundamentals of Statistical Signal Processing*. Englewood Cliffs, NJ: Prentice-Hall, 1993, vol. 1.

Optimal Relay Function in the Low-Power Regime for Distributed Estimation Over a MAC

Marco Guerriero, Stefano Marano, Vincenzo Matta, and Peter Willett, *Fellow, IEEE*

***Abstract*—A random parameter is estimated by a distributed network of sensors that communicate over a common multiple-access channel (MAC). A MAC implies an additive fusion rule, and the goal here is to design a power-constrained forwarding strategy and fusion center post-processing. To get an explicit solution we appeal to asymptotics, meaning that we design the *locally* optimal scheme for the limiting case that the received power goes to zero.**

***Index Terms*— Distributed estimation, MAC, relay.**

I. Introduction and Background

Reliable data delivery from several remote sensors sharing a common transmission medium is possible, and can be realized by employing source and channel coding strategies borrowed from (or extending) classical point-to-point results. This approach decouples the source and channel coding stages; however, it is known that this separation is not necessarily optimal [1] when the sources are correlated and/or one's goal is not direct recovery of the observations.

A basic lesson from [2] is that there exist cases in which a simple amplify-and-forward strategy outperforms the best separate scheme by orders of magnitude. This happens, for instance, for Gaussian estimation problems over a Gaussian MAC [3], and it is due to the perfect match between the (additive) nature of the optimal MMSE estimator and the (additive) channel structure. In this work, we depart from the source/channel Gaussian model and the corresponding amplify-and-forward solution, allowing the local encoders to apply a nonlinear transformation to arbitrarily distributed observations (see Fig. 1). We limit ourselves to the ideal MAC—not necessarily a Gaussian one—that requires perfect synchronization of the transmissions, both in time and phase, at the local sensors, and we operate under a relayed power constraint.

Joint consideration of the estimation problem and the noisy MAC is in [4] and [5], in which in the asymptote of an increasingly large number of sensors an optimal communication/estimation scheme (called type-based multiple access, or TBMA) was proposed for quantized observations. A likelihood-based multiple access (LBMA) scheme, suitable for continuous observations, was discussed in [6], and yields asymptotically efficient estimation over a waveform channel.

Manuscript received September 08, 2009; accepted December 09, 2009. Date of publication January 29, 2010; date of current version April 14, 2010. The associate editor coordinating the review of this manuscript and approving it for publication was Dr. Biao Chen. M. Guerriero and P. Willett were supported by the Office of Naval Research under Contract N00014-07-1-0429 and N00014-07-1-0055.

M. Guerriero and P. Willett are with the Department of Electrical and Computer Engineering, University of Connecticut, U-2157, Storrs, CT 06269 USA (e-mail: marco.guerriero@engr.uconn.edu; willett@engr.uconn.edu; p.willett@ieee.org).

S. Marano and V. Matta are with the Department of Information and Electrical Engineering (DIIIE), University of Salerno, 84084 Fisciano (SA), Italy (e-mail: marano@unisa.it; vmatta@unisa.it).

Color versions of one or more of the figures in this paper are available online at http://ieeexplore.ieee.org.

Digital Object Identifier 10.1109/TSP.2010.2041870

A.2 IEEE-SP-P

M. N. El Korso, A. Renaux, R. Boyer and S. Marcos, "Deterministic Performance Bounds on the Mean Square Error for Near Field Source Localization", en préparation pour *IEEE Transactions on Signal Processing*.

Deterministic Lower Bounds on the Mean Square Error for Near Field Source Localization

Mohammed Nabil EL KORSO, *Student Member, IEEE,* Alexandre RENAUX, *Member, IEEE,* Rémy BOYER, *Member, IEEE* and Sylvie MARCOS

***Abstract*— This correspondence investigates deterministic lower bounds on estimator's mean square error applied to the passive near field source localization. More precisely, we focus on the so-called threshold prediction. As a by product, we give closed form expressions of the McAulay-Seidman, the Hammersley-Chapman-Robbins, the McAulay-Hofstetter bounds and also, a new proposed bound, the so-called Cramér-Rao Fourier bound, for the conditional model observation (*i.e.,* parameterized mean) and the unconditional model observation (*i.e.,* parameterized covariance matrix). Finally, numerical simulations are given to assess the efficiency of these lower bounds to approximate the estimator's mean square error and to predict the threshold effect.**

***Index Terms*—** Near field source localization, performance analysis, mean square error, threshold prediction, deterministic lower bounds.

I. Introduction

The near field source localization is an important and challenging topic with several applications such as sonar, seismology, digital communications, etc. Unlike the far field assumption, in the near field context the curvature of the waves impinging on the sensors is not planar. Consequently, each source is characterized not only by its bearing but, also by its range making the estimation scheme more complex. Nevertheless, one can note the existence of a large number of estimation algorithm adapted to the passive near field source localization [1]–[5].

There exist only a few number of works studying the optimal asymptotic estimation performance in this context [3], [6] (by asymptotic we mean a large signal to noise ratio or a large number of snapshots [7], [8]). More precisely, to characterize the asymptotic performance of an estimator in terms of the mean square error, the Cramér-Rao bound is the most popular tool [9] which is a tight bound under certain mild/general condition [10]. However, the Cramér-Rao bound becomes too optimistic in the non-asymptotic region which has the effect of making the Cramér-Rao bound a not tight and not valid bound in the non-asymptotic region [11]. This non-asymptotic region is delimited by the so-called threshold or breakdown point (*i.e.,* when the estimator's mean square error increases dramatically due to the outlier effect [12]). One should note that the prediction of this threshold is of great important since it delimits the optimal operation zone of the estimator's working range.

The authors are with Laboratoire des Signaux et Systèmes (L2S), Université Paris-Sud XI (UPS), CNRS, SUPELEC, 3 rue Joliot Curie, Gif-Sur-Yvette, 91192, France, phone: +331 6985 1763, fax: +331 6985 1765, {elkorso, remy.boyer, alexandre.renaux, marcos}@lss.supelec.fr. This project is funded by region Île de France and Digeteo Research Park.

However, and to the best of our knowledge, no result can be find in the literature concerning the threshold prediction in the near field source localization. In this correspondence, we fill this lack. More precisely, we consider the two source signal model assumptions (where the observation model is corrupted by a spatially colored noise): the conditional model (*i.e.,* when the signals are assumed to be deterministic) and the unconditional model (*i.e.,* when the signals are assumed to be driven by a Gaussian random process). For each model, we propose to characterize the threshold region using some deterministic lower bounds on the estimator's mean square error. In particular, we derive and analyze the following deterministic lower bounds: the McAulay-Seidman [13], the Hammersley-Chapman-Robbins [14], [15], the McAulay-Hofstetter [16] bounds and also, a new proposed bound, the so-called Cramér-Rao Fourier bound [17].

II. Model setup

Let us considere a uniform and linear array (ULA) composed of N sensors with an inter-element spacing d. We suppose that the ULA recieve a single near-field and narrow-band source. Consequently, the observation model is given as follows [1]:

$$x_n(t) = s(t)e^{j\tau_n} + v_n(t), \quad t = 1, \ldots, T \quad \text{and} \quad n = 0, \ldots, N-1, \tag{1}$$

where T denotes the number of snapshots, whereas, $x_n(t)$ is the observed signal at the output of the $(n+1)$th sensor. The source signal is denoted by $s(t)$. The random process $v_n(t)$ is an additive noise. The time delay τ_n associated with the signal propagation time from the first sensor to the $(n+1)$th sensor is given by [3]:

$$\tau_n = \frac{2\pi r}{\lambda}\left(\sqrt{1 + \frac{n^2 d^2}{r^2} - \frac{2nd\sin\theta}{r}} - 1\right), \tag{2}$$

where λ is the signal wavelength and where r and $\theta \in [0, \pi/2]$ denote the range and the bearing of the source, respectively. In the following we assume that the source is located in the so-called Fresnel region [2], meaning that,

$$0.62(d^3(N-1)^3/\lambda)^{1/2} < r < 2d^2(N-1)^2/\lambda, \tag{3}$$

in this case, the time delay is given by:

$$\tau_n = \omega n + \phi n^2 + O\left(\frac{d^2}{r^2}\right), \tag{4}$$

where $O\left(\frac{d^2}{r^2}\right)$ denotes the terms of order larger or equal to $\frac{d^2}{r^2}$, in which the so-called electrical angles are given by:

$$\omega = -2\pi\frac{d}{\lambda}\sin(\theta), \tag{5}$$

and

$$\phi = \pi\frac{d^2}{\lambda r}\cos^2(\theta). \tag{6}$$

Neglecting $O\left(\frac{d^2}{r^2}\right)$, the time delay τ_n can be approximated by the following quadratic form $\tau_n = \omega n + \phi n^2$. Consequently, the observation vector can be expressed as:

$$\mathbf{x}(t) = [x_1(t)\dots x_N(t)]^T = \mathbf{a}(\omega,\phi)s(t) + \mathbf{v}(t), \tag{7}$$

where $\mathbf{v}(t) = [v_1(t)\dots v_N(t)]^T$, and where, the $(n+1)$th element of the steering vector $\mathbf{a}(\omega,\phi)$ is given by $[\mathbf{a}(\omega,\phi)]_{n+1} = e^{j(\omega n+\phi n^2)}$.

In the remaining of this paper, we will use the following assumptions :

- The noise will be assumed to be a complex circular with zero mean with a known covariance full rank matrix $\mathbf{\Sigma}_{\text{noise}}$.
- For both conditional (*i.e.,* deterministic [7]) and unconditional (*i.e.,* stochastic [18]) model, the unknown vector parameter is given by $\boldsymbol{\xi} = [\omega\ \phi]^T$.

In the following $\boldsymbol{\xi}_0, \omega_0$ and ϕ_0 represent the real value of the candidate parameters $\boldsymbol{\xi}, \omega$ and ϕ, respectively. The joint probability density function of the observations $\boldsymbol{\chi} = [\mathbf{x}^T(1)\dots\mathbf{x}^T(T)]^T \sim \mathcal{CN}(\boldsymbol{\mu}(\boldsymbol{\xi}_0), \mathbf{\Sigma}(\boldsymbol{\xi}_0))$ for a given $\boldsymbol{\xi}_0$, is expressed as:

$$p(\boldsymbol{\chi};\boldsymbol{\xi}_0) = \frac{1}{\pi^{NT}\left|\mathbf{\Sigma}(\boldsymbol{\xi}_0)\right|}e^{-(\boldsymbol{\chi}-\boldsymbol{\mu}(\boldsymbol{\xi}_0))^H\mathbf{\Sigma}(\boldsymbol{\xi}_0)^{-1}(\boldsymbol{\chi}-\boldsymbol{\mu}(\boldsymbol{\xi}_0))}, \tag{8}$$

in which $|.|$ denotes the determinate operator.

III. Deterministic lower bounds derivation

In [17], [19] the authors provide a different unification of some well known lower bounds on the mean square error of unbiased estimators of deterministic parameters. More precisely, in [19], Forster and Larzabal, solved the problem of establishing lower bounds on the mean square error for deterministic parameter estimation using a constrained optimization problem. By imposing some adequate constraints on the bias for the considered optimization problem, they obtained several lower bounds as the Cramér-Rao, the Barankin and the Battacharya bounds. In [17], Todros and Tabrikian propose a new class of performance lower bounds using the so-called integral transform which generalizes the derivative applied on the likelihood-ratio function. Thus, they showed that some well known lower bounds (as the Cramér-Rao, the McAulay-Seidman and the Battacharya bounds) are obtained by a proper choice of the kernel of the integral transform.

A. Deterministic lower bounds unification

The two unifications presented in [17], [19] are formulated differently but lead to the same result. In the remanning of this correspondence, we chose to adopt the unification presented in [17]. It is shown that each lower bound can be written in the following form:

$$\int_{\mathbb{C}^{NT}}\left(\hat{\boldsymbol{\xi}}-\boldsymbol{\xi}_0\right)\left(\hat{\boldsymbol{\xi}}-\boldsymbol{\xi}_0\right)^T p(\boldsymbol{\chi};\boldsymbol{\xi}_0)d\boldsymbol{\chi} \succcurlyeq \boldsymbol{C} = \mathbf{\Gamma}\boldsymbol{K}^{-1}\mathbf{\Gamma}^H \tag{9}$$

with $\boldsymbol{K} = E_{\boldsymbol{\chi};\boldsymbol{\xi}_0}\left\{\boldsymbol{\gamma}\boldsymbol{\gamma}^H\right\}$, where $\hat{\boldsymbol{\xi}}$ denotes the estimate of the true value parameter $\boldsymbol{\xi}_0$, $E_{\boldsymbol{\chi};\boldsymbol{\xi}_0}\{.\}$ is the expectation *w.r.t.* $p(\boldsymbol{\chi};\boldsymbol{\xi}_0)$, $\boldsymbol{C}$ is a lower bound matrix, $\boldsymbol{A} \succcurlyeq \boldsymbol{B}$ means that the matrix $\boldsymbol{A}-\boldsymbol{B}$ is non-negative defined. Consequently, for a specific choice of the couple $(\mathbf{\Gamma},\boldsymbol{\gamma})$, one obtains a specific lower bound. In this way, the Cramér-Rao bound (CRB) can be defined using the following couple:

$$\begin{cases}\mathbf{\Gamma}_{\text{CRB}} &= \mathbf{1}_2,\\ \boldsymbol{\gamma}_{\text{CRB}} &= \frac{\partial \ln p(\boldsymbol{x};\boldsymbol{\xi})}{\partial\boldsymbol{\xi}}|_{\boldsymbol{\xi}=\boldsymbol{\xi}_0},\end{cases} \tag{10}$$

where $\mathbf{1}_2$ denotes the 2×1 vector filled by ones. For the following couple:

$$\begin{cases}\mathbf{\Gamma}_{\text{MSB}} &= \mathbf{\Phi},\\ \boldsymbol{\gamma}_{\text{MSB}} &= [\nu(\boldsymbol{x};\boldsymbol{\xi}_1)\ \dots\ \nu(\boldsymbol{x};\boldsymbol{\xi}_L)]^T,\end{cases} \tag{11}$$

one obtains the McAulay-Seidman bound (MSB), in which the so-called ratio-likelihood function is given by:

$$\nu(\boldsymbol{x};\boldsymbol{\xi}_l) = \frac{p(\boldsymbol{x};\boldsymbol{\xi}_l)}{p(\boldsymbol{x};\boldsymbol{\xi}_0)}, \tag{12}$$

and where $\boldsymbol{\xi}_l$ for $l = 1,\dots,L$ denotes the L test points, whereas $\mathbf{\Phi} = [\boldsymbol{\xi}_1-\boldsymbol{\xi}_0\ \dots\ \boldsymbol{\xi}_L-\boldsymbol{\xi}_0]^T$. The Hammersley-Chapman-Robbins bound (HCRB) can be defined using $\mathbf{\Gamma}_{\text{HCRB}}$ and $\boldsymbol{\gamma}_{\text{HCRB}}$ in which:

$$\begin{cases}\mathbf{\Gamma}_{\text{HCRB}} &= [\mathbf{0}_2\ \mathbf{\Phi}],\\ \boldsymbol{\gamma}_{\text{HCRB}} &= [1\ \boldsymbol{\gamma}_{\text{MSB}}]^T,\end{cases} \tag{13}$$

where $\mathbf{0}_2$ denotes the 2×1 vector filled by zeros. Finally, one can define the McAulay-Hofstetter bound (MHB) using:

$$\begin{cases}\mathbf{\Gamma}_{\text{MHB}} &= [\boldsymbol{I}_2\ \mathbf{\Phi}],\\ \boldsymbol{\gamma}_{\text{MHB}} &= [\boldsymbol{\gamma}_{\text{CRB}}\ \boldsymbol{\gamma}_{\text{MSB}}]^T,\end{cases} \tag{14}$$

where $\boldsymbol{I}_2$ denotes the 2×2 identity matrix.

Recently, a new deterministic lower bound, called the Cramér-Rao Fourier bound (CRFB), was proposed in [17]. To have a gain in computing time, this latter applies the discrete Fourier transform (DFT) on $\mathbf{\Phi}$ and $\boldsymbol{\gamma}_{\text{BMS}}$. Consequently, it is given thanks to the following couple:

$$\begin{cases}\mathbf{\Gamma}_{\text{CRFB}} &= [\boldsymbol{I}_2\ \mathbf{\Phi}\boldsymbol{W}^H],\\ \boldsymbol{\gamma}_{\text{CRFB}} &= [\boldsymbol{\gamma}_{\text{CRB}}\ \boldsymbol{\gamma}_{\text{MSB}}\boldsymbol{W}^T]^T,\end{cases} \tag{15}$$

where, in the near field context, the bi-dimensional discrete Fourier transform $\boldsymbol{W}$ is given by

$$[\boldsymbol{W}]_{p,l} = \exp(-i\boldsymbol{\Omega}_p^T\boldsymbol{\xi}_l), \tag{16}$$

in which $\boldsymbol{\Omega}_p$ is expressed for the pth frequency test bin $\boldsymbol{f}_p = [f_p \ f'_p]^T$ as

$$\boldsymbol{\Omega}_p = \left[\frac{2\pi f_p}{\Delta_\omega L_1} \ \frac{2\pi f'_p}{\Delta_\phi L_2} \right]^T, \tag{17}$$

where $L = L_1 L_2$, $f_p \in \{1, \ldots, L_1\}$ and $f'_p \in \{1, \ldots, L_2\}$ in which L_1 and L_2 are the number of test points *w.r.t.* ω and ϕ, respectively. Δ_ω and Δ_ϕ denote the uniform inter-test point *w.r.t.* ω and ϕ, respectively. Consequently, the index p is a unique combination of $\left\{f_p, f'_p\right\}$ where the total number of these combinations is denoted by P.

One should note that the aforementioned bounds depend generally on the number of test points L and/or the number of frequency test-bins P. Thus, in the following these bounds are indexed by L and/or P.

B. Deterministic lower bounds matrix expressions

After some straightforwerd calculation it can be shown (see [17, Appendix M]) that the CRFB is expressed as

$$\boldsymbol{C}_{\mathrm{BFCR}}^{(L,P)} = \boldsymbol{C}_{\mathrm{BCR}} + \boldsymbol{Q}\boldsymbol{W}^H \left(\boldsymbol{W}\boldsymbol{R}\boldsymbol{W}^H\right)^{-1} \boldsymbol{W}\boldsymbol{Q}^T, \tag{18}$$

where

$$\boldsymbol{Q} = \boldsymbol{C}_{\mathrm{BCR}}\boldsymbol{D} - \boldsymbol{\Phi}, \tag{19}$$

in which

$$\boldsymbol{D} = \left[\boldsymbol{d}(\boldsymbol{\xi}_1) \quad \ldots \quad \boldsymbol{d}(\boldsymbol{\xi}_L)\right], \tag{20}$$

and

$$\boldsymbol{d}(\boldsymbol{\xi}_l) = -\left(\frac{\partial \mathrm{KLD}\left(p(\boldsymbol{\chi};\boldsymbol{\xi}_l)||p(\boldsymbol{\chi};\boldsymbol{\xi})\right)}{\partial \boldsymbol{\xi}}\right)^T |_{\boldsymbol{\xi}=\boldsymbol{\xi}_0}, \tag{21}$$

where the KLD denotes the kullback-Leibler divergence and

$$\boldsymbol{R} = \boldsymbol{\Psi} - \boldsymbol{D}^T\boldsymbol{C}_{\mathrm{BCR}}\boldsymbol{D} \text{ with } [\boldsymbol{\Psi}]_{m,n} \tag{22}$$

$$= E_{\boldsymbol{\chi};\boldsymbol{\xi}_0}\left\{v(\boldsymbol{\chi},\boldsymbol{\xi}_m)v(\boldsymbol{\chi},\boldsymbol{\xi}_n)\right\} \tag{23}$$

where $m = 1, \ldots, L, \ n = 1, \ldots, L$. Following the same methodology, one can easily obtains the following matrix expressions:

$$\boldsymbol{C}_{\mathrm{BMS}}^{(L)} = \boldsymbol{\Phi}\boldsymbol{\Psi}^{-1}\boldsymbol{\Phi}^T, \tag{24}$$

$$\boldsymbol{C}_{\mathrm{BHCR}}^{(L)} = \boldsymbol{\Phi}\left(\boldsymbol{\Psi} - \mathbf{1}_L\mathbf{1}_L^T\right)^{-1}\boldsymbol{\Phi}^T, \tag{25}$$

$$\boldsymbol{C}_{\mathrm{BMH}}^{(L)} = \boldsymbol{C}_{\mathrm{BCR}} + \boldsymbol{Q}\boldsymbol{R}^{-1}\boldsymbol{Q}^T. \tag{26}$$

In the following we give closed form expression of the elements of $\boldsymbol{C}_{\mathrm{MHB}}^{(L)}$, $\boldsymbol{C}_{\mathrm{MHCB}}^{(L)}$, $\boldsymbol{C}_{\mathrm{MSB}}^{(L)}$ and $\boldsymbol{C}_{\mathrm{CRFB}}^{(L,P)}$. Since the expression of $\boldsymbol{C}_{\mathrm{BCR}}$ is well known for complex circular Gaussian observations $\boldsymbol{\chi} \sim \mathcal{CN}(\boldsymbol{\mu}(\boldsymbol{\xi}_0), \boldsymbol{\Sigma}(\boldsymbol{\xi}_0))$ [20] (see (27)), we focus only on $\boldsymbol{D}$ and $\boldsymbol{\Psi}$.

$$\boldsymbol{C}_{\mathrm{BCR}} = \mathbf{FIM}^{-1} \ \text{ where} \tag{27}$$

$$[\mathbf{FIM}]_{i,k} = \mathrm{tr}\left\{\boldsymbol{\Sigma}(\boldsymbol{\xi}_0)^{-1}\frac{\partial\boldsymbol{\Sigma}(\boldsymbol{\xi}_0)}{\partial\left[\boldsymbol{\xi}_\mathbf{0}\right]_i}\boldsymbol{\Sigma}(\boldsymbol{\xi}_0)^{-1}\frac{\partial\boldsymbol{\Sigma}(\boldsymbol{\xi}_0)}{\partial\left[\boldsymbol{\xi}_\mathbf{0}\right]_k}\right\} \tag{28}$$

$$+ 2\Re\left\{\frac{\partial\boldsymbol{\mu}(\boldsymbol{\xi}_0)^H}{\partial\left[\boldsymbol{\xi}_\mathbf{0}\right]_i}\boldsymbol{\Sigma}(\boldsymbol{\xi}_0)^{-1}\frac{\partial\boldsymbol{\mu}(\boldsymbol{\xi}_0)}{\partial\left[\boldsymbol{\xi}_\mathbf{0}\right]_k}\right\}, \tag{29}$$

in which $\mathrm{tr}\{.\}$ and $\Re\{.\}$ denote the trace operator and the real part, respectively.

1) The conditional case: In the conditional case we assume that $s(t) = \alpha(t)e^{j(2\pi f_0 t + \psi(t))}$ is the source signal with a carrier frequency equals to f_0 where $\alpha(t)$ and $\psi(t)$ are the known real amplitude and the known shift phase, respectively. Consequently, one has an observation model with a parameterized mean such that $\boldsymbol{\chi} \sim \mathcal{CN}(\boldsymbol{\mu}(\boldsymbol{\xi}_0), \boldsymbol{\Sigma}_{\mathrm{noise}})$ where $\boldsymbol{\mu}(\boldsymbol{\xi}_0) = [s(1)\mathbf{a}^T(\omega_0,\phi_0)\ldots s(L)\mathbf{a}^T(\omega_0,\phi_0)]^T$. Consequently, by applying (27) one has

$$[\mathbf{FIM}]_{i,k} = 2\Re\left\{\frac{\partial\boldsymbol{\mu}(\boldsymbol{\xi}_0)^H}{\partial\left[\boldsymbol{\xi}_\mathbf{0}\right]_i}\boldsymbol{\Sigma}_{\mathrm{noise}}^{-1}\frac{\partial\boldsymbol{\mu}(\boldsymbol{\xi}_0)}{\partial\left[\boldsymbol{\xi}_\mathbf{0}\right]_k}\right\}, \ i = 1,2, \ k = 1,2. \tag{30}$$

On one hand, one obtains:

$$\mathrm{KLD}\left(p(\boldsymbol{\chi};\boldsymbol{\xi}_n)||p(\boldsymbol{\chi};\boldsymbol{\xi})\right) = \int_{\mathbb{C}^{NT}} p(\boldsymbol{\chi};\boldsymbol{\xi}_n)\mathrm{Ln}\frac{p(\boldsymbol{\chi};\boldsymbol{\xi}_n)}{p(\boldsymbol{\chi};\boldsymbol{\xi})}d\boldsymbol{\chi}$$

$$= \int_{\mathbb{C}^{NT}} \left[(\boldsymbol{\chi}-\boldsymbol{\mu}(\boldsymbol{\xi}))^H\boldsymbol{\Sigma}_{\mathrm{noise}}^{-1}\right]$$

$$\left[(\boldsymbol{\chi}-\boldsymbol{\mu}(\boldsymbol{\xi})) - (\boldsymbol{\chi}-\boldsymbol{\mu}(\boldsymbol{\xi}_n))^H\boldsymbol{\Sigma}_{\mathrm{noise}}^{-1}(\boldsymbol{\chi}-\boldsymbol{\mu}(\boldsymbol{\xi}_n))\right] \tag{31}$$

$$p(\boldsymbol{\chi};\boldsymbol{\xi}_n)d\boldsymbol{\chi} \tag{32}$$

$$= \int_{\mathbb{C}^{NT}} \left[\boldsymbol{\chi}^H\boldsymbol{\Sigma}_{\mathrm{noise}}^{-1}(\boldsymbol{\mu}(\boldsymbol{\xi}_n)-\boldsymbol{\mu}(\boldsymbol{\xi})) - \boldsymbol{\mu}(\boldsymbol{\xi})^H\boldsymbol{\Sigma}_{\mathrm{noise}}^{-1}(\boldsymbol{\chi}-\boldsymbol{\mu}(\boldsymbol{\xi}))\right]$$

$$f(\boldsymbol{\chi};\boldsymbol{\xi}_n)d\boldsymbol{\chi} \tag{33}$$

$$= (\boldsymbol{\mu}(\boldsymbol{\xi}_n)-\boldsymbol{\mu}(\boldsymbol{\xi}))^H\boldsymbol{\Sigma}_{\mathrm{noise}}^{-1}(\boldsymbol{\mu}(\boldsymbol{\xi}_n)-\boldsymbol{\mu}(\boldsymbol{\xi})). \tag{34}$$

On the other hand, one has:

$$[\boldsymbol{\Psi}]_{m,n} = \int_{\mathbb{C}^{NT}} \frac{1}{\pi\left|\boldsymbol{\Sigma}_{\mathrm{noise}}\right|}\times$$

$$\exp\left(-(\boldsymbol{\chi}-\boldsymbol{\mu}(\boldsymbol{\xi}_m))^H\boldsymbol{\Sigma}_{\mathrm{noise}}^{-1}(\boldsymbol{\chi}-\boldsymbol{\mu}(\boldsymbol{\xi}_m)) - (\boldsymbol{\chi}-\boldsymbol{\mu}(\boldsymbol{\xi}_n))^H\boldsymbol{\Sigma}_{\mathrm{noise}}^{-1}\right)$$

$$\exp\left((\boldsymbol{\chi}-\boldsymbol{\mu}(\boldsymbol{\xi}_n)) + (\boldsymbol{\chi}-\boldsymbol{\mu}(\boldsymbol{\xi}_0))^H\boldsymbol{\Sigma}_{\mathrm{noise}}^{-1}(\boldsymbol{\chi}-\boldsymbol{\mu}(\boldsymbol{\xi}_0))\right)d\boldsymbol{\chi}$$

$$= \alpha(\boldsymbol{\xi}_m,\boldsymbol{\xi}_n),$$

in which

$$\alpha(\boldsymbol{\xi}_m,\boldsymbol{\xi}_n) = \exp(-2\boldsymbol{\mu}(\boldsymbol{\xi}_0)^H\boldsymbol{\Sigma}_{\mathrm{noise}}^{-1}\boldsymbol{\mu}(\boldsymbol{\xi}_0) - \boldsymbol{\mu}(\boldsymbol{\xi}_0)^H\boldsymbol{\Sigma}_{\mathrm{noise}}^{-1}$$
$$(\boldsymbol{\mu}(\boldsymbol{\xi}_m)+\boldsymbol{\mu}(\boldsymbol{\xi}_n)) \tag{35}$$
$$+\boldsymbol{\mu}(\boldsymbol{\xi}_m)^H\boldsymbol{\Sigma}_{\mathrm{noise}}^{-1}(\boldsymbol{\mu}(\boldsymbol{\xi}_n)-\boldsymbol{\mu}(\boldsymbol{\xi}_0)) + \boldsymbol{\mu}(\boldsymbol{\xi}_m)^H\boldsymbol{\Sigma}_{\mathrm{noise}}^{-1} \tag{36}$$
$$(\boldsymbol{\mu}(\boldsymbol{\xi}_n)-\boldsymbol{\mu}(\boldsymbol{\xi}_0))). \tag{37}$$

Consequently, $\boldsymbol{C}_{\mathrm{MHB}}^{(L)}$, $\boldsymbol{C}_{\mathrm{MHCB}}^{(L)}$, $\boldsymbol{C}_{\mathrm{MSB}}^{(L)}$ and $\boldsymbol{C}_{\mathrm{CRFB}}^{(L,P)}$ are given by plugging (30), (34) and (36) into (26), (25), (24) and (18), respectively. See Appendix A for closed form expressions of $\boldsymbol{C}_{\mathrm{CRFB}}^{(L,1)}$ in the case $P = 1$.

2) The unconditional case: Let us consider the unconditional model, *i.e.*, when the signals are assumed to be Gaussian (with zero mean and variance σ_s^2) independent of the noise. Under this assumption, one obtains an observation model with a parameterized covariance matrix such that $\boldsymbol{\chi} \sim \mathcal{CN}(\mathbf{0}, \boldsymbol{\Sigma}(\boldsymbol{\xi}_0))$ where the covariance matrix $\boldsymbol{\Sigma}(\boldsymbol{\xi}_0) = \sigma_s^2\boldsymbol{I}_T \otimes \mathbf{a}(\omega_0,\phi_0)\mathbf{a}^H(\omega_0,\phi_0) + \boldsymbol{\Sigma}_{\mathrm{noise}}$ in which $\otimes$ denotes the Kronecker product. Consequently, the FIM in (27) becomes:

$$[\mathbf{FIM}]_{i,k} = T\ \mathrm{tr}\left\{\boldsymbol{\Sigma}(\boldsymbol{\xi}_0)^{-1}\frac{\partial\boldsymbol{\Sigma}(\boldsymbol{\xi}_0)}{\partial\left[\boldsymbol{\xi}_\mathbf{0}\right]_i}\boldsymbol{\Sigma}(\boldsymbol{\xi}_0)^{-1}\frac{\partial\boldsymbol{\Sigma}(\boldsymbol{\xi}_0)}{\partial\left[\boldsymbol{\xi}_\mathbf{0}\right]_k}\right\}, \tag{38}$$

$i = 1,2, \ k = 1,2.$

First, note that:

$$\mathrm{KLD}\left(p(\boldsymbol{\chi};\boldsymbol{\xi}_n)||p(\boldsymbol{\chi};\boldsymbol{\xi})\right) = \int_{\mathbb{C}^{NT}} p(\boldsymbol{\chi};\boldsymbol{\xi}_n)\mathrm{Ln}\frac{p(\boldsymbol{\chi};\boldsymbol{\xi}_n)}{p(\boldsymbol{\chi};\boldsymbol{\xi})}d\boldsymbol{\chi}$$
$$= \int_{\mathbb{C}^{NT}} \frac{1}{\pi^{NT}\left|\boldsymbol{\Sigma}(\boldsymbol{\xi}_n)\right|}\left(\boldsymbol{\chi}^H\left(\boldsymbol{\Sigma}(\boldsymbol{\xi}_n)^{-1}-\boldsymbol{\Sigma}(\boldsymbol{\xi})^{-1}\right)\boldsymbol{\chi}\right)$$
$$\exp\left(-\boldsymbol{\chi}^H\boldsymbol{\Sigma}(\boldsymbol{\xi}_n)^{-1}\boldsymbol{\chi}\right)d\boldsymbol{\chi} + \mathrm{Ln}\frac{\left|\boldsymbol{\Sigma}(\boldsymbol{\xi})\right|}{\left|\boldsymbol{\Sigma}(\boldsymbol{\xi}_n)\right|} \quad (39)$$
$$= E_{\boldsymbol{\chi};\boldsymbol{\xi}_n}\left\{\boldsymbol{\chi}^H\boldsymbol{\Sigma}(\boldsymbol{\xi})\boldsymbol{\chi}\right\} + E_{\boldsymbol{\chi};\boldsymbol{\xi}_n}\left\{\boldsymbol{\chi}^H\boldsymbol{\Sigma}(\boldsymbol{\xi}_n)\boldsymbol{\chi}\right\} + \mathrm{Ln}\frac{\left|\boldsymbol{\Sigma}(\boldsymbol{\xi})\right|}{\left|\boldsymbol{\Sigma}(\boldsymbol{\xi}_n)\right|}. \quad (40)$$

Noting that:

$$E_{\boldsymbol{\chi};\boldsymbol{\xi}_n}\left\{\boldsymbol{\chi}^H\boldsymbol{\Sigma}(\boldsymbol{\xi})\boldsymbol{\chi}\right\} = \sum_{i=1}^{NT}\sum_{j=1}^{NT} E_{\boldsymbol{\chi};\boldsymbol{\xi}_n}\left\{[\boldsymbol{\chi}]_i^*[\boldsymbol{\chi}]_j\left[\boldsymbol{\Sigma}(\boldsymbol{\xi})^{-1}\right]_{i,j}\right\} \quad (41)$$

$$= \sum_{j=1}^{NT}\left[\boldsymbol{\Sigma}(\boldsymbol{\xi}_n)\boldsymbol{\Sigma}(\boldsymbol{\xi})^{-1}\right]_{j,j} = \mathrm{tr}\left(\boldsymbol{\Sigma}(\boldsymbol{\xi}_n)\boldsymbol{\Sigma}(\boldsymbol{\xi})^{-1}\right) \quad (42)$$

and, in the same way,

$$E_{\boldsymbol{\chi};\boldsymbol{\xi}_n}\left\{\boldsymbol{\chi}^H\boldsymbol{\Sigma}(\boldsymbol{\xi}_0)^{-1}\boldsymbol{\chi}\right\} = NT. \quad (43)$$

Consequently, plugging (41) and (43) into (40) one obtains

$$\mathrm{KLD}\left(p(\boldsymbol{\chi};\boldsymbol{\xi}_n)||f(\boldsymbol{\chi};\boldsymbol{\xi})\right) = \mathrm{Ln}\frac{\left|\boldsymbol{\Sigma}\right|}{\left|\boldsymbol{\Sigma}(\boldsymbol{\xi}_n)\right|} + \mathrm{tr}\left(\boldsymbol{\Sigma}(\boldsymbol{\xi}_n)\boldsymbol{\Sigma}(\boldsymbol{\xi})^{-1}\right) + NT. \quad (44)$$

Second, one has:

$$[\boldsymbol{\Psi}]_{n,m} = \frac{\left|\boldsymbol{\Sigma}(\boldsymbol{\xi}_0)\right|}{\pi^{NT}\left|\boldsymbol{\Sigma}(\boldsymbol{\xi}_m)\right|\left|\boldsymbol{\Sigma}(\boldsymbol{\xi}_n)\right|} \quad (45)$$

$$\underbrace{\int_{\mathbb{C}^{NT}}\exp\left(-\boldsymbol{\chi}^H\left(\boldsymbol{\Sigma}(\boldsymbol{\xi}_m)^{-1}+\boldsymbol{\Sigma}(\boldsymbol{\xi}_n)^{-1}-\boldsymbol{\Sigma}(\boldsymbol{\xi}_0)^{-1}\right)\boldsymbol{\chi}\right)d\boldsymbol{\chi}}_{\pi^{NT}\left|(\boldsymbol{\Sigma}(\boldsymbol{\xi}_m)^{-1}+\boldsymbol{\Sigma}(\boldsymbol{\xi}_n)^{-1}-\boldsymbol{\Sigma}(\boldsymbol{\xi}_0)^{-1})^{-1}\right|} \quad (46)$$

$$= \frac{\left|\boldsymbol{\Sigma}(\boldsymbol{\xi}_0)\right|}{\left|\boldsymbol{\Sigma}(\boldsymbol{\xi}_m)\right|\left|\boldsymbol{\Sigma}(\boldsymbol{\xi}_n)\right|\left|\boldsymbol{\Sigma}(\boldsymbol{\xi}_m)^{-1}+\boldsymbol{\Sigma}(\boldsymbol{\xi}_n)^{-1}-\boldsymbol{\Sigma}(\boldsymbol{\xi}_0)^{-1}\right|} \quad (47)$$

Consequently, using the fact that $\frac{\partial \mathrm{Ln}\left|\boldsymbol{\Sigma}(\boldsymbol{\xi})\right|}{\partial\boldsymbol{\xi}} = \mathrm{tr}\left\{\boldsymbol{\Sigma}(\boldsymbol{\xi})^{-1}\frac{\partial\boldsymbol{\Sigma}(\boldsymbol{\xi})}{\partial\boldsymbol{\xi}}\right\}$ [21] and plugging (38), (44) and (47) into (26), (25), (24) and (18) one obtains $\boldsymbol{C}_{\mathrm{MHB}}^{(L)}$, $\boldsymbol{C}_{\mathrm{MHCB}}^{(L)}$, $\boldsymbol{C}_{\mathrm{MSB}}^{(L)}$ and $\boldsymbol{C}_{\mathrm{CRFB}}^{(L,P)}$, respectively. See Appendix A for closed form expressions of $\boldsymbol{C}_{\mathrm{CRFB}}^{(L,1)}$ in the case $P=1$.

IV. Numerical simulations

The scenario used in these simulations is a ULA of $N=5$ sensors spaced by $d=\frac{\lambda}{2}$. The noise is assumed to be a complex circular white Gaussian random process with zero-mean and known variance σ^2, uncorrelated both temporally and spatially.

To compare the threshold prediction accuracy we plot the MSE *w.r.t.* ω and ϕ using 250 Monte Carlo trials. In both conditional and unconditional cases (see Fig. 1-4), we compute $\boldsymbol{C}_{\mathrm{MHB}}^{(L)}$, $\boldsymbol{C}_{\mathrm{MHCB}}^{(L)}$, $\boldsymbol{C}_{\mathrm{MSB}}^{(L)}$ using $L=2^{10}$ test points (more precisely, we used $L_1=2^5$ test points over the parameter ω and $L_2=2^5$ test points over the parameter ϕ.) The CRFB, $\boldsymbol{C}_{\mathrm{CRFB}}^{(L,1)}$, is obtained using $L=2^{10}$ test points and also by numerical maximization over 2^{10} frequency test bins for $P=1$.

Fig. 1-4 provide an illustration of the usefulness of the aforementioned deterministic lower bounds in the case of conditional and unconditional model assumptions for ω and ϕ. First, one can notice that the MSE of ϕ is lower than the MSE of ω which is expected due the range of those parameters and from the fact that ϕ is the coefficient of the second order, whereas, ω is the coefficient of the first order *w.r.t.* to the time delay (see (4)). Second, one can notice that all the aforementioned bounds provide a *good* prediction of the MSE threshold. Nevertheless, we notice that the MSB is more accurate than the others (error of the threshold prediction less than 4 dB).

Finally, one can note that the advantage of the CRFB is its computational cost (the computational complexity of the CRFB is lower in comparison to the MSB, HCRB and MHB due to the inversion matrix, see (26), (25), (24) and (18) in the case where $P \ll L$.) However, the degradation of the threshold prediction can be explained as follow: applying the DFT on $\boldsymbol{\Phi}$ and $\boldsymbol{\gamma}_{\mathrm{BMS}}$ to obtain the CRFB, is equivalent to compress (to reduce) the constraints on the bias (see Appendix B). Since, the reduction of the constraints will decrease the accuracy of the lower bound [22], then, one expects to obtain a less accurate bound. This loss of accuracy affect only the threshold prediction and does not affect the asymptotic performance prediction of the MLE. This can be argued by the fact that the DFT is applied only on the $\boldsymbol{\Psi}$ and $\boldsymbol{\gamma}_{\mathrm{BMS}}$ compounds without affecting $\boldsymbol{\gamma}_{\mathrm{CRB}}$ (we recall that $\boldsymbol{\gamma}_{\mathrm{CRB}}$ reflects the constraints on the bias used to compute the CRB which is a tight bound in the asymptotic region.)

V. Conclusion

In this paper, we present the derivation of different some deterministic lower bounds on the MSE in near field source localization context. This analysis allowed us to characterize the non-asymptotic performance estimators mean square error. In particular, we focused on the threshold/breakdown prediction. Furthermore, we demonstrated in this study, that Cramér-Rao Fourier bound recently proposed remains less efficient than some of its predecessors as, for example, the McAulay-Hofstetter bound.

Appendix A

In this appendix, we give closed form expression of the CRFB for the case $P=1$. In this case, the matrix $\boldsymbol{W}$ will be reduced to a row vector of dimension L, such that:

$$[\boldsymbol{W}]_{1,l} = \exp\left(-j2\pi\frac{l-1}{L}\right), \quad l=1,\ldots,L. \quad (48)$$

Let $\rho = \boldsymbol{W}\boldsymbol{R}\boldsymbol{W}^H$, consequently, one has:

$$\rho = \sum_{m=1}^{L}\sum_{n=1}^{L}[\boldsymbol{R}]_{m,n}\exp\left(j\pi\frac{n-m}{L}\right). \quad (49)$$

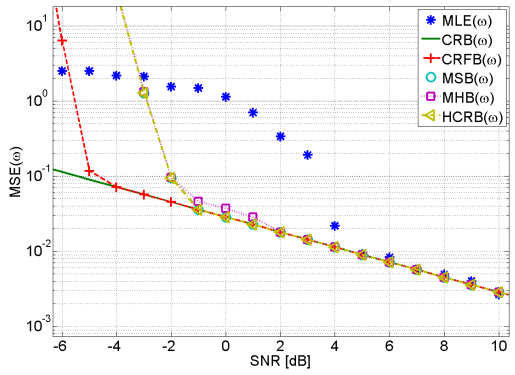

Fig. 1. Conditional deterministic lower bounds on the mean square error *w.r.t.* ω for near field source localization, with $T = 10$ and $(\theta, r) = (45°, 6\lambda)$.

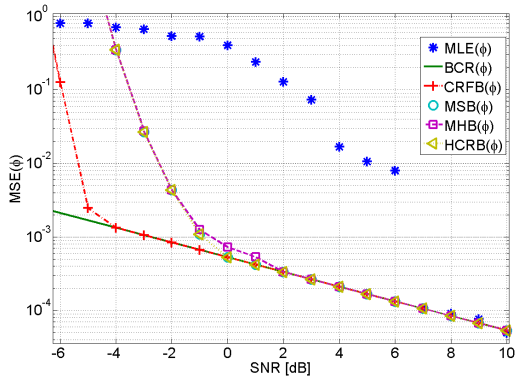

Fig. 2. Conditional deterministic lower bounds on the mean square error *w.r.t.* ϕ for near field source localization, with $T = 10$ and $(\theta, r) = (45°, 6\lambda)$.

On the other hand, using (22), one obtains:

$$[\boldsymbol{R}]_{m,n} = [\boldsymbol{\Psi}]_{m,n} \tag{50}$$

$$- \sum_{p=1}^{2}\sum_{q=1}^{2} \left(\frac{\partial \mathrm{KLD}\left(p(\boldsymbol{x};\boldsymbol{\xi}_m)||p(\boldsymbol{x};\boldsymbol{\xi})\right)}{\partial \left[\boldsymbol{\xi}\right]_p} \right)^T |_{\boldsymbol{\xi}=\boldsymbol{\xi}_0} \tag{51}$$

$$[\boldsymbol{C}_{\mathrm{CRB}}]_{p,q} \left(\frac{\partial \mathrm{KLD}\left(p(\boldsymbol{x};\boldsymbol{\xi}_n)||p(\boldsymbol{x};\boldsymbol{\xi})\right)}{\partial \left[\boldsymbol{\xi}\right]_q} \right)^T |_{\boldsymbol{\xi}=\boldsymbol{\xi}_0}. \tag{52}$$

Consequently, one obtains the closed form expression given in the following

$$\left[\boldsymbol{C}^{(L,1)}_{\mathrm{CRFB}}\right]_{p,q} = [\boldsymbol{C}_{\mathrm{CRB}}]_{p,q} \tag{53}$$

$$+ \frac{1}{\rho} \sum_{m=1}^{L}\sum_{n=1}^{L} \beta(p,m)\beta(q,n) \exp\left(j2\pi \frac{n-m}{L}\right), \tag{54}$$

in which

$$\beta(p,n) = \sum_{q=1}^{2} [\boldsymbol{C}_{\mathrm{CRB}}]_{p,q} \tag{55}$$

$$\left(\frac{\partial \mathrm{KLD}\left(p(\boldsymbol{x};\boldsymbol{\xi}_n)||p(\boldsymbol{x};\boldsymbol{\xi})\right)}{\partial \left[\boldsymbol{\xi}\right]_q} \right)^T |_{\boldsymbol{\xi}=\boldsymbol{\xi}_0} + [\boldsymbol{\xi}_0]_p - [\boldsymbol{\xi}_n]_p. \tag{56}$$

A. The conditional case:

Plugging (34) and (36) into (53), one obtains

$$\left[\boldsymbol{C}^{(L,1)}_{\mathrm{CRFB}}\right]_{p,q} = [\boldsymbol{C}_{\mathrm{CRB}}]_{p,q} \tag{57}$$

$$+ \frac{\sum_{m=1}^{L}\sum_{n=1}^{L} \beta(p,m)\beta(q,n) \exp\left(j2\pi \frac{n-m}{L}\right)}{\sum_{m=1}^{L}\sum_{n=1}^{L} \gamma(m,n) \exp\left(j\pi \frac{n-m}{L}\right)}, \tag{58}$$

where

$$\gamma(m,n) = \alpha(\boldsymbol{\xi}_m, \boldsymbol{\xi}_n) - \sum_{p=1}^{2}\sum_{q=1}^{2} \kappa(m,p)\kappa(n,q) \left[\boldsymbol{C}_{\mathrm{CRB}}\right]_{p,q}, \tag{59}$$

in which

$$\kappa(n,q) = \left(\frac{\partial \left(\boldsymbol{\mu}(\boldsymbol{\xi}_n) - \boldsymbol{\mu}(\boldsymbol{\xi})\right)^H \boldsymbol{\Sigma}^{-1}_{\mathrm{noise}} \left(\boldsymbol{\mu}(\boldsymbol{\xi}_n) - \boldsymbol{\mu}(\boldsymbol{\xi})\right)}{\partial \left[\boldsymbol{\xi}\right]_q} \right) |_{\boldsymbol{\xi}=\boldsymbol{\xi}_0} \tag{60}$$

$$= -\dot{\boldsymbol{\mu}}_q \boldsymbol{\xi}_0^H \boldsymbol{\Sigma}^{-1}_{\mathrm{noise}} \tag{61}$$

$$\times \left(\boldsymbol{\mu}(\boldsymbol{\xi}_n) - \boldsymbol{\mu}(\boldsymbol{\xi})\right) + \left(\boldsymbol{\mu}(\boldsymbol{\xi}_n) - \boldsymbol{\mu}(\boldsymbol{\xi})\right)^H \boldsymbol{\Sigma}^{-1}_{\mathrm{noise}} - \dot{\boldsymbol{\mu}}_q(\boldsymbol{\xi}_0) \tag{62}$$

and where $\dot{\boldsymbol{\mu}}_q(\boldsymbol{\xi}_0) = [s(1) \ \ldots \ s(T)]^T \otimes \left([0 \ \ldots \ (n-1)^q]^T \odot \boldsymbol{a}(\omega_0, \phi_0)\right)$, in which $\odot$ denotes the element wise product and where

$$\beta(p,n) = \sum_{q=1}^{2} [\boldsymbol{C}_{\mathrm{CRB}}]_{p,q} \left(\frac{\partial \kappa(n,q)}{\partial \left[\boldsymbol{\xi}\right]_q} \right) |_{\boldsymbol{\xi}=\boldsymbol{\xi}_0} + [\boldsymbol{\xi}_0]_p - [\boldsymbol{\xi}_n]_p \tag{63}$$

B. The unconditional case:

Plugging (44) and (47) into (53), one obtains

$$\left[\boldsymbol{C}^{(L,1)}_{\mathrm{CRFB}}\right]_{p,q} = [\boldsymbol{C}_{\mathrm{CRB}}]_{p,q} \tag{64}$$

$$+ \frac{\sum_{m=1}^{L}\sum_{n=1}^{L} \beta(p,m)\beta(q,n) \exp\left(j2\pi \frac{n-m}{L}\right)}{\sum_{m=1}^{L}\sum_{n=1}^{L} \gamma(m,n) \exp\left(j\pi \frac{n-m}{L}\right)}, \tag{65}$$

where

$$\gamma(m,n) = \frac{|\boldsymbol{\Sigma}(\boldsymbol{\xi}_0)|}{|\boldsymbol{\Sigma}(\boldsymbol{\xi}_m)|\,|\boldsymbol{\Sigma}(\boldsymbol{\xi}_n)|\,|\boldsymbol{\Sigma}(\boldsymbol{\xi}_m)^{-1} + \boldsymbol{\Sigma}(\boldsymbol{\xi}_n)^{-1} - \boldsymbol{\Sigma}(\boldsymbol{\xi}_0)^{-1}|} \tag{66}$$

$$- \sum_{p=1}^{2}\sum_{q=1}^{2} \kappa(m,p)\kappa(n,q) \left[\boldsymbol{C}_{\mathrm{CRB}}\right]_{p,q}. \tag{67}$$

in which

$$\kappa(n,q) = \left(\frac{\partial \left(\mathrm{Ln} \frac{|\boldsymbol{\Sigma}(\boldsymbol{\xi})|}{|\boldsymbol{\Sigma}(\boldsymbol{\xi}_n)|} + \mathrm{tr}\left(\boldsymbol{\Sigma}(\boldsymbol{\xi}_n)\boldsymbol{\Sigma}(\boldsymbol{\xi})^{-1}\right)\right)}{\partial \left[\boldsymbol{\xi}\right]_q} \right) |_{\boldsymbol{\xi}=\boldsymbol{\xi}_0} = \tag{68}$$

$$\mathrm{tr}\left\{ \boldsymbol{\Sigma}(\boldsymbol{\xi}_0)^{-1} \frac{\partial \boldsymbol{\Sigma}(\boldsymbol{\xi})}{\partial \boldsymbol{\xi}} |_{\boldsymbol{\xi}=\boldsymbol{\xi}_0} + \boldsymbol{\Sigma}(\boldsymbol{\xi}_n) \frac{\partial \boldsymbol{\Sigma}(\boldsymbol{\xi})}{\partial \boldsymbol{\xi}} |_{\boldsymbol{\xi}=\boldsymbol{\xi}_0} \right\} \tag{69}$$

and where

$$\beta(p,n) = \sum_{q=1}^{2} [\boldsymbol{C}_{\mathrm{CRB}}]_{p,q} \left(\frac{\partial \kappa(n,q)}{\partial \left[\boldsymbol{\xi}\right]_q} \right) |_{\boldsymbol{\xi}=\boldsymbol{\xi}_0} + [\boldsymbol{\xi}_0]_p - [\boldsymbol{\xi}_n]_p \tag{70}$$

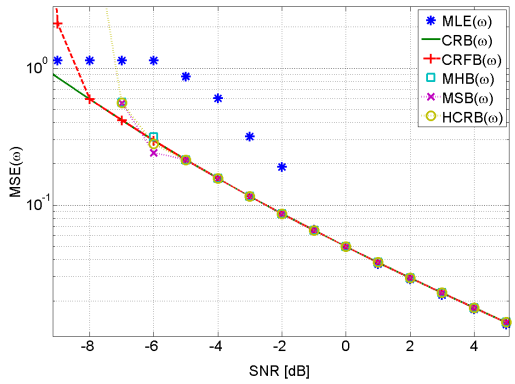

Fig. 3. Unconditional deterministic lower bounds on the mean square error *w.r.t.* ω for near field source localization, with $T = 100$ and $(\theta, r) = (30°, 6\lambda)$.

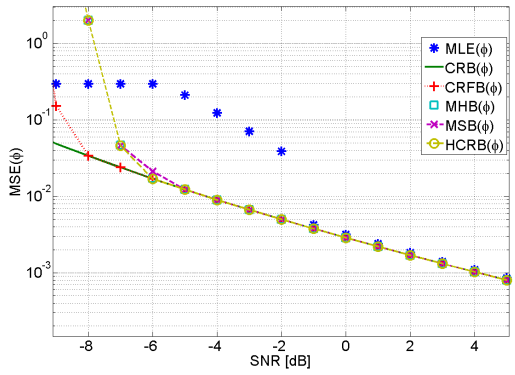

Fig. 4. Unconditional deterministic lower bounds on the mean square error *w.r.t.* ϕ for near field source localization, with $T = 100$ and $(\theta, r) = (30°, 6\lambda)$.

APPENDIX B

In this appendix, we rewrite the CRFB presented in [17] using the minimization formulation as presented in [19]. The aim is then, to explore the constraints on the bias due to the CRFB. In the following, and due to the space limitation, we consider only the case of one unknown parameter denoted ξ. The extension of an unknown vector parameter is tedious/long but straightforward and will not be presented in this appendix.

In the case of one unknown parameter ξ, one has:

$$\boldsymbol{C}_{\text{CRFB}}^{(L,P)} = \boldsymbol{\Gamma}^H \boldsymbol{K}^{-1} \boldsymbol{\Gamma}, \tag{71}$$

where

$$\boldsymbol{\Gamma} = \begin{bmatrix} 1 \\ \boldsymbol{W}\boldsymbol{\Phi} \end{bmatrix}, \tag{72}$$

in which

$$\boldsymbol{\Phi} = \begin{bmatrix} \xi_1 - \xi_0 \\ \vdots \\ \xi_1 - \xi_L \end{bmatrix} \tag{73}$$

and

$$\boldsymbol{K} = \begin{bmatrix} \mathbf{FIM} & \boldsymbol{D}^T \boldsymbol{W}^H \\ \boldsymbol{W}\boldsymbol{D} & \boldsymbol{W}\boldsymbol{\Psi}\boldsymbol{W}^H \end{bmatrix}, \tag{74}$$

in which

$$\boldsymbol{D} = -\begin{bmatrix} \left(\frac{\partial \text{KLD}(p(\boldsymbol{\chi};\xi_1)||p(\boldsymbol{\chi};\xi))}{\partial \xi}\right)|_{\xi=\xi_0} \\ \vdots \\ \left(\frac{\partial \text{KLD}(p(\boldsymbol{\chi};\xi_L)||p(\boldsymbol{\chi};\xi))}{\partial \xi}\right)|_{\xi=\xi_0} \end{bmatrix}. \tag{75}$$

Let us rewrite $\boldsymbol{K}$ as

$$[\boldsymbol{K}]_{m,n} = \int g_m g_n d\boldsymbol{\chi} \tag{76}$$

then,

$$g_1 = \int \frac{\partial \ln p(\boldsymbol{\chi};\xi)}{\partial \xi}|_{\xi=\xi_0} \sqrt{p(\boldsymbol{\chi};\xi_0)} d\boldsymbol{\chi} \tag{77}$$

$$= \int \frac{\partial p(\boldsymbol{\chi};\xi)}{\partial \xi}|_{\xi=\xi_0} \frac{1}{\sqrt{p(\boldsymbol{x};\xi_0)}} d\boldsymbol{\chi}, \tag{78}$$

and

$$[\boldsymbol{K}]_{m,1} = \sum_{n=1}^{L} \int \frac{\partial \ln p(\boldsymbol{\chi};\xi)}{\partial \xi}|_{\xi=\xi_0} p(\boldsymbol{\chi};\xi_n) \exp(-j2m\pi \frac{n}{L}) d\boldsymbol{\chi} \tag{79}$$

$$= \sum_{n=1}^{L} \rho(\boldsymbol{\chi},\xi_n) \exp(-j2m\pi \frac{n}{L}), \tag{80}$$

Note that, $[\boldsymbol{K}]_{m,1}$ represents the DFT of the sequence $\{\rho(\boldsymbol{\chi},\xi_n)\}_{n=1}^{L}$ where

$$\rho(\boldsymbol{\chi},\xi_n) = \int \frac{\partial \ln p(\boldsymbol{\chi};\xi)}{\partial \xi}|_{\xi=\xi_0} p(\boldsymbol{\chi};\xi_n) d\boldsymbol{\chi}. \tag{81}$$

On the other hand, we can rewrite $[\boldsymbol{K}]_{m,1}$ as follows

$$[\boldsymbol{K}]_{m,1} = \sum_{n=1}^{L} \int \frac{\partial \ln p(\boldsymbol{\chi};\xi)}{\partial \xi}|_{\xi=\xi_0} \sqrt{p(\boldsymbol{\chi};\xi_0)} \frac{p(\boldsymbol{\chi};\xi_n)}{\sqrt{p(\boldsymbol{\chi};\xi_0)}} \tag{82}$$

$$\exp(-j2m\pi \frac{n}{L}) d\boldsymbol{\chi} = \int g_1 g_m d\boldsymbol{\chi}, \tag{83}$$

in which g_m represents the DFT of the sequence $\left\{\frac{p(\boldsymbol{\chi};\xi_n)}{\sqrt{p(\boldsymbol{\chi};\xi_0)}}\right\}_{n=1}^{L}$ given as follows

$$g_m = \sum_{n=1}^{L} \frac{f(\boldsymbol{\chi};\xi_n)}{\sqrt{p(\boldsymbol{\chi};\xi_0)}} \tag{84}$$

$$\exp(-j2m\pi \frac{n}{L}). \tag{85}$$

Since, $\boldsymbol{\Gamma} = \begin{bmatrix} 1 \\ \boldsymbol{W}\boldsymbol{\Phi} \end{bmatrix}$, then that m^{th} line the vector $\boldsymbol{W}\boldsymbol{\Phi}$ represent the spectrum frequency for the sequence $\{\xi_n - \xi_0\}_{n=1}^{L}$ at the m^{th} frequency. In the same way, each g_m represents the spectrum frequency of the sequence $\left\{\frac{p(\boldsymbol{x};\xi_n)}{\sqrt{p(\boldsymbol{x};\xi_0)}}\right\}_{n=1}^{L}$ at the m^{th} frequency.

Finally, the TTB bound can be viewed as a compression (in the frequency domain) of the Barankin constraints, *i.e.,* the constraint due to the construction of the TTB, are the DFT of a large sequence, this sequence reflects a null bias on several test points.

REFERENCES

[1] Y. D. Huang and M. Barkat, "Near-field multiple source localization by passive sensor array," *IEEE Trans. Antennas Propagat.*, vol. 39, pp. 968–975, 1991.

[2] N. Yuen and B. Friedlander, "Performance analysis of higher order ESPRIT for localization of near-field sources," *IEEE Trans. Signal Processing*, vol. 46, pp. 709–719, 1998.

[3] E. Grosicki, K. Abed-Meraim, and Y. Hua, "A weighted linear prediction method for near-field source localization," *IEEE Trans. Signal Processing*, vol. 53, pp. 3651–3660, 2005.

[4] W. Zhi and M. Chia, "Near-field source localization via symmetric subarrays," *IEEE Signal Processing Lett.*, vol. 14, no. 6, pp. 409–412, 2007.

[5] M. N. El Korso, G. Bouleux, R. Boyer, and S. Marcos, "Sequential estimation of the range and the bearing using the zero-forcing MUSIC approach," in *Proc. EUSIPCO*, Glasgow, Scotland, Aug. 2009, pp. 1404–1408.

[6] M. N. El Korso, R. Boyer, A. Renaux, and S. Marcos, "Nonmatrix closed-form expressions of the Cramér-Rao bounds for near-field localization parameters," in *Proc. of IEEE Int. Conf. Acoust., Speech, Signal Processing*, Taipei, Taiwan, 2009.

[7] P. Stoica and A. Nehorai, "MUSIC, maximum likelihood and the Cramér Rao bound," *IEEE Trans. Acoust., Speech, Signal Processing*, vol. 37, pp. 720–741, May 1989.

[8] ——, "MUSIC, maximum likelihood and the Cramér Rao bound: further results and comparisons," *IEEE Trans. Acoust., Speech, Signal Processing*, vol. 38, pp. 2140–2150, 1990.

[9] H. Cramér, *Mathematical Methods of Statistics*. New York: Princeton University, Press, 1946.

[10] E. L. Lehmann, *Theory of Point Estimation*. New York: Wiley, 1983.

[11] E. Boyer, P. Forster, and P. Larzabal, "Non asymptotic statistical performances of beamforming for deterministic signals," *IEEE Signal Processing Lett.*, vol. 11, no. 1, pp. 20–22, Jan. 2004.

[12] L. Atallah, J. P. Barbot, and P. Larzabal, "SNR threshold indicator in data aided frequency synchronization," *IEEE Signal Processing Lett.*, vol. 11, pp. 652–654, Aug. 2004.

[13] R. J. McAulay and L. P. Seidman, "A useful form of the Barankin lower bound and its application to ppm threshold analysis," *IEEE Trans. Inform. Theory*, vol. 15, pp. 273–279, Mar. 1969.

[14] J. M. Hammersley, "On estimating restricted parametrers," *J. R. Soc. Ser. B*, vol. 12, pp. 192–240, 1950.

[15] L. Atallah, J. P. Barbot, and P. Larzabal, "From Chapman Robbins bound towards Barankin bound in threshold behaviour prediction," *Electronic Letters*, vol. 40, pp. 279–280, Feb. 2004.

[16] R. J. McAulay and E. M. Hofstetter, "Barankin bounds on parameter estimation," *IEEE Trans. Inform. Theory*, vol. 17, pp. 669–676, Nov. 1971.

[17] K. Todros and J. Tabrikian, "General classes of performance lower bounds for parameter estimation Part I: Non-bayesian bounds for unbiased estimators," *IEEE Trans. Inform. Theory*, vol. 56, pp. 5045–5063, Oct. 2010.

[18] P. Stoica and A. Nehorai, "Performances study of conditional and unconditional direction of arrival estimation," *IEEE Trans. Acoust., Speech, Signal Processing*, vol. 38, pp. 1783–1795, Oct. 1990.

[19] P. Forster and P. Larzabal, "On lower bounds for deterministic parameter estimation," in *Proc. of IEEE Int. Conf. Acoust., Speech, Signal Processing*, Orlando, Fl, 2002.

[20] P. Stoica and R. Moses, *Spectral Analysis of Signals*. NJ: Prentice Hall, 2005.

[21] K. B. Petersen and M. S. Pedersen, "The matrix cookbook," available at http://matrixcookbook.com, ver. nov. 14, 2008.

[22] A. Renaux, "Contribution à l'analyse des performances d'estimation en traitement statistique du signal," Ph.D. dissertation, Ecole Normale Supérieure de Cachan, Cachan, FR., Jul. 2006. http://www.satie.ens-cachan.fr/ts/These_Alex.pdf.

Annexe B

Articles sur le seuil de résolution limite pour des signaux monodimensionnels

B.1 IEEE-SP-2011

M. N. El Korso, R. Boyer, A. Renaux and S. Marcos, "Statistical resolution limit of the uniform linear cocentered orthogonal loop and dipole array", *IEEE Transactions on Signal Processing*, Volume : 59, Issue : 1, Jan. 2011, pp. 425-431.

Correspondence

Statistical Resolution Limit of the Uniform Linear Cocentered Orthogonal Loop and Dipole Array

Mohammed Nabil El Korso, Rémy Boyer, Alexandre Renaux, and Sylvie Marcos

***Abstract*—Among the family of polarization sensitive arrays, we can find the so-called cocentered orthogonal loop and dipole uniform linear array (COLD-ULA). The COLD-ULA exhibits some interesting properties, e.g., the insensibility of the polarization vector with respect to the source localization in the plan of the array. In this correspondence, we derive the statistical resolution limit (SRL) characterizing the minimal separation, in terms of direction-of-arrivals, to resolve two closely spaced known polarized sources impinging on a COLD-ULA. Toward this end, nonmatrix closed form expressions of the deterministic Cramér–Rao bound (CRB) are derived and thus, the SRL is deduced. A comparison between the SRL of the COLD-ULA and the classical ULA are given. Particularly, it is shown that, in the case of orthogonal known signal sources, the SRL of the COLD-ULA is equal to the SRL of the ULA, meaning that it is not a function of polarization parameters. Furthermore, due to the derived SRL, it is shown that, under some general conditions, the SRL of the COLD-ULA is smaller than the one of the ULA.**

***Index Terms*—Cocentered orthogonal loop and dipole (COLD) array, polarized sources localization, statistical resolution limit.**

I. Introduction

Polarized sources localization by an array of sensors is an important topic with a large number of applications especially in wireless communication and seismology [1]. Particularly, the context of polarized sources has been investigated in the literature and several algorithms, to estimate the localization and polarization parameters, have been proposed [1]–[4]. Among the different types of arrays, the crossed-dipole array (constituted by several couple of dipoles) is sensitive to the source's polarization and thus, is adequate to this context. In particular, the cocentered orthogonal loop and dipole uniform linear array (COLD-ULA) exhibits some interesting properties [5], [6], as for instance, the insensibility of the polarization vector with respect to the source localization in the plan of the array or, the constant norm of the polarization vector. Note that these properties are not shared by the standard crossed-dipole array [5]. The optimal performance in terms of mean square error by way of the Cramér–Rao bound (CRB) for the COLD-ULA array has already been investigated in [5], [6]. In [5], matrix expressions of the CRB was given, whereas, in [6] the asymptotic (in terms of sensors) CRB was derived. However, to the best of our knowledge, no works has been done on the resolvability of closely polarized sources.

Manuscript received May 10, 2010; accepted September 21, 2010. Date of publication October 07, 2010; date of current version December 17, 2010. This project is funded by region Île de France and Digeteo Research Park. The associate editor coordinating the review of this manuscript and approving it for publication was Prof. Andreas Jakobsson.

The authors are with Laboratoire des Signaux et Systèmes (L2S), Université Paris-Sud XI (UPS), CNRS, SUPELEC, Gif-Sur-Yvette, 91192, France (e-mail: elkorso@lss.supelec.fr; remy.boyer@lss.supelec.fr; alexandre.renaux@lss.supelec.fr; marcos@lss.supelec.fr).

Color versions of one or more of the figures in this correspondence are available online at http://ieeexplore.ieee.org.

Digital Object Identifier 10.1109/TSP.2010.2083657

A common tool to characterize the resolvability between two signals is the so-called statistical resolution limit (SRL). The SRL [7]–[19], defined *as the minimal separation between two signals in terms of the parameter of interest*, is a challenging problem and an essential tool to quantify estimator performance.

One can find in the literature three main approaches to characterize the SRL:

i) The first is based on the concept of mean null spectrum and is relevant to a specific high-resolution algorithm [7], [8].
ii) The second approach is based on a hypothesis test using the generalized likelihood ratio test (GLRT) [9]–[11] or the Bayesian approach [12].
iii) The third method is based on the estimation accuracy concept [13]–[18].

In this context, one can distinguish two main criteria. The first one was introduced by Lee in [13] and states that *two signals are resolvable, w.r.t. the parameter of interest ω_1 and ω_2, if the maximum standard deviation, of ω_1 and ω_2, is less than half the difference between ω_1 and ω_2*. However, one can note that the Lee criterion ignores the coupling between the parameters of interest [19]. To take into account this effect, Smith [16], proposed the second following criterion based on the CRB: *two signals are resolvable if the separation between ω_1 and ω_2, is less than the standard deviation of the separation estimation*. Consequently, the SRL in the Smith sense is defined as the separation between the parameters of interest that is equal to the standard deviation of the separation.

To the best of our knowledge, all the works related to the resolvability of closely spaced sources concern the case of non-polarized sources [7]–[9], [11]–[18], and no studies/results are available concerning the case of polarized sources. The goal of this correspondence is to fill this lack.

Since the mean null spectrum approach is relevant to a specific high-resolution algorithm, in this correspondence we focus mainly on the SRL derivation for known polarized sources in the Smith sense. Furthermore, since it exists a relationship between the SRL based on the Smith criterion and the SRL based on a hypothesis test [11] in the asymptotic case, the SRL based on a hypothesis test is deduced and compared to the derived SRL based on the Smith criterion.

Consequently, in this correspondence, we derive and analyze the minimum direction-of-arrivals (DOA) separation between two known polarized sources that allows a correct sources resolvability for the COLD-ULA in the Smith sense. As a by product, a closed-form expression of the true (non-asymptotic) deterministic CRB is given (which is not available in the literature). Finally, the SRL using an ULA is derived and compared to the SRL using a COLD-ULA. It is shown that, in the case of orthogonal known signal sources, the SRL is not a function of polarization parameters (i.e., the SRL of the COLD-ULA is equal to the SRL of the ULA). Furthermore, in the case of non-orthogonal known signal sources and under some general conditions, the SRL of the COLD-ULA is shown to be smaller than the one of the ULA.

II. Model Setup

Consider a COLD-ULA made from L COLD sensors (a COLD sensor is formed by a loop and a dipole [5]) with interelement spacing d that receives a signal emitted by M radiating far-field and narrowband sources. Assuming that the array and the incident signals are coplanar [5], i.e., the elevation is fixed to $\pi/2$, the observed signal

model on the ℓ^{th} COLD sensor at the t^{th} snapshot is given by[1] [2], [5] $\boldsymbol{x}_\ell(t) = [x_{\text{loop}}(t)\ x_{\text{dipole}}(t)]^T = \sum_{m=1}^{M} \alpha_m(t)\mathbf{u}_m e^{i\ell\omega_m} + \boldsymbol{v}_\ell(t)$, where $\ell = 0 \dots L-1$ and $t = 1 \dots N$, in which N is the number of snapshots. $\omega_m = (2\pi/\lambda)d\sin(\theta_m)$ is the spatial phase factor in which θ_m and λ are the azimuth of the m^{th} source and the wavelength, respectively. The time-varying source is modelled by[2] $\alpha_m(t) = a_m e^{i(2\pi f_0 t + \phi_m(t))}$ in which a_m is the non-zero real amplitude, $\phi_m(t)$ is the time-varying modulating phase and f_0 denotes the carrier frequency of the incident wave. The additive noise is denoted by $\boldsymbol{v}_\ell(t) = [v_{\text{loop}}(t)\ v_{\text{dipole}}(t)]^T$. The polarization state vector $\mathbf{u}_m$ is given by

$$\mathbf{u}_m = \begin{bmatrix} \frac{2i\pi A_{sl}}{\lambda}\cos(\rho_m) \\ -L_{sd}\sin(\rho_m)e^{i\psi_m} \end{bmatrix}$$

where $\rho_m \in [0, \pi/2]$ and $\psi_m \in [-\pi, \pi]$ are the polarization state parameters. From a modelling point of view, each dipole in the array is assumed to be a short dipole (w.r.t. the distance d) with the same length L_{sd} and each loop is assumed to be a short loop (w.r.t. the distance d) with the same area A_{sl}. Under these assumptions, the total output vector received by the COLD-ULA for the t^{th} snapshot can be written as follows:

$$\begin{aligned} \boldsymbol{y}(t) &= \begin{bmatrix} \boldsymbol{x}_0^T(t) & \dots & \boldsymbol{x}_{L-1}^T(t) \end{bmatrix}^T \\ &= \sum_{m=1}^{M} \mathbf{A}_m(t)\mathbf{d}_m + \begin{bmatrix} \boldsymbol{v}_0^T(t) & \dots & \boldsymbol{v}_{L-1}^T(t) \end{bmatrix}^T \end{aligned} \quad (1)$$

where the $(2L) \times L$ matrix $\mathbf{A}_m(t) = \mathbf{I}_L \otimes (\alpha_m(t)\mathbf{u}_m)$ in which the operator $\otimes$ stands for the Kronecker product. The steering vector is defined by $\mathbf{d}_m = [1\ e^{i\omega_m}\ \dots\ e^{i(L-1)\omega_m}]^T$. Since the problem addressed herein is to derive the SRL based on the CRB for the proposed model, we first start by deriving the CRB for (1) in the case of $M = 2$ sources.

III. Deterministic Cramér-Rao Bound Derivation

In the remaining of the correspondence, we will use the following assumptions:

- A1. The noise is assumed to be a complex circular white Gaussian random noise with zero-mean and unknown variance σ^2. In addition, it is assumed to be both temporally and spatially uncorrelated.
- A2. The sources are assumed to be known and deterministic (see, e.g., [20]–[24]). The unknown parameter vector is then given by[3] $\boldsymbol{\xi} = [\omega_1\ \omega_2\ \sigma^2]^T$.
- A3. Furthermore, from a modelling point of view, we can assume, without loss of generality [5], that $L_{sd} = 2\pi A_{sl}/\lambda = 1$.

Using A1, the joint probability density function of the full observation vector $\boldsymbol{\chi} = [\boldsymbol{y}^T(1) \dots \boldsymbol{y}^T(N)]^T$ given $\boldsymbol{\xi}$ can be written as follows:

$$p(\boldsymbol{\chi}|\boldsymbol{\xi}) = \frac{1}{(\pi\sigma^2)^{2NL}} e^{\frac{-1}{\sigma^2}(\boldsymbol{\chi}-\boldsymbol{\mu})^H(\boldsymbol{\chi}-\boldsymbol{\mu})}$$

where $\boldsymbol{\mu} = \sum_{m=1}^{2} [\mathbf{d}_m^T\mathbf{A}_m(1)^T \dots \mathbf{d}_m^T\mathbf{A}_m(N)^T]^T$. Let $E\{(\hat{\boldsymbol{\xi}} - \boldsymbol{\xi})(\hat{\boldsymbol{\xi}} - \boldsymbol{\xi})^T\}$ be the covariance matrix of an unbiased estimator of $\boldsymbol{\xi}$, denoted by $\hat{\boldsymbol{\xi}}$. The covariance inequality principle states that under quite general/weak conditions $\text{MSE}([\hat{\boldsymbol{\xi}}]_i) = E\{([\hat{\boldsymbol{\xi}}]_i - [\boldsymbol{\xi}]_i)^2\} \geq \text{CRB}([\boldsymbol{\xi}]_i)$, where $\text{CRB}([\boldsymbol{\xi}]_i) = [\mathbf{FIM}^{-1}(\boldsymbol{\xi})]_{i,i}$ in which $\mathbf{FIM}(\boldsymbol{\xi})$ denotes the Fisher information matrix (FIM) regarding to the vector parameter $\boldsymbol{\xi}$.

Since we are working with a Gaussian observation model (assumption A1), the $i^{\text{th}}, j^{\text{th}}$ element of the FIM for the parameter vector $\boldsymbol{\xi}$ can be written as [25]

$$[\mathbf{FIM}(\boldsymbol{\xi})]_{i,j} = \frac{NL}{\sigma^4}\frac{\partial\sigma^2}{\partial[\boldsymbol{\xi}]_i}\frac{\partial\sigma^2}{\partial[\boldsymbol{\xi}]_j} + \frac{2}{\sigma^2}\Re\left\{\frac{\partial\boldsymbol{\mu}^H}{\partial[\boldsymbol{\xi}]_i}\frac{\partial\boldsymbol{\mu}}{\partial[\boldsymbol{\xi}]_j}\right\}$$

where $(i,j) \in \{1,2,3\}^2$. $[\boldsymbol{\xi}]_i$ and $\Re\{z\}$ denote the i^{th} element of $\boldsymbol{\xi}$ and the real part of z, respectively. Then, the FIM for the proposed model is block-diagonal

$$\mathbf{FIM}(\boldsymbol{\xi}) = \frac{2}{\sigma^2}\begin{bmatrix} \mathbf{F} & \mathbf{0} \\ \mathbf{0}^T & \frac{NL}{2\sigma^2} \end{bmatrix} \quad (2)$$

where

$$\begin{aligned} [\mathbf{F}]_{m,p} &= \Re\left\{\frac{\partial\boldsymbol{\mu}^H}{\partial\omega_m}\frac{\partial\boldsymbol{\mu}}{\partial\omega_p}\right\} \\ &= N\Re\left\{r_N\left(\mathbf{u}_m^H\mathbf{u}_p\mathbf{d}_m^H\mathbf{D}^2\mathbf{d}_p + K_{mp}\right)\right\}, \quad (m,p) \in \{1,2\}^2 \end{aligned} \quad (3)$$

in which $\mathbf{D} = \text{diag}\{0, \dots, L-1\}$, $r_N = (1/N)\sum_{t=1}^{N}\alpha_1^*(t)\alpha_2(t)$ and

$$K_{mp} = \frac{\partial\mathbf{u}_m^H}{\partial\omega_m}\frac{\partial\mathbf{u}_p}{\partial\omega_p}\mathbf{d}_m^H\mathbf{d}_p - i\mathbf{u}_m^H\frac{\partial\mathbf{u}_p}{\partial\omega_p}\mathbf{d}_m^H\mathbf{D}\mathbf{d}_p + i\frac{\partial\mathbf{u}_m}{\partial\omega_m}\mathbf{u}_p^H\mathbf{d}_m^H\mathbf{D}\mathbf{d}_p.$$

Using the fact that the polarization state vector of a COLD array is not a function of the direction parameter, thus $\partial\mathbf{u}_m/\partial\omega_m = \mathbf{0}$. Consequently $K_{mp} = 0$ and (3) becomes $[\mathbf{F}]_{mp} = N\Re\{r_N\mathbf{u}_m^H\mathbf{u}_p\mathbf{d}_m^H\mathbf{D}^2\mathbf{d}_p\}$. Furthermore, as $\|\mathbf{u}_m\|^2 = 1$, one obtains $[\mathbf{F}]_{i,i} = Na_i^2\alpha$ for $i = 1, 2$ where $\alpha = (1/6)(L-1)L(2L-1)$. The cross terms are given by $[\mathbf{F}]_{1,2} = [\mathbf{F}]_{2,1} = N\Re\{r_N\mathbf{u}_1^H\mathbf{u}_2\eta\}$ where $\mathbf{u}_1^H\mathbf{u}_2 = \cos(\rho_1)\cos(\rho_2) + \sin(\rho_1)\sin(\rho_2)e^{i(\psi_2-\psi_1)}$ and

$$\eta = \sum_{\ell=0}^{L-1}\ell^2 e^{-i(\omega_1-\omega_2)\ell} = \sum_{\ell=0}^{L-1}\ell^2 e^{-i\text{sgn}(\omega_1-\omega_2)\delta_\omega^{(\text{COLD})}\ell} \quad (4)$$

in which $\delta_\omega^{(\text{COLD})} = |\omega_1 - \omega_2|$ and $\text{sgn}(z) = z/|z|$ for $z \neq 0$. To simplify the derivations and without loss of generality, we choose $\omega_1 > \omega_2$ in the following. Consequently, the inverse of the FIM is given by

$$\mathbf{F}^{-1} = \frac{N}{\det\{\mathbf{F}\}}\begin{bmatrix} a_2^2\alpha & -\Re\left\{r_N\mathbf{u}_1^H\mathbf{u}_2\eta\right\} \\ -\Re\left\{r_N\mathbf{u}_1^H\mathbf{u}_2\eta\right\} & a_1^2\alpha \end{bmatrix} \quad (5)$$

where $\det\{\mathbf{F}\} = N^2(a_1^2a_2^2\alpha^2 - \Re^2\{r_N\mathbf{u}_1^H\mathbf{u}_2\eta\})$. Finally, replacing (2) and (5) into $\mathbf{CRB}(\boldsymbol{\xi}) = \mathbf{FIM}^{-1}(\boldsymbol{\xi})$, the CRBs (see Fig. 1) are given by

$$\text{CRB}(\omega_1) \triangleq [\mathbf{F}^{-1}]_{1,1} = \frac{\sigma^2}{2N}\frac{a_2^2\alpha}{a_1^2a_2^2\alpha^2 - \Re^2\left\{r_N\mathbf{u}_1^H\mathbf{u}_2\eta\right\}} \quad (6)$$

$$\text{CRB}(\omega_2) \triangleq [\mathbf{F}^{-1}]_{2,2} = \frac{\sigma^2}{2N}\frac{a_1^2\alpha}{a_1^2a_2^2\alpha^2 - \Re^2\left\{r_N\mathbf{u}_1^H\mathbf{u}_2\eta\right\}} \quad (7)$$

$$\text{CRB}(\omega_1,\omega_2) \triangleq [\mathbf{F}^{-1}]_{1,2} = -\frac{\sigma^2}{2N}\frac{\Re\left\{r_N\mathbf{u}_1^H\mathbf{u}_2\eta\right\}}{a_1^2a_2^2\alpha^2 - \Re^2\left\{r_N\mathbf{u}_1^H\mathbf{u}_2\eta\right\}}. \quad (8)$$

IV. Statistical Resolution Limit

This section is devoted to the derivation of the SRL of the COLD-ULA. Taking advantage of the previously derived CRBs (6), (7), and

[1]One should note that due to the nature of the COLD array sensors, one has twice the number of measurements w.r.t. a ULA array with the same number of sensors and the same array's aperture.

[2]Note that this source model is commonly used in many digital communication systems (see [5] and references therein).

[3]Note that the state parameter vector is assumed to be known. However, this assumption is not severe (since the numerical simulations part).

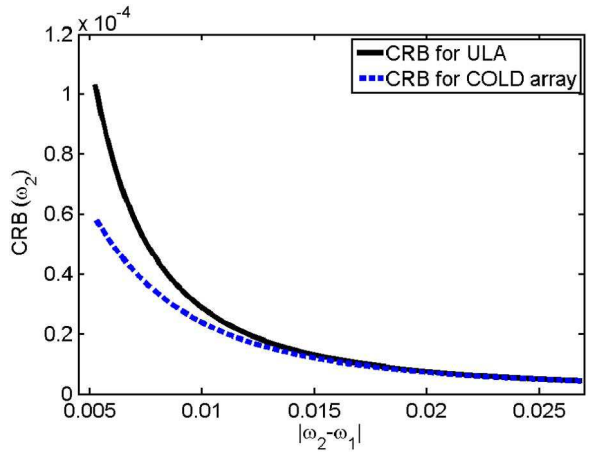

Fig. 1. The CRB for the COLD array and the ULA with $N = 100$ snapshots and $L = 25$ sensors. One can notice that for a small separation the CRB for the ULA goes to infinity faster than the CRB for the COLD array. This can be explained by the additional knowledge about polarization parameters in the case of the COLD array.

(8), the SRL in the Smith sense is derived in Section IV-A. Then, the SRL based on a hypothesis test is deduced in Section IV-B. One should note that the SRL of the ULA according to the model (1) is not derived in the literature. This latter can be derived following the same steps as in Section IV-A leading to

$$\delta_\omega^{(\mathrm{ULA})} = \frac{\sigma}{\sqrt{2N\alpha}}\sqrt{\frac{a_1^2+a_2^2+2\Re\{r_N\}}{a_1^2a_2^2-\Re^2\{r_N\}}}.$$

A. Statistical Resolution Limit for a COLD-ULA

Let $\delta_\omega^{(\mathrm{COLD})}$ denoting the SRL of COLD-ULA according to the model (1). Thus, one obtains (see [19])

$$\mathrm{CRB}\left(\delta_\omega^{(\mathrm{COLD})}\right) = \mathrm{CRB}(\omega_1)+\mathrm{CRB}(\omega_2)-2\mathrm{CRB}(\omega_1,\omega_2). \quad (9)$$

Consequently, the SRL[4] is defined as the minimal separation, denoted $\delta_\omega^{(\mathrm{COLD})}$, which resolves the following implicit equation:

$$\delta_\omega^{(\mathrm{COLD})} = \sqrt{\mathrm{CRB}\left(\delta_\omega^{(\mathrm{COLD})}\right)} \Longleftrightarrow f\left(\delta_\omega^{(\mathrm{COLD})}\right) = A \quad (10)$$

where $f(\delta_\omega^{(\mathrm{COLD})}) = (2/\sigma^2)\det\{\mathbf{F}\}\left(\left(\delta_\omega^{(\mathrm{COLD})}\right)^2 + 2\mathrm{CRB}(\omega_1,\omega_2)\right)$ and $A = (a_1^2+a_2^2)\alpha$. In the following, (10) is solved to obtain the desired SRL for the orthogonal and non-orthogonal signal sources cases.

1) The Orthogonal Signal Sources Case: In the case of orthogonal signal sources [20], one has $r_N = (1/N)\sum_{t=1}^{N}\alpha_1^*(t)\alpha_2(t) = 0$. This implies that the FIM is diagonal (i.e., the parameters of interest are decoupled). Thus, replacing $\mathrm{CRB}(\omega_1,\omega_2) = 0$ and $r_N = 0$ into (10), the SRL in the orthogonal signal sources case, denoted by $\delta_\omega^{(\mathrm{COLD-O})}$, is given by

$$\delta_\omega^{(\mathrm{COLD-O})} = \frac{\sigma}{\sqrt{2N\alpha}}\sqrt{\frac{a_1^2+a_2^2}{a_1^2a_2^2}}. \quad (11)$$

It can be readily checked that the SRL is not a function of the polarization parameters. Consequently, in comparison to the classical ULA array, the use of the COLD array cannot improve the resolvability of the sources in this scenario. Moreover, for equipowered sources ($a_1 = a_2 = a$), one obtains

$$\delta_\omega^{(\mathrm{COLD-O})} = \frac{1}{\sqrt{N\alpha\mathrm{SNR}}} \quad (12)$$

where $\mathrm{SNR} = a^2/\sigma^2$. Furthermore, for equipowered sources and a large number of sensors ($L \gg 1$), the SRL can be approximated by $\delta_\omega^{(\mathrm{COLD-O})} \approx \sqrt{3}/(N^{1/2}\mathrm{SNR}^{1/2}L^{3/2})$. Note that, in this case, the SRL is proportional to the inverse square root of the number of snapshots, to the inverse square root of the SNR and to inverse of $L\sqrt{L}$. Also note that, the SRL obtained here is qualitatively consistent with the SRL derived in [12], [17] in the case of a classical ULA array.

2) The Non-Orthogonal Signal Sources Case: The analysis in the general case of non-orthogonal signal sources (i.e., $r_N \neq 0$) is more complex and needs some approximations. Considering the second-order Taylor expansion of the functional η (see (4)) around $\delta_\omega^{(\mathrm{COLD})} = 0$, one obtains, for $L\delta_\omega^{(\mathrm{COLD})} \ll 1$, $\eta \approx \sum_{\ell=0}^{L-1}\ell^2(1+i\delta_\omega^{(\mathrm{COLD})}\ell) = \alpha + i\beta\delta_\omega^{(\mathrm{COLD})}$, where $\beta = \sum_{\ell=0}^{L-1}\ell^3 = (1/4)(L-1)^2L^2$ (note that this approximation is not severe, since numerical simulation shows that the SRL based on the second-order Taylor expansion of η is close, and in a good agreement with the exact SRL; see Fig. 3). One can note that expression (10), for non-orthogonal signal sources, becomes, for $L\delta_\omega^{(\mathrm{COLD})} \ll 1$,

$$\left(\delta_\omega^{(\mathrm{COLD})}\right)^2 = \frac{\sigma^2}{2N}\frac{A+2B-2\delta_\omega^{(\mathrm{COLD})}\bar{B}}{C^2-\left(B-\delta_\omega^{(\mathrm{COLD})}\bar{B}\right)^2} \quad (13)$$

where $B = \alpha\Re\{r_N\mathbf{u}_1^H\mathbf{u}_2\}$, $\bar{B} = \beta\Im\{r_N\mathbf{u}_1^H\mathbf{u}_2\}$ and $C = a_1a_2\alpha$ in which $\Im\{z\}$ denote the imaginary part of z. Expression (13) is in fact the roots of the following polynomial

$$p(x) = 2N\bar{B}x^4 + 4NB\bar{B}x^3 + 2N(B^2-C^2)x^2 - 2\sigma^2\bar{B}x + \sigma^2(A+2B) \quad (14)$$

where $x = \delta_\omega^{(\mathrm{COLD})}$.

Resolving this polynomial can be facilitated by noticing that, if $\delta_\omega^{(\mathrm{COLD})}$ is a root then $-\delta_\omega^{(\mathrm{COLD})}$ is also a root.[5] Consequently, $p(x)$ can be rewritten as $p(x) = (x-\delta_\omega^{(\mathrm{COLD})})(x+\delta_\omega^{(\mathrm{COLD})})(x-s_1)(x-s_2)$, where s_1 and s_2 are the unwanted roots. From the latter expression and (14), one obtains

$$\begin{cases} s_1+s_2 = 2NB \\ s_1s_2 - \left(\delta_\omega^{(\mathrm{COLD})}\right)^2 = \frac{(B^2-C^2)}{\bar{B}} \\ \left(\delta_\omega^{(\mathrm{COLD})}\right)^2(s_1+s_2) = \frac{-\sigma^2}{N} \\ -\left(\delta_\omega^{(\mathrm{COLD})}\right)^2 s_1s_2 = \frac{\sigma^2(A+2B)}{2N\bar{B}}. \end{cases} \quad (15)$$

Using the second and last equation of (15) one obtains the SRL as the root (we keep only the positive root whatever the sign of $\bar{B}$) of $2N\bar{B}(\delta_\omega^{(\mathrm{COLD})})^4 + 2N(B^2-C^2)(\delta_\omega^{(\mathrm{COLD})})^2 + \sigma^2(A+2B) = 0$. Consequently,

$$(\delta_\omega^{(\mathrm{COLD})})^2 = \frac{C^2-B^2}{2\bar{B}}\left(1-\sqrt{1-2\sigma^2\frac{(A+2B)}{(B^2-C^2)^2}\frac{\bar{B}}{N}}\right).$$

[4]From (9), one should note that the SRL using the Smith criterion [16] takes into account the coupling between the parameters of interest unlike the Lee criterion [13], see Fig. 2 (*right*).

[5]Indeed, using the change variable formula (see [26] p. 45) w.r.t. $\bar{\delta} = -\delta_\omega^{(\mathrm{COLD})}$, the Jacobian matrix $\mathbf{J}$ is reduced to a scalar $J = -1$. Thus, $\mathrm{CRB}(-\delta_\omega^{(\mathrm{COLD})}) = \mathrm{CRB}(\bar{\delta}) = J^2\mathrm{CRB}(\delta_\omega^{(\mathrm{COLD})}) = \mathrm{CRB}(\delta_\omega^{(\mathrm{COLD})})$. Consequently, if $\delta_\omega^{(\mathrm{COLD})}$ is a root of $(\delta_\omega^{(\mathrm{COLD})})^2 = \mathrm{CRB}(\delta_\omega^{(\mathrm{COLD})})$ then $-\delta_\omega^{(\mathrm{COLD})}$ is also a root.

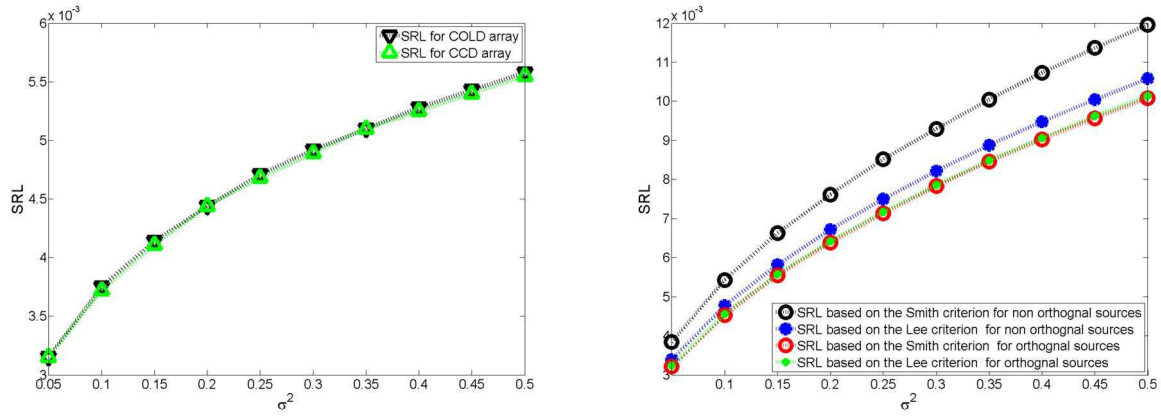

Fig. 2. Left: The SRL using a COLD and a cocentered crossed-dipole (CCD) [5]. One notices that the SRL of a CCD array is in a good agreement with the SRL of a COLD array. However, the SRL closed form expression of the COLD array is easier to derive since the COLD array exhibits some interesting properties, as for instance, the insensibility of the polarization vector to the source localization in the plan of the array and the constant norm of the polarization vector. Right: The SRL based on the Smith and Lee criterion. One can notice that in the case of orthogonal signal sources, the SRL based on the Smith and Lee criterion coincides (upon a normalization factor). However, in the general case (i.e., not orthogonal signal sources) the Lee criterion, unlike the Smith criterion, ignores the coupling terms between the parameters of interest.

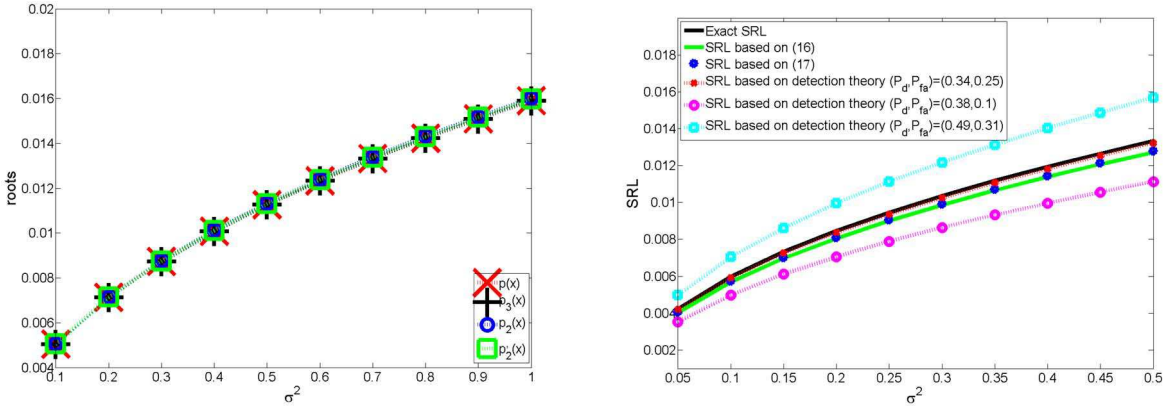

Fig. 3. Left: Illustration of the desired roots of the polynomials $p_2(x), p_2'(x), p_3(x)$ and $p_4(x)$. Right: Comparison with literature results: The SRL versus σ^2 for $N = 100$: the approximated SRL based on (16) and (17) is in good agreement with the exact SRL (i.e., the numerical solution of (10) without any approximation). This validate the closed-form expressions given in (16) and (17). Furthermore, one can notice that, for example, for $P_d = 0.37$ and $P_{\text{fa}} = 0.1$ the SRL based on the SRL (16) and (17) is almost equal to the SRL based on a hypothesis test [11] derived in the asymptotic case. From the case $P_d = 0.49$ and $P_{\text{fa}} = 0.3$ or/and $P_d = 0.32$ and $P_{\text{fa}} = 0.1$, one can notice the influence of the translation factor ρ on the SRL.

One should note that under realistic conditions $\delta_\omega^{(\text{COLD})}$ exists since $\frac{(A+2B)}{(B^2-C^2)^2}\frac{\bar{B}}{N}$ is $o(\frac{1}{NL^5})$ (i.e., $|\frac{(A+2B)}{(B^2-C^2)^2})\frac{\bar{B}}{N}| \ll 1$). Consequently, the desired SRL is given by (we discard the negative root) (see (16), shown at the bottom of the page). Note that, unlike the orthogonal signal sources case, the SRL depends on the state vector parameter.

Remark 1: Note that the latter formula is valid if $\bar{B} \neq 0$. When $\bar{B} = 0$, the roots of $p(x)$ (which become the roots of $p_2(x) \triangleq 2N(B^2 - C^2)x^2 + \sigma^2(A + 2B)$) are given by $x^2 = \frac{-\sigma^2(A+2B)}{2N(B^2-C^2)}$. The real root exists if in particular $C^2 - B^2 > 0$ and $A + 2B \geq 0$. Since $|\Re\{xy\}| \leq |xy| \leq |x||y|$, where $|.|$ denotes the absolute value of a real number or the modulus of a complex number, then, for a fixed value of t, one has $|\Re\{e^{i(\phi_2(t)-\phi_1(t))}\mathbf{u}_1^H\mathbf{u}_2\}| \leq |e^{j(\phi_2(t)-\phi_1(t))}||\mathbf{u}_1^H\mathbf{u}_2| \leq 1$. Thus, $|\Re\{\sum_{t=1}^N e^{i(\phi_2(t)-\phi_1(t))}\mathbf{u}_1^H\mathbf{u}_2\}| \leq \sum_{t=1}^N|\Re\{e^{i(\phi_2(t)-\phi_1(t))}\mathbf{u}_1^H\mathbf{u}_2\}| \leq N \leq N\frac{a_1^2+a_2^2}{2a_1a_2}$. Consequently, $A \geq -2B$ is satisfied. On the other hand, since $\Im\{r_N\mathbf{u}_1^H\mathbf{u}_2\} = 0$, thus, $|\Re\{r_N\mathbf{u}_1^H\mathbf{u}_2\}| = |r_N||\mathbf{u}_1^H\mathbf{u}_2|$. Assuming different polarization state vectors, i.e., $(\rho_1, \psi_1) \neq (\rho_2, \psi_2)$, one obtains $|r_N||\mathbf{u}_1^H\mathbf{u}_2| < |r_N| \leq (a_1a_2/N)\sum_{t=1}^N|e^{i(\phi_2(t)-\phi_1(t))}| = a_1a_2$. Thus, $B^2 < C^2$. Finally, one concludes that the root of (14) in

$$\delta_\omega^{(\text{COLD})} = \sqrt{\frac{C^2-B^2}{2\bar{B}}\left(1-\sqrt{1-2\sigma^2\frac{(A+2B)}{(B^2-C^2)^2}\frac{\bar{B}}{N}}\right)}$$
$$= \alpha\sqrt{\frac{a_1^2a_2^2-\Re^2\{r_N\mathbf{u}_1^H\mathbf{u}_2\}}{2\beta\Im\{r_N\mathbf{u}_1^H\mathbf{u}_2\}}\left(1-\sqrt{1-\frac{2\sigma^2\beta\Im\{r_N\mathbf{u}_1^H\mathbf{u}_2\}}{\alpha N}\frac{((a_1^2+a_2^2)+2\Re\{r_N\mathbf{u}_1^H\mathbf{u}_2\})}{(\Re^2\{r_N\mathbf{u}_1^H\mathbf{u}_2\}-a_1^2a_2^2)^2}}\right)}. \quad (16)$$

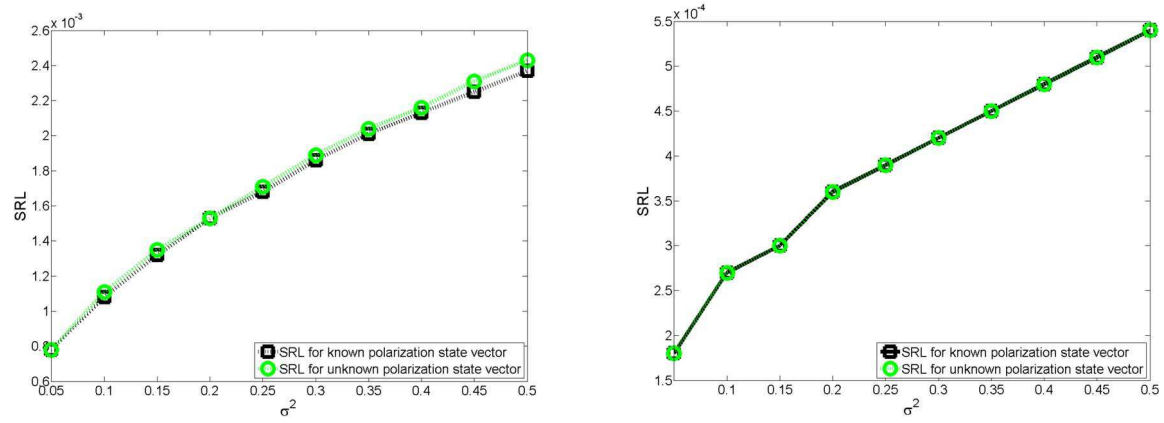

Fig. 4. The SRL of the COLD-ULA with (left) $N = 40$ snapshots and $L = 5$ sensors, and (right) $N = 100$ snapshots and $L = 10$ sensors. Note that the SRL using the assumption of known state parameter vector is almost identical to the SRL of unknown state parameter vector.

the case $\Im\{r_N \mathbf{u}_1^H \mathbf{u}_2\} = 0$ exists and is given by (we discard the negative root)

$$\delta_\omega^{(\mathrm{COLD})} = \frac{\sigma}{\sqrt{2N\alpha}} \sqrt{\frac{a_1^2 + a_2^2 + 2\Re\{r_N \mathbf{u}_1^H \mathbf{u}_2\}}{a_1^2 a_2^2 - \Re^2\{r_N \mathbf{u}_1^H \mathbf{u}_2\}}}. \quad (17)$$

Remark 2: From Fig. 3 (left), one can notice that the desired roots of $p_4(x), p_3(x) \triangleq 4NB\bar{B}x^3 + 2N(B^2 - C^2)x^2 - 2\sigma^2\bar{B}x + \sigma^2(A+2B)$, $p_2(x)$ and $p_2'(x) \triangleq 2N(B^2 - C^2)x^2 - 2\sigma^2\bar{B}x + \sigma^2(A+2B)$ are almost identical for various values of σ^2. Indeed, this is expected since the desired roots, corresponding to the SRL, are small (i.e., $\delta_\omega^{(\mathrm{COLD})} \ll 1$). Furthermore, for a sufficient number of sensors, the coefficient corresponding to the fourth, third and first degree of the polynomial $p(x)$ are small (i.e., $2N\bar{B} \sim O(1)$, $4NB\bar{B} \sim O(1/N)$ and $2\sigma^2\bar{B} \sim O(1/N)$ whereas $2N(B^2 - C^2) \sim O(N)$).

Remark 3: On the other hand, since $|\frac{(A+2B)}{(B^2-C^2)^2}\frac{\bar{B}}{N}| \ll 1$, the second-order Taylor expansion of (16) around $\frac{(A+2B)}{(B^2-C^2)^2}\frac{\bar{B}}{N} = 0$ gives

$$\delta_\omega^{(\mathrm{COLD})} = \frac{\sigma}{\sqrt{2N\alpha}} \sqrt{\frac{a_1^2 + a_2^2 + 2\Re\{r_N \mathbf{u}_1^H \mathbf{u}_2\}}{a_1^2 a_2^2 - \Re^2\{r_N \mathbf{u}_1^H \mathbf{u}_2\}}} \quad (18)$$

which is the same expression as in (17). Furthermore, for orthogonal signal sources, one obtains (11). Consequently, (17) unifies the different cases of the SRL derivation results.

Remark 4: Finally, using (17) and for equipowered sources (i.e., $a_1 = a_2 = a$), one obtains

$$\delta_\omega^{(\mathrm{COLD})} = \frac{1}{\sqrt{N\alpha \mathrm{SNR}}} \sqrt{\frac{1 + \Re\{\tilde{r}_N \mathbf{u}_1^H \mathbf{u}_2\}}{1 - \Re^2\{\tilde{r}_N \mathbf{u}_1^H \mathbf{u}_2\}}} \quad (19)$$

in which $\tilde{r}_N = (1/N)\sum_{t=1}^{N} e^{j(\phi_2(t) - \phi_1(t))}$. Note that, the SRL obtained in (19) is qualitatively consistent with the SRL derived in [12] and [17] in the case of a classical ULA array.

Remark 5: The polarization state vector of a COLD array is not function of the direction parameter (i.e., $\partial \mathbf{u}_m / \partial \omega_m = \mathbf{0}$ for $m = 1, 2$). Remark that this is not the case for Cocentered Crossed-Dipole (CCD) antenna. This nice property of the COLD array allows to greatly simplify the analysis of the SRL, see Fig. 2 (left) for a comparison between the CCD-ULA and the COLD-ULA SRL.

Furthermore, from A2, one can note that the state parameter vector is assumed to be known. However, this assumption is not severe, since numerical simulations show that the SRL of a known state parameter vector is close to the SRL of a unknown state parameter vector (even for a low number of sensors $L = 5$ and/or a low number of snapshots $N = 40$); see Fig. 4.

B. SRL Based on a Hypothesis Test

Another approach to derive the SRL is based on a hypothesis test. In this Subsection, we show that the results of [11] in the case of non-polarized sources can be extended to the polarized sources case. Indeed, using a binary hypothesis test and the same method as in [11], the asymptotic (in terms of snapshots) SRL based on a hypothesis test is given as the root of (proof: see the Appendix)

$$\delta_{\mathrm{detection}} = \rho\sqrt{\mathrm{CRB}(\delta_{\mathrm{detection}})}. \quad (20)$$

The so-called translation factor, ρ, is determined numerically, for a given probability of detection P_d and a given probability of false alarm P_{fa}, as the root of $\mathcal{Q}^{-1}_{\chi'^2_2(\rho)}(P_d) = \mathcal{Q}^{-1}_{\chi^2_2}(P_{\mathrm{fa}})$. In which $\mathcal{Q}^{-1}_{\chi^2_2}(.)$ and $\mathcal{Q}^{-1}_{\chi'^2_2(\rho)}(.)$ denote the inverse of the right tail probability of the central chi-squared pdf χ^2_2 and the noncentral chi-squared pdf $\chi'^2_2(\rho)$, respectively).

Remark 6: The hypothesis test used to derive (20) is a binary one-sided test and the MLE used is an unconstrained estimator (see the Appendix), thus, one can deduce that the GLRT, used to derive the asymptotic SRL, is [27] 1) asymptotically uniformly most powerful (UMP) test among all invariant statistical tests, and 2) has asymptotic constant false-alarm rate (CFAR).

Fig. 3 (right) shows that the derived SRL (17) is in agreement, with respect to the translation factor, with the extension of the SRL based on a UMP and CFAR hypothesis test in the asymptotic case, which assesses the validity of our results. In addition, this figure shows that the derived SRL is tight w.r.t. the exact SRL (i.e., the numerical solution of (10) without any approximation). Furthermore, Fig. 3 (right) assesses remark 2 and 3 since the SRL (17) derived using $p_2(x)$ is almost identical to the SRL (16) derived using $p(x)$.

In the following section, a comparison between the SRL of two polarized sources impinging on a COLD-ULA and on an ULA, is done.

V. Comparison Between the Statistical Resolution Limit of a COLD-ULA and an ULA and Numerical Analysis

Consider two radiating far-field and narrowband sources observed by a classical ULA of L sensors with interelement spacing d [25]. The array and the emitted signals are coplanar. Following the same steps leading to $\delta_\omega^{(\mathrm{COLD-O})}$, one obtains after some algebra calculations the SRL of the ULA denoted by $\delta_\omega^{(\mathrm{ULA-O})}$. The derivations are not reported here since they are similar to the ones presented for the COLD array. As in Section IV, we detail the orthogonal and non-orthogonal signal sources case.

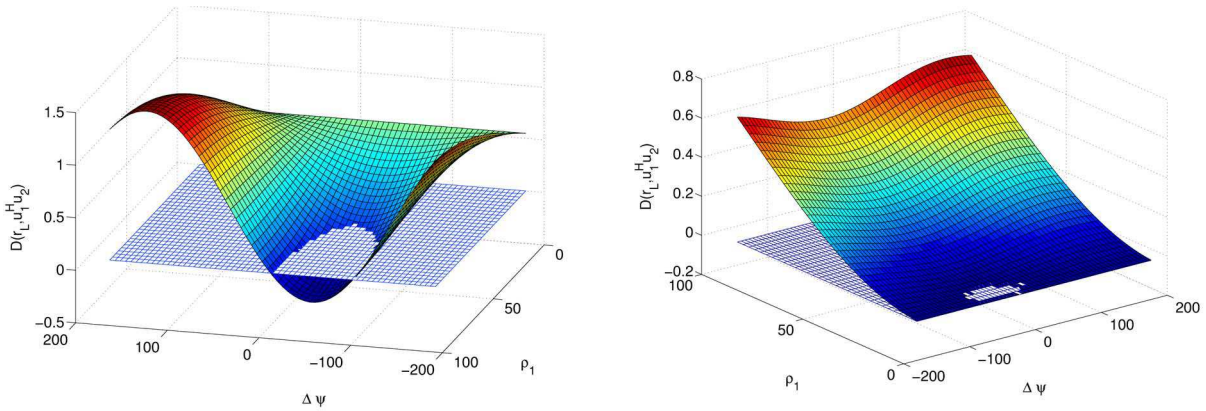

Fig. 5. $D(r_L, \mathbf{u}_1^H \mathbf{u}_2)$ versus the polarization state parameters ρ and ψ; $a_1 = 2, a_2 = 3, r_N = (1+i)/20$ where $N = 20$. (Left) $\rho_2 = 85°$ and (right) $\rho_2 = 5°$.

A. Comparison in the Orthogonal Signal Sources Case

In the case where the signal sources are orthogonal (i.e., $r_N = 0$ [20]), one obtains (after calculus) $\delta_\omega^{(\mathrm{ULA-O})} = \delta_\omega^{(\mathrm{COLD-O})}$ meaning that the COLD-ULA and the classical ULA have the same resolvability capacity.

B. Comparison in the Non-Orthogonal Signal Sources Case

In the following we focus on the SRL given by (18) (see remark 3). After calculus, one obtains the SRL of the ULA

$$\delta_\omega^{(\mathrm{ULA})} = \frac{\sigma}{\sqrt{2N\alpha}} \sqrt{\frac{(a_1^2 + a_2^2) + 2\Re\{r_N\}}{a_1^2 a_2^2 - \Re^2\{r_N\}}}. \tag{21}$$

Thus, from (17) and (21), one can check that

$$\delta_\omega^{(\mathrm{COLD})} \leq \delta_\omega^{(\mathrm{ULA})} \quad \text{iff} \quad \Re\{r_N\} \geq \Re\left\{r_N \mathbf{u}_1^H \mathbf{u}_2\right\}. \tag{22}$$

As $\Re\{r_N \mathbf{u}_1^H \mathbf{u}_2\} = \Re\{r_N\}\Re\{\mathbf{u}_1^H \mathbf{u}_2\} - \Im\{r_N\}\Im\{\mathbf{u}_1^H \mathbf{u}_2\}$ and $\Re\{\mathbf{u}_1^H \mathbf{u}_2\} \leq 1$, condition (22) is satisfied for $\Im\{r_N\} = 0$ or/and $\Im\{\mathbf{u}_1^H \mathbf{u}_2\} = 0$. Consequently, we have $\delta_\omega^{(\mathrm{COLD})} < \delta_\omega^{(\mathrm{ULA})}$ for the following cases:

- C1. if the signals are real and positive, i.e., $\Im\{r_N\} = 0$ or with the same phase, i.e., $\phi_1(t) = \phi_2(t), \forall t$;
- C2. if $\psi_1 = \psi_2$, i.e., $\Im\{\mathbf{u}_1^H \mathbf{u}_2\} = 0$;
- C3. if $\rho_1 = 0$ or $\rho_2 = 0$, i.e., $\Im\{\mathbf{u}_1^H \mathbf{u}_2\} = 0$.

Besides C1., C2., and C3., in Fig. 5 we plot $D(r_L, \mathbf{u}_1^H \mathbf{u}_2) = \Re\{r_N\} - \Re\{r_N \mathbf{u}_1^H \mathbf{u}_2\}$ versus the polarization state parameters ρ and ψ. Consequently, from (22) if $D > 0$ thus $\delta_\omega^{(\mathrm{COLD})} < \delta_\omega^{(\mathrm{ULA})}$. Fig. 5 suggests that generally $\delta_\omega^{(\mathrm{COLD})} < \delta_\omega^{(\mathrm{ULA})}$ while $\delta_\omega^{(\mathrm{COLD})} > \delta_\omega^{(\mathrm{ULA})}$ only for a small region (which corresponds to the part of the plot that is under the horizontal plan). This means that generally, the SRL of the COLD-ULA is smaller than the one for the ULA.

VI. Conclusion

In this correspondence, we derived the deterministic CRB in a non-matrix closed form expression for two polarized far-field time-varying narrowband known sources observed by a COLD-ULA. Taking advantage of these expressions, we deduced the SRL for the COLD-ULA which was compared to the SRL of the ULA. We noticed that, surprisingly, in the case where the signal sources are orthogonal, the SRL of the COLD-ULA is equal to the SRL of the ULA, meaning that it is not a function of polarization parameters. Furthermore, for non-orthogonal signal sources, we have given three sufficient and necessary conditions such that the SRL of the COLD-ULA is less than the SRL of the ULA. By analytical expressions and numerical simulations we have shown that the SRL of the ULA is less than the SRL of the COLD-ULA only for few cases, meaning that generally the performance of the COLD-ULA is better than the performance of the ULA. Note that an interesting work could be to apply the proposed method in the case of Gaussian sources and to compare it to [17, eq.(9)].

Appendix

Let us consider the following binary hypothesis test where $\mathcal{H}_0$ and $\mathcal{H}_1$ represent the presence of one signal and the presence of two signals, respectively. Consequently, following the same line as in [11], one can formulate the hypothesis test, as a simple one-sided binary hypothesis test as follows:

$$\begin{cases} \mathcal{H}_0 : & \delta_{\mathrm{detection}} = 0 \\ \mathcal{H}_1 : & \delta_{\mathrm{detection}} > 0 \end{cases} \tag{23}$$

where $\delta_{\mathrm{detection}}$ denotes the SRL based on a hypothesis test such that $\delta_{\mathrm{detection}} = |\omega_1 - \omega_2|$. To derive the SRL based on a hypothesis test, we consider the GLRT [27]:

$$L_G(\boldsymbol{y}) = \frac{p(\boldsymbol{y}|\hat{\delta}_{\mathrm{detection}}, \hat{\sigma}_1, \mathcal{H}_1)}{p(\boldsymbol{y}|\hat{\sigma}_0, \mathcal{H}_0)} \gtrless^{\mathcal{H}_1} \varsigma' \tag{24}$$

where $\hat{\delta}_{\mathrm{detection}}$, $\hat{\sigma}_1$ and $\hat{\sigma}_0$ denote the maximum likelihood estimates (MLE) of $\delta_{\mathrm{detection}}$ under $\mathcal{H}_1$, the MLE of σ under $\mathcal{H}_1$ and the MLE of σ_0 under $\mathcal{H}_0$, respectively, in which ς' denotes the test threshold (the central spatial phase factor is implicitly assumed unknown). From (24), one obtains

$$T_G(\boldsymbol{y}) = \mathrm{Ln} L_G(\boldsymbol{y}) \gtrless^{\mathcal{H}_1} \varsigma = \mathrm{Ln}\varsigma'. \tag{25}$$

Deriving and analyzing the SRL from (25) seems to be hard and even intractable in some cases (especially due to the derivation of $\hat{\delta}_{\mathrm{detection}}$). Consequently, in the following we consider the asymptotic case. In [27] it has been proved that, for a large number of snapshots, the statistic $T_G(\boldsymbol{y})$ in (25) follows:

$$T_G(\boldsymbol{y}) \sim \begin{cases} \chi_2^2 & \text{under } \mathcal{H}_0 \\ \chi'^2_2(\rho') & \text{under } \mathcal{H}_1 \end{cases} \tag{26}$$

where χ_2^2 and $\chi'^2_2(\rho')$ denote the central chi-square pdf and the noncentral chi-square pdf both with two degrees of freedom. The noncentral parameter ρ' is given by [27]

$$\rho' = \hat{\delta}^2_{\mathrm{detection}} \left(\mathrm{CRB}(\delta_{\mathrm{detection}})\right)^{-1}. \tag{27}$$

Since we consider the asymptotic case $\hat{\delta}_{\mathrm{detection}} \approx \delta_{\mathrm{detection}}$, thus (27) becomes $\delta^2_{\mathrm{detection}} = \rho' \mathrm{CRB}(\delta_{\mathrm{detection}})$. Consequently, $\delta_{\mathrm{detection}} =$

$\rho\sqrt{\mathrm{CRB}(\delta_{\mathrm{detection}})}$ where $\sqrt{\rho} = \rho'$ represents the so-called translation factor [11] which is determined due to the probability of detection P_d and the probability of false alarm P_{fa} as follows: $P_{\mathrm{fa}} = \mathcal{Q}_{\chi_2^2}(\varsigma)$ and $P_d = \mathcal{Q}_{\chi'^2_2(\rho^2)}(\varsigma)$ where $\mathcal{Q}_{\chi_2^2}(.)$ and $\mathcal{Q}_{\chi'^2_2(\rho^2)}(.)$ denote the right tail probability of χ_2^2 and $\chi'^2_2(\rho^2)$, respectively. This conclude the proof.

REFERENCES

[1] D. Donno, A. Nehorai, and U. Spagnolini, "Seismic velocity and polarization estimation for wavefield separation," *IEEE Trans. Signal Process.*, vol. 56, no. 10, pp. 4794–4809, Oct. 2008.

[2] J. Li and R. Compton, "Angle and polarization estimation using esprit with a polarization sensitive array," *IEEE Trans. Antennas Propag.*, vol. 39, no. 9, pp. 1376–1383, Sep. 1991.

[3] I. Ziskind, M. Wax, and H. Rafael, "Maximum likelihood localization of diversely polarized sources by simulated annealing," *IEEE Trans. Antennas Propag.*, vol. 38, no. 7, pp. 1111–1114, Jul. 1990.

[4] K. Wong and M. Zoltowski, "Uni-vector-sensor ESPRIT for multi-source azimuth, elevation, and polarization estimation," *IEEE Trans. Antennas Propag.*, vol. 45, no. 10, pp. 1467–1474, Oct. 1997.

[5] J. Li, P. Stoica, and D. Zheng, "Efficient direction and polarization estimation with a COLD array," *IEEE Trans. Antennas Propag.*, vol. 44, no. 4, pp. 539–547, Apr. 1996.

[6] R. Boyer, "Analysis of the COLD uniform linear array," presented at the IEEE Int. Work. Signal Processing, Advanced, Wireless Communications, Perugia, Italy, 2009.

[7] H. Cox, "Resolving power and sensitivity to mismatch of optimum array processors," *J. Acoust. Soc. Amer.*, vol. 54, no. 3, pp. 771–785, 1973.

[8] K. Sharman and T. Durrani, "Resolving power of signal subspace methods for finite data lengths," in *Proc. IEEE Int. Conf. Acoust., Speech, Signal Processing*, 1995, pp. 1501–1504.

[9] M. Shahram and P. Milanfar, "On the resolvability of sinusoids with nearby frequencies in the presence of noise," *IEEE Trans. Signal Process.*, vol. 53, no. 7, pp. 2579–2588, Jul. 2005.

[10] M. Shahram and P. Milanfar, "Statistical and information-theoretic analysis of resolution in imaging," *IEEE Trans. Inf. Theory*, vol. 52, no. 8, pp. 3411–34377, Aug. 2006.

[11] Z. Liu and A. Nehorai, "Statistical angular resolution limit for point sources," *IEEE Trans. Signal Process.*, vol. 55, no. 11, pp. 5521–5527, Nov. 2007.

[12] A. Amar and A. Weiss, "Fundamental limitations on the resolution of deterministic signals," *IEEE Trans. Signal Process.*, vol. 56, no. 11, pp. 5309–5318, Nov. 2008.

[13] H. B. Lee, "The Cramér-Rao bound on frequency estimates of signals closely spaced in frequency," *IEEE Trans. Signal Process.*, vol. 40, no. 6, pp. 1507–1517, 1992.

[14] H. B. Lee, "The Cramér-Rao bound on frequency estimates of signals closely spaced in frequency (unconditional case)," *IEEE Trans. Signal Process.*, vol. 42, no. 6, pp. 1569–1572, 1994.

[15] E. Dilaveroglu, "Nonmatrix Cramér–Rao bound expressions for high-resolution frequency estimators," *IEEE Trans. Signal Process.*, vol. 46, no. 2, pp. 463–474, Feb. 1998.

[16] S. T. Smith, "Statistical resolution limits and the complexified Cramér–Rao bound," *IEEE Trans. Signal Process.*, vol. 53, no. 5, pp. 1597–1609, May 2005.

[17] J.-P. Delmas and H. Abeida, "Statistical resolution limits of DOA for discrete sources," in *Proc. IEEE Int. Conf. Acoust., Speech, Signal Processing*, Toulouse, France, 2006, vol. 4, pp. 889–892.

[18] J. Kusuma and V. Goyal, "On the accuracy and resolution of powersum-based sampling methods," *IEEE Trans. Signal Process.*, vol. 57, no. 1, pp. 182–193, Jan. 2009.

[19] M. N. El Korso, R. Boyer, A. Renaux, and S. Marcos, "Statistical resolution limit for multiple signals and parameters of interest," presented at the IEEE Int. Conf. Acoust., Speech, Signal Processing, Dallas, TX, 2010.

[20] J. Li and R. T. Compton, "Maximum likelihood angle estimation for signals with known waveforms," *IEEE Trans. Signal Process.*, vol. 41, pp. 2850–2862, Sep. 1993.

[21] J. Li, B. Halder, P. Stoica, and M. Viberg, "Computationally efficient angle estimation for signals with known waveforms," *IEEE Trans. Signal Process.*, vol. 43, pp. 2154–2163, Sep. 1995.

[22] M. Cedervall and R. L. Moses, "Efficient maximum likelihood DOA estimation for signals with known waveforms in presence of multipath," *IEEE Trans. Signal Process.*, vol. 45, pp. 808–811, Mar. 1997.

[23] A. Renaux, "Weiss–Weinstein bound for data aided carrier estimation," *IEEE Signal Process. Lett.*, vol. 14, no. 4, pp. 283–286, Apr. 2007.

[24] B. Ng and C. See, "Sensor-array calibration using a maximum-likelihood approach," *IEEE Trans. Antennas Propag.*, vol. 44, pp. 827–835, Jun. 1996.

[25] P. Stoica and R. Moses, *Spectral Analysis of Signals*. Englewood Cliffs, NJ: Prentice-Hall, 2005.

[26] S. M. Kay, *Fundamentals of Statistical Signal Processing: Estimation Theory*. Englewood Cliffs, NJ: Prentice-Hall, 1993, vol. 1.

[27] S. M. Kay, *Fundamentals of Statistical Signal Processing: Detection Theory*. Englewood Cliffs, NJ: Prentice-Hall, 1998, vol. 2.

A Barankin-Type Bound on Direction Estimation Using Acoustic Sensor Arrays

Tao Li, Joseph Tabrikian, and Arye Nehorai

***Abstract*—We derive a Barankin-type bound (BTB) on the mean-square error (MSE) in estimating the directions of arrival (DOAs) of far-field sources using acoustic sensor arrays. We consider narrowband and wideband deterministic source signals, and scalar or vector sensors. Our results provide an approximation to the threshold of the signal-to-noise ratio (SNR) below which the performance of the maximum likelihood estimation (MLE) degrades rapidly. For narrowband DOA estimation using uniform linear vector-sensor arrays, we show that this threshold increases with the distance between the sensors. As a result, for medium SNR values the performance does not necessarily improve with this distance.**

***Index Terms*—Acoustic sensor array, acoustic vector sensor, Barankin bound, direction of arrival estimation, threshold SNR.**

I. INTRODUCTION

The Barankin bound [1]–[4] is a useful tool in estimation problems for predicting the threshold region of signal-to-noise ratio (SNR) [5]–[8], below which the accuracy of the maximum likelihood estimation (MLE) degrades rapidly. Identification of the threshold region enables to determine the operation conditions, such as observation time and transmission power, to obtain a desired performance.

In the recent years, many works have been carried out for identification of the threshold region of the MLE. One approach is based on the method of interval estimation (MIE) [9] in which the performance of the MLE in the threshold region is approximated. However,

Manuscript received October 16, 2009; accepted September 07, 2010. Date of publication September 20, 2010; date of current version December 17, 2010. The work of T. Li and A. Nehorai was supported by the ONR Grant N000140910496. The associate editor coordinating the review of this manuscript and approving it for publication was Dr. Xavier Mestre.

T. Li and A. Nehorai are with the Department of Electrical and Systems Engineering, Washington University in St. Louis, St. Louis, MO, 63130 USA (e-mail: litao@ese.wustl.edu; nehorai@ese.wustl.edu).

J. Tabrikian is with the Department of Electrical and Computer Engineering, Ben-Gurion University of the Negev, Beer Sheva 84150, Israel (e-mail: joseph@ee.bgu.ac.il).

Color versions of one or more of the figures in this paper are available online at http://ieeexplore.ieee.org.

Digital Object Identifier 10.1109/TSP.2010.2078809

B.2 Elsevier-SP-S

M. N. El Korso, R. Boyer, A. Renaux and S. Marcos, "On the Statistical Resolvability Of Point Sources in Subspace Interference Using a GLRT-Based Framework", soumis à *Elsevier Signal Processing*.

On the Statistical Resolvability Of Point Sources in Subspace Interference Using a GLRT-Based Framework

Mohammed Nabil EL KORSO, Rémy BOYER, Alexandre RENAUX, and Sylvie MARCOS

Abstract

The Statistical Resolution Limit (SRL), denoted by δ, characterizing the minimal separation to resolve two closely spaced far-field narrowband sources, among a total number of $M \geq 2$, impinging on a linear array is derived. The two Sources Of Interest (SOI) are corrupted by (1) the interference resulting from the $M-2$ remaining sources (called here subspace interference (SI)) and by (2) a broadband noise. Toward this end, a hypothesis test formulation is conducted. Depending on the *a priori* knowledge on the SOI, on the interfering sources and on the noise variance, the (constrained) Maximum Likelihood Estimators (MLE) of the SRL subject to $\delta \in \mathbb{R}$ and/or in the context of the matched subspace detector theory are derived. Finally, we show that the SRL which is the minimum separation that allows a correct resolvability for given probabilities of false alarm and of detection can always be linked to a particular form of the Cramér-Rao Bound (CRB), called the Interference CRB (I-CRB), which takes into account the $M-2$ interfering sources. As a by product, we give the theoretical Signal-to-Interference-plus-Noise Ratio (SINR) threshold for a given SRL and for several typical scenarios.

Keywords: Statistical resolution limit, SNR threshold, performance analysis, subspace interference.

1. Introduction

The context of narrowband far-field sources localization has been widely investigated in the literature [1]. However, the ultimate performance in terms of resolution limit have not been fully investigated. The Statistical Resolution Limit (SRL) [2, 3, 4, 5, 6, 7, 8, 9, 10, 11, 12], defined as the minimal separation between two signals in terms of parameter of interest, is a challenging problem [13] and an essential tool to quantify estimator performance. A closely related problem is to derive the signal-to-noise ratio threshold (SNR), *i.e.*, the minimal SNR above which the two signals are resolvable [14].

Among all the different approaches to characterize the SRL, one can find three families. The first and oldest one is based on the null spectrum [2, 3]. A second one is based on the estimation accuracy [5, 6, 7, 8] and the last one and maybe the most promising one is based on detection theory in the context of the hypothesis test formulation. One can find in the literature several works related to the SRL or to the SNR threshold using an hypothesis test formulation [9, 10, 11, 12, 14]. Specifically, in [11], Liu and Nehorai have derived the so-called statistical angular resolution limit (*i.e.*, the SRL) *w.r.t.* Direction-Of-Arrival (DOA) using the asymptotic equivalence expression (in terms of number snapshots) of the Generalized Likelihood Ratio Test (GLRT). More recently, Amar and Weiss [12] have proposed to determine the SRL of two complex sinusoids with nearby frequencies using the Bayesian approach for a given correct decision probability. Finally, Sharman and Milanfar [10] have considered the resolvability of sinusoids with nearby frequencies by deriving the theoretical SNR threshold based on the GLRT.

In this paper, we focus our analysis on a GLR based hypothesis test formulation. This choice is motivated by the following arguments: (1) unlike the SRL based on the mean null spectrum [2, 3], the SRL based on detection theory is claimed to be appropriate for all high-resolution algorithms since it is not related to a specific algorithm, (2) it exists a relationship between the SRL based on the estimation accuracy [7] (*i.e.,* the Cramér-Rao bound (CRB)) and the SRL based on detection theory [11] (see subsections *3.4, 4.4, 5.4* and *6.4*), (3) unlike the Bayesian approach, the use of the GLRT does not require any *prior* knowledge on the parameter of interest, (4) since the separation term is unknown to the user, it is impossible to design an optimal detector in the Neyman-Pearson sense [15] but the GLRT applied to our model is Uniformly Most Powerful invariant (UMP-invariant) test among all the invariant statistical tests [16], which is considered as the strongest statement of optimality that one could expect to obtain [17].

It is important to note that all the existing works have been derived only for two sources of interest (SOI) and thus the influence of the other (interfering) sources is neglected. Another important point is that most of the contributions have been made in the case of spectral analysis and thus the impact of the array geometry on the resolution has not been studied in the context of statistical array processing with complex sources.

In this work, the considered model can be described by

two narrowband far-field closely spaced SOI, among a total number of $M \geq 2$ sources, imbedded in a competitive environment constituted by (1) the interference resulting from the $M-2$ remaining sources (called here subspace interference (SI)) and by (2) a broadband noise. For this general model, we derive the theoretical signal-to-interference-plus-noise ratio (SINR) threshold *w.r.t.* the SRL for linear arrays.

The paper is organized as follows. We first begin by introducing the observation model and the problem setup in Section 2. Sections 3 to 6 are devoted to the SINR threshold and SRL derivations depending on the assumptions on the SOI, on the subspace interference and on the noise variance. Section 7 gives a summary of the main results and compares the SINR thresholds. Furthermore, in Section 8, numerical simulations are given to assess the effect of the array geometry, of the aperture, of the *prior* sources knowledge and the effect of the subspace interference. Finally, Section 9 concludes this work.

2. Problem setup and assumptions

Let us consider a Linear Array (LA) with N sensors that receives at the t^{th} snapshot, a signal emitted by M deterministic far-field and narrow-band sources, denoted by $\{s_1(t), \ldots, s_M(t)\}$. For the n^{th} sensor and for the t^{th} snapshot, the observation model is given by [1]

$$y_n(t) = \sum_{m=1}^{M} s_m(t) \exp(j\omega_m d_n) + v_n(t) \qquad (1)$$

$t = 1, \ldots, L, \quad n = 0, \ldots, N-1$, where L stands for the number of snapshots,

$$\omega_m = -2\pi \sin(\theta_m)/\nu$$

is the parameter of interest of the m^{th} source which is a function of the bearing θ_m and of the signal wavelength ν. d_n stands for the (known) distance between a reference sensor (the first sensor herein) and the n^{th} sensor[1]. The additive noise $v_n(t)$ is assumed to be a complex random process. Consequently, the observation vector at the t^{th} snapshot, can be expressed as

$$\boldsymbol{y}(t) = \begin{bmatrix} y_0(t) & \ldots & y_{N-1}(t) \end{bmatrix}^T = \begin{bmatrix} \boldsymbol{a}_1 & \ldots & \boldsymbol{a}_M \end{bmatrix} \breve{\boldsymbol{s}}(t) + \boldsymbol{v}(t),$$

where $\boldsymbol{v}(t) = [v_0(t) \ldots v_{N-1}(t)]^T$ and $\breve{\boldsymbol{s}}(t) = [s_1(t) \ \ldots \ s_M(t)]^T$, in which the $(n+1)^{th}$ entry of the steering vector $\boldsymbol{a}_m$ is given by $[\boldsymbol{a}_m]_{n+1} = \exp(j\omega_m d_n)$, $m = 1, 2, \ldots, M$. Finally, the "vectorized" full observation vector is as follows:

$$\boldsymbol{y} \triangleq \begin{bmatrix} \boldsymbol{y}^T(1) & \boldsymbol{y}^T(2) & \ldots & \boldsymbol{y}^T(L) \end{bmatrix}^T.$$

[1]For instance, in the case of the Uniform LA (ULA), $d_n = nd$ where d denotes the inter-element space between two successive sensors.

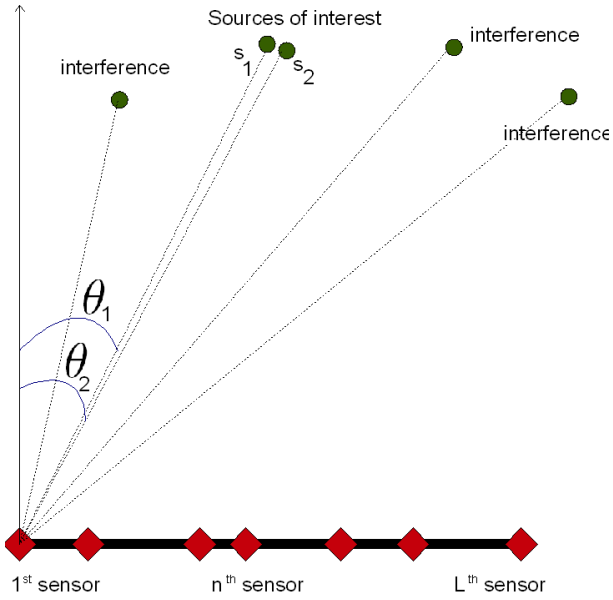

Figure 1: Two closely-spaced SOI imbedded in three interfering sources observed by a linear array with $L = 7$ sensors.

2.1. Hypothesis test formulation of the SRL in subspace interference

2.1.1. SRL in subspace interference

The aim of this work is to derive the theoretical SINR threshold and the SRL, denoted by δ, in the context of the scenario depicted on Fig. 1. More precisely,

1. Two closely-spaced sources are of interest (SOI). Without loss of generality, we consider that these two sources are $\boldsymbol{s}_1$ and $\boldsymbol{s}_2$ (such that $\boldsymbol{s}_1 \neq \boldsymbol{s}_2$). So, the SRL (*i.e.,* the separation) is defined as $\delta \triangleq \omega_2 - \omega_1$.
2. The $M-2$ remaining sources, denoted by $\{\boldsymbol{s}_3, \ldots, \boldsymbol{s}_M\}$, are viewed as an interference (also called Subspace Interference (SI) [18]). Each pair of sources is considered widely-spaced. A sufficient condition is that the minimal separation over all the combination of pairs of interfering sources, denoted by Δ_ω, must satisfy $\Delta_\omega > \delta$.
3. The background broadband noise is assumed to be a complex circular white Gaussian random process with zero-mean and variance σ^2.

Consequently, the problem setup can be viewed as deriving the theoretical SINR threshold and the SRL for two closely-spaced SOI imbedded in a structured interference (the $M-2$ remaining sources) and an unstructured interference (*i.e.*, the broadband noise).

2.1.2. Hypothesis test formulation

The problem of resolving *only* two closely-spaced SOI in the context of a binary hypothesis test has been already (partially) tackled in [9, 10, 11, 12]. But in these references, the model is restricted to *only* two closely-spaced

SOI. In this work, we consider a more general model described in the previous section. This model has a rich structure since the impact of $M-2$ interfering sources is taken into account. Consequently, the theoretical SINR threshold and the SRL derived in this paper are appropriate to the realistic situation where $M \geq 2$ sources belong to the field of view of a LA (see Fig. 1).
Let the hypothesis $\mathcal{H}_0$ represents the case where the two SOI are combined into a single signal, whereas the hypothesis $\mathcal{H}_1$ embodies the situation where the two SOI are resolvable. Consequently, a convenient binary hypothesis test (see [9, 10, 11, 12]) is given by

$$\begin{cases} \mathcal{H}_0 : & \delta = 0, \\ \mathcal{H}_1 : & \delta \neq 0. \end{cases} \tag{2}$$

Since the separation term δ is unknown, it is impossible to design an optimal detector in the Neyman-Pearson sense. In this case, the Generalized Likelihood Ratio Test (GLRT) [15] is a well-known statistic test to solve such a problem and is given by

$$G(\boldsymbol{y}) = \frac{\max_{\delta,\boldsymbol{\rho}_1} p(\boldsymbol{y};\delta,\boldsymbol{\rho}_1,\mathcal{H}_1)}{\max_{\boldsymbol{\rho}_0} p(\boldsymbol{y};\boldsymbol{\rho}_0,\mathcal{H}_0)} = \frac{p(\boldsymbol{y};\hat{\delta},\hat{\boldsymbol{\rho}}_1,\mathcal{H}_1)}{p(\boldsymbol{y};\hat{\boldsymbol{\rho}}_0,\mathcal{H}_0)} \underset{\mathcal{H}_0}{\overset{\mathcal{H}_1}{\gtrless}} \eta', \tag{3}$$

in which $p(\boldsymbol{y};\boldsymbol{\rho}_0,\mathcal{H}_0)$ and $p(\boldsymbol{y};\delta,\boldsymbol{\rho}_1,\mathcal{H}_1)$ denote the probability density functions (pdf) under $\mathcal{H}_0$ and $\mathcal{H}_1$, respectively, and where η', $\hat{\delta}$ and $\hat{\boldsymbol{\rho}}_i$ denote the detection threshold, the Maximum Likelihood Estimate (MLE) of δ under $\mathcal{H}_1$ and the MLE of the parameter vector $\boldsymbol{\rho}_i$ (containing all the unknown nuisance and/or unwanted parameters) under $\mathcal{H}_i, i = 0, 1$. If the statistic $G(\boldsymbol{y})$ is greater than a given threshold η', then the signals are said to be resolvable.
Unfortunately, closed-form expressions of $\hat{\delta}$, $\hat{\boldsymbol{\rho}}_1$ and $\hat{\boldsymbol{\rho}}_0$ are not available (this is mainly due to the derivation of $\hat{\delta}$ which is, in this case, a highly non linear and intractable optimization problem [19]). However, since the two SOI are closely-spaced (this assumption can be argued by the fact that the high resolution algorithms have asymptotically an infinite resolving power [20, 9, 7, 10, 11, 12]), one can approximate model (1) into a new model which is linear *w.r.t.* the parameter δ.

2.2. Linear form of the model with subspace interference

First, let us introduce the center parameter $\omega_c = \frac{\omega_1+\omega_2}{2}$. As in [9, 10, 11, 12], using the assumption of a small angular separation of the two SOI, a first-order Taylor expansion around $\delta = 0$ leads to

$$\boldsymbol{y} \overset{1}{=} \boldsymbol{A}\boldsymbol{s}_+ + \delta \boldsymbol{B}\boldsymbol{s}_- + \boldsymbol{e} + \boldsymbol{v}, \tag{4}$$

where $\boldsymbol{e} = \boldsymbol{C}\boldsymbol{s}$, $\boldsymbol{C} = [\boldsymbol{A}_3 \ \ldots \ \boldsymbol{A}_M]$, $\boldsymbol{s} = [\boldsymbol{s}_3^T \ \ldots \ \boldsymbol{s}_M^T]^T$ and

$$\boldsymbol{s}_+ = \boldsymbol{s}_1 + \boldsymbol{s}_2, \tag{5}$$

$$\boldsymbol{s}_- = \boldsymbol{s}_2 - \boldsymbol{s}_1, \tag{6}$$

in which $\boldsymbol{s}_i = [s_i(1) \ \ldots \ s_i(L)]^T$. Furthermore, the signal $\boldsymbol{e}$ encompasses the interference of all the sources apart from the two closest ones (*i.e.*, the first and the second one). In addition, denoting $\boldsymbol{I}_L$ the $L \times L$ identity matrix, $\boldsymbol{d} = [d_0 \ d_1 \ \ldots \ d_{N-1}]^T$ and $\boldsymbol{a}$ the steering vector considered for the center parameter ω_c (*i.e.*, $[\boldsymbol{a}]_{n+1} \triangleq \exp(j\omega_c d_n)$, $n = 0, \ldots, N-1$), we define

$$\boldsymbol{A} \triangleq \begin{bmatrix} \boldsymbol{a} & & \boldsymbol{0} \\ & \ddots & \\ \boldsymbol{0} & & \boldsymbol{a} \end{bmatrix}_{(NL)\times L} = \boldsymbol{I}_L \otimes \boldsymbol{a}, \tag{7}$$

$$\boldsymbol{B} \triangleq \frac{j}{2}\boldsymbol{I}_L \otimes \dot{\boldsymbol{a}}, \quad \text{where} \quad \dot{\boldsymbol{a}} \triangleq \boldsymbol{a} \odot \boldsymbol{d}, \tag{8}$$

$$\boldsymbol{A}_m \triangleq \boldsymbol{I}_L \otimes \boldsymbol{a}_m, \quad \text{for } m = 3, \ldots, M, \tag{9}$$

where $\otimes$ and $\odot$ stand for the Kronecker and the Hadamard products, respectively. In the rest of the paper, and as in [10, 11], the parameter ω_c is assumed to be known or previously estimated. Furthermore, we consider that the matrix $\boldsymbol{C}$ is known or previously estimated [21]. Note that the case of unknown ω_c and/or unknown $\boldsymbol{C}$ leads to an untractable solution of the GLRT and, consequently, is beyond the scope of this paper.

2.3. Defintion of the SNR and the SINR

A standard measure for the point source without interference is the Signal-to-Noise Ratio defined as

$$\text{SNR} \triangleq \frac{\sum_{m=1}^{2} ||\boldsymbol{s}_m||^2}{\sigma^2}. \tag{10}$$

But a more convenient measure in case of interference is the Signal to Interference plus Noise Ratio defined according to

$$\text{SINR} \triangleq \frac{\sum_{m=1}^{2} ||\boldsymbol{s}_m||^2}{\|\boldsymbol{s}\|^2 + \sigma^2}. \tag{11}$$

Obviously, we have SINR $\leq$ SNR. Let INR$\triangleq \frac{\|\boldsymbol{s}\|^2}{\sigma^2}$ be the Interference to Noise Ratio. Straightforward relations between the SNR and the SINR are

$$\text{SINR} = \frac{1}{1+\alpha}\text{SNR}, \quad \text{if} \quad \text{INR} = \alpha, \tag{12}$$

$$\text{SINR} = \text{SNR}, \quad \text{if} \quad \text{INR} = 0, \tag{13}$$

$$\text{SINR} \approx \text{SNR}, \quad \text{if} \quad \text{INR} \ll 1. \tag{14}$$

In this work, the theoretical SINR and SNR are derived for a given SRL in the scenarios listed above. More precisely, relation (12) means that if the INR is fixed to the constant α then the SINR is proportional to the SNR. Relation (13) is a particular case of relation (12) and stands for the situation where there is no subspace interference. The last relation (14) means that the subspace interference is dominated by the noise.

3. Case 1: known SOI, SI and noise variance

First, let us consider the scenario where the two SOI, the SI and the noise variance are known, *i.e.*, $\boldsymbol{s}_1$, $\boldsymbol{s}_2$, $\boldsymbol{s}$ and σ^2 are known vectors. Let δ_1 be the SRL for the considered case. Let us define the new observation vector $\boldsymbol{z} \triangleq \boldsymbol{y} - \boldsymbol{A}\boldsymbol{s}_+ - \boldsymbol{C}\boldsymbol{s}$.

3.1. Binary hypothesis test

With the aforementioned framework, the hypothesis test (2) becomes

$$\begin{cases} \mathcal{H}_0: & \boldsymbol{z} = \boldsymbol{v} \sim \mathcal{CN}(\boldsymbol{0}, \sigma^2\boldsymbol{I}), \\ \mathcal{H}_1: & \boldsymbol{z} = \boldsymbol{w}\delta_1 + \boldsymbol{v} \sim \mathcal{CN}(\boldsymbol{w}\delta_1, \sigma^2\boldsymbol{I}), \end{cases} \tag{15}$$

in which $\boldsymbol{w} \triangleq \boldsymbol{B}\boldsymbol{s}_-$.

3.2. Constrained MLE (CMLE) and GLRT

As $\delta_1 \in \mathbb{R}$, one has to find the Constrained MLE (CMLE) of δ_1. More precisely, the constrained optimization problem can be written according to

$$\arg\min_{\delta_1} L(\boldsymbol{z}, \delta_1) \;\text{ subject to }\; \delta_1 \in \mathbb{R}$$

where $L(\boldsymbol{z}, \delta_1)$ is the negative log-likelihood function. According to Appendix A.1, the CMLE is

$$\hat{\delta}_1 = \frac{\Re\left\{\boldsymbol{w}^H\boldsymbol{z}\right\}}{\|\boldsymbol{w}\|^2} \tag{16}$$

where $\|\boldsymbol{w}\|^2 = \boldsymbol{s}_-^H\boldsymbol{B}^H\boldsymbol{B}\boldsymbol{s}_- = \frac{1}{4}||\boldsymbol{s}_-||^2||\dot{\boldsymbol{a}}||^2$. Using (16), the statistic of the GLRT is then given by

$$G(\boldsymbol{z}) = \frac{p(\boldsymbol{z}; \hat{\delta}_1, \mathcal{H}_1)}{p(\boldsymbol{z}; \mathcal{H}_0)} = \exp\left(\frac{1}{\sigma^2}\left(||\boldsymbol{z}||^2 - ||\boldsymbol{z} - \boldsymbol{w}\hat{\delta}_1||^2\right)\right) \underset{\mathcal{H}_0}{\overset{\mathcal{H}_1}{\gtrless}} \eta'. \tag{17}$$

Plugging (16) into (17), and defining a new statistic, denoted by $T(\boldsymbol{z})$, one obtains

$$\begin{aligned} T(\boldsymbol{z}) \triangleq 2\ln G(\boldsymbol{z}) &= \frac{2}{\sigma^2}\left(\hat{\delta}_1\boldsymbol{z}^H\boldsymbol{w} + \hat{\delta}_1\boldsymbol{w}^H\boldsymbol{z} - \hat{\delta}_1^2\|\boldsymbol{w}\|^2\right) \\ &= \frac{2\Re\left\{\boldsymbol{w}^H\boldsymbol{z}\right\}}{\sigma^2\|\boldsymbol{w}\|^2}\left(\boldsymbol{w}^H\boldsymbol{z} + \boldsymbol{z}^H\boldsymbol{w} - \Re\left\{\boldsymbol{w}^H\boldsymbol{z}\right\}\right) \\ &= \frac{\Re^2\left\{\boldsymbol{w}^H\boldsymbol{z}\right\}}{\|\boldsymbol{w}\|^2\frac{\sigma^2}{2}}. \end{aligned} \tag{18}$$

Using the result of Appendix B, we have

$$T(\boldsymbol{z}) \sim \begin{cases} \chi_1^2 & \text{under } \mathcal{H}_0, \\ \chi_1^2\left(\lambda_1\left(P_{fa}, P_d\right)\right) & \text{under } \mathcal{H}_1, \end{cases}$$

where

$$\lambda_1\left(P_{fa}, P_d\right) = \frac{2\delta_1^2}{\sigma^2}\|\boldsymbol{w}\|^2 = \frac{\delta_1^2}{2\sigma^2}||\boldsymbol{s}_-||^2||\dot{\boldsymbol{a}}||^2, \tag{19}$$

and where χ_1^2 denotes the central distribution with one degree of freedom. Since $G(\boldsymbol{z}) \underset{\mathcal{H}_0}{\overset{\mathcal{H}_1}{\gtrless}} \eta' \iff T(\boldsymbol{z}) \underset{\mathcal{H}_0}{\overset{\mathcal{H}_1}{\gtrless}} \eta \triangleq \ln\eta'$, the probability of false alarm and the probability of detection are then given by

$$P_{fa} = Q_{\chi_1^2}(\eta)$$

and

$$P_d = Q_{\chi_1^2(\lambda_1(P_{fa},P_d))}(\eta),$$

respectively, in which $Q_{\chi_1^2}(.)$ and $Q_{\chi_1^2(\lambda_1(P_{fa},P_d))}(.)$ denote the right tail of the χ_1^2 pdf and the $\chi_1^2(\lambda_1\left(P_{fa}, P_d\right))$ pdf, respectively. In practice $\lambda_1\left(P_{fa}, P_d\right)$ can be derived for a given P_{fa} and P_d as the solution of $Q_{\chi_1^2}^{-1}(P_{fa}) = Q_{\chi_1^2(\lambda_1(P_{fa},P_d))}^{-1}(P_d)$.

3.3. Theoretical SINR derivation

Result 1. *The SINR threshold with respect to the SRL δ_1 required to resolve two closely spaced known SOI imbedded in $M-2$ known sources in a known noise variance, is given by*

$$SINR_1 \;=\; \frac{\|\boldsymbol{s}_1\|^2 + \|\boldsymbol{s}_2\|^2}{\|\boldsymbol{s}\|^2 + \delta_1^2\frac{2\|\boldsymbol{w}\|^2}{\lambda_1(P_{fa},P_d)}}. \quad \blacksquare \tag{20}$$

Result 2. *The SNR threshold with respect to the SRL δ_1 required to resolve two closely spaced known SOI in a known noise variance, is given by*

$$SNR_1 = \lambda_1\left(P_{fa}, P_d\right)\frac{||\boldsymbol{s}_1||^2 + ||\boldsymbol{s}_2||^2}{2\delta_1^2\|\boldsymbol{w}\|^2}. \quad \blacksquare \tag{21}$$

Result 3. *If the SOI are orthogonal signals, i.e., $\boldsymbol{s}_1^H\boldsymbol{s}_2 = \boldsymbol{s}_2^H\boldsymbol{s}_1 = 0$, then $||\boldsymbol{s}_-||^2 = ||\boldsymbol{s}_1||^2 + ||\boldsymbol{s}_2||^2$. The SNR threshold is given by*

$$SNR_{1o} = \frac{2\lambda_1\left(P_{fa}, P_d\right)}{\delta_1^2\|\dot{\boldsymbol{a}}\|^2}. \quad \blacksquare \tag{22}$$

The last result means that the SNR threshold for orthogonal SOI is invariant to the source powers.

3.4. Alternative expression of the non-centrality parameter

Let $[\delta_1 \;\; \sigma^2]^T$ be the vector collecting the parameters under $\mathcal{H}_1$. The associated CRB(δ_1) which is derived in appendix C.1, is given by

$$\mathrm{CRB}(\delta_1) = \frac{\sigma^2}{2\|\boldsymbol{w}\|^2} = \frac{2\sigma^2}{\|\boldsymbol{s}_-\|^2\|\dot{\boldsymbol{a}}\|^2}.$$

Consequently, (19) can be rewritten *w.r.t.* the CRB as

$$\lambda_1\left(P_{fa}, P_d\right) = \delta_1^2\mathrm{CRB}^{-1}(\delta_1). \tag{23}$$

Note that (23) is an expression where δ_1 is the unknown variable. This is in agreement with the formulation introduced in reference [7].

4. Case 2: known SOI, unknown SI, known noise variance

4.1. Binary hypothesis test

In the following, we consider the case where two known SOI are imbedded in $M-2$ unknown interfering sources. In addition, the noise variance is assumed to be known. Consequently, the observations under each hypothesis are given by

$$\begin{cases} \mathcal{H}_0: & \boldsymbol{z} \triangleq \boldsymbol{y} - \boldsymbol{A}\boldsymbol{s}_+ = \boldsymbol{C}\boldsymbol{s} + \boldsymbol{v} \sim \mathcal{CN}(\boldsymbol{C}\boldsymbol{s}, \sigma^2\boldsymbol{I}), \\ \mathcal{H}_1: & \boldsymbol{z} = \delta_2\boldsymbol{w} + \boldsymbol{C}\boldsymbol{s} + \boldsymbol{v} \sim \mathcal{CN}(\delta_2\boldsymbol{w} + \boldsymbol{C}\boldsymbol{s}, \sigma^2\boldsymbol{I}). \end{cases} \tag{24}$$

where δ_2 denotes the SRL.

4.2. Joint CMLE and GLRT

As $\delta_2 \in \mathbb{R}$, one has to find jointly the CMLE of the SRL and the MLE of interfering sources. Let us reorganize the observation according to $\boldsymbol{z} = \boldsymbol{Q}\boldsymbol{p} + \boldsymbol{v}$ where $\boldsymbol{Q} = [\boldsymbol{w}\ \boldsymbol{C}]$ and $\boldsymbol{p} = [\delta_2\ \boldsymbol{s}^T]^T$, then the constrained optimization problem can be written according to

$$\arg\min_{\boldsymbol{p}} L(\boldsymbol{z}, \boldsymbol{p}) \quad \text{subject to} \quad \boldsymbol{e}_1^T\boldsymbol{p} \in \mathbb{R} \tag{25}$$

where $\boldsymbol{e}_1 = [1\ 0 \dots 0]^T$ and $L(\boldsymbol{z}, \boldsymbol{p})$ is the negative log-likelihood function of the observation. According to Appendix A.2, we have

$$\hat{\delta}_2 = \frac{\Re\{\boldsymbol{w}^H\boldsymbol{P}_{\boldsymbol{C}}^{\perp}\boldsymbol{z}\}}{||\boldsymbol{P}_{\boldsymbol{C}}^{\perp}\boldsymbol{w}||^2}, \tag{26}$$

$$\hat{\boldsymbol{s}}_{\mathcal{H}_0} = \boldsymbol{C}^{\dagger}\boldsymbol{z}, \tag{27}$$

$$\hat{\boldsymbol{s}}_{\mathcal{H}_1} = \boldsymbol{C}^{\dagger}(\boldsymbol{z} - \hat{\delta}\boldsymbol{w}), \tag{28}$$

where $\dagger$ stands for the Moore-Penrose pseudo-inverse [22]. Consequently using (26), (27) and (28), one obtains

$$\begin{cases} \hat{\boldsymbol{v}}_{\mathcal{H}_0} = \boldsymbol{P}_{\boldsymbol{C}}^{\perp}\boldsymbol{z} & \text{under } \mathcal{H}_0, \\ \hat{\boldsymbol{v}}_{\mathcal{H}_1} = \boldsymbol{P}_{\boldsymbol{C}}^{\perp}\boldsymbol{z} - \boldsymbol{P}_{\boldsymbol{C}}^{\perp}\boldsymbol{w}\frac{\Re\{\boldsymbol{w}^H\boldsymbol{P}_{\boldsymbol{C}}^{\perp}\boldsymbol{z}\}}{||\boldsymbol{P}_{\boldsymbol{C}}^{\perp}\boldsymbol{w}||^2} & \text{under } \mathcal{H}_1. \end{cases} \tag{29}$$

Now, we are ready to use the statistic $\breve{T}(\boldsymbol{y})$ based on the GLRT which is defined as follows:

$$\breve{T}(\boldsymbol{z}) \triangleq 2\ln G(\boldsymbol{z}) = \frac{2}{\sigma^2}(\|\hat{\boldsymbol{v}}_{\mathcal{H}_0}\|^2 - \|\hat{\boldsymbol{v}}_{\mathcal{H}_1}\|^2). \tag{30}$$

Plugging (29) in (30) and after some calculus, one obtains

$$\breve{T}(\boldsymbol{z}) = \frac{2}{\sigma^2}\frac{\Re^2\{\boldsymbol{w}^H\boldsymbol{P}_{\boldsymbol{C}}^{\perp}\boldsymbol{z}\}}{||\boldsymbol{P}_{\boldsymbol{C}}^{\perp}\boldsymbol{w}||^2} = \frac{\Re^2\{\breve{\boldsymbol{w}}^H\breve{\boldsymbol{z}}\}}{\frac{\sigma^2}{2}\|\breve{\boldsymbol{w}}\|^2}, \tag{31}$$

where $\breve{\boldsymbol{z}} = \breve{\boldsymbol{U}}^H\boldsymbol{z}$ and where $\breve{\boldsymbol{w}} = \breve{\boldsymbol{U}}^H\boldsymbol{w}$ in which $\boldsymbol{P}_{\boldsymbol{C}}^{\perp} = \breve{\boldsymbol{U}}\breve{\boldsymbol{U}}^H$ is any orthogonal decomposition for which $\breve{\boldsymbol{U}}^H\breve{\boldsymbol{U}} = \boldsymbol{I}$ [23, eq (A.4.7)]. The statistics of the random variable $\breve{\boldsymbol{z}}$ follow:

$$\begin{cases} \breve{\boldsymbol{z}}_{\mathcal{H}_0} \sim \mathcal{CN}(\boldsymbol{0}, \sigma^2\boldsymbol{I}) & \text{under } \mathcal{H}_0, \\ \breve{\boldsymbol{z}}_{\mathcal{H}_1} \sim \mathcal{CN}(\breve{\boldsymbol{w}}\delta_2, \sigma^2\boldsymbol{I}) & \text{under } \mathcal{H}_1, \end{cases} \tag{32}$$

since $\breve{\boldsymbol{U}}^H\boldsymbol{C} = \boldsymbol{0}$. Expressions (31) and (32) are formally similar to the case studied in Appendix B. So, we can conclude

$$\breve{T}(\boldsymbol{z}) \sim \begin{cases} \chi_1^2 & \text{under } \mathcal{H}_0 \\ \chi_1^2(\lambda_2(P_{fa}, P_d)) & \text{under } \mathcal{H}_1, \end{cases} \tag{33}$$

where

$$\lambda_2(P_{fa}, P_d) = \frac{2\delta_2^2}{\sigma^2}||\boldsymbol{P}_{\boldsymbol{C}}^{\perp}\boldsymbol{w}||^2. \tag{34}$$

4.3. Theoretical SINR derivation

From (34), one can state the following results:

Result 4. *The SINR threshold with respect to the SRL δ_2 required to resolve two closely spaced known SOI imbedded in $M-2$ unknown sources in a known noise variance, is given by*

$$SINR_2 = \frac{\|\boldsymbol{s}_1\|^2 + \|\boldsymbol{s}_2\|^2}{\|\boldsymbol{s}\|^2 + \delta_2^2\frac{2||\boldsymbol{P}_{\boldsymbol{C}}^{\perp}\boldsymbol{w}||^2}{\lambda_2(P_{fa}, P_d)}}. \quad \blacksquare \tag{35}$$

Result 5. *The SNR threshold with respect to the SRL δ_2 required to resolve two closely spaced known SOI with a known noise variance is obtained for $\boldsymbol{P}_{\boldsymbol{C}}^{\perp} = \boldsymbol{I}$ and $\boldsymbol{s} = \boldsymbol{0}$ and thus is given by*

$$SNR_2 = \lambda_2(P_{fa}, P_d)\frac{\|\boldsymbol{s}_1\|^2 + \|\boldsymbol{s}_2\|^2}{2\delta_2^2||\boldsymbol{w}||^2}. \quad \blacksquare \tag{36}$$

Result 6. *If the SOI are orthogonal. The SNR threshold is given by*

$$SNR_{2o} = \frac{2\lambda_2(P_{fa}, P_d)}{\delta_2^2\|\dot{\boldsymbol{a}}\|^2}. \quad \blacksquare \tag{37}$$

The last result means that the SNR threshold for orthogonal SOI is invariant to the source powers.

4.4. Alternative expression of the non-centrality parameter

In [24], the Interference Cramér-Rao Bound (I-CRB) has been introduced. This bound is the CRB for the unknown parameter $[\delta_2\ \sigma^2]^T$ and for the projected observation $\breve{\boldsymbol{z}} = \breve{\boldsymbol{U}}^H\boldsymbol{z}$. So, this bound integrates the subspace interference related to $\langle\boldsymbol{C}\rangle$. More precisely, this bound takes the following form:

$$\text{I-CRB}(\delta_2) = \frac{\sigma^2}{2||\boldsymbol{P}_{\boldsymbol{C}}^{\perp}\boldsymbol{w}||^2}.$$

See Appendix C.2 for the proof. Consequently, using (34), one deduces the relationship between the I-CRB and the non-centrality parameter

$$\lambda_2(P_{fa}, P_d) = \delta_2^2\text{I-CRB}^{-1}(\delta_2). \tag{38}$$

5. Case 3: unknown SOI, SI and known noise variance

5.1. Binary hypothesis test

In the following, we consider the case where two unknown sources are imbedded in $M-2$ unknown sources. The noise variance is assumed to be known. Consequently, the observations under each hypothesis are given by

$$\begin{cases} \mathcal{H}_0: & \boldsymbol{y} = \boldsymbol{D}\boldsymbol{g} + \boldsymbol{v} \sim \mathcal{CN}(\boldsymbol{D}\boldsymbol{g}, \sigma^2\boldsymbol{I}), \\ \mathcal{H}_1: & \boldsymbol{y} = \boldsymbol{B}\boldsymbol{\theta} + \boldsymbol{D}\boldsymbol{g} + \boldsymbol{v} \sim \mathcal{CN}(\boldsymbol{B}\boldsymbol{\theta} + \boldsymbol{D}\boldsymbol{g}, \sigma^2\boldsymbol{I}), \end{cases} \tag{39}$$

where $\boldsymbol{D} \triangleq [\boldsymbol{A}\ \boldsymbol{C}] \in \mathbb{C}^{NL\times(M-1)L}$, in which the unknown vector parameter $\boldsymbol{\theta}$ and $\boldsymbol{g}$ are defined by

$$\begin{aligned} \boldsymbol{\theta} &\triangleq \delta_3 \boldsymbol{s}_-, \\ \boldsymbol{g} &\triangleq \begin{bmatrix} \boldsymbol{s}_+ \\ \boldsymbol{s} \end{bmatrix}. \end{aligned}$$

where δ_3 is the SRL.

5.2. Unconstrained MLE and GLRT

The unconstrained MLEs of the unknown parameters are given by [18]:

$$\hat{\boldsymbol{\theta}} = (\boldsymbol{B}^H\boldsymbol{P}_{\boldsymbol{D}}^{\perp}\boldsymbol{B})^{-1}\boldsymbol{B}^H\boldsymbol{P}_{\boldsymbol{D}}^{\perp}\boldsymbol{y}, \tag{40}$$

$$\hat{\boldsymbol{g}}_{\mathcal{H}_0} = (\boldsymbol{D}^H\boldsymbol{D})^{-1}\boldsymbol{D}^H\boldsymbol{y}, \tag{41}$$

$$\hat{\boldsymbol{g}}_{\mathcal{H}_1} = (\boldsymbol{D}^H\boldsymbol{P}_{\boldsymbol{B}}^{\perp}\boldsymbol{D})^{-1}\boldsymbol{D}^H\boldsymbol{P}_{\boldsymbol{B}}^{\perp}\boldsymbol{y}, \tag{42}$$

where $\boldsymbol{P}_{\boldsymbol{D}}^{\perp} \triangleq \boldsymbol{I} - \boldsymbol{P}_{\boldsymbol{D}}$, in which $\boldsymbol{P}_{\boldsymbol{D}}$ denotes the orthogonal projector onto the subspace spanned by the columns of the matrix $\boldsymbol{D}$.

Consequently, the MLEs of the noise are

$$\begin{cases} \hat{\boldsymbol{v}}_{\mathcal{H}_0} = \boldsymbol{P}_{\boldsymbol{D}}^{\perp}\boldsymbol{y} & \text{under } \mathcal{H}_0, \\ \hat{\boldsymbol{v}}_{\mathcal{H}_1} = \boldsymbol{P}_{[\boldsymbol{B}\boldsymbol{D}]}^{\perp}\boldsymbol{y} & \text{under } \mathcal{H}_1, \end{cases} \tag{43}$$

where the oblique projectors $\boldsymbol{E}_{\boldsymbol{B}\boldsymbol{D}}$ and $\boldsymbol{E}_{\boldsymbol{D}\boldsymbol{B}}$ are defined as

$$\boldsymbol{E}_{\boldsymbol{B}\boldsymbol{D}} = \boldsymbol{B}(\boldsymbol{B}^H\boldsymbol{P}_{\boldsymbol{D}}^{\perp}\boldsymbol{B})^{-1}\boldsymbol{B}^H\boldsymbol{P}_{\boldsymbol{D}}^{\perp}, \tag{44}$$

$$\boldsymbol{E}_{\boldsymbol{D}\boldsymbol{B}} = \boldsymbol{D}(\boldsymbol{D}^H\boldsymbol{P}_{\boldsymbol{B}}^{\perp}\boldsymbol{D})^{-1}\boldsymbol{D}^H\boldsymbol{P}_{\boldsymbol{B}}^{\perp}. \tag{45}$$

Now, we are ready to use the statistic $T'(\boldsymbol{y})$ based on the GLRT and defined as follows

$$T'(\boldsymbol{y}) \triangleq 2\ln G(\boldsymbol{y}) = \frac{2}{\sigma^2}\left(\|\hat{\boldsymbol{v}}_{\mathcal{H}_0}\|^2 - \|\hat{\boldsymbol{v}}_{\mathcal{H}_1}\|^2\right) \tag{46}$$

$$= \frac{1}{\sigma^2}\boldsymbol{y}^H\left(\boldsymbol{P}_{\boldsymbol{D}}^{\perp} - \boldsymbol{P}_{[\boldsymbol{B}\boldsymbol{D}]}^{\perp}\right)\boldsymbol{y}. \tag{47}$$

Using [16, eq (3.7)] and [18, eq (19)], one has $\boldsymbol{P}_{\boldsymbol{D}}^{\perp} - \boldsymbol{P}_{[\boldsymbol{B}\boldsymbol{D}]}^{\perp} = \boldsymbol{P}_{\boldsymbol{D}}^{\perp}\boldsymbol{E}_{\boldsymbol{B}\boldsymbol{D}}\boldsymbol{P}_{\boldsymbol{D}}^{\perp} = \boldsymbol{P}_{\boldsymbol{P}_{\boldsymbol{D}}^{\perp}\boldsymbol{B}}$. Thus,

$$T'(\boldsymbol{y}) = \frac{2}{\sigma^2}\boldsymbol{y}^H\boldsymbol{P}_{\boldsymbol{P}_{\boldsymbol{D}}^{\perp}\boldsymbol{B}}\boldsymbol{y}. \tag{48}$$

Let $\boldsymbol{P}_{\boldsymbol{P}_{\boldsymbol{D}}^{\perp}\boldsymbol{B}} = \boldsymbol{U}\boldsymbol{U}^H$ be any orthogonal decomposition [23] of the projector $\boldsymbol{P}_{\boldsymbol{P}_{\boldsymbol{D}}^{\perp}\boldsymbol{B}}$ such that $\boldsymbol{U}^H\boldsymbol{U} = \boldsymbol{I}$ and define an auxiliary random variable $\tilde{\boldsymbol{y}} = \boldsymbol{U}^H\boldsymbol{y}$. One should note that

$$\begin{cases} \tilde{\boldsymbol{y}} = \boldsymbol{U}^H\boldsymbol{v} \sim \mathcal{CN}(\boldsymbol{0}, \sigma^2\boldsymbol{I}) & \text{under } \mathcal{H}_0, \\ \tilde{\boldsymbol{y}} = \boldsymbol{U}^H\boldsymbol{B}\boldsymbol{\theta} + \boldsymbol{U}^H\boldsymbol{v} \sim \mathcal{CN}(\boldsymbol{U}^H\boldsymbol{B}\boldsymbol{\theta}, \sigma^2\boldsymbol{I}) & \text{under } \mathcal{H}_1. \end{cases} \tag{49}$$

Consequently,

$$T'(\boldsymbol{y}) \sim \begin{cases} \chi^2_{2r} & \text{under } \mathcal{H}_0, \\ \chi^2_{2r}(\lambda_3(P_{fa}, P_d)) & \text{under } \mathcal{H}_1, \end{cases} \tag{50}$$

where [17] $r = \mathrm{trace}(\boldsymbol{P}_{\boldsymbol{P}_{\boldsymbol{D}}^{\perp}\boldsymbol{B}}) = \mathrm{rank}(\boldsymbol{P}_{\boldsymbol{P}_{\boldsymbol{D}}^{\perp}\boldsymbol{B}}) = L$ and

$$\lambda_3(P_{fa}, P_d) = \frac{\boldsymbol{\theta}^H\boldsymbol{B}^H\boldsymbol{U}\boldsymbol{U}^H\boldsymbol{B}\boldsymbol{\theta}}{\sigma^2/2} = \frac{2\delta_3^2}{\sigma^2}\,||\boldsymbol{P}_{\boldsymbol{D}}^{\perp}\boldsymbol{w}||^2. \tag{51}$$

Note that the non-centrality parameter $\lambda_3(P_{fa}, P_d)$ can be numerically computed as the solution of $\mathcal{Q}^{-1}_{\chi^2_{2L}}(P_{fa}) = \mathcal{Q}^{-1}_{\chi^2_{2L}(\lambda_3(P_{fa},P_d))}(P_d)$.

5.3. Theoretical SINR derivation

From (51), one can state the following results:

Result 7. *The SINR threshold with respect to the SRL δ_3 required to resolve two closely spaced unknown SOI imbedded in $M-2$ unknown sources with a known noise variance, is given by*

$$SINR_3 = \frac{\|\boldsymbol{s}_1\|^2 + \|\boldsymbol{s}_2\|^2}{\|\boldsymbol{s}\|^2 + \delta_3^2\frac{2||\boldsymbol{P}_{\boldsymbol{D}}^{\perp}\boldsymbol{w}||^2}{\lambda_3(P_{fa},P_d)}}. \quad \blacksquare \tag{52}$$

Result 8. *The SNR threshold with respect to the SRL δ_3 required to resolve two closely spaced unknown SOI with a known noise variance, is given by*

$$SNR_3 = \lambda_3(P_{fa}, P_d)\,\frac{\|\boldsymbol{s}_1\|^2 + \|\boldsymbol{s}_2\|^2}{2\delta_3^2||\boldsymbol{P}_{\boldsymbol{A}}^{\perp}\boldsymbol{w}||^2}. \quad \blacksquare \tag{53}$$

A straightforward derivation leads to

$$||\boldsymbol{P}_{\boldsymbol{A}}^{\perp}\boldsymbol{w}||^2 = \frac{1}{4}||\boldsymbol{s}_-||^2||\boldsymbol{b}||^2, \tag{54}$$

where $\boldsymbol{b} = \dot{\boldsymbol{a}} - \frac{\boldsymbol{a}^H\dot{\boldsymbol{a}}}{L}\boldsymbol{a}$ and $||\boldsymbol{b}||^2 = ||\dot{\boldsymbol{a}}||^2 - \frac{|\boldsymbol{a}^H\dot{\boldsymbol{a}}|^2}{L}$.

Result 9. *If the SOI are orthogonal. The SNR threshold is given by*

$$SNR_{3o} = \frac{2\lambda_3(P_{fa}, P_d)}{\delta_3^2\,\|\boldsymbol{b}\|^2}. \quad \blacksquare \tag{55}$$

The last result means that the SNR threshold for orthogonal SOI is invariant to the source powers.

5.4. Alternative expression of the non-centrality parameter

In the case of unknown SOI, the FIM is not invertible, therefore the CRB of δ_3 does not exist. This arises due to the lack of indentifiability in model (39) because of multiplicative ambiguity in the product $\delta_3 \boldsymbol{s}_-$. To obtain an invertible FIM, it is necessary to assume known SOI as in case 1 and 2. Note that if, as in case 3 (and also the following case, *i.e.*, case 4), the vector of interest is $\boldsymbol{\theta} = \delta_3 \boldsymbol{s}_-$, there is no ambiguity and it exists an unbiased estimator (and thus the CRB) of $\boldsymbol{\theta}$. Keeping in mind this fact, it is interesting to note that the I-CRB (as derived in Appendix C.2) for the unknown parameters δ_3 *w.r.t.* the interference subspace $\langle \boldsymbol{D} \rangle$ and for known SOI, is given by

$$\text{I-CRB}(\delta_3) = \frac{\sigma^2}{2||\boldsymbol{P}_{\boldsymbol{D}}^{\perp}\boldsymbol{w}||^2}.$$

This can be linked to the non-centrality parameter in (51) according to

$$\lambda_3\left(P_{fa}, P_d\right) = \delta_3^2 \text{I-CRB}^{-1}(\delta_3). \tag{56}$$

6. Case 4: unknown SOI, SI and noise variance

6.1. Binary hypothesis test

In the following, we consider the general case where two unknown sources are imbedded in $M-2$ unknown sources. In addition, σ^2 is assumed to be unknown. Let δ_4 be the SRL. The observations under each hypothesis are given by

$$\begin{cases} \mathcal{H}_0: & \boldsymbol{y} = \boldsymbol{D}\boldsymbol{g} + \boldsymbol{v} \sim \mathcal{CN}(\boldsymbol{D}\boldsymbol{g}, \sigma^2\boldsymbol{I}), \\ \mathcal{H}_1: & \boldsymbol{y} = \boldsymbol{B}\boldsymbol{\theta} + \boldsymbol{D}\boldsymbol{g} + \boldsymbol{v} \sim \mathcal{CN}(\boldsymbol{B}\boldsymbol{\theta} + \boldsymbol{D}\boldsymbol{g}, \sigma^2\boldsymbol{I}). \end{cases} \tag{57}$$

6.2. The GLRT derivation

From (57), the GLRT is given by

$$G(\boldsymbol{y}) = \frac{\hat{\sigma}_0^2}{\hat{\sigma}_1^2} = \frac{||\hat{\boldsymbol{v}}_{\mathcal{H}_0}||^2}{||\hat{\boldsymbol{v}}_{\mathcal{H}_1}||^2}, \tag{58}$$

where the MLE of the noise variance under each hypothesis is given by [25]

$$\hat{\sigma}_i^2 = \frac{1}{NL}||\hat{\boldsymbol{v}}_{\mathcal{H}_i}||^2. \tag{59}$$

After some straightforward derivations, we obtain

$$\begin{cases} \hat{\boldsymbol{v}}_{\mathcal{H}_0} = \boldsymbol{P}_{\boldsymbol{D}}^{\perp}\boldsymbol{y} & \text{under } \mathcal{H}_0, \\ \hat{\boldsymbol{v}}_{\mathcal{H}_1} = \boldsymbol{P}_{[\boldsymbol{B}\boldsymbol{D}]}^{\perp}\boldsymbol{y} & \text{under } \mathcal{H}_1, \end{cases} \tag{60}$$

and where $\hat{\boldsymbol{\theta}}$, $\hat{\boldsymbol{g}}_{\mathcal{H}_0}$ and $\hat{\boldsymbol{g}}_{\mathcal{H}_1}$ are given by (40)-(42), respectively. In this case it is more convenient to define the statistic $T''(\boldsymbol{y})$ as follows

$$T''(\boldsymbol{y}) \triangleq \left(\ln G(\boldsymbol{y})\right)^{\frac{1}{NL}} - 1 = \frac{T'(\boldsymbol{y})}{N(\boldsymbol{y})} \tag{61}$$

where $N(\boldsymbol{y}) = \frac{1}{\sigma^2}\boldsymbol{y}^H\boldsymbol{P}_{[\boldsymbol{B}\boldsymbol{D}]}^{\perp}\boldsymbol{y}$. In addition, using any orthogonal decomposition [23], one has $\boldsymbol{P}_{[\boldsymbol{B}\boldsymbol{D}]}^{\perp} = \boldsymbol{U}'\boldsymbol{U}'^H$. Consequently, $N(\boldsymbol{y}) = ||\bar{\boldsymbol{y}}||^2$, in which $\bar{\boldsymbol{y}} = \boldsymbol{U}'^H\boldsymbol{y}$. Thus,

$$T''(\boldsymbol{y}) = \frac{||\tilde{\boldsymbol{y}}||^2}{||\bar{\boldsymbol{y}}||^2}, \tag{62}$$

and

$$\begin{cases} \bar{\boldsymbol{y}} = \boldsymbol{U}'^H\boldsymbol{v} \sim \mathcal{CN}(\boldsymbol{0}, \sigma^2\boldsymbol{I}) & \text{under } \mathcal{H}_0, \\ \bar{\boldsymbol{y}} = \boldsymbol{U}'^H\boldsymbol{v} \sim \mathcal{CN}(\boldsymbol{0}, \sigma^2\boldsymbol{I}) & \text{under } \mathcal{H}_1, \end{cases}$$

then,

$$\begin{cases} N(\boldsymbol{y}) \sim \chi^2_{2r'} & \text{under } \mathcal{H}_0, \\ N(\boldsymbol{y}) \sim \chi^2_{2r'}(0) & \text{under } \mathcal{H}_1, \end{cases}$$

where $r' = \text{trace}(\boldsymbol{P}_{[\boldsymbol{B}\boldsymbol{D}]}^{\perp}) = NL - \text{rank}(\boldsymbol{P}_{[\boldsymbol{B}\boldsymbol{D}]}) = (N-M)\,L$.

Furthermore, one can notice that the random variables $||\bar{\boldsymbol{y}}||^2$ and $||\tilde{\boldsymbol{y}}||^2$ are independent (see Appendix D). Consequently, a new statistic $V(\boldsymbol{y})$ is described as follows

$$V(\boldsymbol{y}) \triangleq (N-M)T''(\boldsymbol{y}) \sim \tag{63}$$

$$\begin{cases} F_{2L,2(N-M)L} & \text{under } \mathcal{H}_0, \\ F_{2L,2(N-M)L}(\lambda_4\left(P_{fa}, P_d\right)) & \text{under } \mathcal{H}_1, \end{cases}$$

where $F_{2L,2(N-M)L}$ and $F_{2L,2(N-M)L}(\lambda_4\left(P_{fa}, P_d\right))$ denote the F central and noncentral distributions [15], respectively, of $2L$ and $2(N-M)L$ degrees of freedom, in which the non-centrality parameter is given by

$$\lambda_4\left(P_{fa}, P_d\right) = \frac{2\delta_4^2}{\sigma^2}||\boldsymbol{P}_{\boldsymbol{D}}^{\perp}\boldsymbol{w}||^2. \tag{64}$$

Once again, note that the non-centrality parameter $\lambda_4(P_{fa}, P_d)$ can be computed numerically as the solution of $\mathcal{Q}^{-1}_{F_{2L,2(N-M)L}}(P_{fa}) = \mathcal{Q}^{-1}_{F_{2L,2(N-M)L}(\lambda_4(P_{fa},P_d))}(P_d)$ with $2L$ and $2(N-M)L$ degree of freedom, where $\mathcal{Q}^{-1}_{F_{2L,2(N-M)L}}(\beta)$ and $\mathcal{Q}^{-1}_{F_{2L,2(N-M)L}(\lambda_4(P_{fa},P_d))}(\beta)$ denote the right tail of the pdf $F_{2L,2(N-M)L}$ and $F_{2L,2(N-M)L}(\lambda_4(P_{fa}, P_d))$, respectively, starting at β.

6.3. Theoretical SINR derivation

From (64), one can state the following results:

Result 10. *The SINR threshold with respect to the SRL δ_4 required to resolve two closely spaced unknown SOI imbedded in $M-2$ unknown sources with an unknown noise variance, is given by*

$$SINR_4 = \frac{\|\boldsymbol{s}_1\|^2 + \|\boldsymbol{s}_2\|^2}{\|\boldsymbol{s}\|^2 + \delta_4^2 \frac{2||\boldsymbol{P}_{\boldsymbol{D}}^{\perp}\boldsymbol{w}||^2}{\lambda_4(P_{fa},P_d)}}. \quad \blacksquare \tag{65}$$

Result 11. *The SNR threshold with respect to the SRL δ_4 required to resolve two closely spaced unknown SOI with an unknown noise variance is given by*

$$SNR_4 = \lambda_4\left(P_{fa}, P_d\right) \frac{\|\boldsymbol{s}_1\|^2 + \|\boldsymbol{s}_2\|^2}{2\delta_4^2||\boldsymbol{P}_{\boldsymbol{A}}^{\perp}\boldsymbol{w}||^2}. \quad \blacksquare \tag{66}$$

As in the case 3, the SNR threshold for orthogonal SOI is given by the following result:

Result 12. *If the SOI are orthogonal. The SNR threshold is given by*

$$SNR_{4o} = \frac{2\lambda_4\left(P_{fa}, P_d\right)}{\delta_4^2 \left\|\boldsymbol{b}\right\|^2}. \quad \blacksquare \tag{67}$$

The last result means that the SNR threshold for orthogonal SOI is invariant to the source powers.

6.4. Alternative expression of the non-centrality parameter

As in the case 3, the I-CRB defined in Appendix C.2 for the unknown parameter $[\delta_4\ \sigma^2]^T$ *w.r.t.* the interference subspace $\langle \boldsymbol{D} \rangle$ with known SOI can be linked to the non-centrality parameter, given in (64), according to

$$\lambda_4\left(P_{fa}, P_d\right) = \delta_4^2 \text{I-CRB}^{-1}(\delta_4). \tag{68}$$

7. Summary of results and discussion

The studied cases are summarized in table 1 [2].

Toward the comparison of the studied cases, we formulate the three following propositions:

P1. First, as shown in Fig. 2, an increasing the number of the unknown parameter increases the degree of freedom of the χ_n^2 distribution used to derive λ, which will increase the value of λ and consequently,

$$\lambda_1 = \lambda_2 \leq \lambda_3. \tag{69}$$

P2. Second, considering the noise variance as unknown parameter will produce a F distribution to compute the desired non-centrality parameter (see case 4). As a consequence, the non-centrality parameter computed *w.r.t.* χ_n^2 distribution is lower than the non-centrality parameter computed *w.r.t.* F distribution for any $P_d > P_{fa}$ [26], meaning that

$$\lambda_3 \leq \lambda_4. \tag{70}$$

P3. On the other hand, note that $\langle \boldsymbol{C} \rangle \subset \langle \boldsymbol{D} \rangle$, where $\langle \boldsymbol{C} \rangle$ and $\langle \boldsymbol{D} \rangle$ denote the subspace spanned by the column of the matrices $\boldsymbol{C}$ and $\boldsymbol{D}$, respectively. Consequently we have $\forall \boldsymbol{w}$: $\boldsymbol{w}^H \boldsymbol{P}_{\boldsymbol{C}} \boldsymbol{w} \leq \boldsymbol{w}^H \boldsymbol{P}_{\boldsymbol{D}} \boldsymbol{w}$ and thus

$$||\boldsymbol{P}_{\boldsymbol{D}}^{\perp} \boldsymbol{w}||^2 \leq ||\boldsymbol{P}_{\boldsymbol{C}}^{\perp} \boldsymbol{w}||^2 \leq \|\boldsymbol{w}\|^2. \tag{71}$$

From **P1.**, **P2.** and **P3.** and for the same SRL (*i.e.*, $\delta_1 = \delta_2 = \delta_3 = \delta_4$), one deduces that

$$\text{SINR}_1 \leq \text{SINR}_2 \leq \text{SINR}_3 \leq \text{SINR}_4.$$

[2] In this section, P_{fa}, P_d are dropped from $\lambda\left(P_{fa}, P_d\right)$ for sake of simplicity.

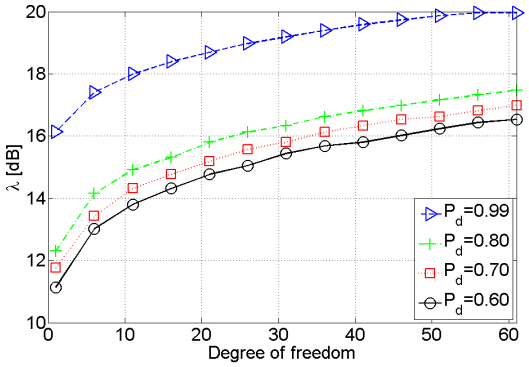

Figure 2: Behavior of the noncentral parameter of χ_n^2 versus n the degree of freedom for different value of P_d and for a fixed $P_{fa} = 0.01$.

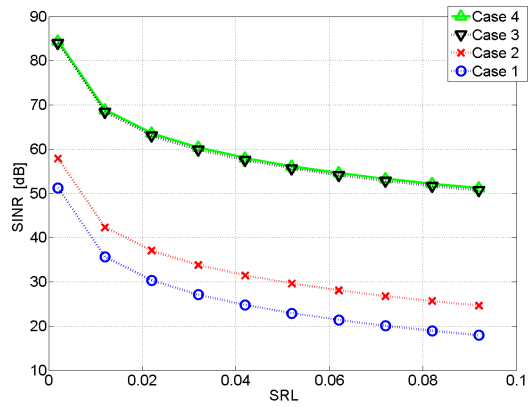

Figure 3: SINR threshold *w.r.t.* the SRL for the studied cases.

The same analysis can be done in the case of $M = 2$ (no interference), *i.e.*,

$$\text{SNR}_1 \leq \text{SNR}_2 \leq \text{SNR}_3 \leq \text{SNR}_4,$$
$$\text{SNR}_{1o} \leq \text{SNR}_{2o} \leq \text{SNR}_{3o} \leq \text{SNR}_{4o}.$$

In Fig. 3, we have reported the SINR threshold *w.r.t.* the SRL obtained in all cases. The gap between the case 1 and the case 2 is evaluated around 10 dB and it is especially due to the projector $\boldsymbol{P}_{\boldsymbol{C}}^{\perp}$. The difference between the case 2 and the case 3 is around 25 dB. This loss is considerably high because it is due to the projector $\boldsymbol{P}_{\boldsymbol{D}}^{\perp}$ but also to the higher degree of freedom for λ_3. Finally, the gap between the case 3 and the case 4 is about only 0.5 dB and it is produced by the difference in the distribution used to compute the desired λ_4. In conclusion, the difference between the studied cases is mainly due to

- the non-centrality parameter numerical value,
- the effect of the subspace interference according to the projection onto $\langle \boldsymbol{C} \rangle$ or $\langle \boldsymbol{D} \rangle$.

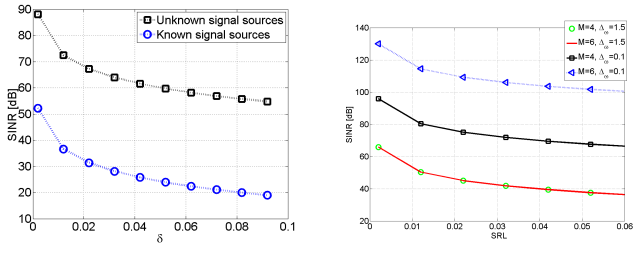

Figure 4: *(left)* SINR threshold to resolve two known/unknown closely far-field SOI with known noise variance for an ULA where $N = 10$, $d = \frac{\nu}{2}$ and $M = 4$ in which $\Delta_\omega = 0.75$. *(right)* The SINR threshold for an ULA where $N = 10$, $d = \frac{\nu}{2}$, for different number of sources and Δ_ω.

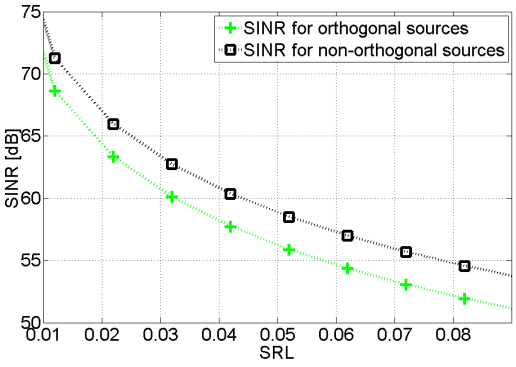

Figure 5: The required SINR to resolve two BPSK unknown orthogonal/non-orthogonal closely far-field sources for an ULA where $N = 10$, $d = \frac{\nu}{2}$ and $M = 4$.

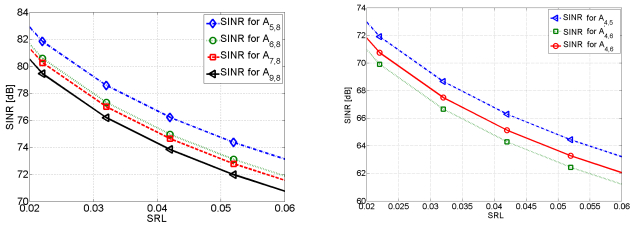

Figure 6: *(left)* The required SINR to resolve two unknown closely sources with known noise variance for different array geometries and same aperture which $N = 10$, $d = \frac{\nu}{2}$ and $M = 4$ in which $\Delta_\omega = 1.5$. *(right)* The required SNR to resolve two known sources using ULA, Type 4 and Type 5 geometries where $P_{fa} = 0.01$ and $P_d = 0.99$.

8. Numerical Analysis

This section is devoted to the numerical analysis of the SINR threshold *w.r.t.* the SRL. Furthermore, we have considered equal interference's power and broadband noise's power (INR= 1) and thus SINR $= \frac{1}{2}$SNR. The number of snapshots is equal to $L = 100$ where $\nu = 0.5m$ and $(P_{fa}, P_d) = (0.01, 0.99)$. The SRL *w.r.t.* the two closest sources (the SOI) is denoted by δ, where all the remain sources are equally spaced by Δ_ω (where $\Delta_\omega > \delta$).

8.1. Effect on the source prior

The *prior* knowledge on the source amplitudes and source phases is known to have a considerable effect on the estimation accuracy [27]. One could expect the same behavior concerning the resolution limit. From Fig. 4*(left)* one can notice the effect of the sources *prior* knowledge on the SRL. Indeed, the SRL depends strongly on the *prior* sources knowledge, *e.g.*, the SINR threshold needed to resolve two known signal sources *w.r.t.* δ is approximatively 40 dB less than the SINR threshold needed to resolve two unknown sources.

8.2. Effect of the subspace interference

In Fig. 4*(right)*, we have reported the effect of additional sources (considered as a subspace interference) on the SINR threshold. One can distinguish two cases:

1. The first one represents the scenario where $\Delta_\omega \gg \delta$. In this case, one can notice that the additional sources do not affect the SINR. This can be explained by the fact that the high resolution algorithms have asymptotically an infinite resolving power [20].
2. The second scenario is for $\Delta_\omega > \delta$. In this case, one can notice the drastic effect of the interfering sources. For example, the SINR gap between $M = 4$ and $M = 6$ scenarios is evaluated around 30 dB.

8.3. Orthogonal SOI

From an estimation point of view, it is well-known that the estimation accuracy for orthogonal signal sources outperforms the estimation accuracy for the non-orthogonal signal sources [28]. One expect the same behavior concerning the SINR threshold. In fact, as shown in Fig. 5, the SINR threshold in the case of non-orthogonal Binary Phase-Shift Keying (BPSK) signal sources is greater than the case of orthogonal BPSK signal sources. This loss is around 3 dB.

8.4. Analysis for nonuniform arrays

The effect of the nonuniform antenna array is studied in the following. The linear array will be specified by their array aperture and their sensor positions[3].

• First, let us study the effect of the number of sensors on the SRL (or, equivalently, on the minimum required SINR to resolve two closely spaced sources). In Table 2 are listed different array geometries with 5, 6, 7 and 9 sensors. The array with 9 sensors is an ULA, whereas the others belong to the so-called "optimal" nonuniform array geometries [30]. More precisely, an exhaustive search has been done to select the minimum redundancy arrays with 5, 6 and 7 sensors with an aperture equals to $8d$ (recall that the minimum redundancy arrays minimize the

[3]For example, an ULA of N sensors will be represented as $A_{N,N-1} = [0, 1, \ldots, N-1]$, where the subscript $N-1$ is related to the array aperture (*i.e.*, the distance between the first and the last sensor is equal to $(N-1)d$ where $d = \frac{\nu}{2}$ [29].)

number of redundant lags R such that no missing lags will be present). From Fig. 6*(left)* one can notice, for the same array aperture, that the SINR threshold to resolve two closely spaced sources is slightly sensitive to the number of sensors. The gap for ULA of 5 sensors and the one for 9 sensors (having the same array aperture) is evaluated at 2 dB.

• Finally, let us consider the case of different LA geometries with the same number of sensors. In Table 3 are reported different array geometries for $N = 4$ sensors with different apertures. One can notice, from Fig. 6*(right)*, that the array aperture affects the SINR threshold to resolve two closely spaced sources around 2 dB. On the other hand, one can notice that the SRL for arrays of the same aperture with different array geometries are affected by only 1 dB (*i.e.*, between the so-called perfect array $A_{4,6}$ and any array $A'_{4,6}$). Meaning that, the SRL is only slightly sensitive to the array design (for the same array aperture).

9. Conclusion

In this paper, we have derived theoretical expressions of the signal-to-interference-plus-noise ratio (SINR) threshold *w.r.t.* the statistical-resolution-limit (SRL) for two closely spaced far-field narrowband sources, among a total number of $M \geq 2$, impinging on a linear nonuniform array. The two Sources Of Interest (SOI) are corrupted by (1) the interference resulting from the $M-2$ remaining sources (called here subspace interference (SI)) and by (2) a broadband noise. Since our approach is based on the detection theory, these expressions provide useful information concerning the resolution limit for a given couple of probability of false alarm and probability of detection. In addition, the theoretical SINR threshold and the SRL have been analyzed with respect to the interference (resulting from the $M-2$ other sources), the array geometry and the aperture, the *prior* sources knowledge or their orthogonality.

10. Appendix

10.1. Derivation of the CMLE for cases 1 and 2

10.1.1. MLEs for case 1

The negative log-likelihood function is given by

$$L(\boldsymbol{z},\delta) = -\ln p(\boldsymbol{z}) = -\ln(\pi\sigma^2)^{-NL/2} + \sigma^{-2}||\boldsymbol{z}-\boldsymbol{w}\delta||^2.$$

The optimization problem is given by

$$\arg\min_{\delta} L(\boldsymbol{z},\delta) \;\text{ subject to }\; \delta \in \mathbb{R}.$$

This problem can also be solved by the Lagrange multiplier method. Let ϑ be a real Lagrange multiplier, then the Lagrange function is given by

$$\mathcal{L}(\delta,\vartheta) = L(\boldsymbol{z},\delta) + \vartheta\Im(\delta).$$

The condition $\Im(\delta) = 0$ can be rewritten according to $-j\frac{1}{2}(\delta-\delta^*) = 0$. So, the partial derivatives of the Lagrange function are

$$\begin{cases} \frac{\partial\mathcal{L}}{\partial\delta} = \sigma^{-2}\left(||\boldsymbol{w}||^2\delta^* - \boldsymbol{z}^H\boldsymbol{w}\right) - j\frac{\vartheta}{2}, \\ \frac{\partial\mathcal{L}}{\partial\vartheta} = \Im(\delta). \end{cases}$$

since $\frac{\partial\delta^*}{\partial\delta} = 0$. By letting $\frac{\partial\mathcal{L}}{\partial\delta}|_{\delta_0} = 0$, we have

$$\delta_0 = \frac{\boldsymbol{w}^H\boldsymbol{z}}{||\boldsymbol{w}||^2} - j\frac{\vartheta\sigma^2}{2||\boldsymbol{w}||^2}. \tag{72}$$

Setting $\frac{\partial\mathcal{L}}{\partial\vartheta}|_{\vartheta_0} = 0$, we have

$$\Im(\delta_0) = \Im\left\{\frac{\boldsymbol{w}^H\boldsymbol{z}}{||\boldsymbol{w}||^2}\right\} - \frac{\vartheta\sigma^2}{2||\boldsymbol{w}||^2} = 0.$$

Consequently, the Lagrange multiplier is given by

$$\vartheta_0 = \frac{2}{\sigma^2}\Im\{\boldsymbol{w}^H\boldsymbol{z}\}.$$

Plugging the above expression in (72), we have

$$\hat{\delta} = \frac{\boldsymbol{w}^H\boldsymbol{z}}{||\boldsymbol{w}||^2} - j\Im\left\{\frac{\boldsymbol{w}^H\boldsymbol{z}}{||\boldsymbol{w}||^2}\right\} = \frac{\Re\left\{\boldsymbol{w}^H\boldsymbol{z}\right\}}{||\boldsymbol{w}||^2}, \tag{73}$$

by using $\Re\{a\} = a - j\Im\{a\}$.

10.1.2. MLEs for case 2

The negative log-likelihood function is given by

$$L(\boldsymbol{z},\boldsymbol{d}) = -\ln p(\boldsymbol{z}) = -\ln(\pi\sigma^2)^{-NL/2} + \sigma^{-2}||\boldsymbol{z}-\boldsymbol{Q}\boldsymbol{p}||^2.$$

The optimization problem is given by

$$\arg\min_{\boldsymbol{p}} L(\boldsymbol{z},\boldsymbol{p}) \;\text{ subject to }\; \boldsymbol{e}_1^T\boldsymbol{p} \in \mathbb{R}$$

where $\boldsymbol{e}_1 = [1\ 0\ldots 0]^T$.

This problem can be solved by the Lagrange multiplier method. Let ϑ be a real Lagrange multiplier, then the Lagrange function is given by

$$\mathcal{L}(\boldsymbol{p},\vartheta) = L(\boldsymbol{z},\boldsymbol{p}) + \vartheta\Im(\boldsymbol{e}_1^T\boldsymbol{p}).$$

The condition $\Im(\boldsymbol{e}_1^T\boldsymbol{p}) = 0$ can be rewritten according to $-j\frac{1}{2}(\boldsymbol{e}_1^T\boldsymbol{p} - \boldsymbol{e}_1^T\boldsymbol{p}^*) = 0$. So, the partial derivatives of the Lagrange function are

$$\begin{cases} \frac{\partial\mathcal{L}}{\partial\boldsymbol{p}} = \sigma^{-2}\left(\boldsymbol{Q}^T\boldsymbol{Q}^*\boldsymbol{p}^* - \boldsymbol{Q}^T\boldsymbol{z}^*\right) - j\frac{\vartheta}{2}\boldsymbol{e}_1, \\ \frac{\partial\mathcal{L}}{\partial\vartheta} = \Im(\boldsymbol{e}_1^T\boldsymbol{p}), \end{cases}$$

since $\frac{\partial\boldsymbol{p}^*}{\partial\boldsymbol{p}} = \boldsymbol{0}$. By letting $\frac{\partial\mathcal{L}}{\partial\boldsymbol{p}}|_{\boldsymbol{p}_0} = 0$, we have

$$\boldsymbol{p}_0 = \boldsymbol{Q}^\dagger\boldsymbol{z} - j\frac{\vartheta\sigma^2}{2}(\boldsymbol{Q}^H\boldsymbol{Q})^{-1}\boldsymbol{e}_1. \tag{74}$$

By setting $\frac{\partial\mathcal{L}}{\partial\vartheta}|_{\vartheta_0} = 0$, we have

$$\Im(\boldsymbol{e}_1^T\boldsymbol{p}_0) = \Im(\boldsymbol{e}_1^T\boldsymbol{Q}^\dagger\boldsymbol{z}) - \frac{\vartheta_0\sigma^2}{2}h = 0$$

where we have defined the real quantity $h = \boldsymbol{e}_1^T(\boldsymbol{Q}^H\boldsymbol{Q})^{-1}\boldsymbol{e}_1$. Consequently, the Lagrange multiplier is given by

$$\vartheta_0 = \frac{2}{\sigma^2 h}\Im(\boldsymbol{e}_1^T\boldsymbol{Q}^\dagger\boldsymbol{z}).$$

Plugging the above expression into (74), we have

$$\hat{\boldsymbol{p}} = \boldsymbol{Q}^\dagger\boldsymbol{z} - j\frac{1}{h}(\boldsymbol{Q}^H\boldsymbol{Q})^{-1}\boldsymbol{e}_1\Im(\boldsymbol{e}_1^T\boldsymbol{Q}^\dagger\boldsymbol{z}). \quad (75)$$

CMLE of the SRL . The estimate of the SRL is given by $\hat{\delta} = \boldsymbol{e}_1^T\hat{\boldsymbol{p}}$ and thus,

$$\hat{\delta} = \boldsymbol{e}_1^T\boldsymbol{Q}^\dagger\boldsymbol{z} - j\Im(\boldsymbol{e}_1^T\boldsymbol{Q}^\dagger\boldsymbol{z}). \quad (76)$$

Now, remark that $\Re\{a\} = a - j\Im\{a\}$, then

$$\hat{\delta} = \Re\{\boldsymbol{e}_1^T\boldsymbol{Q}^\dagger\boldsymbol{z}\}. \quad (77)$$

In addition, using the inverse of a block matrix and the Schur complement [10], we have

$$\boldsymbol{e}_1^T\boldsymbol{Q}^\dagger = \ell\boldsymbol{w}^H + \boldsymbol{u}^H\boldsymbol{C}^H, \quad (78)$$

where

$$\ell = \frac{1}{||\boldsymbol{w}||^2 - \boldsymbol{w}^H\boldsymbol{C}(\boldsymbol{C}^H\boldsymbol{C})^{-1}\boldsymbol{C}^H\boldsymbol{w}} = \frac{1}{||\boldsymbol{P}_{\boldsymbol{C}}^\perp\boldsymbol{w}||^2} \quad (79)$$

$$\boldsymbol{u}^H = -\frac{\boldsymbol{w}^H\boldsymbol{C}(\boldsymbol{C}^H\boldsymbol{C})^{-1}}{||\boldsymbol{P}_{\boldsymbol{C}}^\perp\boldsymbol{w}||^2}. \quad (80)$$

Thus

$$\boldsymbol{e}_1^T\boldsymbol{Q}^\dagger = \frac{\boldsymbol{w}^H\boldsymbol{P}_{\boldsymbol{C}}^\perp}{||\boldsymbol{P}_{\boldsymbol{C}}^\perp\boldsymbol{w}||^2}. \quad (81)$$

Using (77) and (81), we have (26).

MLE of the interfering sources . The estimate of the interfering sources is given by $\hat{\boldsymbol{s}} = \boldsymbol{J}\hat{\boldsymbol{p}}$ where $\boldsymbol{J} = [\boldsymbol{0}_{(M-2)L\times 1}\ \boldsymbol{I}_{(M-2)L}]$ is a $((M-2)L)\times((M-2)L+1)$ selection matrix. We have

$$\hat{\boldsymbol{s}} = \boldsymbol{J}\boldsymbol{Q}^\dagger\boldsymbol{z} - j\frac{1}{h}\boldsymbol{J}(\boldsymbol{Q}^H\boldsymbol{Q})^{-1}\boldsymbol{e}_1\Im\{\boldsymbol{e}_1^T\boldsymbol{Q}^\dagger\boldsymbol{z}\}. \quad (82)$$

Let us define the following matrix:

$$\boldsymbol{G} \triangleq (\boldsymbol{C}^H\boldsymbol{C})^{-1}\left(\boldsymbol{I} + \frac{\boldsymbol{C}^H\boldsymbol{w}\boldsymbol{w}^H\boldsymbol{C}^{\dagger H}}{||\boldsymbol{P}_{\boldsymbol{C}}^\perp\boldsymbol{w}||^2}\right), \quad (83)$$

and observe the following equalities:

$$\boldsymbol{J}\boldsymbol{Q}^\dagger = \boldsymbol{u}\boldsymbol{w}^H + \boldsymbol{G}\boldsymbol{C}^H = \boldsymbol{C}^\dagger - \frac{1}{||\boldsymbol{P}_{\boldsymbol{C}}^\perp\boldsymbol{w}||^2}\boldsymbol{C}^\dagger\boldsymbol{w}\boldsymbol{w}^H\boldsymbol{P}_{\boldsymbol{C}}^\perp,$$

$$\frac{1}{h}\boldsymbol{J}(\boldsymbol{Q}^H\boldsymbol{Q})^{-1}\boldsymbol{e}_1 = \frac{1}{h}\begin{bmatrix}\boldsymbol{u} & \boldsymbol{G}\end{bmatrix}\boldsymbol{e}_1 = \frac{1}{h}\boldsymbol{u} = -\boldsymbol{C}^\dagger\boldsymbol{w}.$$

Plugging the two above expressions and (81) into (82), we obtain

$$\begin{aligned}\hat{\boldsymbol{s}} &= \boldsymbol{C}^\dagger\boldsymbol{z} - \frac{\boldsymbol{C}^\dagger\boldsymbol{w}\boldsymbol{w}^H\boldsymbol{P}_{\boldsymbol{C}}^\perp}{||\boldsymbol{P}_{\boldsymbol{C}}^\perp\boldsymbol{w}||^2}\boldsymbol{z} + j\boldsymbol{C}^\dagger\boldsymbol{w}\Im\left\{\frac{\boldsymbol{w}^H\boldsymbol{P}_{\boldsymbol{C}}^\perp\boldsymbol{z}}{||\boldsymbol{P}_{\boldsymbol{C}}^\perp\boldsymbol{w}||^2}\right\}\\ &= \boldsymbol{C}^\dagger\boldsymbol{z} - \boldsymbol{C}^\dagger\boldsymbol{w}\underbrace{\left(\frac{\boldsymbol{w}^H\boldsymbol{P}_{\boldsymbol{C}}^\perp\boldsymbol{z}}{||\boldsymbol{P}_{\boldsymbol{C}}^\perp\boldsymbol{w}||^2} - j\Im\left\{\frac{\boldsymbol{w}^H\boldsymbol{P}_{\boldsymbol{C}}^\perp\boldsymbol{z}}{||\boldsymbol{P}_{\boldsymbol{C}}^\perp\boldsymbol{w}||^2}\right\}\right)}_{\hat{\delta}}\\ &= \boldsymbol{C}^\dagger\left(\boldsymbol{z} - \boldsymbol{w}\hat{\delta}\right).\end{aligned}$$

10.2. Statistic of the random variable $\frac{\Re^2\{\boldsymbol{w}^H\boldsymbol{y}\}}{\frac{\sigma^2}{2}\|\boldsymbol{w}\|^2}$

Let us consider a random variable $\boldsymbol{y} = \delta\boldsymbol{w} + \boldsymbol{v}$ corrupted by a zero-mean white circular Gaussian noise $\boldsymbol{v}$ of variance σ^2. We recall that a circular random variable means [23] $\Re\{\boldsymbol{v}\} \sim \mathcal{N}(\boldsymbol{0}, \frac{\sigma^2}{2}\boldsymbol{I})$, $\Im\{\boldsymbol{v}\} \sim \mathcal{N}(\boldsymbol{0}, \frac{\sigma^2}{2}\boldsymbol{I})$ and $E(\Re\{\boldsymbol{v}\}\Im\{\boldsymbol{v}\}^T) = E(\Im\{\boldsymbol{v}\}\Re\{\boldsymbol{v}\}^T) = \boldsymbol{0}$. So,

$$\begin{cases}\boldsymbol{y}_{\mathcal{H}_0} \sim \mathcal{CN}(\boldsymbol{0}, \sigma^2\boldsymbol{I}),\\ \boldsymbol{y}_{\mathcal{H}_1} \sim \mathcal{CN}(\delta\boldsymbol{w}, \sigma^2\boldsymbol{I}).\end{cases} \quad (84)$$

Let $u = \Re\{\boldsymbol{w}^H\boldsymbol{y}\}$. The mean of variable u is given by $||\boldsymbol{w}||^2\delta$ and its variance is

$$\begin{aligned}C_u &= E\left\{\left(\Re\{\boldsymbol{w}^H\boldsymbol{y}\} - ||\boldsymbol{w}||^2\delta\right)^2\right\} = E\left\{\Re^2\{\boldsymbol{w}^H\boldsymbol{v}\}\right\}\\ &= E\left\{\left(\Re\{\boldsymbol{w}^H\}\Re\{\boldsymbol{v}\} - \Im\{\boldsymbol{w}^H\}\Im\{\boldsymbol{v}\}\right)^2\right\}\\ &= E\left\{\left(\Re\{\boldsymbol{w}\}^T\Re\{\boldsymbol{v}\} + \Im\{\boldsymbol{w}\}^T\Im\{\boldsymbol{v}\}\right)^2\right\}.\end{aligned}$$

Consequently, using the circularity of the noise, one obtains

$$\begin{aligned}C_u &= \Re\{\boldsymbol{\omega}\}^T\underbrace{E\left(\Re\{\boldsymbol{v}\}\Re\{\boldsymbol{v}\}^T\right)}_{(\sigma^2/2)\boldsymbol{I}}\Re\{\boldsymbol{\omega}\} + \Im\{\boldsymbol{\omega}\}^T\underbrace{E\left(\Im\{\boldsymbol{v}\}\Im\{\boldsymbol{v}\}^T\right)}_{(\sigma^2/2)\boldsymbol{I}}\Im\{\boldsymbol{\omega}\}\\ &+ \Re\{\boldsymbol{\omega}\}^T\underbrace{E\left(\Re\{\boldsymbol{v}\}\Im\{\boldsymbol{v}\}^T\right)}_{\boldsymbol{0}}\Im\{\boldsymbol{\omega}\} + \Im\{\boldsymbol{\omega}\}^T\underbrace{E\left(\Im\{\boldsymbol{v}\}\Re\{\boldsymbol{v}\}^T\right)}_{\boldsymbol{0}}\Re\{\boldsymbol{\omega}\}\\ &= \frac{\sigma^2}{2}\|\boldsymbol{w}\|^2.\end{aligned}$$

Let us define a new statistic as follows:

$$T(\boldsymbol{y}) \triangleq \frac{u^2}{C_u} = \frac{\Re^2\{\boldsymbol{w}^H\boldsymbol{y}\}}{\frac{\sigma^2}{2}\|\boldsymbol{w}\|^2}. \quad (85)$$

Thus, according to [15], we have $T(\boldsymbol{y}) \sim \chi_1^2(\lambda)$ in which $\chi_1^2(\lambda)$ denotes the non-central chi-square distribution with one degree of freedom where the non-centrality parameter is given by

$$\lambda \triangleq \frac{E(u)^2}{C_u} = \frac{2\delta^2||\boldsymbol{w}||^2}{\sigma^2}. \quad (86)$$

10.3. Derivation of the CRB and the I-CRB

In this appendix, we derive the CRB (Cramér-Rao Bound) an the so-called I-CRB (Interference CRB). Let $E\left\{(\hat{\acute{\boldsymbol{\Theta}}} - \acute{\boldsymbol{\Theta}})(\hat{\acute{\boldsymbol{\Theta}}} - \acute{\boldsymbol{\Theta}})^T\right\}$ be the covariance matrix of an unbiased estimator, $\hat{\acute{\boldsymbol{\Theta}}}$, of the deterministic parameter vector $\acute{\boldsymbol{\Theta}}$. The covariance inequality principle states that, under quite general/weak conditions, the variance satisfies: $\text{MSE}([\hat{\acute{\boldsymbol{\Theta}}}]_i) = E\left\{\left([\hat{\acute{\boldsymbol{\Theta}}}]_i - [\acute{\boldsymbol{\Theta}}]_i\right)^2\right\} \geq \left[\mathbf{CRB}(\acute{\boldsymbol{\Theta}})\right]_{i,i}$ where $\mathbf{CRB}(\acute{\boldsymbol{\Theta}}) = \mathbf{FIM}^{-1}(\acute{\boldsymbol{\Theta}})$, in which **FIM** denotes the Fisher Information Matrix. The (i^{th}, k^{th}) element of the FIM for

the parameter vector $\acute{\boldsymbol{\Theta}}$ can be written (for a complex circular Gaussian observation model) as [23]

$$\left[\mathbf{FIM}(\acute{\boldsymbol{\Theta}})\right]_{i,k} = \mathrm{Trace}\left\{\mathbf{R}^{-1}\frac{\partial \mathbf{R}}{\partial\left[\acute{\boldsymbol{\Theta}}\right]_i}\mathbf{R}^{-1}\frac{\partial \mathbf{R}}{\partial\left[\acute{\boldsymbol{\Theta}}\right]_k}\right\} \quad (87)$$

$$+2\Re\left\{\frac{\partial \boldsymbol{\mu}^H}{\partial\left[\acute{\boldsymbol{\Theta}}\right]_i}\mathbf{R}^{-1}\frac{\partial \boldsymbol{\mu}}{\partial\left[\acute{\boldsymbol{\Theta}}\right]_k}\right\},$$

where $\mathbf{R}$ and $\boldsymbol{\mu}$ denote the covariance matrix and the mean of the observation vector model, respectively.

10.3.1. Derivation of the CRB

Let us consider the estimation of the real parameter of interest δ, where the observation model is as follows

$$\boldsymbol{z} = \delta\boldsymbol{w} + \boldsymbol{v} \quad (88)$$

where $\boldsymbol{v} \sim \mathcal{CN}(0, \sigma^2\boldsymbol{I})$ whereas $\delta, \boldsymbol{w}$ and σ^2 are deterministic parameters. Thus $\boldsymbol{z} \sim \mathcal{CN}(\boldsymbol{\mu} = \delta\boldsymbol{w}, \boldsymbol{R} = \sigma^2\boldsymbol{I})$. The unknown deterministic parameter vector is defined as $\acute{\boldsymbol{\Theta}} = [\delta\ \sigma^2]^T$. Using (87), the CRB *w.r.t.* δ for the observation (88) is given by

$$\mathrm{CRB}(\delta) = \left[\frac{2}{\sigma^2}\Re\left\{\left(\frac{\partial \boldsymbol{\mu}}{\partial\delta}\right)^H\frac{\partial \boldsymbol{\mu}}{\partial\delta}\right\}\right]^{-1} = \frac{\sigma^2}{2}\left\|\boldsymbol{w}\right\|^2 \quad (89)$$

since it is well-known that δ and σ^2 are decoupled (diagonal FIM).

10.3.2. Derivation of the I-CRB

Now, let us consider the estimation of the real parameter of interest δ, where the observation model is corrupted by a deterministic structured interference as follows

$$\boldsymbol{z} = \delta\boldsymbol{w} + \boldsymbol{C}\boldsymbol{s} + \boldsymbol{v}. \quad (90)$$

Let us define the orthogonal projector and its orthogonal decomposition according to $\boldsymbol{P}_{\boldsymbol{C}}^{\perp} = \breve{\boldsymbol{U}}\breve{\boldsymbol{U}}^H$ which is a null-steering operator that nulls everything in the interference space $\langle\boldsymbol{C}\rangle$ [18]. Let us defined a new observation based on (90) as follows

$$\breve{\boldsymbol{z}} \triangleq \breve{\boldsymbol{U}}^H\boldsymbol{z} = \delta\breve{\boldsymbol{U}}^H\boldsymbol{w} + \breve{\boldsymbol{v}}, \quad (91)$$

since $\breve{\boldsymbol{U}}^H\breve{\boldsymbol{U}} = \boldsymbol{I}$, one has $\breve{\boldsymbol{v}} = \breve{\boldsymbol{U}}^H\boldsymbol{v} \sim \mathcal{CN}(0, \sigma^2\boldsymbol{I})$ and $\boldsymbol{z} \sim \mathcal{CN}(\boldsymbol{\mu} = \delta\breve{\boldsymbol{U}}^H\boldsymbol{w}, \boldsymbol{R} = \sigma^2\boldsymbol{I})$. The I-CRB [24], is the CRB for the observation (91) related to the projector $\boldsymbol{P}_{\boldsymbol{C}}^{\perp}$ where the unknown vector parameter is given by $\acute{\boldsymbol{\Theta}}$. Consequently, using (87) and after straightforward calculus, one obtains

$$\text{I-CRB}(\delta) = \left[\frac{2}{\sigma^2}\Re\left\{\left(\frac{\partial \boldsymbol{\mu}}{\partial\delta}\right)^H\frac{\partial \boldsymbol{\mu}}{\partial\delta}\right\}\right]^{-1} = \frac{\sigma^2}{2}||\boldsymbol{P}_{\boldsymbol{C}}^{\perp}\boldsymbol{w}||^2 \quad (92)$$

since it is well-known that δ and σ^2 are decoupled (diagonal FIM).

10.4. Independence of $||\bar{\boldsymbol{y}}||^2$ and $||\tilde{\boldsymbol{y}}||^2$

Since $E(\bar{\boldsymbol{y}}) = \boldsymbol{0}$ under $\mathcal{H}_0$ and $\mathcal{H}_1$, one has

$$\begin{aligned}
\mathrm{Cov}(\bar{\boldsymbol{y}}, \tilde{\boldsymbol{y}}) &= E(\bar{\boldsymbol{y}}\tilde{\boldsymbol{y}}^H) = \boldsymbol{U}'^H E(\boldsymbol{y}\boldsymbol{y}^H)\boldsymbol{U} \\
&= \boldsymbol{U}'^H\boldsymbol{U}'\boldsymbol{U}'^H E(\boldsymbol{y}\boldsymbol{y}^H)\boldsymbol{U}\boldsymbol{U}^H\boldsymbol{U} \\
&= \boldsymbol{U}'^H\boldsymbol{P}_{[\boldsymbol{BD}]}^{\perp}E(\boldsymbol{y}\boldsymbol{y}^H)\boldsymbol{P}_{\boldsymbol{P}_{\boldsymbol{D}}^{\perp}\boldsymbol{B}}\boldsymbol{U} \\
&= \boldsymbol{U}'^H\left(\sigma^2\boldsymbol{P}_{[\boldsymbol{BD}]}^{\perp}\boldsymbol{P}_{\boldsymbol{P}_{\boldsymbol{D}}^{\perp}\boldsymbol{B}} + \left(\boldsymbol{P}_{[\boldsymbol{BD}]}^{\perp}\boldsymbol{e}\right)\left(\boldsymbol{P}_{\boldsymbol{P}_{\boldsymbol{D}}^{\perp}\boldsymbol{B}}\boldsymbol{e}\right)^H\right)\boldsymbol{U}
\end{aligned}$$

where $\boldsymbol{e} = \boldsymbol{B}\boldsymbol{\theta} + \boldsymbol{D}\boldsymbol{g}$ under $\mathcal{H}_1$ and $\boldsymbol{e} = \boldsymbol{D}\boldsymbol{g}$ under $\mathcal{H}_0$.

Note $\boldsymbol{P}_{[\boldsymbol{BD}]}^{\perp}\boldsymbol{e} = \boldsymbol{0}$. And, on the other hand,

$$\begin{aligned}
\boldsymbol{P}_{[\boldsymbol{BD}]}^{\perp}\boldsymbol{P}_{\boldsymbol{P}_{\boldsymbol{D}}^{\perp}\boldsymbol{B}} &= \boldsymbol{P}_{\boldsymbol{D}}^{\perp}(\boldsymbol{P}_{\boldsymbol{D}}^{\perp}\boldsymbol{E}_{\boldsymbol{BD}} - \boldsymbol{E}_{\boldsymbol{BD}}\boldsymbol{P}_{\boldsymbol{D}}^{\perp}\boldsymbol{E}_{\boldsymbol{BD}})\boldsymbol{P}_{\boldsymbol{D}}^{\perp} \\
&= (\boldsymbol{P}_{\boldsymbol{D}}^{\perp}\boldsymbol{E}_{\boldsymbol{BD}} - \boldsymbol{P}_{\boldsymbol{D}}^{\perp}\boldsymbol{E}_{\boldsymbol{BD}}\boldsymbol{P}_{\boldsymbol{D}}^{\perp}\boldsymbol{E}_{\boldsymbol{BD}})\boldsymbol{P}_{\boldsymbol{D}}^{\perp} \\
&= (\boldsymbol{P}_{\boldsymbol{D}}^{\perp}\boldsymbol{E}_{\boldsymbol{BD}} - \boldsymbol{P}_{\boldsymbol{D}}^{\perp}\boldsymbol{E}_{\boldsymbol{BD}})\boldsymbol{P}_{\boldsymbol{D}}^{\perp} = \boldsymbol{0}.
\end{aligned}$$

Consequently, $\mathrm{Cov}(\bar{\boldsymbol{y}}, \tilde{\boldsymbol{y}}) = \boldsymbol{0}$. Meaning that $\bar{\boldsymbol{y}}$ and $\tilde{\boldsymbol{y}}$ are uncorrelated. Thus, they are independent in the normal distribution case [25]. Consequently, it is straightforward to conclude that $\|\bar{\boldsymbol{y}}\|^2$ and $\|\tilde{\boldsymbol{y}}\|^2$ are also independent [16].

[1] H. Krim and M. Viberg, "Two decades of array signal processing research: the parametric approach," *IEEE Signal Processing Mag.*, vol. 13, no. 4, pp. 67–94, 1996.

[2] H. Cox, "Resolving power and sensitivity to mismatch of optimum array processors," *J. Acoust. Soc. Am*, vol. 54, no. 3, pp. 771–785, 1973.

[3] K. Sharman and T. Durrani, "Resolving power of signal subspace methods for fnite data lengths," in *Proc. of IEEE Int. Conf. Acoust., Speech, Signal Processing*, Florida, USA, 1995, pp. 1501–1504.

[4] H. B. Lee, "The Cramér-Rao bound on frequency estimates of signals closely spaced in frequency (unconditional case)," *IEEE Trans. Signal Processing*, vol. 42, no. 6, pp. 1569–1572, 1994.

[5] E. Dilaveroglu, "Nonmatrix Cramér-Rao bound expressions for high-resolution frequency estimators," *IEEE Trans. Signal Processing*, vol. 46, no. 2, pp. 463–474, Feb. 1998.

[6] H. B. Lee, "The Cramér-Rao bound on frequency estimates of signals closely spaced in frequency," *IEEE Trans. Signal Processing*, vol. 40, no. 6, pp. 1507–1517, 1992.

[7] S. T. Smith, "Statistical resolution limits and the complexified Cramér-Rao bound," *IEEE Trans. Signal Processing*, vol. 53, pp. 1597–1609, May 2005.

[8] M. N. El Korso, R. Boyer, A. Renaux, and S. Marcos, "Statistical resolution limit for multiple signals and parameters of interest," in *Proc. of IEEE Int. Conf. Acoust., Speech, Signal Processing*, Dallas, TX, 2010.

[9] M. Shahram and P. Milanfar, "Imaging below the diffraction limit: A statistical analysis," *IEEE Trans. Image Processing*, vol. 13, no. 5, pp. 677–689, May 2004.

[10] ——, "On the resolvability of sinusoids with nearby frequencies in the presence of noise," *IEEE Trans. Signal Processing*, vol. 53, no. 7, pp. 2579–2585, Jul. 2005.

[11] Z. Liu and A. Nehorai, "Statistical angular resolution limit for point sources," *IEEE Trans. Signal Processing*, vol. 55, no. 11, pp. 5521–5527, Nov. 2007.

[12] A. Amar and A. Weiss, "Fundamental limitations on the resolution of deterministic signals," *IEEE Trans. Signal Processing*, vol. 56, no. 11, pp. 5309–5318, Nov. 2008.

[13] A. J. den Dekker and A. van den Bos, "Resolution, a survey," *J. Opt. Soc. Amer.*, vol. 14, pp. 547–557, Jan. 1997.

[14] P. Stoica, V. Simonyte, and T. Soderstrom, "On the resolution performance of spectral analysis," *Elsevier Signal Processing*, vol. 44, pp. 153–161, Jan. 1995.

[15] S. M. Kay, *Fundamentals of Statistical Signal Processing : Detection Theory*. NJ: Prentice Hall, 1998, vol. 2.

[16] L. L. Scharf and B. Friedlander, "Matched subspace detectors," *IEEE Trans. Signal Processing*, vol. 42, no. 8, pp. 2146–2157, Aug. 1994.

[17] L. L. Scharf, *Statistical Signal Processing: Detection, Estimation, and Time Series Analysis*. Reading: Addison Wesley, 1991.

[18] R. T. Behrens and L. L. Scharf, "Signal processing applications of oblique projection operators," *IEEE Trans. Signal Processing*, vol. 42, no. 6, pp. 1413–1424, Jun. 1994.

[19] B. Ottersten, M. Viberg, P. Stoica, and A. Nehorai, "Exact and large sample maximum likelihood techniques for parameter estimation and detection in array processing," in *Radar Array Processing*, S. Haykin, J. Litva, and T. J. Shepherd, Eds. Berlin: Springer-Verlag, 1993, ch. 4, pp. 99–151.

[20] H. L. VanTrees, *Detection, Estimation and Modulation theory: Optimum Array Processing*. New York: Wiley, 2002, vol. 4.

[21] R. Behrens, "Subspace signal processing in structured noise," Ph.D. dissertation, University of Colorado, Boulder, US-CO, 1990.

[22] G. H. Golub and C. F. V. Loan, *Matrix Computations*. London: Johns Hopkins, 1989.

[23] P. Stoica and R. Moses, *Spectral Analysis of Signals*. NJ: Prentice Hall, 2005.

[24] R. Boyer, "Oblique projection for source estimation in a competitive environment: Algorithm and statistical analysis," *Elsevier Signal Processing*, vol. 89, pp. 2547–2554, Dec. 2009.

[25] S. M. Kay, *Fundamentals of Statistical Signal Processing : Estimation Theory*. NJ: Prentice Hall, 1993, vol. 1.

[26] M. Shahram, "Statistical and information-theoretic analysis of resolution in imaging and array processing," Ph.D. dissertation, University of California, Santa Cruz, 2005.

[27] Y. Abramovich, B. Johnson, and N. Spencer, "Statistical non-identifiability of close emitters: Maximum-likelihood estimation breakdown," in *EUSIPCO*, Glasgow, Scotland, Aug. 2009.

[28] H. L. VanTrees, *Detection, Estimation and Modulation Theory*. New York: Wiley, 1968, vol. 1.

[29] Y. Meurisse and J. Delmas, "Bounds for sparse planar and volume arrays," *IEEE Trans. Signal Processing*, vol. 47, pp. 464–468, Jan. 2001.

[30] Y. I. Abramovich, N. K. Spencer, and A. Y. Gorokhov, "Positive-definite toeplitz completion in DOA estimation for nonuniform linear antenna arrays. II: Partially augmentable arrays," *IEEE Trans. Signal Processing*, vol. 47, no. 6, pp. 1502–1521, Jun. 1999.

	SOI	SI	Noise variance	The distribution used to compute λ	SINR for $M \geq 2$	SNR for $M = 2$
Case 1	known	known	known	χ_1^2	$\frac{\|\boldsymbol{s}_1\|^2+\|\boldsymbol{s}_2\|^2}{\|\boldsymbol{s}\|^2+\frac{2}{\lambda_1}\delta_1^2\|\boldsymbol{w}\|^2}$	$\lambda_1 \frac{\|\boldsymbol{s}_1\|^2+\|\boldsymbol{s}_2\|^2}{2\delta_1^2\|\boldsymbol{w}\|^2}$
Case 2	known	unknown	known	χ_1^2	$\frac{\|\boldsymbol{s}_1\|^2+\|\boldsymbol{s}_2\|^2}{\|\boldsymbol{s}\|^2+\frac{2}{\lambda_2}\delta_2^2\|\|\boldsymbol{P}_{\boldsymbol{C}}^{\perp}\boldsymbol{w}\|\|^2}$	$\lambda_2 \frac{\|\boldsymbol{s}_1\|^2+\|\boldsymbol{s}_2\|^2}{2\delta_2^2\|\boldsymbol{w}\|^2}$
Case 3	unknown	unknown	known	χ_{2L}^2	$\frac{\|\boldsymbol{s}_1\|^2+\|\boldsymbol{s}_2\|^2}{\|\boldsymbol{s}\|^2+\frac{2}{\lambda_3}\delta_3^2\|\|\boldsymbol{P}_{\boldsymbol{D}}^{\perp}\boldsymbol{w}\|\|^2}$	$\lambda_3 \frac{\|\boldsymbol{s}_1\|^2+\|\boldsymbol{s}_2\|^2}{2\delta_3^2\|\|\boldsymbol{P}_{\boldsymbol{A}}^{\perp}\boldsymbol{w}\|\|^2}$
Case 4	unknown	unknown	unknown	$F_{2L,2(N-M)L}$	$\frac{\|\boldsymbol{s}_1\|^2+\|\boldsymbol{s}_2\|^2}{\|\boldsymbol{s}\|^2+\frac{2}{\lambda_4}\delta_4^2\|\|\boldsymbol{P}_{\boldsymbol{D}}^{\perp}\boldsymbol{w}\|\|^2}$	$\lambda_4 \frac{\|\boldsymbol{s}_1\|^2+\|\boldsymbol{s}_2\|^2}{2\delta_4^2\|\|\boldsymbol{P}_{\boldsymbol{A}}^{\perp}\boldsymbol{w}\|\|^2}$

Table 1: Summary of results with $\boldsymbol{w} = \boldsymbol{B}\boldsymbol{s}_{-}$ and $\boldsymbol{D} = [\boldsymbol{A}\ \boldsymbol{C}]$.

Array type	Sensor positions	N	Aperture	Redundant lags	Missing gaps
Minimum redundancy $A_{5,8}$	$[0,1,2,5,8]$	5	$8d$	$R = \{1,3\}$	$G = \{\}$
Minimum redundancy $A_{6,8}$	$[0,1,2,3,6,8]$	6	$8d$	$R = \{1,2,3,5,6\}$	$G = \{\}$
Minimum redundancy $A_{7,8}$	$[0,1,2,4,5,6,8]$	7	$8d$	$R = \{1,2,3,4,5,6\}$	$G = \{\}$
ULA $A_{9,8}$	$[0,1,2,3,4,5,6,7,8]$	9	$8d$	$R = \{1,2,3,4,5,6,7\}$	$G = \{\}$

Table 2: Characteristic of different array geometries with different number of sensors and with the same array aperture.

Array type	Sensor positions	N	Aperture	Redundant lags	Missing gaps
Perfect array $A_{4,6}$	$[0,1,4,6]$	4	$6d$	$R = \{\}$	$G = \{\}$
$A'_{4,6}$	$[0,1,2,6]$	4	$6d$	$R = \{1\}$	$G = \{3\}$
Minimum redundancy $A_{4,5}$	$[0,1,2,5]$	4	$5d$	$R = \{1\}$	$G = \{\}$

Table 3: Characteristic of different array geometries with the same number of sensors and different array aperture. The so-called perfect array contains no redundancy lag and no gap.

Annexe C

Articles sur le seuil de résolution limite pour des signaux multidimensionnels

C.1 IEEE-ICASSP-2010

M. N. El Korso, R. Boyer, A. Renaux and S. Marcos, "Statistical resolution limits for multiple parameters of interest and for multiple signals", in Proc. of *IEEE International Conference on Acoustics, Speech, and Signal Processing, ICASSP-10,* Dallas, TX, USA.

STATISTICAL RESOLUTION LIMIT FOR MULTIPLE PARAMETERS OF INTEREST AND FOR MULTIPLE SIGNALS

Mohammed Nabil El Korso, Remy Boyer, Alexandre Renaux and Sylvie Marcos

Laboratoire des Signaux et Systémes (L2S)
Université Paris-Sud XI (UPS), CNRS, SUPELEC,
Gif-Sur-Yvette, France
{elkorso, remy.boyer, alexandre.renaux, marcos}@lss.supelec.fr

ABSTRACT

The concept of Statistical Resolution Limit (SRL), which is defined as the minimal separation to resolve two closely spaced signals, is an important tool to quantify performance in parametric estimation problems. This paper generalizes the SRL based on the Cramér-Rao bound to multiple parameters of interest per signal and for multiple signals. We first provide a fresh look at the SRL in the sense of Smith's criterion by using a proper change of variable formula. Second, based on the Minkowski distances, we extend this criterion to the important case of multiple parameters of interest per signal and to multiple signals. The results presented herein can be applied to any estimation problem and are not limited to source localization problems.

Index Terms— Statistical resolution limit, performance analysis, Cramér-Rao bound.

1. INTRODUCTION

Characterizing the ability of resolving closely spaced signals is an important step to quantify estimators performance. The concept of Statistical Resolution Limit (SRL), i.e., the minimum distance between two closely spaced signals that allows a correct resolvability, is rising in several applications (especially in parameter estimation problems such as radar, sonar, spectral estimation [1] etc.) There essentially exist two approaches to obtain a SRL: (1) the first is based on the estimation accuracy [2, 3] while (2) the second is based on the detection theory [4]. In this paper we consider the SRL based on the estimation accuracy. The Cramér-Rao Bound (CRB) does not directly point out the best resolution that can be achieved by an unbiased estimator. However, since it expresses a lower bound on the covariance matrix of any unbiased estimator, it can be used to obtain the SRL. We distinguish two main criteria on the SRL based on the CRB. The first one was introduced by Lee in [2]: *two signals* (for example parameterized by the Direction Of Arrivals (DOA) θ_1 and θ_2) *are said to be resolvable w.r.t. the DOA if the maximum standard deviation is less than twice the difference between* θ_1 *and* θ_2. Assuming that the CRB is a tight bound (under mild conditions), the standard deviation, σ_{θ_1} and σ_{θ_2}, of an unbiased estimator can be approximated by $\sqrt{\text{CRB}(\theta_1)}$ and $\sqrt{\text{CRB}(\theta_2)}$, respectively. Consequently, the SRL δ_θ is defined, in Lee's criterion sense, as $2\max\left\{\sqrt{\text{CRB}(\theta_1)}, \sqrt{\text{CRB}(\theta_2)}\right\}$. Lee [2] and Dilaveroglu [5] used this criterion to obtain the SRL of frequency estimates. Swingler [6] used the same criterion for close frequencies in the case of complex spaced sinusoids. However, the main problem of this criterion is that the coupling between parameters is ignored. To overcome this problem, Smith [3] proposed the following criterion: *two signals are resolvable w.r.t. the DOA if the difference between the DOA is greater than the standard deviation of the DOA difference estimation according to the CRB*. Consequently, the SRL, in Smith's criterion sense, is defined as δ_θ for which $\delta_\theta < \sqrt{\text{CRB}\left(\delta_\theta\right)}$ is achieved. This means that, the SRL is obtained by resolving the implicit equation $\delta_\theta^2 = \text{CRB}\left(\delta_\theta\right)$. In [7], an example of study of the SRL for DOA of discrete signals based on Smith's criterion has been considered.
In several estimation problems, the signals are parameterized by more than one parameter of interest per signal, for example in the context of, near-field source localization [8] (bearing, elevation and range), polarized source [9] (DOA and the polarization state parameters) and more generally in communication applications [10]. However, Lee and Smith's criteria were introduced only when the signal is parameterized by only one parameter (for example frequency, DOA etc.) To the best of our knowledge, no results are avalaible on the extension of the SRL to multiple parameters of interest per signal. Thus, the aim of this paper is to fill this lack. We first begin by giving a fresh look at Smith's criterion using a proper change of variable formula. Then we show that the extension to the multiple parameters per signal case is not straighforward. Finally, we propose an extension to the case of multiple parameters of interest and multiple signals using the k-norm distance. One should note that, the SRL presented herein can be applied to any estimation problem and is not limited to the source localization problem.

2. PROBLEM SETUP AND BACKGROUND

The observation model for M signals following the waveform described by the functional $\boldsymbol{f}(.)$ is given by

$$\mathbf{x} = \sum_{m=1}^{M} \boldsymbol{f}(\boldsymbol{\xi}_m) + \mathbf{n}, \tag{1}$$

where $\mathbf{n}$ denotes the additive noise. The parameters are collected in $\bar{\boldsymbol{\xi}} = [\boldsymbol{\xi}_1^T \dots \boldsymbol{\xi}_M^T]^T$, with a proper rearrangement of $\bar{\boldsymbol{\xi}}$ one can obtain $\boldsymbol{\xi} = [\boldsymbol{\omega}^T \ \boldsymbol{\rho}^T]^T$ where $\boldsymbol{\omega}$ is the $(MP) \times 1$ vector of the parameters of interest and $\boldsymbol{\rho}$ denotes the vector obtained by concatenation of the unwanted and nuisance parameters. This means that we consider P parameters of interest for each signal. To the best of our knowledge, the state of art [3] tackles this problem only in the case of $M = 2$ and $P = 1$. The problem addressed herein is to derive the Statistical Resolution Limit (SRL) based on the Cramér-Rao Bound (CRB) in

This project is funded by both the Région Île-de-France and the Digiteo Research Park.

the case of $P \geq 1$ and $M \geq 2$.
First, let us consider the SRL for two impinging signals w.r.t. one parameter of interest per signal. Consequently, the vector of the parameters of interest is given by $\boldsymbol{\omega} = [\omega_1\ \omega_2]^T$, where we assume that $\omega_1 \neq \omega_2$. Under mild conditions, $E\left\{\left(\left[\hat{\boldsymbol{\xi}}\right]_i - [\boldsymbol{\xi}]_i\right)^2\right\} \geq [\mathbf{CRB}(\boldsymbol{\xi})]_{i,i}$ where $\hat{\boldsymbol{\xi}}$ denotes an unbiased estimator of $\boldsymbol{\xi}$ and $\mathbf{CRB}(\boldsymbol{\xi}) = \mathbf{FIM}^{-1}(\boldsymbol{\xi})$, in which $\mathbf{FIM}(\boldsymbol{\xi})$ denotes the Fisher Information Matrix for model (1) regarding to $\boldsymbol{\xi}$ [11]. In the following, for sake of simplicity, the notation $\mathbf{CRB}([\boldsymbol{\xi}]_{1:i})$ will be used instead of the *Matlab* notation $[\mathbf{CRB}(\boldsymbol{\xi})]_{1:i,1:i}$.
Having $\mathbf{CRB}(\boldsymbol{\xi})$, one can deduce $\mathbf{CRB}(\breve{\boldsymbol{\xi}})$, where $\breve{\boldsymbol{\xi}} = \mathbf{g}(\boldsymbol{\xi}) = [\delta\ \boldsymbol{\rho}^T]^T$, by using the change of variable formula (see [12] p. 45)

$$\mathbf{CRB}(\breve{\boldsymbol{\xi}}) = \mathbf{J}\ \mathbf{CRB}(\boldsymbol{\xi})\ \mathbf{J}^T, \tag{2}$$

where the separation is given by $\delta = |\omega_1 - \omega_2|$ and where the Jacobian matrix is given by $[\mathbf{J}]_{i,j} = \frac{\partial[\mathbf{g}(\boldsymbol{\xi})]_i}{\partial[\boldsymbol{\xi}]_j}$. Consequently, $\mathbf{J} = \begin{bmatrix}\mathbf{h}^T & \mathbf{0}\\ \mathbf{0} & \mathbf{I}\end{bmatrix}$ where $\mathbf{h} = \mathrm{sgn}(\omega_1 - \omega_2)[1\ \ -1]^T$ and $\mathrm{sgn}(\omega_1 - \omega_2) = \frac{\omega_1 - \omega_2}{|\omega_1 - \omega_2|}$. Using the Jacobian matrix above and (2), one obtains

$$\mathbf{CRB}(\breve{\boldsymbol{\xi}}) = \begin{bmatrix}\mathbf{h}^T & \mathbf{0}\\ \mathbf{0} & \mathbf{I}\end{bmatrix}\begin{bmatrix}\mathrm{CRB}(\omega_1) & \mathrm{CRB}(\omega_1,\omega_2) & \times\\ \mathrm{CRB}(\omega_2,\omega_1) & \mathrm{CRB}(\omega_2) & \times\\ \times & \times & \times\end{bmatrix}\begin{bmatrix}\mathbf{h} & \mathbf{0}\\ \mathbf{0} & \mathbf{I}\end{bmatrix},$$

where $\mathrm{CRB}(\omega_i)$ and $\mathrm{CRB}(\omega_1,\omega_2) \triangleq \left[\mathbf{CRB}(\breve{\boldsymbol{\xi}})\right]_{1,2}$ denote the CRB on ω_i and the cross terms between ω_1 and ω_2, respectively. Consequently,

$$\begin{aligned}\mathrm{CRB}(\delta) &\triangleq \mathbf{CRB}\left(\left[\breve{\boldsymbol{\xi}}\right]_1\right) = \mathrm{sgn}^2(\omega_1-\omega_2)\mathrm{CRB}(\omega_1)+\\ &(-\mathrm{sgn}(\omega_1-\omega_2))^2\mathrm{CRB}(\omega_2) - 2\mathrm{sgn}^2(\omega_1-\omega_2)\mathrm{CRB}(\omega_1,\omega_2)\\ &= \mathrm{CRB}(\omega_1) + \mathrm{CRB}(\omega_2) - 2\mathrm{CRB}(\omega_1,\omega_2).\end{aligned} \tag{3}$$

From (3) we notice that the SRL using Smith's criterion [3] takes into account the coupling between the parameters of interest. Consequently, using Smith's criterion, the SRL can be re-written as δ which resolves the following equation

$$\delta^2 = \mathrm{CRB}(\omega_1) + \mathrm{CRB}(\omega_2) - 2\mathrm{CRB}(\omega_1,\omega_2). \tag{4}$$

Finally, note that, as in [7], for the case where the parameters of interest are decoupled, one obtains the SRL by resolving the following equation $\delta^2 = \mathrm{CRB}(\omega_1) + \mathrm{CRB}(\omega_2)$.
One should note that, unlike Smith's criterion, Lee's criterion[1] [2] does not take into account the coupling between the parameters that becomes important when the signal parameters are close. In the following section, we will extend the previous SRL to multiple parameters of interest per signal in the case of two emitting signals.

3. STATISTICAL RESOLUTION LIMIT FOR MULTIPLE PARAMETERS OF INTEREST PER SIGNAL

Before introducing a scheme to derive the SRL for multiple parameters of interest per signal, we begin by showing that generalizing Smith's approach to derive the SRL for multiple parameters is not straightforward. For that purpose, let us consider the simple case of $M = 2$ parameters, denoted $\omega_i^{(1)}$ and $\omega_i^{(2)}$, of interest for the i^{th} signal. Let $\tilde{\boldsymbol{\delta}} = [\delta_1\ \delta_2]^T$ where $\delta_1 = |\omega_1^{(1)} - \omega_2^{(1)}|$ and $\delta_2 = |\omega_1^{(2)} - \omega_2^{(2)}|$ denote the separation w.r.t. $\omega^{(1)}$ and $\omega^{(2)}$, respectively. Consequently

$$\tilde{\boldsymbol{\delta}} = \boldsymbol{H}\boldsymbol{\omega} \ \text{ with } \ \boldsymbol{H} = \begin{bmatrix}a_1 & 0 & -a_1 & 0\\ 0 & a_2 & 0 & -a_2\end{bmatrix},$$

where $a_p = \mathrm{sgn}(\omega_1^{(p)} - \omega_2^{(p)})$ and $\boldsymbol{\omega} = [\omega_1^{(1)}\ \omega_1^{(2)}\ \omega_2^{(1)}\ \omega_2^{(2)}]^T$. From $\mathbf{CRB}(\boldsymbol{\xi})$, one can deduce $\mathbf{CRB}(\breve{\boldsymbol{\xi}})$ by using the change of variable formula (2), where $\boldsymbol{\xi} = [\boldsymbol{\omega}^T\ \boldsymbol{\rho}^T]^T$ and $\breve{\boldsymbol{\xi}} = [\tilde{\boldsymbol{\delta}}^T\ \boldsymbol{\rho}^T]^T$. The Jacobian matrix is then given by $\mathbf{J} = \begin{bmatrix}\boldsymbol{H} & \mathbf{0}\\ \mathbf{0} & \mathbf{I}\end{bmatrix}$. Consequently,

$$\mathbf{CRB}(\breve{\boldsymbol{\xi}}) = \begin{bmatrix}\boldsymbol{H} & \mathbf{0}\\ \mathbf{0} & \mathbf{I}\end{bmatrix}\begin{bmatrix}\mathbf{CRB}(\boldsymbol{\omega}) & \times\\ \times & \times\end{bmatrix}\begin{bmatrix}\boldsymbol{H}^T & \mathbf{0}\\ \mathbf{0} & \mathbf{I}\end{bmatrix}.$$

Using the same method as in (4), one obtains

$$\begin{aligned}\mathrm{CRB}(\delta_1) \triangleq \mathbf{CRB}\left(\left[\breve{\boldsymbol{\xi}}\right]_1\right) =& \mathrm{CRB}(\omega_1^{(1)}) + \mathrm{CRB}(\omega_2^{(1)})\\ &- 2\mathrm{CRB}(\omega_1^{(1)},\omega_2^{(1)}),\end{aligned} \tag{5}$$

and

$$\begin{aligned}\mathrm{CRB}(\delta_2) \triangleq \mathbf{CRB}\left(\left[\breve{\boldsymbol{\xi}}\right]_2\right) =& \mathrm{CRB}(\omega_1^{(2)}) + \mathrm{CRB}(\omega_2^{(2)})\\ &- 2\mathrm{CRB}(\omega_1^{(2)},\omega_2^{(2)}).\end{aligned} \tag{6}$$

From (5) and (6), we notice that the CRB on the separation w.r.t. $\omega^{(1)}$ is viewed independently from the separation w.r.t. $\omega^{(2)}$ and *vice-versa*. Consequently, deducing the SRL in the case of multiple parameters of interest per signal using (5) and (6) can be meaningless. As an example, Fig. 1a shows that, thanks to the second parameter of interest, even if $\omega_1^{(1)}$ is very close to $\omega_2^{(1)}$, the signals can still be well resolvable. However, Fig. 1b shows that even if $\omega_1^{(1)}$ is not too close to $\omega_2^{(1)}$ as in Fig. 1a, the signals might not be resolvable.

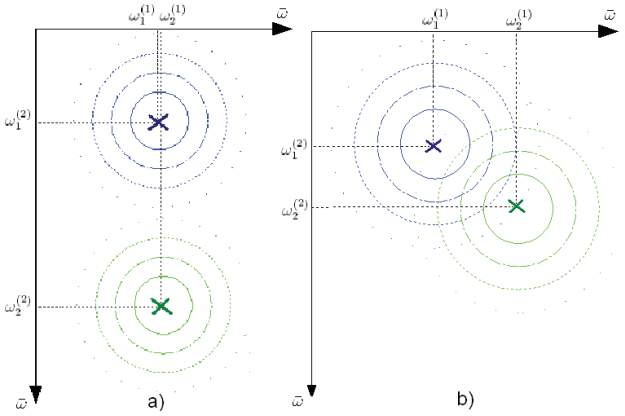

Fig. 1. Localization of two point signals thanks to two parameters of interest where $\bar{\omega}$ denotes the unit of measurement.

[1]Recall that the SRL based on Lee's criterion [2] is defined as δ such that $\delta = 2\max\left\{\sqrt{\mathrm{CRB}(\omega_1)}, \sqrt{\mathrm{CRB}(\omega_2)}\right\}$.

3.1. Proposed solution

Let us assume that we have P parameters of interest per signal denoted by $C = \left\{\omega^{(1)}, \omega^{(2)}, \ldots, \omega^{(P)}\right\}$. The question herein addressed is *how can we define the SRL such that all the P parameters of interest are taken into account?* A natural idea is to consider the distance between the set of the P parameters of interest of the first signal, $C_1 = \left\{\omega_1^{(1)}, \omega_1^{(2)}, \ldots, \omega_1^{(P)}\right\}$ and the set of the P parameters of interest of the second signal, $C_2 = \left\{\omega_2^{(1)}, \omega_2^{(2)}, \ldots, \omega_2^{(P)}\right\}$. Let

$$\delta \triangleq k\text{-norm distance}(C_1, C_2) = \left(\sum_{p=1}^{P} \delta_p^k\right)^{1/k}, \quad (7)$$

define the SRL w.r.t. the sets C_1 and C_2 (such that $C_1 \neq C_2$) where $\delta_p = \left|\omega_1^{(p)} - \omega_2^{(p)}\right|$. The k-norm distance(C_1, C_2) is the so-called Minkowski distance of order k. Having $\mathbf{CRB}(\boldsymbol{\xi})$ where $\boldsymbol{\xi} = [\boldsymbol{\omega}^T \ \boldsymbol{\rho}^T]^T$ in which

$$\boldsymbol{\omega} = [\omega_1^{(1)} \ \omega_2^{(1)} \ \omega_1^{(2)} \ \omega_2^{(2)} \ \ldots \ \omega_1^{(P)} \ \omega_2^{(P)}]^T,$$

one can deduce $\mathbf{CRB}(\tilde{\boldsymbol{\xi}})$ where $\tilde{\boldsymbol{\xi}} = [\delta \ \boldsymbol{\rho}^T]^T$. Consequently, the Jacobian matrix is given by $\mathbf{J} = \begin{bmatrix} \mathbf{h}^T & \mathbf{0} \\ \mathbf{0} & \mathbf{I} \end{bmatrix}$ where

$$\mathbf{h} = \begin{bmatrix} g_1 & -g_1 & g_2 & -g_2 & \ldots & g_P & -g_P \end{bmatrix}^T,$$

in which $g_p = \frac{\partial \delta}{\partial \omega_1^{(p)}} = -\frac{\partial \delta}{\partial \omega_2^{(p)}}$. Since $|x|^k = \sqrt{x^{2k}}$ for $x \neq 0$, one has

$$\begin{aligned} g_p &= \frac{\partial \left(\sum_{q=1}^{P} \sqrt{\left(\omega_1^{(q)} - \omega_2^{(q)}\right)^{2k}}\right)^{1/k}}{\partial \omega_1^{(p)}} \\ &= \left(\sum_{q=1}^{P} \sqrt{\left(\omega_1^{(q)} - \omega_2^{(q)}\right)^{2k}}\right)^{\frac{1}{k}-1} \sqrt{\left(\omega_1^{(p)} - \omega_2^{(p)}\right)^{2(k-1)}} \\ &= \delta^{1-k} \delta_p^{k-1}. \end{aligned} \quad (8)$$

Again, by using the change of variable formula (2), one obtains

$$\mathbf{CRB}(\tilde{\boldsymbol{\xi}}) = \begin{bmatrix} \mathbf{h}^T \mathbf{CRB}(\boldsymbol{\omega}) \mathbf{h} & \times \\ \times & \mathbf{I} \end{bmatrix}.$$

Consequently, after some calculus, one obtains

$$\begin{aligned} \mathrm{CRB}(\delta) \triangleq \mathbf{CRB}\left(\left[\tilde{\boldsymbol{\xi}}\right]_1\right) &= \sum_{p=1}^{P}\sum_{q=1}^{P} g_p g_q \Big([\mathbf{CRB}(\boldsymbol{\xi})]_{2p,2q} + \\ [\mathbf{CRB}(\boldsymbol{\xi})]_{2p-1,2q-1} &- [\mathbf{CRB}(\boldsymbol{\xi})]_{2p,2q-1} - [\mathbf{CRB}(\boldsymbol{\xi})]_{2p-1,2q} \Big) \\ &= \delta^{2(1-k)} \left(A_{\mathrm{direct}} + A_{\mathrm{cross}}\right), \end{aligned} \quad (9)$$

where $A_{\mathrm{direct}} = \sum_{p=1}^{P} \delta_p^{2(k-1)} \Big(\mathrm{CRB}(\omega_1^{(p)}) + \mathrm{CRB}(\omega_2^{(p)}) - 2\mathrm{CRB}(\omega_1^{(p)}, \omega_2^{(p)})\Big)$ represents the contribution of the parameters of interest for the same parameter p and where $A_{\mathrm{cross}} = \sum_{p=1}^{P} \sum_{\substack{q=1 \\ q \neq p}}^{P} \delta_p^{k-1} \delta_q^{k-1} \Big(\mathrm{CRB}(\omega_1^{(p)}, \omega_1^{(q)}) + \mathrm{CRB}(\omega_2^{(p)}, \omega_2^{(q)}) - 2\mathrm{CRB}(\omega_1^{(p)}, \omega_2^{(q)})\Big)$ represents the contribution of the cross terms between parameters of interest.

Despite of the fact that the 2-norm is the most commonly used norm, it is often more interesting to use the 1-norm to solve[2] $\delta^2 = CRB(\delta)$. Indeed, by doing this, the separation remains linear w.r.t. the parameters. This implies that its first order derivative is parameter independent. In fact, and as expected, if $P = 1$ and considering the 1-norm distance, one notices that $g_1 = 1$ and consequently, using (9), one obtains, $\mathrm{CRB}(\delta) = [\mathbf{CRB}(\boldsymbol{\xi})]_{1,1} + [\mathbf{CRB}(\boldsymbol{\xi})]_{2,2} - 2[\mathbf{CRB}(\boldsymbol{\xi})]_{1,2}$ which is the same expression as (4).

Remark 1: Let us now consider the case where $P = 2$, and let us assume, for sake of simplicity, that the parameters $\omega_1^{(p)}$ and $\omega_2^{(q)}$ $\forall p, q$ are decoupled. Applying (9) one obtains,

$$\begin{aligned} \mathrm{CRB}(\delta) = \delta^{2(1-k)} \Big[&\delta_1^{2(k-1)} \Big(\mathrm{CRB}\left(\omega_1^{(1)}\right) + \mathrm{CRB}\left(\omega_2^{(1)}\right) \Big) \\ &+ \delta_2^{2(k-1)} \Big(\mathrm{CRB}\left(\omega_1^{(2)}\right) + \mathrm{CRB}\left(\omega_2^{(2)}\right) \Big) \\ &+ 2\delta_1^{k-1}\delta_2^{k-1} \Big(\mathrm{CRB}\left(\omega_1^{(1)}, \omega_1^{(2)}\right) + \mathrm{CRB}\left(\omega_2^{(1)}, \omega_2^{(2)}\right) \Big) \Big]. \end{aligned} \quad (10)$$

We notice that, unlike (5) and (6), equation (10) takes into account the effect of parameters of different nature thanks to the cross terms $\mathrm{CRB}\left(\omega_i^{(1)}, \omega_j^{(2)}\right)$.

Remark 2: In the case where we are interested by deriving the SRL w.r.t. multiple physical parameters of interest having *different* units of measurement, we cannot use directly formula (9). To illustrate how to derive the SRL in this case, we consider for instance the problem of the localisation of two near-field sources parameterized by two physical parameters, namely the bearing θ in radian and the range r in meter. Toward the derivation of the SRL, we have to

1. Derive the CRB w.r.t. to the physical parameters corresponding to $[\theta_1 \ \theta_2 \ r_1 \ r_2 \ \boldsymbol{\rho}^T]^T$.
2. Deduce the CRB w.r.t. to the non-physical parameters corresponding to $[\omega_1^{(1)} \ \omega_2^{(1)} \ \omega_1^{(2)} \ \omega_2^{(2)} \ \boldsymbol{\rho}^T]^T$ thanks to a proper change of variable. This change of variable is deduced from the definition of the electric angles $\omega_i^{(1)} = -2\pi d/\lambda \sin(\theta_i)$ and $\omega_i^{(2)} = \pi^2 (d^2/\lambda) \cos^2(\theta_i)/r_i$ where d is the distance inter-sensor and λ is the signal wavelength [13].
3. Choose k and deduce the $\mathrm{CRB}(\delta)$ where δ is defined in (7) using formula (9).
4. Finally, solve the implicit equation $\delta^2 = \mathrm{CRB}(\delta)$ which provides the SRL.

In the following, this result is extended to the case of $M \geq 2$ signals where each signal is parameterized by P parameters of interest per signal.

4. STATISTICAL RESOLUTION LIMIT FOR MULTIPLE SIGNALS

We begin by deriving the SRL for each couple of signals. Using the Newton's binomial theorem for M signals, the number of signal's couples is equal to $\frac{M(M-1)}{2}$. Then, the SRL will be the worst SRL, i.e., the maximum of all the minimal distances between each couple of two closely spaced signals that allows a correct resolvability.

[2] However, if $\exists p \in [1 \ldots P]$ such that $\omega_1^{(p)} = \omega_2^{(p)}$, then $\frac{\partial \delta}{\partial \omega_1^{(p)}}$ exists only if the k-norm distance is such that k is an even number.

From $\mathbf{CRB}(\boldsymbol{\xi})$, one can deduce $\mathbf{CRB}(\breve{\boldsymbol{\xi}})$ using the change of variable formula (2) where $\boldsymbol{\xi} = \begin{bmatrix}\boldsymbol{\omega}^T & \boldsymbol{\rho}^T\end{bmatrix}^T$ with

$$\boldsymbol{\omega} = \left[\left(\boldsymbol{\omega^{(1)}}\right)^T \quad \dots \quad \left(\boldsymbol{\omega^{(P)}}\right)^T\right]^T,$$

in which $\boldsymbol{\omega^{(p)}} = [\omega_1^{(p)}\ \omega_2^{(p)} \dots \omega_M^{(p)}]^T$ and $\breve{\boldsymbol{\xi}} = \mathbf{g}(\boldsymbol{\xi}) = [\boldsymbol{\delta}^T\ \boldsymbol{\rho}^T]^T$ such that $\boldsymbol{\delta} = [\delta_{12}\ \delta_{13} \dots \delta_{1M}\ \delta_{23} \dots \delta_{(M-1)M}]^T$ where $\delta_{ij} = \left(\sum_{p=1}^{P}\left(\delta_p^{(ij)}\right)^k\right)^{1/k}$ and $\delta_p^{(ij)} = \left|\omega_i^{(p)} - \omega_j^{(p)}\right|$. The separation δ_{ij} is the k-norm distance between the i^{th} and the j^{th} signal. Thus, the Jacobian matrix is given by $\mathbf{J} = \begin{bmatrix}\boldsymbol{H} & \mathbf{0}\\ \mathbf{0} & \mathbf{I}\end{bmatrix}$ in which $\boldsymbol{H}$ is a $\left(\frac{M(M-1)}{2}\right) \times (MP)$ matrix given by $\boldsymbol{H} = [\boldsymbol{\alpha}_{12}\ \boldsymbol{\alpha}_{13}\ \dots\ \boldsymbol{\alpha}_{(M-1)M}]^T$ where $\boldsymbol{\alpha}_{ij} = \begin{bmatrix}\boldsymbol{\eta}_{ij1}^T & \dots & \boldsymbol{\eta}_{ijP}^T\end{bmatrix}^T$ in which

$$\left[\boldsymbol{\eta}_{ijp}\right]_q = \begin{cases}\frac{\partial \delta_{ij}}{\partial \omega_i^{(p)}} & \text{for } q = i\\ -\frac{\partial \delta_{ij}}{\partial \omega_i^{(p)}} & \text{for } q = j\\ 0 & \text{otherwise}\end{cases}$$

where $\frac{\partial \delta_{ij}}{\partial \omega_i^{(p)}} = \delta_{ij}^{1-k}\left(\delta_p^{(ij)}\right)^{k-1}$.

We have $\mathbf{CRB}(\breve{\boldsymbol{\xi}}) = \begin{bmatrix}\boldsymbol{H}\mathbf{CRB}(\boldsymbol{\omega})\boldsymbol{H}^T & \times\\ \times & \mathbf{I}\end{bmatrix}$. Finally, taking into account only the main diagonal terms, one obtains

$$\begin{aligned}\mathrm{CRB}(\delta_{ij}) &= \sum_{p=1}^{MP}\sum_{q=1}^{MP}\left[\boldsymbol{\alpha}_{ij}\right]_p\left[\boldsymbol{\alpha}_{ij}\right]_q\left[\mathbf{CRB}(\boldsymbol{\xi})\right]_{p,q}\\ &= \sum_{p=1}^{P}\sum_{q=1}^{P}\frac{\partial \delta_{ij}}{\partial \omega_i^{(p)}}\frac{\partial \delta_{ij}}{\partial \omega_i^{(q)}}\Big(\left[\mathbf{CRB}(\boldsymbol{\xi})\right]_{i+M(p-1),i+M(q-1)} +\\ &\left[\mathbf{CRB}(\boldsymbol{\xi})\right]_{j+M(p-1),j+M(q-1)} - \left[\mathbf{CRB}(\boldsymbol{\xi})\right]_{i+M(p-1),j+M(q-1)}\\ &- \left[\mathbf{CRB}(\boldsymbol{\xi})\right]_{j+M(p-1),i+M(q-1)}\Big)\\ &= \delta_{ij}^{2(1-k)}\left(A_{\mathrm{direct}}^{(ij)} + A_{\mathrm{cross}}^{(ij)}\right), \end{aligned} \tag{11}$$

where $A_{\mathrm{direct}}^{(ij)} = \sum_{p=1}^{P}\left(\delta_p^{(ij)}\right)^{2(k-1)}\Big(\mathrm{CRB}(\omega_i^{(p)}) + \mathrm{CRB}(\omega_j^{(p)}) - 2\mathrm{CRB}(\omega_i^{(p)}, \omega_j^{(p)})\Big)$ represents the contribution of the parameters of interest for the same p and for the i^{th} and j^{th} signals and

$$A_{\mathrm{cross}}^{(ij)} = \sum_{p=1}^{P}\sum_{\substack{q=1\\ q\neq p}}^{P}\left(\delta_p^{(ij)}\right)^{k-1}\left(\delta_q^{(ij)}\right)^{k-1} \times$$

$$\Big(\mathrm{CRB}(\omega_i^{(p)}, \omega_i^{(q)}) + \mathrm{CRB}(\omega_j^{(p)}, \omega_j^{(q)}) - 2\mathrm{CRB}(\omega_i^{(p)}, \omega_j^{(q)})\Big),$$

represents the contribution of the cross terms between parameters of interest for the i^{th} and j^{th} signals. Using (11) one can deduce the SRL as the maximum SRL for each couple of signals, i.e.,

$$\delta = \max\left\{\delta_{ij} \quad \text{for } i < j \quad \text{and } i, j \leq M\right\}.$$

One should note that even if we derive the SRL for each couple of signals, we are also taking into account the influence of the other signals thanks to the use of the CRB regarding to the full vector of parameters $\boldsymbol{\xi}$. As an example, for $M = 2$, applying (11) one obtains (9). And for $M = 2$, $P = 1$ and $k = 1$ one obtains the equivalent Smith's equation written in (4).

5. CONCLUSION

In this paper, we extended the Statistical Resolution Limit to multiple parameters of interest per signal and multiple signals. Toward this end, we give a fresh look at Smith's criterion and defined an *extended* SRL thanks to the Minkowski distances of order k. By using proper changes of variable formula, we obtain general results on the SRL for multiple parameters of interest per signal and multiple signals. The results presented herein can be applied to any estimation problem and are not limited to the source localization problems.

6. REFERENCES

[1] H. L. VanTrees, *Detection, Estimation and Modulation Theory*. New York: Wiley, 1968, vol. 1.

[2] H. B. Lee, "The Cramér-Rao bound on frequency estimates of signals closely spaced in frequency," *IEEE Trans. Signal Processing*, vol. 40, no. 6, pp. 1507–1517, 1992.

[3] S. T. Smith, "Statistical resolution limits and the complexified Cramér Rao bound," *IEEE Trans. Signal Processing*, vol. 53, pp. 1597–1609, May 2005.

[4] A. Amar and A. Weiss, "Fundamental limitations on the resolution of deterministic signals," *IEEE Trans. Signal Processing*, vol. 56, no. 11, pp. 5309–5318, Nov. 2008.

[5] E. Dilaveroglu, "Nonmatrix Cramér-Rao bound expressions for high-resolution frequency estimators," *IEEE Trans. Signal Processing*, vol. 46, no. 2, pp. 463–474, Feb. 1998.

[6] D. Swingler, "Frequency estimation for closely spaced sinsoids: Simple approximations to the Cramér-Rao lower bound," *IEEE Trans. Signal Processing*, vol. 41, no. 1, pp. 489–495, Jan. 1993.

[7] J.-P. Delmas and H. Abeida, "Statistical resolution limits of DOA for discrete sources," in *Proc. IEEE Int. Conf. Acoust., Speech, Signal Processing*, vol. 4, Toulouse, France, 2006, pp. 889–892.

[8] E. Grosicki, K. Abed-Meraim, and Y. Hua, "A weighted linear prediction method for near-field source localization," *IEEE Trans. Signal Processing*, vol. 53, pp. 3651–3660, 2005.

[9] J. Li, P. Stoica, and D. Zheng, "Efficient direction and polarization estimation with a cold array," *IEEE Trans. Antennas Propagat.*, vol. 44, no. 4, pp. 539–547, Apr. 1996.

[10] L. Godara, "Applications of antenna arrays to mobile communications: II. beam-forming and direction of arrival considerations," *IEEE Trans. Antennas Propagat.*, vol. 85, no. 8, pp. 1195–1245, Aug. 1997.

[11] H. Cramér, *Mathematical Methods of Statistics*. New York: Princeton University, Press, 1946.

[12] S. M. Kay, *Fundamentals of Statistical Signal Processing*. NJ: Prentice Hall, 1993, vol. 1.

[13] M. N. El Korso, R. Boyer, A. Renaux, and S. Marcos, "Non-matrix closed-form expressions of the Cramér-Rao bounds for near-field localization parameters," in *Proc. IEEE Int. Conf. Acoust., Speech, Signal Processing*, Taipei, Taiwan, 2009, pp. 3277–3280.

C.2 IEEE-SSP-2011

M. N. El Korso, R. Boyer, A. Renaux and S. Marcos, "A GLRT-based frameword for the multidimensional statistical resolution limit", in Proc. of *IEEE Workshop on Statistical Signal Processing SSP-10,* Nice, France.

A GLRT-BASED FRAMEWORK FOR THE MULTIDIMENSIONAL STATISTICAL RESOLUTION LIMIT

Mohammed Nabil El Korso, Rémy Boyer, Alexandre Renaux and Sylvie Marcos

Laboratoire des Signaux et Systèmes (L2S)
Université Paris-Sud XI, CNRS, SUPELEC
Gif-Sur-Yvette, France

ABSTRACT

Recently, a criterion for Multidimensional Statistical Resolution Limit (MSRL) evaluation, which is defined as the minimal separation to resolve two closely spaced signals depending on several parameters, was empirically proposed in [1] but without a statistical analysis. In this paper, we fill this lack by demonstrating that this MSRL criterion is asymptotically equivalent (upon to a translator factor) to a UMP (Uniformly Most Powerful) test among all invariant statistical tests. This result is an extension of a previous work on mono-dimensional SRL (*i.e.,* when the signals only depend on one parameter). As an illustrative example, the 3-D harmonic retrieval case for wireless channel sounding is treated to show the good agreement of the proposed result.

INDEX TERMS[1]

Multidimensional statistical resolution limit, Cramér-Rao bound, uniformly most powerful test, performance analysis.

1. INTRODUCTION

Characterizing the ability of resolving closely spaced signals is an important step to quantify performance in array signal processing. The concept of Statistical Resolution Limit (SRL), *i.e.,* the minimum distance between two closely spaced signals that allows a correct resolvability, is rising in several applications (especially in parameter estimation problems such as radar, sonar, spectral estimation [2], etc.)

It is important to note that, in several estimation problems, the signals are parameterized by more than one parameters of interest per signal, for example, in the context of, near-field source localization (bearing, elevation and range), polarized source localization (DOA and the polarization state parameters) and more generally in communication applications. However, the SRL has only been defined/derived in the mono-dimensional case [3–7] (*i.e.,* for only one parameter of interest per signal.) This is way we recently have proposed an intuitive extension of the SRL for the multidimensional case [1], called the Multidimensional Statistical Resolution Limit (MSRL). This criterion is based on the extension of the so-called Smith criterion [5] (*i.e.,* based on a Cramér-Rao Bound (CRB) approach) using the k-norm distance.

Nevertheless, no analysis on the MSRL (which was proposed in [1]) was done to check its behavior. Thus, the aim of this paper is to fill this lack. First, we link the concept of the MSRL to a binary hypothesis test which is a slight extension of [4].Second, we prove that the MSRL criterion [1] is asymptotically equivalent to a Uniformly Most Powerful (UMP) test among all invariant statistical tests (which is, in the asymptotic case, considered as the strongest statement of optimality that one could expect to obtain [8]). Note that, while the aforementioned equivalence is derived in the context of 1-norm distance, the same conclusion can be extended for the MSRL based on other k-norm distances ($k \geq 2$ with k integer). Finally, we illustrate our result in the case of a 3-D harmonic retrieval model for wireless channel sounding.

[1]This project is funded by region Île de France and Digiteo Research Park.

2. PROBLEM SETUP AND BACKGROUND

Let $\left\{\Omega, \mathcal{F}, \mathbf{y}, \mathcal{Y}, \mathcal{A}, \mathcal{P}_{\boldsymbol{\xi}}, \boldsymbol{\xi} \subseteq \mathbb{R}^{2P+Q}\right\}$ be the statistical experiment generated by a random vector $\mathbf{y}$ taking values on the measurable space $\{\mathcal{Y}, \mathcal{A}\}$. An observation $\mathbf{y}(\omega)$ is the realization of the random vector $\mathbf{y}$ where ω takes its value on the measurable space $\{\Omega, \mathcal{F}\}$. The distribution of $\mathbf{y}$ is assumed to belong to a family of probability measures $\mathcal{P}_{\boldsymbol{\xi}}$ on $\mathcal{Y}$ and parameterized by the vector $\boldsymbol{\xi} \subseteq \mathbb{R}^{2P+Q}$. It is also assumed that $\mathcal{P}_{\boldsymbol{\xi}}$ is absolutely continuous w.r.t. a σ-finite positive measure μ on $\mathcal{Y}$, such that the Radon-Nikodym derivative (*i.e.,* the likelihood function) $p(\mathbf{y}|\boldsymbol{\xi}) \triangleq d\mathcal{P}_{\boldsymbol{\xi}}(\mathbf{y}) / d\mu(\mathbf{y}), \forall \boldsymbol{\xi} \subseteq \mathbb{R}^{2P+Q}$ exists. More precisely, the observation model is assumed to be structured as follows

$$\mathbf{y} = \boldsymbol{f}(\boldsymbol{\xi}_1) + \boldsymbol{f}(\boldsymbol{\xi}_2) + \mathbf{n}, \tag{1}$$

where, from a signal processing point of view, $\mathbf{y} \in \mathbb{R}^N$ and $\mathbf{n} \in \mathbb{R}^N$ denote the noisy received data[2] and the additive noise with a known probability density function (pdf). The noiseless received data are assumed to be the sum of two signals $\mathbf{f}(\boldsymbol{\xi}_m)$, $m = 1, 2$ each one modelled from the same deterministic known waveform $\mathbf{f}(.)$ parameterized by a set of deterministic unknown vectors $\boldsymbol{\xi}_m \subseteq \mathbb{R}^{P+q_m}$, $m = 1, 2$ in which $q_1 + q_2 = Q$. The function $\mathbf{f}(.)$ is assumed to be measurable and the model (1) is assumed to be parameter identifiable (*i.e.,* the Fisher information matrix considered through this paper is non singular). All the parameters are collected in $\boldsymbol{\xi} = \left[\boldsymbol{\xi}_1^T \boldsymbol{\xi}_2^T\right]^T \subseteq \mathbb{R}^{2P+Q}$. With a proper rearrangement[3] of $\boldsymbol{\xi}$ one obtains $\boldsymbol{\xi} = \left[\boldsymbol{\omega}^T \ \boldsymbol{\rho}^T\right]^T$ where $\boldsymbol{\omega} \subseteq \mathbb{R}^{2P}$ and $\boldsymbol{\rho} \subseteq \mathbb{R}^Q$ denote, respectively, the parameter vector of interest, and the unwanted or nuisance parameters vector. This means that we consider P parameters of interest for each signal. To the best of our knowledge, the result of the literature [5] on the SRL have been only proposed in the case of

[2]Let us note that the study where the observation are complex can be handled by the real model (1) by stacking the real and imaginary parts of the observation vector.

[3]To avoid a complication of notation, $\boldsymbol{\xi}$ denote both the vector parameter before and after the rearrangement. In the following we will only use the vector parameter after the rearrangement.

one parameter of interest per signal. Nevertheless, the problem of deriving the so-called Multidimensional Statistical Resolution Limit (MSRL) based on the Cramér-Rao Bound (CRB) in the case of more than one parameter of interest per signal was recently studied in [1]. The assumptions used for the MSRL derivation are the following:

- **A1.** The element of the $\boldsymbol{\omega}$ are of the same nature, *i.e.,* the parameters of interest have the same unit measurement. If no, please refer to [1, Remark 2] to overcome this assumption.
- **A2.** Each parameter of interest w.r.t. to the first signal, $\omega_1^{(p)}$, can be as close as possible to the parameter of interest w.r.t. to the second signal $\omega_2^{(p)}$, but not equal. This is not really a restrictive assumptions, since in most applications, having two or more identical parameters of interest is a zero probability event [9, p74]. Nevertheless, in the case where it exists p such that $\omega_1^{(p)} = \omega_2^{(p)}$, please refer to [1, Subsection 3.1] to overcome this assumption.

Under these assumptions, the intuitive MSRL criterion is defined in [1] as follows:

Criterion 1 *The MSRL, denoted by δ, for the model (1) in the case of two signals and P parameters of interest per signal is given as the implicit solution of the following equation*

$$\delta^2 = CRB\left(\delta\right) \tag{2}$$

where

$$\delta = \sum_{p=1}^{P} \delta_p \tag{3}$$

in which the so-called local SRLs are given by $\delta_p \triangleq \left|\omega_2^{(p)} - \omega_1^{(p)}\right|$ and where $CRB\left(\delta\right)$ denotes the CRB w.r.t. *δ for the observation model (1).*

In the following the latter MSRL criterion is shown to be asymptotically equivalent (upon to a translator factor) to a UMP test among all invariant statistical tests.

3. ANALYSIS OF THE MSRL

3.1. Hypothesis test formulation

Resolving two closely spaced sources, with respect to their parameter of interest, can be formulated as a binary hypothesis test [6,7,10]. Let us consider the hypothesis $\mathcal{H}_0$ which represents the case where the two emitted signal sources are combined into one signal (*i.e.*, $\forall p \in [1 \dots P]$, $\omega_1^{(p)} = \omega_2^{(p)}$), whereas the hypothesis $\mathcal{H}_1$ embodies the situation where the two signals are resolvable (*i.e.*, $\exists p \in [1 \dots P]$, such that $\omega_1^{(p)} \neq \omega_2^{(p)}$). Consequently, one can formulate the hypothesis test as a simple one-sided binary hypothesis test as follows:

$$\begin{cases} \mathcal{H}_0 : & \delta_{\text{detection}} = 0 \\ \mathcal{H}_1 : & \delta_{\text{detection}} > 0 \end{cases} \tag{4}$$

where $\delta_{\text{detection}}$ denotes a distance between two sets containing the parameters of interest. Let us denote these sets as C_1 and C_2 where $C_q = \left\{\omega_q^{(1)}, \omega_q^{(2)}, \dots, \omega_q^{(P)}\right\}$, $q = 1, 2$. Consequently, $\delta_{\text{detection}}$ can be defined as

$$\delta_{\text{detection}} \triangleq \sum_{p=1}^{P} \left|\omega_2^{(p)} - \omega_1^{(p)}\right|. \tag{5}$$

Since the separation term $\delta_{\text{detection}}$ is unknown, it is impossible to design an optimal detector in the Neyman-Pearson sense. Alternatively, the Generalized Likelihood Ratio Test (GLRT) [8,11] is a well known approach appropriate to solve such a problem. The GLRT is expressed as:

$$\begin{aligned} L_G(\mathbf{y}) &= \frac{\max_{\delta_{\text{detection}}, \boldsymbol{\rho}_1} \; p(\mathbf{y}|\delta_{\text{detection}}, \boldsymbol{\rho}_1, \mathcal{H}_1)}{\max_{\boldsymbol{\rho}_0} \; p(\mathbf{y}|\boldsymbol{\rho}_0, \mathcal{H}_0)} \\ &= \frac{p(\mathbf{y}|\hat{\delta}_{\text{detection}}, \hat{\boldsymbol{\rho}}_1, \mathcal{H}_1)}{p(\mathbf{y}|\hat{\boldsymbol{\rho}}_0, \mathcal{H}_0)} \underset{\mathcal{H}_0}{\overset{\mathcal{H}_1}{\gtrless}} \varsigma' \end{aligned} \tag{6}$$

where $\hat{\delta}_{\text{detection}}$, $\hat{\boldsymbol{\rho}}_1$ and $\hat{\boldsymbol{\rho}}_0$ denote the Maximum Likelihood Estimator (MLE) of $\delta_{\text{detection}}$ under $\mathcal{H}_1$, the MLE of $\boldsymbol{\rho}$ under $\mathcal{H}_1$ and the MLE of $\boldsymbol{\rho}$ under $\mathcal{H}_0$. ς' denotes the test threshold. We rewrite (6) to obtain

$$T_G(\mathbf{y}) = \text{Ln}\, L_G(\mathbf{y}) \underset{\mathcal{H}_0}{\overset{\mathcal{H}_1}{\gtrless}} \varsigma = \text{Ln}\varsigma', \tag{7}$$

in which Ln denotes the natural logarithm.

3.2. Asymptotic equivalence of the GLRT

To find the analytical expression of $T_G(\mathbf{y})$ in (7) is generally intractable. This is mainly due to the fact that the derivation of $\hat{\delta}_{\text{detection}}$ is a highly non linear optimization problem [12] (aside from the linear parameter model [8, 13]). Consequently, in the following, and as in [6], we consider the asymptotic case (in terms of number of samples). In [11, eq (6C.1)] it has been proved that, for a large number of snapshots, the statistic $T_G(\mathbf{y})$ follows a chi-squared pdf under $\mathcal{H}_0$ and $\mathcal{H}_1$ given by

$$T_G(\mathbf{y}) \sim \begin{cases} \chi_1^2 & \text{under } \mathcal{H}_0 \\ {\chi'}_1^2(\kappa'\left(P_{fa}, P_d\right)) & \text{under } \mathcal{H}_1 \end{cases} \tag{8}$$

where χ_1^2 and ${\chi'}_1^2(\kappa'\left(P_{fa}, P_d\right))$ denote the central chi-square and the noncentral chi-square pdf with one degree of freedom. P_{fa} and P_d are, respectively, the probability of false alarm and the probability of detection w.r.t. hypothesis test (4). Whereas, assuming that $\text{CRB}(\delta_{\text{detection}})$ exist, the the noncentral parameter $\kappa'\left(P_{fa}, P_d\right)$ is given by [11, p.239]

$$\kappa'\left(P_{fa}, P_d\right) = \delta_{\text{detection}}^2 \left(\text{CRB}(\delta_{\text{detection}})\right)^{-1}. \tag{9}$$

On the other hand, one can notice that the noncentral parameter $\kappa'\left(P_{fa}, P_d\right)$ can be determined exclusively by the choice of P_{fa} and P_d [6, 8] as the solution of

$$\mathcal{Q}_{\chi_1^2}^{-1}(P_{fa}) = \mathcal{Q}_{{\chi'}_1^2(\kappa'\left(P_{fa}, P_d\right))}^{-1}(P_d), \tag{10}$$

in which $\mathcal{Q}_{\chi_1^2}^{-1}$ and $\mathcal{Q}_{{\chi'}_1^2(\kappa'(P_{fa}, P_d))}^{-1}$ are the inverse of the right tail of the χ_1^2 and ${\chi'}_1^2(\kappa'(P_{fa}, P_d))$ pdf.

Finally, (9) and (10) leads to

$$\delta_{\text{detection}} = \kappa(P_{fa}, P_d)\sqrt{\text{CRB}(\delta_{\text{detection}})} \tag{11}$$

where $\sqrt{\kappa(P_{fa}, P_d)} = \kappa'(P_{fa}, P_d)$ is the so-called translation factor which is determined for a given probability of false alarm and probability of detection (see Fig. 1).

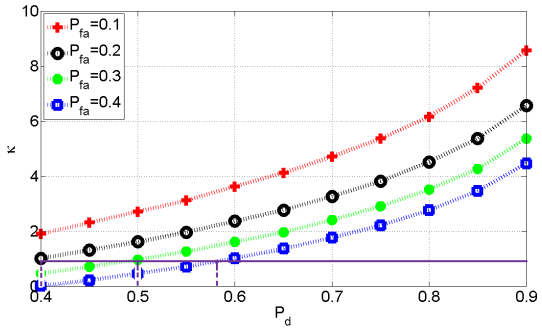

Fig. 1. The translator factor κ vs. the probability of detection P_d and P_{fa}. One can notice that increasing P_d or decreasing P_{fa} has the effect to increase the value of the translator factor κ. This is expected since increasing P_d or decreasing P_{fa} leads to a more selective decision [8, 11].

Remark 1 *It is worth noting that, the hypothesis test (4) is a binary one-sided test and that the MLE used is an unconstrained estimator. Thus, one can deduce that the GLRT, used to derive the asymptotic SRL, is [6, 11]: i) the asymptotically uniformly most powerful test among all invariant statistical tests, and ii) has an asymptotic Constant False-Alarm Rate (CFAR). This is, in the asymptotic case, considered as the strongest statement of optimality that one could hope to obtain [8].*

Finally, from (2) and (11), one can state the following result:

Result 1 *The asymptotic MSRL based on the empirical extension of the Smith criterion given in (2) is equivalent (upon to a translation factor) to the binary one-sided hypothesis test given in (4). Consequently, it is equivalent to an asymptotically uniformly most powerful test among all invariant statistical tests.*

Remark 2 *Consequently, one should note that the MSRL based on the Smith criterion is exactly equal to the MSRL based on the detection approach for all values of P_{fa} and P_d such that $\kappa(P_{fa}, P_d) = 1$ (cf, Fig. 1).*

4. NUMERICAL EXAMPLE

In this Section we present a numerical example of the MSRL applied to the 3-D Harmonic retrieval model for wireless channel sounding [9, 14]. First we briefly introduce the considered model, then, we numerically derive its MSRL.

4.1. Model setup

The observation model can be written as [9]

$$[\boldsymbol{\mathcal{Y}}(t)]_{k,l,m} = [\boldsymbol{\mathcal{X}}(t)]_{k,l,m} + [\boldsymbol{\mathcal{N}}(t)]_{k,l,m}, \quad t = 1, \ldots, T,$$

for $k = 1 \ldots K, l = 1 \ldots L, m = 1 \ldots M$, in which K, L and M denote the number of acquired data samples per channel, the number of receive antenna sensors and the number of transmit antenna sensors, respectively. $\boldsymbol{\mathcal{Y}}(t)$, $\boldsymbol{\mathcal{X}}(t)$ and $\boldsymbol{\mathcal{N}}(t)$ denote the noisy observation multiway array, the noiseless observation multiway array and the noise multiway array at the t^{th} snapshot, respectively. Whereas, the noiseless observation multiway array is given by [14]

$$[\boldsymbol{\mathcal{X}}(t)]_{k,l,m} = \sum_{q}^{2} s_q(t) e^{j\omega_q^{(1)} k} e^{j\omega_q^{(2)} l} e^{j\omega_q^{(3)} m}, \tag{12}$$

where the so-called electrical angles are given by

$$\begin{aligned}
\omega_q^{(1)} &\triangleq \frac{-2\pi}{K}\tau_q, \\
\omega_q^{(2)} &\triangleq \frac{-2\pi d_R}{\lambda}\cos(\phi_q), \\
\omega_q^{(3)} &\triangleq \frac{-2\pi d_T}{\lambda}\cos(\theta_q),
\end{aligned}$$

and τ_q, ϕ_q, θ_q denote delay, direction of arrival, and direction of departure, of the the q^{th} multipath, respectively. d_R, d_T and λ are the inter-element spacings of the transmit and receive array and the carrier wavelength, respectively. $s_q(t)$ is the q^{th} complex amplitude path [9]. It can be proved that the 3-D harmonic retrieval model for wireless channel sounding follows a PARAFAC (PARallel FACtor) decomposition [15] given by

$$\boldsymbol{\mathcal{X}}(t) = \sum_{q=1}^{2} s_q(t) \left(\boldsymbol{a}(\omega_q^{(1)}) \circ \boldsymbol{a}(\omega_q^{(2)}) \circ \boldsymbol{a}(\omega_q^{(3)}) \right), \tag{13}$$

where $\left[\boldsymbol{a}(\omega_q^{(p)})\right]_i = e^{j\omega_q^{(p)}(i-1)}$ and $\circ$ denotes the multiway array outer-product [16]. After vectorization, the full noise free observation vector is given by

$$\boldsymbol{x} = \left[\text{vec}^T\left(\boldsymbol{\mathcal{X}}(1)\right) \quad \ldots \quad \text{vec}^T\left(\boldsymbol{\mathcal{X}}(L)\right)\right]^T.$$

In the same way, we define $\mathbf{y}$, the noisy observation vector, and $\mathbf{n}$, the noise vector, by the concatenation of the proper multiway array's entries.

4.2. MSRL derivation

First we derive the CRB for the 3-D Harmonic retrieval model. Then, we use the change of variable formula [13, p 45] to deduce CRB(δ). Assuming *i.i.d.* complex circular white Gaussian noise with zero-mean and unknown variance $\sigma^2\mathbf{I}$, the joint pdf of $\mathbf{y}$ for a given unknown deterministic parameter vector $\boldsymbol{\xi}$ is

$$\begin{aligned}
p(\mathbf{y}|\,\boldsymbol{\xi}) &= \prod_{t=1}^{T} p(\text{vec}\,(\boldsymbol{\mathcal{Y}}(t))|\,\boldsymbol{\xi}) \\
&= \frac{1}{(\pi\sigma^2)^{TLMK}} e^{\frac{-1}{\sigma^2}(\mathbf{y}-\mathbf{x})^H(\mathbf{y}-\mathbf{x})}.
\end{aligned} \tag{14}$$

The unknown parameter vector is given by

$$\boldsymbol{\xi} = \left[\omega_1^{(1)} \quad \omega_1^{(2)} \quad \omega_1^{(3)} \quad \omega_1^{(1)} \quad \omega_1^{(2)} \quad \omega_1^{(3)} \quad \sigma^2\right]^T,$$

where the parameters of interest are $\omega_1^{(1)}, \omega_1^{(2)}, \omega_2^{(1)}, \omega_2^{(2)}$ (representing the direction of arrival and the direction of departure of each sources). After some calculus, the Fisher information matrix of the noisy observations $\mathbf{y}$ for orthogonal known amplitudes, is given by

$$\mathbf{FIM}(\boldsymbol{\xi}) = \frac{2}{\sigma^2}\begin{bmatrix} \mathbf{F}_{\boldsymbol{\omega}} & \mathbf{0} \\ \mathbf{0} & \times \end{bmatrix}, \tag{15}$$

where,

$$\mathbf{F}_{\boldsymbol{\omega}} = TKML(\boldsymbol{\Delta} \otimes \mathbf{G}), \tag{16}$$

in which

$$\boldsymbol{\Delta} = \begin{bmatrix} \sum_{t=1}^{T} \|s_1(t)\|^2 & 0 \\ 0 & \sum_{t=1}^{T} \|s_2(t)\|^2 \end{bmatrix}$$

and

$$\mathbf{G} = \begin{bmatrix} \frac{(2K-1)(K-1)}{6} & \frac{(K-1)(L-1)}{2} & \frac{(K-1)(M-1)}{2} \\ \frac{(L-1)(K-1)}{2} & \frac{(2L-1)(L-1)}{6} & \frac{(L-1)(M-1)}{2} \\ \frac{(M-1)(K-1)}{2} & \frac{(M-1)(L-1)}{2} & \frac{(2M-1)(M-1)}{6} \end{bmatrix}.$$

Now one can apply Criterion 1. From (15), one deduces numerically $\mathbf{CRB}(\boldsymbol{\xi}) = (\mathbf{FIM}(\boldsymbol{\xi}))^{-1}$. Then, applying the change of variable formula [13, p 45], one obtains

$$\mathrm{CRB}(\delta) = \sum_{p=1}^{2}\sum_{q=1}^{2} \mathrm{CRB}(\omega_q^{(p)}) + \sum_{q=1}^{2} \mathrm{CRB}(\omega_q^{(1)}, \omega_q^{(2)}).$$

Finally, solving numerically the implicit equation $\delta^2 = \mathrm{CRB}(\delta)$ gives the desired MSRL as reported in Fig. 2.

From Fig. 2 one can notice that the numerical MSRL based on Criterion 1 is in good agreement with the MSRL derived using the hypothesis test approach. One can notice that, for $P_d = 0.37$ and $P_{fa} = 0.1$ the MSRL based on Criterion 1 is exactly equal to the MSRL based on the hypothesis test derived in the asymptotic case. From the case $P_d = 0.49$ and $P_{fa} = 0.3$ and $P_d = 0.32$ and $P_{fa} = 0.1$, one can notice the influence of the multiplicative factor κ on the MSRL.

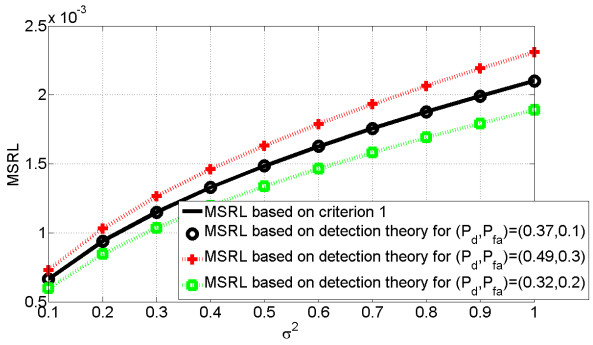

Fig. 2. MSRL vs. σ^2 for L = 100: one can notice that the MSRL based on the Criterion 1 is in good agreement with the MSRL based on the hypothesis test approach (which uses an asymptotically uniformly most powerful test among all invariant statistical tests).

5. CONCLUSION

In this paper, we have analyzed the multidimensional statistical resolution limit based on the empirical extension of the Smith criterion. More precisely, it has been demonstrated that the empirical MSRL criterion based on the 1-norm distance is asymptotically equivalent (upon to a translator factor) to a uniformly most powerful test which is (in the asymptotic case) considered as the strongest statement of optimality that one could expect to obtain.

6. REFERENCES

[1] M. N. El Korso, R. Boyer, A. Renaux, and S. Marcos, "Statistical resolution limit for multiple signals and parameters of interest," in *Proc. of IEEE Int. Conf. Acoust., Speech, Signal Processing*, Dallas, TX, 2010.

[2] H. L. VanTrees, *Detection, Estimation and Modulation Theory*. New York: Wiley, 1968, vol. 1.

[3] H. B. Lee, "The Cramér-Rao bound on frequency estimates of signals closely spaced in frequency," *IEEE Trans. Signal Processing*, vol. 40, no. 6, pp. 1507–1517, 1992.

[4] M. Shahram and P. Milanfar, "Imaging below the diffraction limit: A statistical analysis," *IEEE Trans. Image Processing*, vol. 13, no. 5, pp. 677–689, May 2004.

[5] S. T. Smith, "Statistical resolution limits and the complexified Cramér Rao bound," *IEEE Trans. Signal Processing*, vol. 53, pp. 1597–1609, May 2005.

[6] Z. Liu and A. Nehorai, "Statistical angular resolution limit for point sources," *IEEE Trans. Signal Processing*, vol. 55, no. 11, pp. 5521–5527, Nov. 2007.

[7] A. Amar and A. Weiss, "Fundamental limitations on the resolution of deterministic signals," *IEEE Trans. Signal Processing*, vol. 56, no. 11, pp. 5309–5318, Nov. 2008.

[8] L. L. Scharf, *Statistical Signal Processing: Detection, Estimation, and Time Series Analysis*. Reading: Addison Wesley, 1991.

[9] A. Gershman and N. Sidiropoulos, *Space-time processing for MIMO communications*. New York: Wiley, 2005.

[10] M. Shahram and P. Milanfar, "On the resolvability of sinusoids with nearby frequencies in the presence of noise," *IEEE Trans. Signal Processing*, vol. 53, no. 7, pp. 2579–2585, July 2005.

[11] S. M. Kay, *Fundamentals of Statistical Signal Processing : Detection Theory*. NJ: Prentice Hall, 1998, vol. 2.

[12] B. Ottersten, M. Viberg, P. Stoica, and A. Nehorai, "Exact and large sample maximum likelihood techniques for parameter estimation and detection in array processing," in *Radar Array Processing*, S. Haykin, J. Litva, and T. J. Shepherd, Eds. Berlin: Springer-Verlag, 1993, ch. 4, pp. 99–151.

[13] S. M. Kay, *Fundamentals of Statistical Signal Processing*. NJ: Prentice Hall, 1993, vol. 1.

[14] K. Mokios, N. Sidiropoulos, M. Pesavento, and C. Mecklenbrauker, "On 3-D harmonic retrieval for wireless channel sounding," in *Proc. of IEEE Int. Conf. Acoust., Speech, Signal Processing*, vol. 2, Philadelphia, U.S.A., 2004, pp. 89–92.

[15] R. Harshman, *Foundations of the PARAFAC procedure: Models and conditions for an "explanatory" multi-modal factor analysis*. UCLA Working Papers in Phonetics, 1970.

[16] G. H. Golub and C. F. V. Loan, *Matrix Computations*. London: Johns Hopkins, 1989.

C.3 EURASIP-ASP-2011

M. N. El Korso, R. Boyer, A. Renaux and S. Marcos, "Statistical Resolution Limit for the Multidimensional Harmonic Retrieval Model : Hypothesis Test and Cramer-Rao Bound Approaches", *EURASIP Journal on Advances in Signal Processing*, special issue on "Advances in Angle-of-Arrival and Multidimensional Signal Processing for Localization and Communications", Jun. 2011, p. 1-14, doi :10.1186/1687-6180-2011-12.

EURASIP Journal on Advances in Signal Processing
a SpringerOpen Journal

RESEARCH Open Access

Statistical resolution limit for the multidimensional harmonic retrieval model: hypothesis test and Cramér-Rao Bound approaches

Mohammed Nabil El Korso*, Rémy Boyer, Alexandre Renaux and Sylvie Marcos

Abstract

The statistical resolution limit (SRL), which is defined as the minimal separation between parameters to allow a correct resolvability, is an important statistical tool to quantify the ultimate performance for parametric estimation problems. In this article, we generalize the concept of the SRL to the multidimensional SRL (MSRL) applied to the multidimensional harmonic retrieval model. In this article, we derive the SRL for the so-called multidimensional harmonic retrieval model using a generalization of the previously introduced SRL concepts that we call multidimensional SRL (MSRL). We first derive the MSRL using an hypothesis test approach. This statistical test is shown to be asymptotically an uniformly most powerful test which is the *strongest* optimality statement that one could expect to obtain. Second, we link the proposed asymptotic MSRL based on the hypothesis test approach to a new extension of the SRL based on the Cramér-Rao Bound approach. Thus, a closed-form expression of the asymptotic MSRL is given and analyzed in the framework of the multidimensional harmonic retrieval model. Particularly, it is proved that the optimal MSRL is obtained for equi-powered sources and/or an equi-distributed number of sensors on each multi-way array.

Keywords: Statistical resolution limit, Multidimensional harmonic retrieval, Performance analysis, Hypothesis test, Cramér-Rao bound, Parameter estimation, Multidimensional signal processing

Introduction

The multidimensional harmonic retrieval problem is an important topic which arises in several applications [1]. The main reason is that the multidimensional harmonic retrieval model is able to handle a large class of applications. For instance, the joint angle and carrier estimation in surveillance radar system [2,3], the underwater acoustic multisource azimuth and elevation direction finding [4], the 3-D harmonic retrieval problem for wireless channel sounding [5,6] or the detection and localization of multiple targets in a MIMO radar system [7,8].

One can find many estimation schemes adapted to the multidimensional harmonic retrieval estimation problem, see, e.g., [1,2,4-7,9,10]. However, to the best of our knowledge, no work has been done on the resolvability of such a multidimensional model.

The resolvability of closely spaced signals, in terms of parameter of interest, for a given scenario (e.g., for a given signal-to-noise ratio (SNR), for a given number of snapshots and/or for a given number of sensors) is a former and challenging problem which was recently updated by Smith [11], Shahram and Milanfar [12], Liu and Nehorai [13], and Amar and Weiss [14]. More precisely, the concept of statistical resolution limit (SRL), i.e., the minimum distance between two closely spaced signals[a] embedded in an additive noise that allows a correct resolvability/parameter estimation, is rising in several applications (especially in problems such as radar, sonar, and spectral analysis [15].)

The concept of the SRL was defined/used in several manners [11-14,16-24], which could turn in it to a confusing concept. There exist essentially three approaches

* Correspondence: elkorso@lss.supelec.fr
Laboratoire des Signaux et Systèmes (L2S), Université Paris-Sud XI (UPS), CNRS, SUPELEC, 3 Rue Joliot Curie, Gif-Sur-Yvette 91192, France

to define/obtain the SRL. (i) The first is based on the concept of mean null spectrum: assuming, e.g., that two signals are parameterized by the frequencies f_1 and f_2, the Cox criterion [16] states that these sources are resolved, w.r.t. a given high-resolution estimation algorithm, *if the mean null spectrum at each frequency f_1 and f_2 is lower than the mean of the null spectrum at the midpoint* $\frac{f_1+f_2}{2}$. Another commonly used criterion, also based on the concept of the mean null spectrum, is the Sharman and Durrani criterion [17], which states that two sources are resolved *if the second derivative of the mean of the null spectrum at the midpoint* $\frac{f_1+f_2}{2}$ *is negative*. It is clear that the SRL based on the mean null spectrum is relevant to a specific high-resolution algorithm (for some applications of these criteria one can see [16-19] and references therein.) (ii) The second approach is based on detection theory: the main idea is to use a hypothesis test to decide if one or two closely spaced signals are present in the set of the observations. Then, the challenge herein is to link the minimum separation, between two sources (e.g., in terms of frequencies) that is detectable at a given SNR, to the probability of false alarm, P_{fa} and/or to the probability of detection P_{d}. In this spirit, Sharman and Milanfar [12] have considered the problem of distinguishing whether the observed signal contains one or two frequencies at a given SNR using the generalized likelihood ratio test (GLRT). The authors have derived the SRL expressions w.r.t. P_{fa} and P_{d} in the case of real received signals, and unequal and unknown amplitudes and phases. In [13], Liu and Nehorai have defined a statistical angular resolution limit using the asymptotic equivalence (in terms of number of observations) of the GLRT. The challenge was to determine the minimum angular separation, in the case of complex received signals, which allows to resolve two sources knowing the direction of arrivals (DOAs) of one of them for a given P_{fa} and a given P_{d}. Recently, Amar and Weiss [14] have proposed to determine the SRL of complex sinusoids with nearby frequencies using the Bayesian approach for a given correct decision probability. (iii) The third approach is based on a estimation accuracy criteria independent of the estimation algorithm. Since the Cramér-Rao Bound (CRB) expresses a lower bound on the covariance matrix of any unbiased estimator, then it expresses also the ultimate estimation accuracy [25,26]. Consequently, it could be used to describe/obtain the SRL. In this context, one distinguishes two main criteria for the SRL based on the CRB: (1) the first one was introduced by Lee [20] and states that: *two signals are said to be resolvable w.r.t. the frequencies if the maximum standard deviation is less than twice the difference between f_1 and f_2*. Assuming that the CRB is a tight bound (under mild/weak conditions), the standard deviation, $\sigma_{\hat{f}_1}$ and $\sigma_{\hat{f}_2}$, of an unbiased estimator $\hat{f} = [\hat{f}_1\ \hat{f}_2]^{\text{T}}$ is given by $\sqrt{\text{CRB}(f_1)}$ and $\sqrt{\text{CRB}(f_2)}$, respectively. Consequently, the SRL is defined, in the Lee criterion sense, as $2\max\left\{\sqrt{\text{CRB}(f_1)}, \sqrt{\text{CRB}(f_2)}\right\}$. One can find some results and applications in [20,21] where this criterion is used to derive a matrix-based expression (i.e., without analytic inversion of the Fisher information matrix) of the SRL for the frequency estimates in the case of the conditional and unconditional signal source models. On the other hand, Dilaveroglu [22] has derived a closed-form expression of the frequency resolution for the real and complex conditional signal source models. However, one can note that the coupling between the parameters, $\text{CRB}(f_1, f_2)$ (i.e., the CRB for the cross parameters f_1 and f_2), is ignored by this latter criterion. (2) To extend this, Smith [11] has proposed the following criterion: *two signals are resolvable w.r.t. the frequencies if the difference between the frequencies, δ_f, is greater than the standard deviation of the DOA difference estimation*. Since, the standard deviation can be approximated by the CRB, then, the SRL, in the Smith criterion sense, is defined as the limit of δ_f for which $\delta_f < \sqrt{\text{CRB}(\delta_f)}$ is achieved. This means that, the SRL is obtained by solving the following implicit equation

$$\delta_f^2 = \text{CRB}(\delta_f) = \text{CRB}(f_1) + \text{CRB}(f_2) - 2\text{CRB}(f_1, f_2).$$

In [11,23], Smith has derived the SRL for two closely spaced sources in terms of DOA, each one modeled by one complex pole. In [24], Delmas and Abeida have derived the SRL based on the Smith criterion for DOA of discrete sources under QPSK, BPSK, and MSK model assumptions. More recently, Kusuma and Goyal [27] have derived the SRL based on the Smith criterion in sampling estimation problems involving a powersum series.

It is important to note that all the criteria listed before take into account only one parameter of interest per signal. Consequently, all the criteria listed before cannot be applied to the aforementioned the multidimensional harmonic model. To the best of our knowledge, no results are available on the SRL for multiple parameters of interest per signal. The goal of this article is to fill this lack by proposing and deriving the so-called MSRL for the multidimensional harmonic retrieval model.

More precisely, in this article, the MSRL for multiple parameters of interest per signal using a hypothesis test is derived. This choice is motivated by the following arguments: (i) the hypothesis test approach is not specific to a certain high-resolution algorithm (unlike the mean null spectrum approach), (ii) in this article, we

link the asymptotic MSRL based on the hypothesis test approach to a new extension of the MSRL based on the CRB approach. Furthermore, we show that the MSRL based on the CRB approach is equivalent to the MSRL based on the hypothesis test approach for a fixed couple (P_{fa}, P_d), and (iii) the hypothesis test is shown to be asymptotically an uniformly most powerful test which is the *strongest* statement of optimality that one could expect to obtain [28].

The article is organized as follows. We first begin by introducing the multidimensional harmonic model, in section "Model setup". Then, based on this model, we obtain the MSRL based on the hypothesis test and on the CRB approach. The link between theses two MSRLs is also described in section "Determination of the MSRL for two sources" followed by the derivation of the MSRL closed-form expression, where, as a by product the exact closed-form expressions of the CRB for the multi-dimensional retrieval model is derived (note that to the best of our knowledge, no exact closed-form expressions of the CRB for such model is available in the literature). Furthermore, theoretical and numerical analyses are given in the same section. Finally, conclusions are given.

Glossary of notation

The following notations are used through the article. Column vectors, matrices, and multi-way arrays are represented by lower-case bold letters ($\boldsymbol{a}$, ...), upper-case bold letters ($\boldsymbol{A}$, ...) and bold calligraphic letters ($\boldsymbol{\mathcal{A}}$, ...), whereas

- $\mathbb{R}$ and $\mathbb{C}$ denote the body of real and complex values, respectively,
- $\mathbb{R}^{D_1\times D_2\times\cdots\times D_I}$ and $\mathbb{C}^{D_1\times D_2\times\cdots\times D_I}$ denote the real and complex multi-way arrays (also called tensors) body of dimension $D_1 \times D_2 \times ... \times D_I$, respectively,
- j = the complex number $\sqrt{-1}$.
- $\mathbf{I}_Q$ = the identity matrix of dimension Q,
- $\mathbf{0}_{Q_1\times Q_2}$ = the $Q_1 \times Q_2$ matrix filled by zeros,
- $[\boldsymbol{a}]_i$ = the ith element of the vector $\boldsymbol{a}$,
- $[\boldsymbol{A}]_{i_1,i_2}$ = the i_1th row and the i_2th column element of the matrix $\boldsymbol{A}$,
- $[\boldsymbol{\mathcal{A}}]_{i_1,i_2,...,i_N}$ = the $(i_1, i_2, ..., i_N)$th entry of the multi-way array $\boldsymbol{\mathcal{A}}$,
- $[\boldsymbol{A}]_{i,p:q}$ = the row vector containing the $(q - p + 1)$ elements $[\boldsymbol{A}]_{i,k}$, where $k = p, ..., q$,
- $[\boldsymbol{A}]_{p:q,k}$ = the column vector containing the $(q - p + 1)$ elements $[\boldsymbol{A}]_{i,k}$, where $i = p, ..., q$,
- the derivative of vector $\boldsymbol{a}$ *w.r.t.* to vector $\boldsymbol{b}$ is defined as follows: $\left[\frac{\partial \boldsymbol{a}}{\partial \boldsymbol{b}}\right]_{i,j} = \frac{\partial [\boldsymbol{a}]_i}{\partial [\boldsymbol{b}]_j}$,
- $\boldsymbol{A}^{\mathrm{T}}$ = the transpose of the matrix $\boldsymbol{A}$,
- $\boldsymbol{A}^*$ = the complex conjugate of the matrix $\boldsymbol{A}$,
- $\boldsymbol{A}^{\mathrm{H}} = (\boldsymbol{A}^*)^{\mathrm{T}}$,
- tr $\{\boldsymbol{A}\}$ = the trace of the matrix $\boldsymbol{A}$,
- det $\{\boldsymbol{A}\}$ = the determinant of the matrix $\boldsymbol{A}$,
- $\Re\{a\}$ = the real part of the complex number a,
- $\mathbb{E}\{a\}$ = the expectation of the random variable a,
- $||\boldsymbol{a}||^2 = \frac{1}{L}\sum_{t=1}^{L}[\boldsymbol{a}]_t^2$ denotes the normalized norm of the vector $\boldsymbol{a}$ (in which L is the size of $\boldsymbol{a}$),
- sgn (a) = 1 if $a \geq 0$ and -1 otherwise.
- diag($\boldsymbol{a}$) is the diagonal operator which forms a diagonal matrix containing the vector $\boldsymbol{a}$ on its diagonal,
- vec(.) is the vec-operator stacking the columns of a matrix on top of each other,
- $\odot$ stands for the Hadamard product,
- $\otimes$ stands for the Kronecker product,
- $\circ$ denotes the multi-way array outer-product (recall that for a given multi-way arrays $\boldsymbol{\mathcal{A}} \in \mathbb{C}^{A_1\times A_2\times\cdots\times A_I}$ and $\boldsymbol{\mathcal{B}} \in \mathbb{C}^{B_1\times B_2\times\cdots\times B_J}$, the result of the outer-product of $\boldsymbol{\mathcal{A}}$ and $\boldsymbol{\mathcal{B}}$ denoted by $\boldsymbol{\mathcal{C}}^{A_1\times\cdots\times A_I\times B_1\times\cdots\times B_J}$ is given by $[\boldsymbol{\mathcal{C}}]_{a_1,...,a_I,b_1,...,b_J} = [\boldsymbol{\mathcal{A}}\circ\boldsymbol{\mathcal{B}}]_{a_1,...,a_I,b_1,...,b_J} = [\boldsymbol{\mathcal{A}}]_{a_1,...,a_I}[\boldsymbol{\mathcal{B}}]_{b_1,...,b_J}$).

Model setup

In this section, we introduce the multidimensional harmonic retrieval model in the multi-way array form (also known as *tensor form* [29]). Then, we use the PARAFAC (PARallel FACtor) decomposition to obtain a vector form of the observation model. This vector form will be used to derive the closed-form expression of the MSRL.

Let us consider a multidimensional harmonic model consisting of the superposition of two harmonics each one of dimension P contaminated by an additive noise. Thus, the observation model is given as follows [8,9,26,30-32]:

$$[\boldsymbol{\mathcal{Y}}(t)]_{n_1,...,n_P} = [\boldsymbol{\mathcal{X}}(t)]_{n_1,...,n_P} + [\boldsymbol{\mathcal{N}}(t)]_{n_1,...,n_P}, \quad t = 1, \ldots, L, \quad \text{and} \quad n_p = 0, \ldots, N_p - 1, \tag{1}$$

where $\boldsymbol{\mathcal{Y}}(t)$, $\boldsymbol{\mathcal{X}}(t)$, and $\boldsymbol{\mathcal{N}}(t)$ denote the noisy observation, the noiseless observation, and the noise multi-way array at the tth snapshot, respectively. The number of snapshots and the number of sensors on each array are denoted by L and $(N_1, ..., N_P)$, respectively. The noiseless observation multi-way array can be written as follows[b] [26,30-32]:

$$[\boldsymbol{\mathcal{X}}(t)]_{n_1,...,n_P} = \sum_{m=1}^{2} s_m(t)\prod_{p=1}^{P} e^{j\omega_m^{(p)}n_p}, \tag{2}$$

where $\omega_m^{(p)}$and $s_m(t)$ denote the mth frequency viewed along the pth dimension or array and the mth complex signal source, respectively. Furthermore, the signal source is given by $s_m(t) = \alpha_m(t)e^{j\phi_m(t)}$ where $\alpha_m(t)$ and

$\varphi_m(t)$ denote the real positive amplitude and the phase for the mth signal source at the tth snapshot, respectively.

Since,

$$\prod_{p=1}^{P} e^{j\omega_m^{(p)} n_p} = \left[\boldsymbol{a}(\omega_m^{(1)}) \circ \boldsymbol{a}(\omega_m^{(2)}) \circ \cdots \circ \boldsymbol{a}(\omega_m^{(P)})\right]_{n_1,n_2,\ldots,n_P},$$

where $\boldsymbol{a}(.)$ is a Vandermonde vector defined as

$$\boldsymbol{a}(\omega_m^{(p)}) = \left[1 \quad e^{j\omega_m^{(p)}} \quad \cdots \quad e^{j}(N_p - 1)\omega_m^{(p)}\right]^{\mathrm{T}},$$

then, the multi-way array $\boldsymbol{\mathcal{X}}(t)$ follows a PARAFAC decomposition [7,33]. Consequently, the noiseless observation multi-way array can be rewritten as follows:

$$\boldsymbol{\mathcal{X}}(t) = \sum_{m=1}^{2} s_m(t)\left(\boldsymbol{a}(\omega_m^{(1)}) \circ \boldsymbol{a}(\omega_m^{(2)}) \circ \cdots \circ \boldsymbol{a}(\omega_m^{(P)})\right). \quad (3)$$

First, let us vectorize the noiseless observation as follows:

$$\mathrm{vec}(\boldsymbol{\mathcal{X}}(t)) = [[\boldsymbol{\mathcal{X}}(t)]_{0,0,\ldots,0} \cdots [\boldsymbol{\mathcal{X}}(t)]_{N_1-1,0,\cdots,0} [\boldsymbol{\mathcal{X}}(t)]_{0,1,\ldots,0} \cdots [\boldsymbol{\mathcal{X}}(t)]_{N_1-1,N_2-1,\ldots,N_P-1}]^{\mathrm{T}}. \quad (4)$$

Thus, the full noise-free observation vector is given by

$$\mathbf{x} = \left[\mathrm{vec}^{\mathrm{T}}(\boldsymbol{\mathcal{X}}(1)) \quad \mathrm{vec}^{\mathrm{T}}(\boldsymbol{\mathcal{X}}(2)) \cdots \mathrm{vec}^{\mathrm{T}}(\boldsymbol{\mathcal{X}}(L))\right]^{\mathrm{T}}.$$

Second, and in the same way, we define $\mathbf{y}$, the noisy observation vector, and $\mathbf{n}$, the noise vector, by the concatenation of the proper multi-way array's entries, i.e.,

$$\mathrm{y} = \left[\mathrm{vec}^{\mathrm{T}}(\boldsymbol{\mathcal{Y}}(1)) \quad \mathrm{vec}^{\mathrm{T}}(\boldsymbol{\mathcal{Y}}(2)) \cdots \mathrm{vec}^{\mathrm{T}}(\boldsymbol{\mathcal{Y}}(L))\right]^{\mathrm{T}} = \mathbf{x} + \mathbf{n}. \quad (5)$$

Consequently, in the following, we will consider the observation model in (5). Furthermore, the unknown parameter vector is given by

$$\boldsymbol{\xi} = \left[\boldsymbol{\omega}^{\mathrm{T}} \boldsymbol{\rho}^{\mathrm{T}}\right]^{\mathrm{T}}, \quad (6)$$

where $\boldsymbol{\omega}$ denotes the unknown parameter vector of interest, i.e., containing all the unknown frequencies

$$\boldsymbol{\omega} = \left[\left(\boldsymbol{\omega}^{(1)}\right)^{\mathrm{T}} \cdots \left(\boldsymbol{\omega}^{(P)}\right)^{\mathrm{T}}\right]^{\mathrm{T}},$$

in which

$$\boldsymbol{\omega}^{(p)} = \left[\omega_1^{(p)} \; \omega_2^{(p)}\right]^{\mathrm{T}}. \quad (7)$$

whereas $\boldsymbol{\rho}$ contains the unknown nuisance/unwanted parameters vector, i.e., characterizing the noise covariance matrix and/or amplitude and phase of each source (e.g., in the case of a covariance noise matrix equal to $\sigma^2 \mathbf{I}_{LN_1 \ldots N_P}$ and unknown deterministic amplitudes and phases, the unknown nuisance/unwanted parameters vector $\boldsymbol{\rho}$ is given by $\boldsymbol{\rho} = [\alpha_1(1) \ldots \alpha_2(L)\varphi_1(1) \ldots \varphi_2(L)\sigma^2]^{\mathrm{T}}$.

In the following, we conduct a hypothesis test formulation on the observation model (5) to derive our MSRL expression in the case of two sources.

Determination of the MSRL for two sources

Hypothesis test formulation

Resolving two closely spaced sources, with respect to their parameters of interest, can be formulated as a binary hypothesis test [12-14] (for the special case of P = 1). To determine the MSRL (i.e., $P \geq 1$), let us consider the hypothesis $\mathcal{H}_0$ which represents the case where the two emitted signal sources are combined into one signal, i.e., the two sources have the same parameters (this hypothesis is described by $\forall p \in [1 \ldots P], \omega_1^{(p)} = \omega_2^{(p)}$), whereas the hypothesis $\mathcal{H}_1$ embodies the situation where the two signals are resolvable (the latter hypothesis is described by $\exists p \in [1 \ldots P]$, such that $\omega_1^{(p)} \neq \omega_2^{(p)}$). Consequently, one can formulate the hypothesis test, as a simple one-sided binary hypothesis test as follows:

$$\begin{cases} \mathcal{H}_0 : \delta = 0, \\ \mathcal{H}_1 : \delta > 0, \end{cases} \quad (8)$$

where the parameter δ is the so-called MSRL which indicates us in which hypothesis our observation model belongs. Thus, the question addressed below is how can we define the MSRL δ such that all the P parameters of interest are taken into account? A natural idea is that δ reflects a distance between the P parameters of interest. Let the MSRL denotes the l_1 norm[c] between two sets containing the parameters of interest of each source (which is the naturally used norm, since in the mono-parameter frequency case that we extend here, the SRL is defined as $\delta = f_1 - f_2$ [13,14,34]). Meaning that, if we denote these sets as C_1 and C_2 where $C_m = \left\{\omega_m^{(1)}, \omega_m^{(2)}, \ldots, \omega_m^{(P)}\right\}$, m = 1,2, thus, δ can be defined as

$$\delta \triangleq \sum_{p=1}^{P} \left|\omega_2^{(p)} - \omega_1^{(p)}\right|. \quad (9)$$

First, note that the proposed MSRL describes well the hypothesis test (8) (i.e., δ = 0 means that the two emitted signal sources are combined into one signal and $\delta \neq 0$ the two signals are resolvable). Second, since the MSRL δ is unknown, it is impossible to design an optimal detector in the Neyman-Pearson sense. Alternatively, the GLRT [28,35] is a well-known approach appropriate to solve such a problem. To conduct the GLRT on (8), one has to express the probability density function (pdf) of (5) w.r.t. δ. Assuming (without loss of generality) that $\omega_1^{(1)} > \omega_2^{(1)}$, one can notice that $\boldsymbol{\xi}$ is known if and only if δ and $\boldsymbol{\vartheta} \triangleq \left[\omega_2^{(1)} \left(\boldsymbol{\omega}^{(2)}\right)^{\mathrm{T}} \ldots \left(\boldsymbol{\omega}^{(P)}\right)^{\mathrm{T}}\right]^{\mathrm{T}}$

are fixed (i.e., there is a one to one mapping between δ, $\boldsymbol{\vartheta}$, and ξ). Consequently, the pdf of (5) can be described as $p(\mathbf{y}|\delta,\boldsymbol{\vartheta})$. Now, we are ready to conduct the GLRT for this problem:

$$L_G(\mathbf{y}) = \frac{\max_{\delta,\boldsymbol{\vartheta}_1} p(\mathbf{y}|\delta,\boldsymbol{\vartheta}_1,\mathcal{H}_1)}{\max_{\boldsymbol{\vartheta}_0} p(\mathbf{y}|\boldsymbol{\vartheta}_0,\mathcal{H}_0)} = \frac{p(\mathbf{y}|\hat{\delta},\hat{\boldsymbol{\vartheta}}_1,\mathcal{H}_1)}{p(\mathbf{y}|\hat{\boldsymbol{\vartheta}}_0,\mathcal{H}_0)} \underset{\mathcal{H}_0}{\overset{\mathcal{H}_1}{\gtrless}} \varsigma', \tag{10}$$

where $\hat{\delta}$, $\hat{\boldsymbol{\vartheta}}_1$, and $\hat{\boldsymbol{\vartheta}}_0$ denote the maximum likelihood estimates (MLE) of δ under $\mathcal{H}_1$, the MLE of $\boldsymbol{\vartheta}$ under $\mathcal{H}_1$ and the MLE of $\boldsymbol{\vartheta}$ under $\mathcal{H}_0$, respectively, and where ς' denotes the test threshold. From (10), one obtains

$$T_G(\mathbf{y}) = \mathrm{Ln}\, L_G(\mathbf{y}) \underset{\mathcal{H}_0}{\overset{\mathcal{H}_1}{\gtrless}} \varsigma = \mathrm{Ln}\varsigma', \tag{11}$$

in which Ln denotes the natural logarithm.

Asymptotic equivalence of the MSRL

Finding the analytical expression of $T_G(\mathbf{y})$ in (11) is not tractable. This is mainly due to the fact that the derivation of $\hat{\delta}$ is impossible since from (2) one obtains a multimodal likelihood function [36]. Consequently, in the following, and as in[d] [13], we consider the asymptotic case (in terms of the number of snapshots). In [35, eq (6C.1)], it has been proven that, for a large number of snapshots, the statistic $T_G(\mathbf{y})$ follows a chi-square pdf under $\mathcal{H}_0$ and $\mathcal{H}_1$ given by

$$T_G(\mathbf{y}) \sim \begin{cases} \chi^2_1 & \text{under } \mathcal{H}_0, \\ \chi'^2_1(\kappa'(P_{\mathrm{fa}},P_{\mathrm{d}})) & \text{under } \mathcal{H}_1, \end{cases} \tag{12}$$

where χ^2_1 and $\chi'^2_1(\kappa'(P_{\mathrm{fa}},P_{\mathrm{d}}))$ denote the central chi-square and the noncentral chi-square pdf with one degree of freedom, respectively. P_{fa} and P_{d} are, respectively, the probability of false alarm and the probability of detection of the test (8). In the following, CRB(δ) denotes the CRB for the parameter δ where the unknown vector parameter is given by $[\delta\ \boldsymbol{\vartheta}^{\mathrm{T}}]^{\mathrm{T}}$. Consequently, assuming that CRB(δ) exists (under $\mathcal{H}_0$ and $\mathcal{H}_1$), is well defined (see section "MSRL closed-form expression" for the necessary[e] and sufficient conditions) and is a tight bound (i.e., achievable under quite general/weak conditions [36,37]), thus the noncentral parameter $\kappa'(P_{\mathrm{fa}}, P_{\mathrm{d}})$ is given by [[35], p. 239]

$$\kappa'(P_{\mathrm{fa}},P_{\mathrm{d}}) = \delta^2(\mathrm{CRB}(\delta))^{-1}. \tag{13}$$

On the other hand, one can notice that the noncentral parameter $\kappa'(P_{\mathrm{fa}}, P_{\mathrm{d}})$ can be determined numerically by the choice of P_{fa} and P_{d} [13,28] as the solution of

$$\mathcal{Q}^{-1}_{\chi^2_1}(P_{\mathrm{fa}}) = \mathcal{Q}^{-1}_{\chi'^2_1(\kappa'(P_{\mathrm{fa}},P_{\mathrm{d}}))}(P_{\mathrm{d}}), \tag{14}$$

in which $\mathcal{Q}^{-1}_{\chi^2_1}(\varpi)$ and $\mathcal{Q}^{-1}_{\chi'^2_1(\kappa'(P_{\mathrm{fa}},P_{\mathrm{d}}))}(\varpi)$ are the inverse of the right tail of the χ^2_1 and $\chi'^2_1(\kappa'(P_{\mathrm{fa}},P_{\mathrm{d}}))$ pdf starting at the value ϖ. Finally, from (13) and (14) one obtains[f]

$$\delta = \kappa(P_{\mathrm{fa}},\ P_{\mathrm{d}})\sqrt{\mathrm{CRB}(\delta)}, \tag{15}$$

where $\sqrt{\kappa(P_{\mathrm{fa}},P_{\mathrm{d}})} = \kappa'(P_{\mathrm{fa}},P_{\mathrm{d}})$ is the so-called translation factor [13] which is determined for a given probability of false alarm and probability of detection (see Figure 1 for the behavior of the translation factor versus P_{fa} and P_{d}).

Result 1: The asymptotic MSRL for model (5) in the case of P parameters of interest per signal ($P \geq 1$) is given by δ which is the solution of the following equation:

$$\delta^2 - \kappa^2(P_{\mathrm{fa}},P_{\mathrm{d}})(A_{\mathrm{direct}} + A_{\mathrm{cross}}) = 0, \tag{16}$$

where A_{direct} denotes the contribution of the parameters of interest belonging to the same dimension as follows

$$A_{\mathrm{direct}} = \sum_{p=1}^{P} \mathrm{CRB}(\omega_1^{(p)}) + \mathrm{CRB}(\omega_2^{(p)}) - 2\mathrm{CRB}(\omega_1^{(p)},\omega_2^{(p)}),$$

and where A_{cross} is the contribution of the cross terms between distinct dimension given by

$$A_{\mathrm{cross}} = \sum_{p=1}^{P}\sum_{\substack{p'=1 \\ p'\neq p}}^{P} g_p g_{p'}(\mathrm{CRB}(\omega_1^{(p)},\omega_1^{(p')}) + \mathrm{CRB}(\omega_2^{(p)},\omega_2^{(p')}) - 2\mathrm{CRB}(\omega_1^{(p)},\omega_2^{(p')})),$$

in which $g_p = \mathrm{sgn}\left(\omega_1^{(p)} - \omega_2^{(p)}\right)$.

Proof see Appendix 1.

Remark 1: It is worth noting that the hypothesis test (8) is a binary one-sided test and that the MLE used is

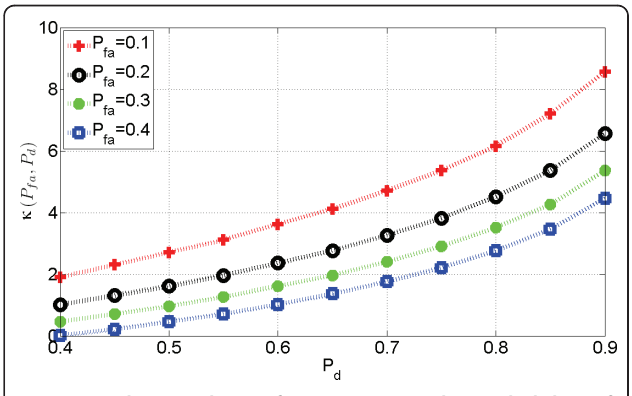

Figure 1 The translation factor κ versus the probability of detection P_{d} and P_{fa}. One can notice that increasing P_{d} or decreasing P_{fa} has the effect to increase the value of the translation factor κ. This is expected since increasing P_{d} or decreasing P_{fa} leads to a more selective decision [28,35].

an unconstrained estimator. Thus, one can deduce that the GLRT, used to derive the asymptotic MSRL [13,35]: (i) is the asymptotically uniformly most powerful test among all invariant statistical tests, and (ii) has an asymptotic constant false-alarm rate (CFAR). Which is, in the asymptotic case, considered as the *strongest* statement of optimality that one could expect to obtain [28].

- *Existence of the MSRL*: It is natural to assume that the CRB is a non-increasing (i.e., decreasing or constant) function on $\mathbb{R}^+$ w.r.t. δ since it is more difficult to estimate two closely spaced signals than two largely-spaced ones. In the same time the left hand side of (15) is a monotonically increasing function w. r.t. δ on $\mathbb{R}^+$. Thus for a fixed couple $(P_{\text{fa}}, P_{\text{d}})$, the solution of the implicit equation given by (15) always exists. However, theoretically, there is no assurance that the solution of equation (15) is unique.
- Note that, in practical situation, the case where CRB(δ) is not a function of δ is important since in this case, CRB(δ) is constant w.r.t. δ and thus the solution of (15) exists and is unique (see section "MSRL closed-form expression").

In the following section, we study the explicit effect of this so-called translation factor.

The relationship between the MSRL based on the CRB and the hypothesis test approaches

In this section, we link the asymptotic MSRL (derived using the hypothesis test approach, see Result 1) to a new proposed extension of the SRL based on the Smith criterion [11]. First, we recall that the Smith criterion defines the SRL in the case of $P = 1$ only. Then, we extend this criterion to $P \geq 1$ (i.e., the case of the multidimensional harmonic model). Finally, we link the MSRL based on the hypothesis test approach (see Result 1) to the MSRL based on the CRB approach (i.e., the extended SRL based on the Smith criterion).

The Smith criterion: Since the CRB expresses a lower bound on the covariance matrix of any unbiased estimator, then it expresses also the ultimate estimation accuracy. In this context, Smith proposed the following criterion for the case of two source signals parameterized each one by only one frequency [11]: *two signals are resolvable if the difference between their frequency,* $\delta_{\boldsymbol{\omega}^{(1)}} = \omega_2^{(1)} - \omega_1^{(1)}$, *is greater than the standard deviation of the frequency difference estimation.* Since, the standard deviation can be approximated by the CRB, then, the SRL, in the Smith criterion sense, is defined as the limit of $\delta_{\boldsymbol{\omega}^{(1)}}$ for which $\delta_{\boldsymbol{\omega}^{(1)}} < \sqrt{\text{CRB}(\delta_{\boldsymbol{\omega}^{(1)}})}$ is achieved. This means that, the SRL is the solution of the following implicit equation

$$\delta^2_{\boldsymbol{\omega}^{(1)}} = \text{CRB}(\delta_{\boldsymbol{\omega}^{(1)}}).$$

The extension of the Smith criterion to the case of $P \geq 1$: Based on the above framework, a straightforward extension of the Smith criterion to the case of $P \geq 1$ for the multidimensional harmonic model is as follows: *two multidimensional harmonic retrieval signals are resolvable if the distance between* C_1 *and* C_2, *is greater than the standard deviation of the* δ_{CRB} *estimation.* Consequently, assuming that the CRB exists and is well defined, the MSRL δ_{CRB} is given as the solution of the following implicit equation

$$\begin{cases} \delta^2_{\text{CRB}} = \text{CRB}(\delta_{\text{CRB}}) \\ \text{s.t.} \quad \delta_{\text{CRB}} = \sum_{p=1}^{P} |\omega_2^{(p)} - \omega_1^{(P)}|. \end{cases} \tag{17}$$

Comparison and link between the MSRL based on the CRB approach and the MSRL based on the hypothesis test approach: The MSRL based on the hypothesis test approach is given as the solution of

$$\begin{cases} \delta = \kappa(P_{\text{fa}}, P_{\text{d}})\sqrt{\text{CRB}(\delta)}, \\ \text{s.t.} \quad \delta = \sum_{p=1}^{P} \left|\omega_2^{(p)} - \omega_1^{(p)}\right|, \end{cases}$$

whereas the MSRL based on the CRB approach is given as the solution of (17). Consequently, one has the following result:

Result 2: Upon to a translation factor, the asymptotic MSRL based on the hypothesis test approach (i.e., using the binary one-sided hypothesis test given in (8)) is equivalent to the proposed MSRL based on the CRB approach (i. e., using the extension of the Smith criterion). Consequently, the criterion given in (17) is equivalent to an asymptotically uniformly most powerful test among all invariant statistical tests for $\kappa(P_{\text{fa}}, P_{\text{d}}) = 1$ (see Figure 2 for the values of $(P_{\text{fa}}, P_{\text{d}})$ such that $\kappa\ (P_{\text{fa}}, P_{\text{d}}) = 1$).

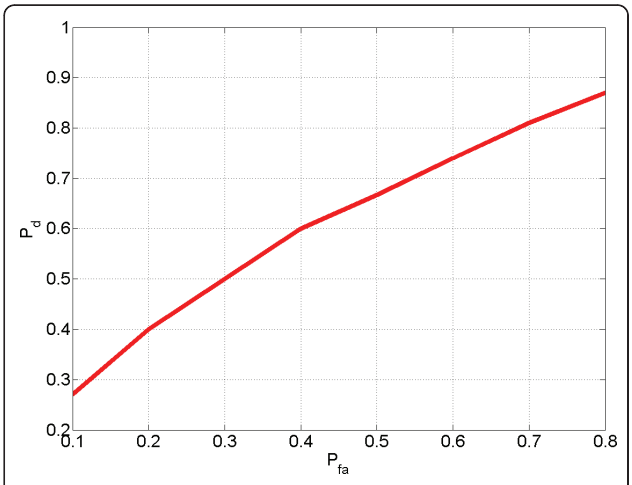

Figure 2 All values of $(P_{\text{fa}}, P_{\text{d}})$ such that $\kappa(P_{\text{fa}}, P_{\text{d}}) = 1$.

The following section is dedicated to the analytical computation of closed-form expression of the MSRL. In section "Assumptions," we introduce the assumptions used to compute the MSRL in the case of a Gaussian random noise and orthogonal waveforms. Then, we derive non matrix closed-form expressions of the CRB (note that to the best of our knowledge, no closed-form expressions of the CRB for such model is available in the literature). In "MSRL derivation" and thanks to these expressions, the MSRL wil be deduced using (16). Finally, the MSRL analysis is given.

MSRL closed-form expression

in section "Determination of the MSRL for two sources" we have defined the general model of the multidimensional harmonic model. To derive a closed-form expression of the MSRL, we need more assumptions on the covariance noise matrix and/or on the signal sources.

Assumptions

- The noise is assumed to be a complex circular white Gaussian random process i.i.d. with zero-mean and unknown variance $\sigma^2\mathbf{I}_{LN_1\dots N_P}$.
- We consider a multidimensional harmonic model due to the superposition of two harmonics each of them of dimension $P \geq 1$. Furthermore, for sake of simplicity and clarity, the sources have been assumed known and orthogonal (e.g., [7,38]). In this case, the unknown parameter vector is fixed and does not grow with the number of snapshots. Consequently, the CRB is an achievable bound [36].
- Each parameter of interest w.r.t. to the first signal, $\omega_1^{(p)}$ $p = 1 \dots P$, can be as close as possible to the parameter of interest w.r.t. to the second signal $\omega_2^{(p)}$ $p = 1 \dots P$, but not equal. This is not really a restrictive assumption, since in most applications, having two or more identical parameters of interest is a zero probability event [[9], p. 53].

Under these assumptions, the joint probability density function of the noisy observations y for a given unknown deterministic parameter vector $\boldsymbol{\xi}$ is as follows:

$$p(\mathbf{y}|\boldsymbol{\xi}) = \prod_{t=1}^{L} p(\mathrm{vec}(\boldsymbol{\mathcal{Y}}(t))|\boldsymbol{\xi}) = \frac{1}{(\pi\sigma^2)^{LN}} e^{\frac{-1}{\sigma^2}(\mathbf{y}-\mathbf{x})^{\mathrm{H}}(\mathbf{y}-\mathbf{x})},$$

where $N = \prod_{p=1}^{P} N_p$. The multidimensional harmonic retrieval model with known sources is considered herein, and thus, the parameter vector is given by

$$\boldsymbol{\xi} = \left[\boldsymbol{\omega}^{\mathrm{T}}\sigma^2\right]^{\mathrm{T}}, \tag{18}$$

where

$$\boldsymbol{\omega} = \left[\left(\boldsymbol{\omega}^{(1)}\right)^{\mathrm{T}} \cdots \left(\boldsymbol{\omega}^{(P)}\right)^{\mathrm{T}}\right]^{\mathrm{T}},$$

in which

$$\boldsymbol{\omega}^{(p)} = \left[\omega_1^{(p)}\omega_2^{(p)}\right]^{\mathrm{T}}. \tag{19}$$

CRB for the multidimensional harmonic model with orthogonal known signal sources

The Fisher information matrix (FIM) of the noisy observations $\mathbf{y}$ w.r.t. a parameter vector $\boldsymbol{\xi}$ is given by [39]

$$\mathbf{FIM}(\boldsymbol{\xi}) = \mathbb{E}\left\{\frac{\partial \ln p(\mathbf{y}|\boldsymbol{\xi})}{\partial \boldsymbol{\xi}}\left(\frac{\partial \ln p(\mathbf{y}|\boldsymbol{\xi})}{\partial \boldsymbol{\xi}}\right)^{\mathrm{H}}\right\}.$$

For a complex circular Gaussian observation model, the (ith, kth) element of the FIM for the parameter vector $\boldsymbol{\xi}$ is given by [34]

$$[\mathbf{FIM}(\boldsymbol{\xi})]_{i,k} = \frac{LN}{\sigma^4}\frac{\partial\sigma^2}{\partial[\boldsymbol{\xi}]_i}\frac{\partial\sigma^2}{\partial[\boldsymbol{\xi}]_k} + \frac{2}{\sigma^2}\Re\left\{\frac{\partial\mathbf{x}^{\mathrm{H}}}{\partial[\boldsymbol{\xi}]_i}\frac{\partial\mathbf{x}}{\partial[\boldsymbol{\xi}]_k}\right\} \quad (i,k) = \{1,\dots,2P+1\}^2. \tag{20}$$

Consequently, one can state the following lemma.

Lemma 1: The FIM for the sum of two P-order harmonic models with orthogonal known sources, has a block diagonal structure and is given by

$$\mathbf{FIM}(\boldsymbol{\xi}) = \frac{2}{\sigma^2}\begin{bmatrix}\mathbf{F}_{\boldsymbol{\omega}} & \mathbf{0}_{2P\times 1}\\ \mathbf{0}_{1\times 2P} & \times\end{bmatrix}, \tag{21}$$

where, the $(2P) \times (2P)$ matrix $\mathbf{F}_{\boldsymbol{\omega}}$ is also a block diagonal matrix given by

$$\mathbf{F}_{\boldsymbol{\omega}} = LN(\boldsymbol{\Delta} \otimes \mathbf{G}), \tag{22}$$

in which $\boldsymbol{\Delta} = \mathrm{diag}\{||\boldsymbol{\alpha}_1||^2, ||\boldsymbol{\alpha}_2||^2\}$ where

$$\boldsymbol{\alpha}_m = \begin{bmatrix}\alpha_m(1) & \dots & \alpha_m(L)\end{bmatrix}^{\mathrm{T}} \quad \text{for} \quad m \in \{1,2\}, \tag{23}$$

and

$$[\mathbf{G}]_{k,l} = \begin{cases}\dfrac{(2N_k-1)(N_k-1)}{6} & \text{for} \quad k = l,\\ \dfrac{(N_k-1)(N_l-1)}{2} & \text{for} \quad k \neq l.\end{cases}$$

Proof see Appendix 2.

After some calculation and using Lemma 1, one can state the following result.

Result 3: The closed-form expressions of the CRB for the sum of two P-order harmonic models with orthogonal known signal sources are given by

$$\mathrm{CRB}(\omega_m^{(p)}) = \frac{6}{LN\mathrm{SNR}_m}C_p, \quad m \in \{1,2\}, \tag{24}$$

where $\mathrm{SNR}_m = \frac{||\boldsymbol{\alpha}_m||^2}{\sigma^2}$ denotes the SNR of the mth source and where

$$C_p = \frac{N_p(1-3V_P)+3V_P+1}{(N_p+1)(N_p^2-1)} \quad \text{in which} \quad V_P = \frac{1}{1+3\sum_{p=1}^{P}\frac{N_p-1}{N_p+1}}.$$

Furthermore, the cross-terms are given by

$$\mathrm{CRB}(\omega_m^{(p)}, \omega_{m'}^{(p')}) = \begin{cases} 0 & \text{for } m \neq m', \\ \dfrac{-6}{LN\mathrm{SNR}_m}\tilde{C}_{p,p'} & \text{for } m = m' \text{ and } p \neq p', \end{cases} \quad (25)$$

where

$$\tilde{C}_{p,p'} = \frac{3V_P}{(N_p+1)(N_{p'}+1)}.$$

Proof see Appendix 3.

MSRL derivation

Using the previous result, one obtains the unique solution of (16), thus, the MSRL for model (1) is given by the following result:

Result 4: The MSRL for the sum of P-order harmonic models with orthogonal known signal sources, is given by

$$\delta = \sqrt{\frac{6}{LN\mathrm{ESNR}}\left(\sum_{p=1}^{P} C_p - \sum_{\substack{p,p'=1 \\ p\neq p'}}^{P} g_p g_{p'} \tilde{C}_{p,p'}\right)}, \quad (26)$$

where the so-called extended SNR is given by $\mathrm{ESNR} = \frac{\mathrm{SNR}_1\mathrm{SNR}_2}{\mathrm{SNR}_1+\mathrm{SNR}_2}$.

Proof see Appendix 4.

Numerical analysis

Taking advantage of the latter result, one can analyze the MSRL given by (26):

- First, from Figure 3 note that the numerical solution of the MSRL based on (12) is in good agreement with the analytical expression of the MSRL (23), which validate the closed-form expression given in (23). On the other hand, one can notice that, for $P_{\mathrm{d}} = 0.37$ and $P_{\mathrm{fa}} = 0.1$ the MSRL based on the CRB is exactly equal to the MSRL based on hypothesis test approach derived in the asymptotic case. From the case $P_{\mathrm{d}} = 0.49$ and $P_{\mathrm{fa}} = 0.3$ or/and $P_{\mathrm{d}} = 0.32$ and $P_{\mathrm{fa}} = 0.1$, one can notice the influence of the translation factor $\kappa(P_{\mathrm{fa}}, P_{\mathrm{d}})$ on the MSRL.

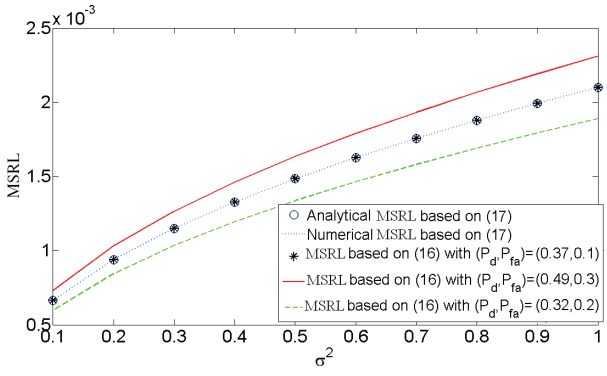

Figure 3 MSRL versus σ^2 for $L = 100$.

- The $\mathrm{MSRL}^{\mathrm{g}}$ is $O\left(\sqrt{\frac{1}{\mathrm{ESNR}}}\right)$ which is consistent with some previous results for the case $P = 1$ (e.g., [12,14,24]).
- From (26) and for a large number of sensors $N_1 = N_2 = \ldots = N_P = N \gg 1$, one obtains a simple expression

$$\delta = \sqrt{\frac{12}{LN^{P+1}\mathrm{ESNR}}\frac{P}{1+3P}},$$

meaning that, the SRL is $O\left(\sqrt{\frac{1}{N^{P+1}}}\right)$.

- Furthermore, since P ≥ 1, one has

$$\frac{(P+1)(3P+1)}{P(3P+4)} < 1,$$

and consequently, the ratio between the MSRL of a multidimensional harmonic retrieval with P parameters of interest, denoted by δ_P and the MSRL of a multidimensional harmonic retrieval with $P + 1$ parameters of interest, denoted by δ_{P+1}, is given by

$$\frac{\delta_{P+1}}{\delta_P} = \sqrt{\frac{(P+1)(3P+1)}{NP(3P+4)}}, \quad (27)$$

meaning that the MSRL for $P + 1$ parameters of interest is less than the one for P parameters of interest (see Figure 4). This, can be explained by the estimation additional parameter and also by an increase of the received noisy data thanks to the additional dimension. One should note that this property is proved theoretically thanks to (27) using the assumption of an equal and large number of sensors. However, from Figure 4 we notice that, in practice, this can be verified even for a

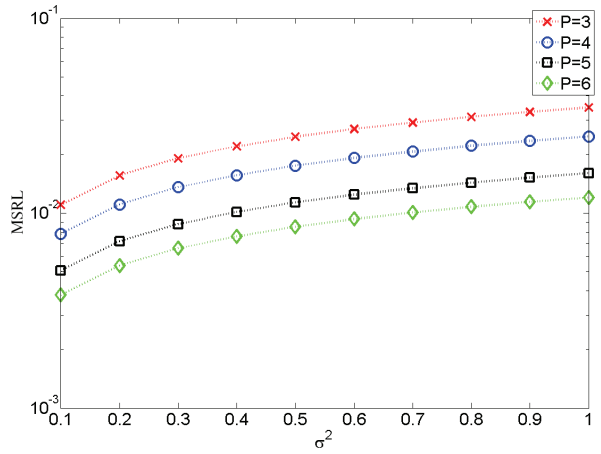

Figure 4 The SRL for multidimensional harmonic retrieval with orthogonal known sources for M equally powered sources, where P = 3, 4, 5, 6, L = 100, and the numbers of sensors are given by N_1 = 3, N_2 = 5, N_3 = 4, N_4 = 4, N_5 = 4, and N_6 = 3.

small number of sensors (e.g., in Figure 4 one has $3 \leq N_p \leq 5$ for p = 3, ..., 6).

- Furthermore, since

$$\sqrt{\frac{4}{LN^{P+1}\mathrm{ESNR}}} \leq \delta_P < \delta_{P-1} < \cdots < \delta_1$$

one can note that, the SRL is lower bounded by $\sqrt{\frac{4}{LN^{P+1}\mathrm{ESNR}}}$.

- One can address the problem of finding the optimal distribution of power sources making the SRL the smallest as possible (s.t. the constraint of constant total source power). In this issue, one can state the following corollary: *Corollary 1:* The optimal power's source distribution that ensures the smallest MSRL is obtained only for the equi-powered sources case.

Proof see Appendix 5.

This result was observed numerically for P = 1 in [12] (see Figure 5 for the multidimensional harmonic model). Moreover, it has been shown also by simulation for the case P = 1 that the so-called maximum likelihood breakdown (i.e., when the mean square error of the MLE increases rapidly) occurs at higher SNR in the case of different power signal sources than in the case of equi-powered signal sources [40]. The authors explained it by the fact that one source grabs most of the total power, then, this latter will be estimated more accurately, whereas the second one, will take an arbitrary parameter

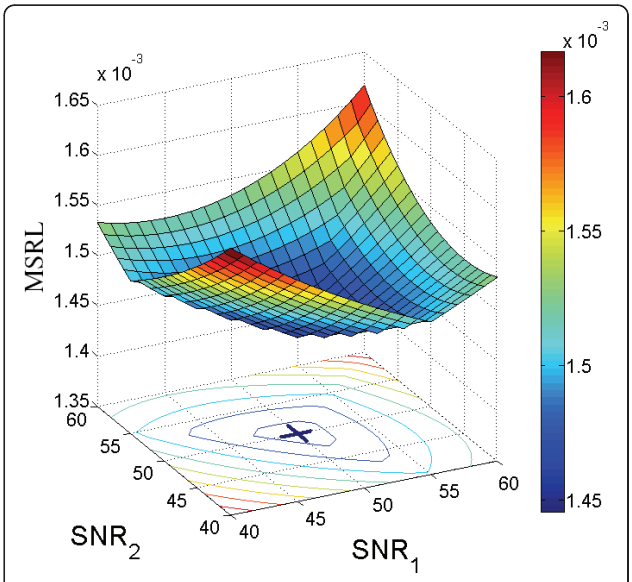

Figure 5 MSRL versus SNR_1, the SNR of the first source, and SNR_2, the SNR of the second source. One can notice that the optimal distribution of the SNR (which corresponds to the lowest MSLR) corresponds to $\mathrm{SNR}_1 = \mathrm{SNR}_2 = \frac{\mathrm{SNR}_{\mathrm{total}}}{2}$ as predicted by Corollary 1.

estimation which represents an outlier.

- In the same way, let us consider the problem of the optimal placement of the sensors[h] N_1, ...,N_P , making the minimum MSRL s.t. the constraint that the total number of sensors is constant (i.e., $N_{\mathrm{total}} = \sum_{p=1}^{P} N_p$ in which we suppose that N_{total} is a multiple of P).

Corollary 2: If the total number of sensors N_{total}, is a multiple of P, then an optimal placement of the sensors that ensure the lowest MSRL is (see Figure 6 and 7)

$$N_1 = \cdots = N_P = \frac{N_{\mathrm{total}}}{P}. \tag{28}$$

Proof see Appendix 6.

Remark 3: Note that, in the case where N_{total} is not a multiple of P, one expects that the optimal MSRL is given in the case where the sensors distribution approaches the equi-sensors distribution situation given in corollary 3. Figure 7 confirms that (in the case of P = 3, N_1 = 8 and a total number of sensors N = 22). From Figure 7, one can notice that the optimal distribution of the number of sensors corresponds to $N_2 = N_3$ = 7 and N_1 = 8 which is the nearest situation to the equi-sensors distribution.

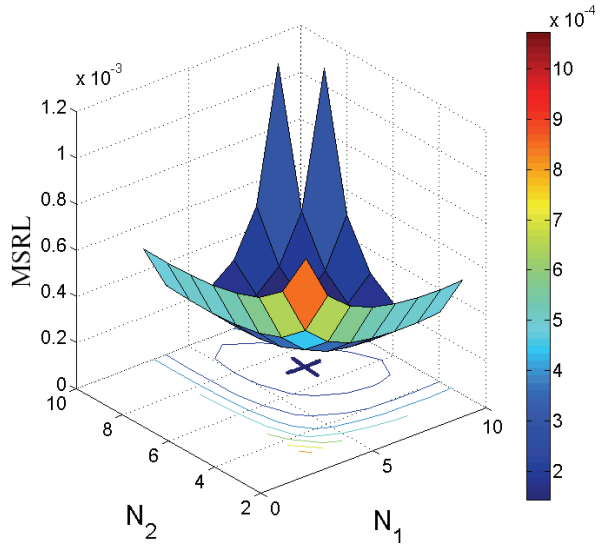

Figure 6 The MSRL versus N_1 and N_2 in the case of $P = 3$ and a total number of sensors $N_{\text{total}} = 21$. One can notice that the optimal distribution of the number of sensors (which corresponds to the lowest SLR) corresponds to $N_1 = N_2 = N_3 = \frac{N_{\text{total}}}{3}$ as predicted by (28).

Conclusion

In this article, we have derived the MSRL for the multi-dimensional harmonic retrieval model. Toward this end, we have extended the concept of SRL to multiple parameters of interest per signal. First, we have used a hypothesis test approach. The applied test is shown to be asymptotically an uniformly most powerful test which is the *strongest* statement of optimality that one could hope to obtain. Second, we have linked the asymptotic MSRL based on the hypothesis test approach to a new extension of the SRL based on the Cramér-Rao bound approach. Using the Cramér-Rao bound and a proper change of variable formula, closed-form expression of the MSRL are given.

Finally, note that the concept of the MSRL can be used to optimize, for example, the waveform and/or the array geometry for a specific problem.

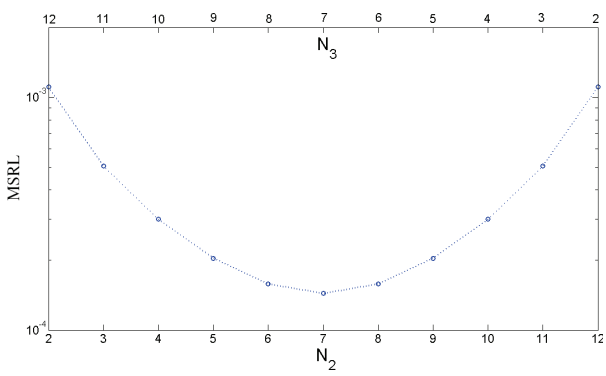

Figure 7 The plot of the MSRL versus N_2 in the case of $P = 3$, $N_1 = 8$ and a total number of sensors $N = 22$.

Appendix 1

The proof of Result 1

Appendix 1.1: In this appendix, we derive the MSRL using the l_1 norm.

From $\mathbf{CRB}(\boldsymbol{\xi})$ where $\boldsymbol{\xi} = [\boldsymbol{\omega}^{\mathrm{T}}\ \boldsymbol{\rho}^{\mathrm{T}}]\mathrm{T}$ in which $\boldsymbol{\omega} = [\omega_1^{(1)}\omega_2^{(1)}\omega_1^{(2)}\omega_2^{(2)}\cdots\omega_1^{(P)}\omega_2^{(P)}]^{\mathrm{T}}$, one can deduce $\mathbf{CRB}(\breve{\boldsymbol{\xi}})$ where $\breve{\boldsymbol{\xi}} = \mathbf{g}(\boldsymbol{\xi}) = [\delta\ \boldsymbol{\vartheta}^{\mathrm{T}}]^{\mathrm{T}}$ in which $\boldsymbol{\vartheta} \triangleq [\omega_2^{(1)}(\boldsymbol{\omega}^{(2)})^{\mathrm{T}}\cdots(\boldsymbol{\omega}^{(P)})^{\mathrm{T}}]^{\mathrm{T}}$. Thanks to the Jacobian matrix given by

$$\frac{\partial \mathbf{g}(\boldsymbol{\xi})}{\partial \boldsymbol{\xi}} = \begin{bmatrix} \mathbf{h}^{\mathrm{T}} & \mathbf{0} \\ \mathbf{A} & \mathbf{0} \\ \mathbf{0} & \mathbf{I} \end{bmatrix},$$

where $\mathbf{h} = [g_1 g_2\ \ldots\ g_P\ ]^{\mathrm{T}} \otimes [1\ -\ 1]^{\mathrm{T}}$, in which $g_p = \frac{\partial \delta}{\partial \omega_1^{(p)}} = -\frac{\partial \delta}{\partial \omega_2^{(p)}} = \mathrm{sgn}\,(\omega_1^{(p)} - \omega_2^{(p)})$ and $\mathbf{A} = [\mathbf{0}\ \mathbf{I}]$. Using the change of variable formula

$$\mathbf{CRB}(\breve{\boldsymbol{\xi}}) = \frac{\partial \mathbf{g}(\breve{\boldsymbol{\xi}})}{\partial \breve{\boldsymbol{\xi}}} \mathbf{CRB}(\boldsymbol{\xi}) \left(\frac{\partial \mathbf{g}(\breve{\boldsymbol{\xi}})}{\partial \breve{\boldsymbol{\xi}}}\right)^{\mathrm{T}}, \tag{29}$$

one has

$$\mathbf{CRB}(\breve{\boldsymbol{\xi}}) = \begin{bmatrix} \mathbf{h}^{\mathrm{T}}\mathbf{CRB}(\boldsymbol{\omega})\mathbf{h} & \times \\ \times & \mathbf{I} \end{bmatrix}.$$

Consequently, after some calculus, one obtains

$$\begin{aligned} \mathbf{CRB}(\delta) &\triangleq [\mathbf{CRB}(\breve{\boldsymbol{\xi}})]_{1,1} = \mathbf{h}^{\mathrm{T}}\mathbf{CRB}(\boldsymbol{\omega})\mathbf{h} \\ &= \sum_{p=1}^{2P}\sum_{p'=1}^{2P} [\mathbf{h}]_p [\mathbf{h}]_{p'} [\mathbf{CRB}(\boldsymbol{\omega})]_{p,p'} \\ &= \sum_{p=1}^{P}\sum_{p'=1}^{P} g_p g_{p'} \left([\mathbf{CRB}(\boldsymbol{\xi})]_{2p,2p'} + [\mathbf{CRB}(\boldsymbol{\xi})]_{2p-1,2p'-1} - [\mathbf{CRB}(\boldsymbol{\xi})]_{2p,2p'-1} - [\mathbf{CRB}(\boldsymbol{\xi})]_{2p-1,2p'} \right) \\ &\triangleq A_{\text{direct}} + A_{\text{cross}}, \end{aligned} \tag{30}$$

where

$A_{\text{direct}} = \sum_{p=1}^{P} \mathrm{CRB}(\omega_1^{(p)}) + \mathrm{CRB}(\omega_2^{(p)}) - 2\mathrm{CRB}(\omega_1^{(p)}, \omega_2^{(p)})$

and where $A_{\text{cross}}(k) = \sum_{p=1}^{P}\sum_{\substack{p'=1 \\ p'\neq p}}^{P} g_p g_{p'} \left(\mathrm{CRB}(\omega_1^{(p)}, \omega_1^{(p')}) + \mathrm{CRB}(\omega_2^{(p)}, \omega_2^{(p')}) - 2\mathrm{CRB}(\omega_1^{(p)}, \omega_2^{(p')}) \right)$

Finally using (30) one obtains (16)

Appendix 1.2: In this part, we derive the MSRL using the l_k norm for a given integer $k \geq 1$. The aim of this part is to support the endnote a, which stays that using the l_1 norm computing the MSRL using the l_1 norm is for the calculation convenience.

Once again, from $\mathbf{CRB}(\xi)$, one can deduce $\mathbf{CRB}(\breve{\xi}_k)$ where $\breve{\xi}_k = \mathbf{g}_k(\boldsymbol{\xi}) = [\delta(k)\ \boldsymbol{\vartheta}^{\mathrm{T}}]^{\mathrm{T}}$ in which the distance between C_1 and C_2 using the l_k norm is given by $\delta(k) \triangleq$

k-norm $\text{distance}(\mathcal{C}_1, \mathcal{C}_2) = \left(\sum_{p=1}^{P} \delta_p^k\right)^{1/k}$ and where $\boldsymbol{\vartheta} \triangleq [\omega_2^{(1)}(\boldsymbol{\omega}^{(2)})^{\mathrm{T}} \dots (\boldsymbol{\omega}^{(P)})^{\mathrm{T}}]^{\mathrm{T}}$. The Jacobian matrix is given by

$$\frac{\partial \mathbf{g}(\boldsymbol{\xi})}{\partial \boldsymbol{\xi}} = \begin{bmatrix} \mathbf{h}_k^{\mathrm{T}} & \mathbf{0} \\ \mathbf{A} & \mathbf{0} \\ \mathbf{0} & \mathbf{I} \end{bmatrix},$$

where $\mathbf{h}_k = [1 \; -1]^{\mathrm{T}} \otimes [g_1(k) g_2(k) \dots g_P(k)]^{\mathrm{T}}$, in which $g_p(k) = \dfrac{\partial \delta(k)}{\partial \omega_1^{(p)}} = -\dfrac{\partial \delta(k)}{\partial \omega_2^{(p)}}$ and $\mathbf{A} = [\mathbf{0}\mathbf{I}]$. Since $|x|^k$ can be written as $\sqrt{x^{2k}}$. Thus, for $\times \neq 0$, one has

$$\begin{aligned} g_p(k) &= \frac{\partial\left(\sum_{p'=1}^{P}\sqrt{\left(\omega_1^{(p')}-\omega_2^{(p')}\right)^{2k}}\right)^{1/k}}{\partial \omega_1^{(p)}} = \frac{1}{k}\left(\sum_{i=1}^{P}\sqrt{\left(\omega_1^{(i)}-\omega_2^{(i)}\right)^{2k}}\right)^{\frac{1}{k}-1}\frac{\partial\sqrt{\left(\omega_1^{(i)}-\omega_2^{(i)}\right)^{2k}}}{\partial \omega_1^{(i)}} \\ &= \operatorname{sgn}(\omega_1^{(p)}-\omega_2^{(p)})\left(\sum_{p=1}^{P}\sqrt{\left(\omega_1^{(p')}-\omega_2^{(p')}\right)^{2k}}\right)^{\frac{1}{k}-1}\sqrt{\left(\omega_1^{(p)}-\omega_2^{(p)}\right)^{2(k-1)}} = \operatorname{sgn}(\omega_1^{(p)}-\omega_2^{(p)})\delta^{1-k}\delta_p^{k-1}. \end{aligned} \tag{31}$$

Again, using the change of variable formula (29), one has

$$\mathbf{CRB}(\breve{\boldsymbol{\xi}}_k) = \begin{bmatrix} \mathbf{h}_k^{\mathrm{T}}\mathbf{CRB}(\boldsymbol{\omega})\mathbf{h}_k & \times \\ \times & \mathbf{I} \end{bmatrix}.$$

Consequently, after some calculus, one obtains

$$\begin{aligned} \mathrm{CRB}(\delta(k)) &\triangleq [\mathbf{CRB}(\breve{\boldsymbol{\xi}}_k)]_{1,1} \\ &= \sum_{p=1}^{P}\sum_{p'=1}^{P} g_p(k) g_{p'}(k)([\mathbf{CRB}(\boldsymbol{\xi})]_{2p,2p'} + [\mathbf{CRB}(\boldsymbol{\xi})]_{2p-1,2p'-1} - [\mathbf{CRB}(\boldsymbol{\xi})]_{2p,2p'-1} - [\mathbf{CRB}(\boldsymbol{\xi})]_{2p-1,2p'}) \\ &= (\delta(k))^{2(1-k)}(A_{\mathrm{direct}}(k) + A_{\mathrm{cross}}(k)), \end{aligned} \tag{32}$$

where

$A_{\mathrm{direct}}(k) = \sum_{p=1}^{P} \delta_p^{2(k-1)}\left(\mathrm{CRB}(\omega_1^{(p)}) + \mathrm{CRB}(\omega_2^{(p)}) - 2\mathrm{CRB}(\omega_1^{(p)}, \omega_2^{(p)})\right)$ and where $A_{\mathrm{cross}}(k) = \sum_{p=1}^{P}\sum_{\substack{p'=1 \\ p'\neq p}}^{P} \delta_p^{k-1}\delta_{p'}^{k-1}\operatorname{sgn}(\omega_1^{(p)}-\omega_2^{(p)})\operatorname{sgn}(\omega_1^{(p')}-\omega_2^{(p')})\left(\mathrm{CRB}(\omega_1^{(p)}, \omega_1^{(p')}) + \mathrm{CRB}(\omega_2^{(p)}, \omega_2^{(p')}) - 2\mathrm{CRB}(\omega_1^{(p)}, \omega_2^{(p')})\right)$.

Consequently, note that resolving analytically the implicit equation (32) w.r.t. $\delta(k)$ is intractable (aside from some special cases). Whereas, resolving analytically the implicit equation (30) can be tedious but feasible (see section "MSRL closed form expression").

Furthermore, denoting $g_p(1) = g_p$, $A_{\mathrm{cross}}(1) \triangleq A_{\mathrm{cross}}$ and $A_{\mathrm{direct}}(1) \triangleq A_{\mathrm{direct}}$ and using (32) one obtains (16).

Appendix 2

Proof of Lemma 1

From (20) one can note the well-known property that the model signal parameters are decoupled from the noise variance [42]. Consequently, the block-diagonal structure in (21) is self-evident.

Now, let us prove (22). From (4), one obtains

$$\frac{\partial \mathrm{vec}(\boldsymbol{\mathcal{X}}(t))}{\partial \omega_m^{(p)}} = j s_m(t)\left(\boldsymbol{a}(\omega_m^{(1)}) \otimes \boldsymbol{a}(\omega_m^{(2)}) \otimes \cdots \otimes \boldsymbol{a}'(\omega_m^{(p)}) \otimes \cdots \otimes \boldsymbol{a}(\omega_m^{(P)})\right),$$

where

$$\boldsymbol{a}'(\omega_m^{(p)}) = \left[0 \quad e^{j\omega_m^{(p)}} \quad \dots \quad (Np-1)e^{j(Np-1)\omega_m^{(p)}}\right]^{\mathrm{T}}.$$

Thus,

$$\frac{\partial \mathbf{x}}{\partial \omega_m^{(p)}} = j\boldsymbol{s}_m \otimes \left(\boldsymbol{a}(\omega_m^{(1)}) \otimes \boldsymbol{a}(\omega_m^{(2)}) \otimes \cdots \otimes \boldsymbol{a}'(\omega_m^{(p)}) \otimes \cdots \otimes \boldsymbol{a}(\omega_m^{(P)})\right),$$

where $s_m = [s_m(1) \dots s_m(L)]^{\mathrm{T}}$. Using the distributivity of the Hermitian operator over the Kronecker product and the mixed-product property of the Kronecker product [43] and assuming, without loss of generality that $p' < p$, one obtains

$$\begin{aligned} \left(\frac{\partial \mathbf{x}}{\partial \omega_m^{(p)}}\right)^{\mathrm{H}}\frac{\partial \mathbf{x}}{\partial \omega_m^{(p')}} &= \left(\boldsymbol{s}_{m'}^{\mathrm{H}} \otimes \left[\boldsymbol{a}^{\mathrm{H}}(\omega_{m'}^{(1)}) \otimes \boldsymbol{a}^{\mathrm{H}}(\omega_{m'}^{(2)}) \otimes \cdots \otimes \boldsymbol{a}'^{\mathrm{H}}(\omega_{m'}^{(p')}) \otimes \cdots \otimes \boldsymbol{a}^{\mathrm{H}}(\omega_{m'}^{(P)})\right]\right) \\ &\quad \times \left(\boldsymbol{s}_m \otimes \left[\boldsymbol{a}(\omega_m^{(1)}) \otimes \boldsymbol{a}(\omega_m^{(2)}) \otimes \cdots \otimes \boldsymbol{a}'(\omega_m^{(p)}) \otimes \cdots \otimes \boldsymbol{a}(\omega_m^{(P)})\right]\right) \\ &= (\boldsymbol{s}_{m'}^{\mathrm{H}}, \boldsymbol{s}_m) \otimes \left(\boldsymbol{a}^{\mathrm{H}}(\omega_{m'}^{(1)})\boldsymbol{a}(\omega_m^{(1)})\right) \otimes \cdots \otimes \left(\boldsymbol{a}'^{\mathrm{H}}(\omega_{m'}^{(p)})\boldsymbol{a}(\omega_m^{(p)})\right) \otimes \dots \\ &\quad \dots \otimes \left(\boldsymbol{a}^{\mathrm{H}}(\omega_m^{(p')})\boldsymbol{a}'(\omega_{m'}^{(p')})\right) \otimes \cdots \otimes \left(\boldsymbol{a}^{\mathrm{H}}(\omega_{m'}^{(P)})\boldsymbol{a}(\omega_m^{(P)})\right). \end{aligned} \tag{33}$$

On the other hand, one has

$$\boldsymbol{a}^{\mathrm{H}}(\omega_m^{(p)})\boldsymbol{a}(\omega_m^{(p)}) = N_p, \tag{34}$$

whereas

$$\boldsymbol{a}^{\mathrm{H}}(\omega_m^{(p)})\boldsymbol{a}'(\omega_m^{(p)}) = \frac{N_p(N_p-1)}{2} \quad \text{and} \quad \boldsymbol{a}'^{\mathrm{H}}(\omega_m^{(p)})\boldsymbol{a}'(\omega_m^{(p)}) = \frac{N_p(2N_p-1)(N_p-1)}{6} \tag{35}$$

Finally, assuming known orthogonal wavefronts [38] (i.e., $\boldsymbol{s}_{m'}^{\mathrm{H}}\boldsymbol{s}_m = 0$) and replacing (35) and (34) into (33), one obtains

$$\left(\frac{\partial \mathbf{x}}{\partial \omega_m^{(p)}}\right)^{\mathrm{H}}\frac{\partial \mathbf{x}}{\partial \omega_{m'}^{(p')}} = \begin{cases} 0 & \text{for } m \neq m', \\ L||\boldsymbol{\alpha}_m||^2 N\dfrac{(N_p-1)(N_{p'}-1)}{4} & \text{for } m = m' \text{ and } p \neq p', \\ L||\boldsymbol{\alpha}_m||^2 N\dfrac{(2N_p-1)(N_p-1)}{6} & \text{for } m = m' \text{ and } p = p', \end{cases} \tag{36}$$

where $\boldsymbol{\alpha}_m = [\alpha_m(1) \dots \alpha_m(L)]$ for $m \in \{1, 2\}$: Consequently, using (36), $\mathbf{F}_{\boldsymbol{\omega}}$ can be expressed as a block diagonal matrix

$$\mathbf{F}_{\boldsymbol{\omega}} = \begin{bmatrix} \mathbf{J}_1 & \mathbf{0} \\ \mathbf{0} & \mathbf{J}_2 \end{bmatrix}, \tag{37}$$

where each $P \times P$ block $\mathbf{J}_m$ is defined by

$$\mathbf{J}_m = L||\boldsymbol{\alpha}_m||^2 N\mathbf{G}, \tag{38}$$

where

$$\mathbf{G} = \begin{bmatrix} \dfrac{(N_1-1)(2N_1-1)}{6} & \dfrac{(N_1-1)(N_2-1)}{4} & \cdots & \dfrac{(N_1-1)(N_P-1)}{4} \\ \dfrac{(N_2-1)(N_1-1)}{4} & \dfrac{(N_2-1)(2N_2-1)}{6} & \cdots & \dfrac{(N_2-1)(N_P-1)}{4} \\ \vdots & \vdots & \ddots & \vdots \\ \dfrac{(N_P-1)(N_1-1)}{4} & \dfrac{(N_2P-1)(N_2-1)}{4} & \cdots & \dfrac{(N_P-1)(2N_P-1)}{6} \end{bmatrix}.$$

Consequently, from (37) and (38) one obtains (22).

Appendix 3

Proof of Result 3

Using (22) one obtains

$$\mathbf{CRB}(\boldsymbol{\omega}) = \frac{\sigma^2}{2}\mathbf{F}_{\boldsymbol{\omega}}^{-1} = \frac{\sigma^2}{2LN}(\boldsymbol{\Delta}^{-1} \otimes \mathbf{G}^{-1}) \tag{39}$$

where $\boldsymbol{\Delta}^{-1} = \text{diag}\left\{\frac{1}{||\boldsymbol{\alpha}_1||^2}, \frac{1}{||\boldsymbol{\alpha}_2||^2}\right\}$. In the following, we give a closed-form expression of $\mathbf{G}^{-1}$. One can notice that the matrix $\mathbf{G}$ has a particular structure such that it can be rewritten as the sum of a diagonal matrix and of a rank-one matrix: $\mathbf{G} = \mathbf{Q} + \boldsymbol{\gamma}\boldsymbol{\gamma}^{\mathrm{T}}$ where $\mathbf{Q} = \frac{1}{12}\text{diag}\{N_1^2 - 1, \ldots, N_P^2 - 1\}$ and $\boldsymbol{\gamma} = \frac{1}{2}[N_1 - 1, \ldots, N_P - 1]^{\mathrm{T}}$ Thanks to this particular structure, an analytical inverse of $\mathbf{G}$ can easily be obtained. Indeed, using the matrix inversion lemma

$$\begin{aligned}\mathbf{G}^{-1} &= (\mathbf{Q} + \boldsymbol{\gamma}\boldsymbol{\gamma}^{\mathrm{T}})^{-1} \\ &= \mathbf{Q}^{-1} - \frac{\mathbf{Q}^{-1}\boldsymbol{\gamma}\boldsymbol{\gamma}^{\mathrm{T}}\mathbf{Q}^{-1}}{1 + \boldsymbol{\gamma}^{\mathrm{T}}\mathbf{Q}^{-1}\boldsymbol{\gamma}}.\end{aligned} \tag{40}$$

A straightforward calculus leads to the following results,

$$\mathbf{Q}^{-1}\boldsymbol{\gamma}\boldsymbol{\gamma}^{\mathrm{T}}\mathbf{Q}^{-1} = 36\begin{bmatrix} \frac{1}{(N_1+1)^2} & \frac{1}{(N_1+1)(N_2+1)} & \cdots & \frac{1}{(N_1+1)(N_P+1)} \\ \frac{1}{(N_2+1)(N_1+1)} & \frac{1}{(N_2+1)^2} & \cdots & \frac{1}{(N_2+1)(N_P+1)} \\ \vdots & \vdots & \ddots & \vdots \\ \frac{1}{(N_P+1)(N_1+1)} & \frac{1}{(N_P+1)(N_2+1)} & \cdots & \frac{1}{(N_P+1)^2} \end{bmatrix}, \tag{41}$$

and

$$\boldsymbol{\gamma}^{\mathrm{T}}\mathbf{Q}^{-1}\boldsymbol{\gamma} = 3\sum_{p=1}^{P}\frac{N_p - 1}{N_p + 1}. \tag{42}$$

Consequently, replacing (41) and (42) into (40), one obtains

$$[\mathbf{G}^{-1}]_{k,l} = \begin{cases} 12\frac{N_p(1 - 3V_P) + 3V_P + 1}{(N_p + 1)(N_p^2 - 1)} & \text{for} \quad k = l, \\ -\frac{36V_P}{(N_p + 1)(N_{p'} + 1)} & \text{for} \quad k \neq l, \end{cases} \tag{43}$$

where $V_P = \left(1 + 3\sum_{p=1}^{P}\frac{N_p - 1}{N_p + 1}\right)^{-1}$. Finally, replacing (43) into (39) one finishes the proof.

Appendix 4

Proof of Result 4

Using Results 1 and 3, one has

$$\begin{aligned}A_{\text{direct}} &= \sum_{p=1}^{P}\left(\text{CRB}(\omega_1^{(p)}) + CRB\,(\omega_2^{(p)})\right) \\ &= \frac{6\sigma^2}{LN}\left(\frac{1}{||\boldsymbol{\alpha}_1||^2} + \frac{1}{||\boldsymbol{\alpha}_2||^2}\right)\sum_{p=1}^{P}\frac{N_p(1 - 3V_P) + 3V_P + 1}{(N_p + 1)(N_p^2 - 1)},\end{aligned} \tag{44}$$

and

$$\begin{aligned}A_{\text{cross}} &= \sum_{p=1}^{P}\sum_{\substack{p'=1 \\ p' \neq p}}^{P} g_p g_{p'}\left(\text{CRB}(\omega_1^{(p)}, \omega_1^{(p')}) + \text{CRB}(\omega_2^{(p)}, \omega_2^{(p')})\right) \\ &= -\frac{6\sigma^2}{LN}\left(\frac{1}{||\boldsymbol{\alpha}_1||^2} + \frac{1}{||\boldsymbol{\alpha}_2||^2}\right)\sum_{\substack{p,p'=1 \\ p \neq p'}}^{P}\frac{3g_p g_{p'} V_P}{(N_p + 1)(N_{p'} + 1)}.\end{aligned} \tag{45}$$

Consequently, replacing (44) and (45) into (16), one finishes the proof.

Appendix 5

Proof of Corollary 1

In this appendix, we minimize the MSRL under the constraint $\text{SNR}_1 + \text{SNR}_2 = \text{SNR}_{\text{total}}$ (where $\text{SNR}_{\text{total}}$ is a real fixed value). Since, the term $\left(\sum_{p=1}^{P} C_p - \sum_{\substack{p,p'=1 \\ p \neq p'}}^{P} g_p g_{p'}\tilde{C}_{p,p'}\right)$ is independent from SNR_1 and SNR_2, minimizing δ is equivalent to minimize $\mathcal{G}(\text{SNR}_1, \text{SNR}_2)$ where

$$\mathcal{G}(\text{SNR}_1, \text{SNR}_2) = \delta^2\frac{LN}{6}\left(\sum_{p=1}^{P} C_p - \sum_{\substack{p,p'=1 \\ p \neq p'}}^{P} g_p g_{p'}\tilde{C}_{p,p'}\right)^{-1} = \frac{\text{SNR}_1 + \text{SNR}_2}{\text{SNR}_1\text{SNR}_2}.$$

Using the method of Lagrange multipliers, the problem is as follows:

$$\begin{cases} \min_{\text{SNR}_1, \text{SNR}_2}\mathcal{G}(\text{SNR}_1, \text{SNR}_2) \\ \text{s.t.} \\ \text{SNR}_1 + \text{SNR}_2 = \text{SNR}_{\text{total}} \end{cases}$$

Thus, the Lagrange function is given by $\mathcal{F}(\text{SNR}_1, \text{SNR}_2, \lambda) = \mathcal{G}(\text{SNR}_1, \text{SNR}_2) + \lambda(\text{SNR}_1 + \text{SNR}_2 - \text{SNR}_{\text{total}})$ where λ denotes the so-called Lagrange multiplier. A simple derivation leads to,

$$\frac{\partial\mathcal{F}(\text{SNR}_1, \text{SNR}_2)}{\partial\ \text{SNR}_1} = \frac{-1}{\text{SNR}_1^2} + \lambda = 0 \tag{46}$$

$$\frac{\partial\mathcal{F}(\text{SNR}_1, \text{SNR}_2)}{\partial\ \text{SNR}_2} = \frac{-1}{\text{SNR}_2^2} + \lambda = 0 \tag{47}$$

$$\frac{\partial\mathcal{F}(\text{SNR}_1, \text{SNR}_2)}{\partial\lambda} = \text{SNR}_1 + \text{SNR}_2 - \text{SNR}_{\text{total}} = 0. \tag{48}$$

Consequently, from (46) and (47), one obtains $\text{SNR}_1 = \text{SNR}_1$. Using (48), one obtains $\text{SNR}_1 = \text{SNR}_2 = \frac{\text{SNR}_{\text{total}}}{2}$. Using the constraint $\text{SNR}_1 + \text{SNR}_2 = \text{SNR}_{\text{total}}$ one deduces *corollary* 1.

Appendix 6

Minimizing δ w.r.t. N_1, ..., N_P is equivalent to minimizing the function $f(\boldsymbol{N}) = \sum_{p=1}^{P} C_p - \sum_{\substack{p,p'=1 \\ p,\neq p'}}^{P} g_p g_{p'}\tilde{C}_{p,p'}$,

where $\boldsymbol{N} = [N_1 \dots N_P]^{\mathrm{T}}$. However, since the numbers of sensors on each array, $N_1, \dots, N_P$, are integers, the derivation of $f(\boldsymbol{N})$ *w.r.t.* $\boldsymbol{N}$ is meaningless. Consequently, let us define the function $\bar{f}(.)$ exactly as $f(.)$ where the set of definition is $\mathbb{R}^P$ instead of $\mathbb{N}^P$. Consequently,

$$\bar{f}(\bar{\boldsymbol{N}})|_{\bar{N}=N} = f(\boldsymbol{N}), \quad \text{where} \quad \bar{\boldsymbol{N}} = [\bar{N}_1 \dots \bar{N}_P]^{\mathrm{T}},$$

in which $\bar{N}_1, \dots, \bar{N}_P$ are real (continuous) variables.

Using the method of Lagrange multipliers, the problem is as follows:

$$\begin{cases} \min_{\bar{N}} \bar{f}(\bar{N}) \\ \sum_{p=1}^{P} \bar{N}_p = \bar{N}_{\text{total}} \end{cases}$$

where $\bar{N}_{\text{total}}$ is a real positive constant value. Thus, the Lagrange function is given by $\Lambda(\bar{\boldsymbol{N}}, \lambda) = \bar{f}(\bar{\boldsymbol{N}}) + \lambda \left(\sum_{p=1}^{P} \bar{N}_p - \bar{N}_{\text{total}} \right)$ where λ denotes the Lagrange multiplier. For a sufficient number of sensors, the Lagrange function can be approximated by

$$\Lambda(\bar{\boldsymbol{N}}, \lambda) \approx \sum_{p=1}^{P} \frac{\bar{N}_p(1-3V)+3V+1}{\bar{N}_p^3} - \sum_{\substack{p,p'=1 \\ p \neq p'}}^{P} \frac{3 g_p g_{p'} V}{\bar{N}_p \bar{N}_{p'}} + \lambda \left(\sum_{p=1}^{P} \bar{N}_p - \bar{N}_{\text{total}} \right)$$

where $V = \dfrac{1}{1+3P}$. A simple derivation leads to,

$$\frac{\partial \Lambda(\bar{\boldsymbol{N}}, \lambda)}{\partial \bar{N}_1} = \frac{3(V-1)}{\bar{N}_1^3} - \frac{3V+1}{\bar{N}_1^4} + \frac{3V}{\bar{N}_1^2} \sum_{\substack{p,p'=1 \\ p \neq p'}}^{P} \frac{g_p g_{p'}}{\bar{N}_{p'}} + \lambda = 0$$

$$\vdots$$

$$\frac{\partial \Lambda(\bar{\boldsymbol{N}}, \lambda)}{\partial \bar{N}_P} = \frac{3(V-1)}{\bar{N}_P^3} - \frac{3V+1}{\bar{N}_P^4} + \frac{3V}{\bar{N}_P^2} \sum_{\substack{p,p'=1 \\ p \neq p'}}^{P} \frac{g_p g_{p'}}{\bar{N}_{p'}} + \lambda = 0$$

$$\frac{\partial \Lambda(\bar{\boldsymbol{N}}, \lambda)}{\partial \lambda} = \sum_{p=1}^{P} \bar{N}_p - \bar{N}_{\text{total}} = 0.$$

This system of equations seems hard to solve. However, an obvious solution is given by $\bar{N}_1 = \dots = \bar{N}_P = \bar{N}$ and $\lambda = \dfrac{3V+1}{\bar{N}^4} - 3\dfrac{V(P\nu - 1) + V - 1}{\bar{N}^3}$ in which $\nu = \sum_{\substack{p,p'=1 \\ p \neq p'}}^{P} g_p g_{p'}$. Since, $\sum_{p=1}^{P} N_p = \bar{N}_{\text{total}}$, thus the trivial solution is given by $\bar{N}_1 = \dots = \bar{N}_P = \dfrac{\bar{N}_{\text{total}}}{P}$. Consequently, if $\bar{N}_{\text{total}}$ is a multiple of P then, the solution of minimizing the function $\bar{f}(\bar{\boldsymbol{N}})$ in $\mathbb{R}^P$ coincides the solution of minimizing the function $f(\boldsymbol{N})$ in $\mathbb{N}^P$. Thus, the optimal placement minimizing the MSRL is $N_1 = \dots = N_P = \dfrac{\bar{N}_{\text{total}}}{P}$. This conclude the proof.

Endnotes

[a]The notion of distance and closely spaced signals used in the following, is w.r.t. to the metric space (d, C), where $d : C \times C \to \mathbb{R}$ in which d and C denote a metric and the set of the parameters of interest, respectively. [b]See [2-9] for some practical examples for the multidimensional harmonic retrieval model. [c]This study can be straightforwardly extended to other norms. The choice of the l_1 is motivated by its calculation convenience (see the derivation of Result 1 and Appendix 1). Furthermore, since the MSRL is considered to be small (this assumption can be argued by the fact that the high-resolution algorithms have asymptotically an infinite resolving power [44]), thus all continuous p-norms are similar to (i.e., *looks like*) the l_1 norm. More importantly, in a finite dimensional vector space, all continuous p-norms are equivalent [[45], p. 53], thus the choice of a specific norm is free. [d]Note that, due to the specific definition of the SRL in [13] (i.e., using the same notation as in [13], $\delta = \cos(\boldsymbol{u}_1^{\mathrm{T}} \boldsymbol{u}_2)$)and the restrictive assumption in [13] ($\boldsymbol{u}_1$ and $\boldsymbol{u}_2$ belong to the same plan), the SRL as defined in [13] cannot be used in the multidimensional harmonic context. [e]One of the necessary conditions regardless the noise pdf is that $\omega_1^{(p)} \neq \omega_2^{(p)}$. Meaning that each parameter of interest w.r.t. to the first signal $\omega_1^{(p)}$ can be as close as possible to the parameter of interest w.r.t. to the second signal $\omega_2^{(p)}$, but not equal. This is not really a restrictive assumptions, since in most applications, having two or more identical parameters of interest is *a zero probability event* [[9], p. 53]. [f]Note that applying (15) for $P = 1$ and for $\kappa(P_{\text{fa}}, P_{\text{d}}) = 1$, one obtains the Smith criterion [11]. [g]Where $O(.)$ denotes the Landau notation [46]. [h]One should note, that we assumed a uniform linear multi-array, and the problem is to find the optimal distribution of the number of sensors on each array. The more general case, i.e., where the optimization problem considers the non linearity of the multi-way array, is beyond the scope of the problem addressed herein.

Abbreviations

CRB: Cramér-Rao Bound; DOAs: direction of arrivals; FIM: Fisher information matrix; GLRT: generalized likelihood ratio test; MLE: maximum likelihood estimates; MSRL: multidimensional SRL; PARAFAC: PARallel FACtor; pdf: probability density function; SNR: signal-to-noise ratio; SRL: statistical resolution limit.

Acknowledgements

This project is funded by region Île de France and Digiteo Research Park. This work has been partially presented in communication [41].

Competing interests

The authors declare that they have no competing interests.

Received: 10 November 2010 Accepted: 13 June 2011
Published: 13 June 2011

References

1. T Jiang, N Sidiropoulos, J ten Berge, Almost-sure identifiability of multidimensional harmonic retrieval. IEEE Trans. Signal Processing. 49(9), 1849–1859 (2001). doi:10.1109/78.942615

2. F Vanpoucke, *Algorithms and Architectures for Adaptive Array Signal Processing*. (Universiteit Leuven, Leuven, Belgium: Ph. D. dissertation, 1995)
3. M Haardt, J Nossek, 3-D unitary ESPRIT for joint 2-D angle and carrier estimation. Proc. of IEEE Int. Conf. Acoust., Speech, Signal Processing, Munich, Germany. **1**, 255–258 (1997)
4. K Wong, M Zoltowski, Uni-vector-sensor ESPRIT for multisource azimuth, elevation, and polarization estimation. IEEE Trans. Antennas Propagat. **45**(10), 1467–1474 (1997)
5. K Mokios, N Sidiropoulos, M Pesavento, C Mecklenbrauker, On 3-D harmonic retrieval for wireless channel sounding. in *Proc. of IEEE Int. Conf. Acoust., Speech, Signal Processing*, vol. 2, (Philadelphia, USA., 2004). pp. 89–92
6. C Schneider, U Trautwein, W Wirnitzer, R Thoma, Performance verification of MIMO concepts using multi-dimensional channel sounding. in *Proc. EUSIPCO,* Florence, Italy, Sep. 2006
7. D Nion, N Sidiropoulos, A PARAFAC-based technique for detection and localization of multiple targets in a MIMO radar system. in *Proc. of IEEE Int. Conf. Acoust., Speech, Signal Processing*, Taipei, Taiwan, 2009
8. D Nion, D Sidiropoulos, Tensor algebra and multi-dimensional harmonic retrieval in signal processing for MIMO radar. IEEE Trans. Signal Processing. **58**, 5693–5705 (nov. 2010)
9. A Gershman, N Sidiropoulos, *Space-time processing for MIMO communications*, (New York: Wiley, 2005)
10. R Boyer, Decoupled root-MUSIC algorithm for multidimensional harmonic retrieval. in *Proc. IEEE Int. Work. Signal Processing, Wireless Communications*, Recife, Brazil. 16–20 (2008)
11. ST Smith, Statistical resolution limits and the complexified Cramér Rao bound. IEEE Trans. Signal Processing. **53**, 1597–1609 (2005)
12. M Shahram, P Milanfar, On the resolvability of sinusoids with nearby frequencies in the presence of noise. IEEE Trans. Signal Processing. **53**(7), 2579–2585 (2005)
13. Z Liu, A Nehorai, Statistical angular resolution limit for point sources. IEEE Trans. Signal Processing. **55**(11), 5521–5527 (2007)
14. A Amar, A Weiss, Fundamental limitations on the resolution of deterministic signals. IEEE Trans. Signal Processing. **56**(11), 5309–5318 (2008)
15. HL VanTrees, in Detection, Estimation and Modulation Theory, vol. 1. (New York: Wiley, 1968)
16. H Cox, Resolving power and sensitivity to mismatch of optimum array processors. J Acoust Soc Am. **54**(3), 771–785 (1973). doi:10.1121/1.1913659
17. K Sharman, T Durrani, Resolving power of signal subspace methods for fnite data lengths. in *Proc. of IEEE Int. Conf. Acoust., Speech, Signal Processing*, Florida, USA. 1501–1504 (1995)
18. M Kaveh, A Barabell, The statistical performance of the MUSIC and the minimum-norm algorithms in resolving plane waves in noise. Proc. ASSP Workshop on Spectrum Estimation and Modeling. **34**(2), 331–341 (1986)
19. H Abeidam, J-P Delmas, Statistical performance of MUSIC-like algorithms in resolving noncircular sources. IEEE Trans. Signal Processing. **56**(6), 4317–4329 (2008)
20. HB Lee, The Cramér-Rao bound on frequency estimates of signals closely spaced in frequency. IEEE Trans. Signal Processing. **40**(6), 1507–1517 (1992)
21. The Cramér-Rao bound on frequency estimates of signals closely spaced in frequency (unconditional case), IEEE Trans. Signal Processing. **42**(6), 1569–1572 (1994)
22. E Dilaveroglu, Nonmatrix Cramér-Rao bound expressions for high-resolution frequency estimators. IEEE Trans. Signal Processing. **46**(2), 463–474 (1998)
23. ST Smith, Accuracy and resolution bounds for adaptive sensor array processing. Proceedings in the ninth IEEE SP Workshop on Statistical Signal and Array Processing. 37–40 (1998)
24. J-P Delmas, H Abeida, Statistical resolution limits of DOA for discrete sources. Proc. of IEEE Int. Conf. Acoust., Speech, Signal Processing, Toulouse, France. **4**, 889–892 (2006)
25. X Liu, N Sidiropoulos, Cramér-Rao lower bounds for low-rank decomposition of multidimensional arrays. IEEE Trans. Signal Processing. **49**, 2074–2086 (2002)
26. R Boyer, Deterministic asymptotic Cramér-Rao bound for the multidimensional harmonic model. Signal Processing. **88**, 2869–2877 (2008). doi:10.1016/j.sigpro.2008.06.011
27. J Kusuma, V Goyal, On the accuracy and resolution of powersum-based sampling methods. IEEE Trans. Signal Processing. **57**(1), 182–193 (2009)
28. LL Scharf, *Statistical Signal Processing: Detection, Estimation, and Time Series Analysis*. (Reading: Addison Wesley, 1991)
29. C Westin, A Tensor Framework For Multidimensional Signal Processing. (Citeseer, 1994)
30. M Haardt, J Nossek, Simultaneous Schur decomposition of several nonsymmetric matrices to achieve automatic pairing in multidimensional harmonic retrieval problems. IEEE Trans. Signal Processing. **46**(1), 161–169 (1998)
31. F Roemer, M Haardt, GD Galdo, Higher order SVD based subspace estimation to improve multi-dimensional parameter estimation algorithms. in *Proc. IEEE Int. Conf. Signals, Systems, and Computers Work*. (2007)
32. M Pesavento, C Mecklenbrauker, J Bohme, Multidimensional rank reduction estimator for parametric MIMO channel models. EURASIP Journal on Applied Signal Processing. **9**, 1354–1363 (2004)
33. R Harshman, Foundations of the PARAFAC procedure: Models and conditions for an "explanatory" multi-modal factor analysis. UCLA Working Papers in Phonetics. (1970)
34. P Stoica, R Moses, *Spectral Analysis of Signals*. (NJ: Prentice Hall, 2005)
35. SM Kay, in Fundamentals of Statistical Signal Processing: Detection Theory, vol. 2. (NJ: Prentice Hall, 1998)
36. B Ottersten, M Viberg, P Stoica, A Nehorai, Exact and large sample maximum likelihood techniques for parameter estimation and detection in array processing. in *Radar Array Processing*, vol. ch 4, ed. by Haykin S, Litva J, Shepherd TJ (Berlin: Springer-Verlag, 1993), pp. 99–151
37. A Renaux, P Forster, E Chaumette, P Larzabal, On the high SNR conditional maximum-likelihood estimator full statistical characterization. IEEE Trans. Signal Processing. **12**(54), 4840–4843 (2006)
38. J Li, RT Compton, Maximum likelihood angle estimation for signals with known waveforms. IEEE Trans. Signal Processing. **41**, 2850–2862 (1993). doi:10.1109/78.236507
39. H Cramér, *Mathematical Methods of Statistics*. (New York: Princeton University, Press, 1946)
40. Y Abramovich, B Johnson, N Spencer, Statistical nonidentifiability of close emitters: Maximum-likelihood estimation breakdown. EUSIPCO, Glasgow, Scotland. (2009)
41. MN El Korso, R Boyer, A Renaux, S Marcos, Statistical resolution limit for multiple signals and parameters of interest. in *Proc. of IEEE Int. Conf. Acoust., Speech, Signal Processing*, (Dallas, TX, 2010)
42. SM Kay, in Fundamentals of Statistical Signal Processing, vol. 1. (NJ: Prentice Hall, 1993)
43. KB Petersen, MS Pedersen, The matrix cookbook http://matrixcookbook.com. ver. nov. 14, 2008
44. HL VanTrees, in Detection, Estimation and Modulation theory: Optimum Array Processing, vol. 4. (New York: Wiley, 2002)
45. GH Golub, CFV Loan, *Matrix Computations*. (London: Johns Hopkins, 1989)
46. T Cormen, C Leiserson, R Rivest, *Introduction to algorithms*. (The MIT press, 1990)

doi:10.1186/1687-6180-2011-12
Cite this article as: El Korso *et al.*: **Statistical resolution limit for the multidimensional harmonic retrieval model: hypothesis test and Cramér-Rao Bound approaches.** *EURASIP Journal on Advances in Signal Processing* 2011 **2011**:12.

C.4 Elsevier-SP-2011

M. N. El Korso, R. Boyer, A. Renaux and S. Marcos, "Statistical analysis of achievable resolution limit in the near field context using nonuniform and lacunar array", accepté à *Elsevier Signal Processing*.

STATISTICAL ANALYSIS OF ACHIEVABLE RESOLUTION LIMIT IN THE NEAR FIELD SOURCE LOCALIZATION CONTEXT USING NONUNIFORM AND LACUNAR ARRAY

Mohammed Nabil EL KORSO, *Student Member, IEEE,* Rémy BOYER, *Member, IEEE,* Alexandre RENAUX, *Member, IEEE* and Sylvie MARCOS

***Abstract*— In this correspondance, we derive the Statistical Resolution Limit (SRL), characterizing the minimal parameter separation, to resolve two closely spaced known near-field sources impinging on nonuniform and lacunar linear arrays. Toward this goal, we conduct on the first-order Taylor expansion of the observation model a Generalized Likelihood Ratio Test (GLRT) based on a Constrained Maximum Likelihood Estimator (CMLE) of the SRL. More precisely, the minimum separation between two near-field sources, that is detectable for a given probability of false alarm and a given probability of detection, is derived herein. Finally, numerical simulations are done to quantify the impact of the array geometry, of the signal sources power distribution and of the array aperture on the statistical resolution limit.**

INDEX TERMS

Statistical resolution limit, near-field, performance analysis.

I. INTRODUCTION

Passive sources localization by an array of sensors is an important topic with a large number of applications, such as sonar, seismology, digital communications, etc. One can find many estimation schemes adapted to the so-called near-field source localization (*e.g.,* [1]–[5]). However, to the best of our knowledge, no work has been done on the resolvability of closely spaced near-field sources.

A common tool to characterize the resolvability between two closely spaced signals is the so-called Statistical Resolution Limit (SRL). The SRL [6]–[12], defined as the minimal separation between two signals in terms of parameters of interest which allows a correct resolvability, is a challenging problem and an essential tool to quantify estimators performance.

The idea herein is to use the detection theory in order to derive/link the SRL to the probability of false alarm, P_{fa} and to the probability of detection P_d. In this spirit Sharman and Milanfar [9] have studied the problem of distinguishing whether the observed signal contains one or two frequencies at a given SNR using the Generalized Likelihood Ratio Test (GLRT). In [11], Liu and Nehorai defined a statistical angular resolution limit using the asymptotic equivalence of the GLRT (in terms of snapshots). Recently, Amar and Weiss [12] proposed to determine the SRL of complex sinusoids with nearby frequencies using the Bayesian approach for a given correct decision probability.

The authors are with Laboratoire des Signaux et Systèmes (L2S), Université Paris-Sud XI (UPS), CNRS, SUPELEC, 3 rue Joliot Curie, Gif-Sur-Yvette, 91192, France, phone: +331 6985 1763, fax: +331 6985 1765, {elkorso, remy.boyer, alexandre.renaux, marcos}@lss.supelec.fr. This project is funded by region Île de France and Digeteo Research Park.

It is important to note that all the references listed before have been conducted in the spectral analysis context or for the far-field source localization problem. To the best of our knowledge, no study/result is available concerning the near-field sources localization problem. The goal of this correspondance is to fill this lack. More precisely, we consider the context of deriving the SRL for two complex narrow-band time-varying closely spaced near-field sources using a binary hypothesis test approach. Since the separation term is an unknown parameter, it is impossible to design an optimal detector in the Neyman-Pearson sense [13], [14]. Consequently, the GLRT is applied herein. The choice of the hypothesis test strategy is motivated by the following arguments: (1) the SRL based on detection theory takes into account the statistical coupling between parameters (unlike the Lee criterion [6]), (2) it exists a relationship between the SRL based on the Smith criterion [7] and the SRL based on detection theory in the asymptotic case [11] (in terms of snapshots). Taking advantage of this relationship, one could deduce the SRL in the Smith sense, and finally, (3) unlike the Bayesian approach [12], the use of the GLRT does not require any *prior* knowledge on the unknown parameter of interest [15]. Consequently, in this correspondance we derive the SRL for two closely spaced near-field sources that allows a correct sources resolvability for nonuniform and lacunar linear arrays following the GLRT strategy.

II. PROBLEM SETUP AND ASSUMPTIONS

Let us consider a received signal composed of two emitted near-field and narrow-band sources impinging on a nonuniform linear array of N sensors. The observation model is given by

$$y_n(t) = \sum_{m=1}^{2} s_m(t) e^{j\tau_{nm}} + v_n(t), \tag{1}$$

$t = 1, \ldots, L,\ n = 0, \ldots, N-1$ where $y_n(t)$ and $v_n(t)$ denote the noisy observed signal and the additive noise at the output of the n^{th} sensor, respectively, whereas, $s_m(t)$ denoted the m^{th} deterministic source signal. The number of snapshots is denoted by L and τ_{nm} is the delay associated with the signal propagation time from the first sensor to the n^{th} sensor w.r.t. the m^{th} source which is given by [4]

$$\tau_{nm} = \frac{2\pi r_m}{\nu}\left(\sqrt{1 + \frac{d_n^2}{r_m^2} - \frac{2d_n \sin\theta_m}{r_m}} - 1\right) \tag{2}$$

where ν, r_m and $\theta_m \in \left[0, \frac{\pi}{2}\right]$ denote the signal wavelength, the range and the bearing of the m^{th} source, respectively. The distance between a reference sensors (the first sensor herein) and the n^{th} sensor is denoted by d_n (*e.g.,* in the case of Uniform Linear Array (ULA), $d_n = nd$ where d is the inter-element space between two successive sensors). It is well known that, if the source range is inside of the so-called Fresnel region [4], [16], *i.e.,*

$$0.62\left(D^3\nu\right)^{1/2} < r_m < 2D^2\frac{(N-1)^2}{\nu}, \tag{3}$$

where D is the array aperture, then the delay τ_{nm} can be approximated by

$$\tau_{nm} = \rho_m d_n + \kappa_m d_n^2 + o\left(\frac{d_n^2}{r_m^2}\right), \tag{4}$$

in which $\rho_m = \frac{-2\pi}{\nu}\sin(\theta_m)$ and $\kappa_m = \frac{\pi}{\nu r_m}\cos^2(\theta_m)$ denote the parameters of interest. Neglecting the term $o\left(\frac{d_n^2}{r_m^2}\right)$, the observation model becomes

$$y_n(t) = \sum_{m=1}^{2} s_m(t) e^{j\left(\rho_m d_n + \kappa_m d_n^2\right)} + v_n(t). \tag{5}$$

Consequently, the observation vector can be expressed as

$$\begin{aligned} \mathbf{y}(t) &= [y_0(t) \dots y_{N-1}(t)]^T & (6)\\ &= [\mathbf{a}(\rho_1,\kappa_1)\ \mathbf{a}(\rho_2,\kappa_2)]\mathbf{s}(t) + \mathbf{v}(t), & (7) \end{aligned}$$

in which $\mathbf{v}(t) = [v_0(t) \dots v_{N-1}(t)]^T$, $\mathbf{s}(t) = [s_1(t)\ s_2(t)]^T$ and where

$$[\mathbf{a}(\rho_m,\kappa_m)]_{n+1} = e^{j(\rho_m d_n + \kappa_m d_n^2)}. \tag{8}$$

Finally, the full observation vector can be written as

$$\mathbf{y} \triangleq [\mathbf{y}^T(1)\ \mathbf{y}^T(2)\ \dots\ \mathbf{y}^T(L)]^T. \tag{9}$$

Throughout the rest of the correspondance, the following assumptions are assumed to hold:

- **A1.** The additive noise is assumed to be a complex circular white Gaussian random process (uncorrelated both temporally and spatially) with zero-mean and known [9] or previously estimated [17] variance σ^2.
- **A2.** The parameters $\rho_c = \frac{\rho_1+\rho_2}{2}$ and $\kappa_c = \frac{\kappa_1+\kappa_2}{2}$ (which represent the center parameters) are assumed to be known [11] or previously estimated [9]. However, in the following we prove that this assumption does not affect the SRL (since the SRL is independent of ρ_c and κ_c).
- **A3.** The sources and the array geometry are known.

III. Near-Field Statistical Resolution Limit

A. Hypothesis test formulation

In the following, we conduct a binary hypothesis test formulation to derive the SRL. Let the hypothesis $\mathcal{H}_0$ represent the case where the two signal sources combine into one single signal (*i.e.*, it represents the case of two unresolvable targets), whereas the hypothesis $\mathcal{H}_1$ embodies the situation where the two signals are resolvable [9], [11], [12]. Then, the hypothesis test is given by

$$\begin{cases} \mathcal{H}_0: & \boldsymbol{\delta} \triangleq \mathbf{0}, \\ \mathcal{H}_1: & \boldsymbol{\delta} \neq \mathbf{0}, \end{cases} \tag{10}$$

where the SRL $\boldsymbol{\delta} \triangleq [\delta_\rho\ \delta_\kappa]^T$ in which $\delta_\rho = \rho_2 - \rho_1$ and $\delta_\kappa = \kappa_2 - \kappa_1$. The Generalized Likelihood Ratio Test (GLRT) is a well known approach to solve a composite binary hypothesis test [14]. It is expressed as follows

$$\begin{aligned} G(\mathbf{y}) &= \max_{\delta_\rho,\delta_\kappa} \frac{p(\mathbf{y};\delta_\rho,\delta_\kappa,\mathcal{H}_1)}{p(\mathbf{y};\mathcal{H}_0)} \\ &= \frac{p(\mathbf{y};\hat{\delta}_\rho,\hat{\delta}_\kappa,\mathcal{H}_1)}{p(\mathbf{y};\mathcal{H}_0)} \underset{\mathcal{H}_0}{\overset{\mathcal{H}_1}{\gtrless}} \gamma, \end{aligned} \tag{11}$$

in which $p(\mathbf{y};.)$ denotes the pdf of $\mathbf{y} \sim \mathcal{CN}(E\{\mathbf{y}\}, \sigma^2\boldsymbol{I})$, $\boldsymbol{s}_i = [s_i(1)\ \dots\ s_i(L)]^T$ for $i = 1, 2$, and where γ, $\hat{\delta}_\rho$ and $\hat{\delta}_\kappa$ denote the detection threshold, the Maximum Likelihood Estimate (MLE) under $\mathcal{H}_1$ of δ_ρ and δ_κ, respectively. One can note that the difficult task to derive the GLRT, is to obtain an analytical expressions of $\hat{\delta}_\rho$ and $\hat{\delta}_\kappa$ since the near-field model is highly nonlinear. The key idea to overcome this problem, is to consider that a small separation [9]. This assumption can be argued by the fact the high resolution algorithms have, asymptotically, an infinite resolving power [18]. Consequently, in the following, we show that the near-field model can be linearized by considering small separation on ρ and κ.

B. Linearized Near-Field Model

Using parameters ρ_c and κ_c, a first-order Taylor expansion of the observation model around $(\delta_\rho, \delta_\kappa) = (0, 0)$ leads to

$$\mathbf{y} = \mathbf{A}\boldsymbol{s}_+ + \mathbf{D}\boldsymbol{\delta} + \mathbf{v}, \tag{12}$$

where $\boldsymbol{s}_+ = \boldsymbol{s}_1 + \boldsymbol{s}_2$ and $\mathbf{D} = [\mathbf{B}\boldsymbol{s}_-\ \mathbf{C}\boldsymbol{s}_-]$ in which $\boldsymbol{s}_- = \boldsymbol{s}_2 - \boldsymbol{s}_1$ ($\boldsymbol{s}_1 \neq \boldsymbol{s}_2$). Denoting, $\boldsymbol{d} = [d_0\ d_1\ \dots\ d_{N-1}]^T$, $\otimes$ the Kronecker product, $\odot$ the Hadamard product and $\mathbf{I}_L$ the identity matrix of dimension $L \times L$, we have

$$\mathbf{A} = \mathbf{I}_L \otimes \boldsymbol{a}(\rho_c,\kappa_c), \tag{13}$$

$$\mathbf{B} = \frac{j}{2}\mathbf{I}_L \otimes (\boldsymbol{a}(\rho_c,\kappa_c) \odot \boldsymbol{d}), \tag{14}$$

and

$$\mathbf{C} = \frac{j}{2}\mathbf{I}_L \otimes (\boldsymbol{a}(\rho_c,\kappa_c) \odot \boldsymbol{d} \odot \boldsymbol{d}). \tag{15}$$

C. Constrained MLE (CMLE) of the SRL

Since, ρ_c, κ_c, $\boldsymbol{s}_1$ and $\boldsymbol{s}_2$ are known, observation model (12) can be simplified according to

$$\mathbf{z} \triangleq \mathbf{y} - \mathbf{A}\boldsymbol{s}_+ = \mathbf{D}\boldsymbol{\delta} + \mathbf{v}. \tag{16}$$

As $\boldsymbol{\delta} \in \mathbb{R}^2$, one has to find the Constrained MLE (CMLE) of $\boldsymbol{\delta}$ in order to use correctly the GLRT. More precisely, the constrained optimization problem can be written according to

$$\arg\max_{\boldsymbol{\delta}} L(\mathbf{z},\boldsymbol{\delta}) \ \text{ subject to } \ \Im\{\boldsymbol{\delta}\} = \mathbf{0}, \tag{17}$$

where $L(\mathbf{z},\boldsymbol{\delta}) = \ln p(\mathbf{z};\boldsymbol{\delta},\mathcal{H}_1)$ is the log-likelihood function, $\Im\{.\}$ denotes the imaginary part. The Lagrange function adapted to this problem can be defined as

$$\mathcal{L}(\boldsymbol{\delta},\boldsymbol{\vartheta}) = L(\mathbf{z},\boldsymbol{\delta}) - \frac{j\boldsymbol{\vartheta}^T}{2}(\boldsymbol{\delta} - \boldsymbol{\delta}^*) \tag{18}$$

$$\Rightarrow \begin{cases} \frac{\partial\mathcal{L}}{\partial\boldsymbol{\delta}} = \frac{-1}{\sigma^2}\mathbf{D}^T(\mathbf{z} - \mathbf{D}\boldsymbol{\delta})^* - j\frac{\boldsymbol{\vartheta}}{2} \\ \frac{\partial\mathcal{L}}{\partial\boldsymbol{\vartheta}} = \Im\{\boldsymbol{\delta}\}, \end{cases} \tag{19}$$

where $\boldsymbol{\vartheta}$ is the Lagrange multiplier. Setting $\frac{\partial \mathcal{L}}{\partial \boldsymbol{\delta}}|_{\hat{\boldsymbol{\delta}}_0} = \mathbf{0}$ one has

$$\hat{\boldsymbol{\delta}}_0 = \left(\mathbf{D}^H\mathbf{D}\right)^{-1}\left(\mathbf{D}^H\mathbf{z} - \frac{j}{2}\sigma^2\boldsymbol{\vartheta}\right), \tag{20}$$

where

$$\mathbf{D}^H\mathbf{D} = \frac{\|\boldsymbol{s}_-\|^2}{4}\mathbf{F} \tag{21}$$

in which

$$\mathbf{F} = \begin{bmatrix} f_2 & f_3 \\ f_3 & f_4 \end{bmatrix} \tag{22}$$

and

$$f_i = \sum_{n=0}^{N-1} (d_n)^i. \tag{23}$$

Thus, note that $\mathbf{D}^H\mathbf{D}$ is a real matrix. Consequently, using $\frac{\partial \mathcal{L}}{\partial \boldsymbol{\vartheta}}|_{\boldsymbol{\vartheta}_0} = \mathbf{0}$ and (20), one obtains

$$\boldsymbol{\vartheta}_0 = \frac{2}{\sigma^2}\Im\left\{\mathbf{D}^H\mathbf{z}\right\}. \tag{24}$$

Plugging (24) into (20) one obtains

$$\hat{\boldsymbol{\delta}} = \left(\mathbf{D}^H\mathbf{D}\right)^{-1}\Re\left\{\mathbf{D}^H\mathbf{z}\right\}. \tag{25}$$

D. Near-field SRL derivation

In the light of the above framework, the new binary hypothesis test is given by

$$\begin{cases} \mathcal{H}_0: & \mathbf{z} = \mathbf{v}, \\ \mathcal{H}_1: & \mathbf{z} = \mathbf{D}\boldsymbol{\delta} + \mathbf{v}. \end{cases} \tag{26}$$

The GLRT is then expressed as,

$$G(\mathbf{z}) = \frac{p(\mathbf{z}; \hat{\boldsymbol{\delta}}, \mathcal{H}_1)}{p(\mathbf{z}; \mathcal{H}_0)} = e^{\left(\frac{\|\mathbf{z}\|^2}{\sigma^2} - \frac{\|\mathbf{z}-\mathbf{D}\hat{\boldsymbol{\delta}}\|^2}{\sigma^2}\right)} \underset{\mathcal{H}_0}{\overset{\mathcal{H}_1}{\gtrless}} \eta'. \tag{27}$$

Thus,

$$\ln G(\mathbf{z}) = \frac{1}{\sigma^2}\left(\mathbf{z}^H\mathbf{D}\hat{\boldsymbol{\delta}} + \hat{\boldsymbol{\delta}}^T\mathbf{D}^H\mathbf{z} - \hat{\boldsymbol{\delta}}^T\mathbf{D}^H\mathbf{D}\hat{\boldsymbol{\delta}}\right). \tag{28}$$

Plugging (25) into (28), one obtains

$$\ln G(\mathbf{z}) = \frac{1}{\sigma^2}\Re\left\{\mathbf{z}^H\mathbf{D}\right\}\left(\mathbf{D}^H\mathbf{D}\right)^{-1}\Re\left\{\mathbf{D}^H\mathbf{z}\right\}. \tag{29}$$

Let us define the new statistic

$$T(\mathbf{z}) \overset{\Delta}{=} 2\ln G(\mathbf{z}) \underset{\mathcal{H}_0}{\overset{\mathcal{H}_1}{\gtrless}} \eta = 2\ln\eta'. \tag{30}$$

According to the Appendix, one obtains

$$T(\mathbf{z}) \sim \begin{cases} \chi_2^2(0) = \chi_2^2 & \text{under } \mathcal{H}_0, \\ \chi_2^2\left(\lambda(P_{fa}, P_d)\right) & \text{under } \mathcal{H}_1, \end{cases} \tag{31}$$

where χ_2^2 and $\chi_2^2\left(\lambda(P_{fa}, P_d)\right)$ denote the central and the non-central chi-square distribution of 2 degrees of freedom, respectively, in which

$$\lambda(P_{fa}, P_d) = \frac{2\|\boldsymbol{s}_-\|^2}{\sigma^2}\boldsymbol{\delta}^T\mathbf{F}\boldsymbol{\delta}. \tag{32}$$

Moreover, the probability of false alarm and the probability of detection are given by

$$P_{fa} = Q_{\chi_2^2}(\eta) \tag{33}$$

and

$$P_d = Q_{\chi_2^2(\lambda(P_{fa},P_d))}(\eta), \tag{34}$$

where $Q_{\chi_2^2}(\eta)$ and $Q_{\chi_2^2(\lambda(P_{fa},P_d))}(\eta)$ denote the right tail of the χ_2^2 and $\chi_2^2(\lambda(P_{fa}, P_d))$ pdf starting from η. Thus, the non-centrality parameter $\lambda(P_{fa}, P_d)$ can also be expressed as the solution of

$$Q^{-1}_{\chi_2^2}(P_{fa}) = Q^{-1}_{\chi_2^2(\lambda(P_{fa},P_d))}(P_d), \tag{35}$$

where $Q^{-1}_{\chi_2^2}$ and $Q^{-1}_{\chi_2^2(\lambda(P_{fa},P_d))}$ are the inverse of the right tail of the χ_2^2 and $\chi_2^2(\lambda(P_{fa}, P_d))$ pdf. Consequently, one can state the following results:

Result 1: The relationship between the SRL and the minimum SNR required to resolve two non-orthogonal closely spaced known near-field sources, is given by

$$\begin{aligned} \textit{SNR} &\overset{\Delta}{=} \frac{\|\boldsymbol{s}_1\|^2 + \|\boldsymbol{s}_2\|^2}{\sigma^2} \\ &= \lambda(P_{fa}, P_d)\frac{\|\boldsymbol{s}_1\|^2 + \|\boldsymbol{s}_2\|^2}{2\|\boldsymbol{s}_-\|^2\boldsymbol{\delta}^T\mathbf{F}\boldsymbol{\delta}} \blacksquare \end{aligned} \tag{36}$$

Result 2: The relationship between the SRL and the minimum SNR required to resolve two orthogonal (i.e., $\boldsymbol{s}_1^H\boldsymbol{s}_2 = 0$) closely spaced known near-field sources, is given by

$$\textit{SNR}_o = \frac{\lambda(P_{fa}, P_d)}{2\boldsymbol{\delta}^T\mathbf{F}\boldsymbol{\delta}}, \tag{37}$$

since $||\boldsymbol{s}_-||^2 = ||\boldsymbol{s}_1||^2 + ||\boldsymbol{s}_2||^2$. ■

Note that $\textit{SNR}_o$ is invariant in comparison with the source powers.

IV. Simulation results

Two complex near-field narrow-band sources belonging to the so-called Fresnel region are impigng on a linear array (the geometry is detailled of each scenarios). The probability of false alarm and the probability of detection are, for example, setted to $P_{fa} = 0.01$ and $P_d = 0.99$.

- From Result 1, one can notice that the SRL does not depend on the parameters ρ_c and κ_c. Furthermore, from the Cramér-Rao bound point of view, one can easily prove that the CRB w.r.t. ρ_1 and ρ_2 (or, κ_1 and κ_2), for two known signal sources, depends only on δ_ρ and δ_κ and does not depend directly on ρ_1 and ρ_2 (or, κ_1 and κ_2) themselves (*i.e.,* $\text{CRB}(\rho_i) = f(\delta_\rho, \delta_\kappa)$ and $\text{CRB}(\kappa_i) = f'(\delta_\rho, \delta_\kappa)$). Consequently, since the estimation accuracy depends only on the parameter separation, it is natural to expect that the SRL does not depend on ρ_c or κ_c. Indeed, and as expected, from Fig. 1 one notices that the SRLs using the exact values ρ_c and κ_c and the estimated values $\hat{\rho}_c$ and $\hat{\kappa}_c$ are the same. One concludes that the assumption **A2** is not restrictive at all.
- On the other hand we consider now, the ratio of $\textit{SNR}_o$, given in (37), over the *SNR*, given in (36). Assuming the same signal sources power in the orthognal and non-orthogonal cases, one obtains

$$\frac{\textit{SNR}_o}{\textit{SNR}} = \frac{\|\boldsymbol{s}_1\|^2 + \|\boldsymbol{s}_2\|^2 - 2\Re\left\{\boldsymbol{s}_2^H\boldsymbol{s}_1\right\}}{\|\boldsymbol{s}_1\|^2 + \|\boldsymbol{s}_2\|^2}.$$

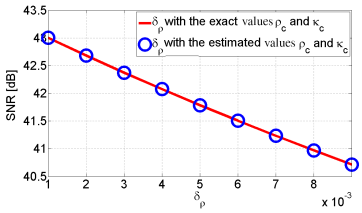

Fig. 1. The required SNR to resolve two known closely spaced near-field sources using the exact and the estimated (using the 2D-MUSIC algorithm [5]) parameters ρ_c and κ_c, for an ULA of $N = 7$ sensors with $L = 25$ snapshots. The same behavior is noticed w.r.t. δ_κ.

For example, in the case of Binary Phase-Shift Keying (BPSK) [19] $SNR_o > SNR$ as shown in Fig. 2. The gain is around 3 dB. The necessary and sufficient condition to have $SNR_o < SNR$ is $\Re\left\{\boldsymbol{s}_2^H \boldsymbol{s}_1\right\} > 0$.

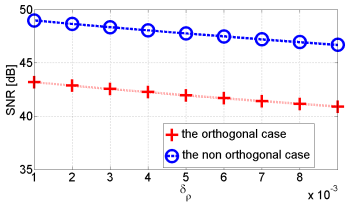

Fig. 2. The required SNR to resolve two closely spaced BPSK near-field sources in the case of real orthogonal signal sources and non orthogonal signal sources, for an ULA of $N = 7$ sensors with $L = 25$ snapshots. The same behavior is noticed w.r.t. δ_κ.

- Finally, we study the impact of nonuniform array geomtries on the SRL. Different configurations are considered herein as shown in Table I; type 1 configuration were the three missing sensors causes a diminution of the array aperture; type 2 and type 3 two any configurations where the three missing sensors do not affect the array aperture; and the filled ULA configuration. From Fig. 3, one can deduce that a loss of sensors has an important impact on the SRL if the sensors are located in the extremity of the array (this loss is around 2.5 dB). However, this problem is largely mitigated if the missing sensors do not modify the array aperture. Nevertheless, note that it is preferable to remove the sensors located near the origin sensors (*i.e.*, to maximize f_i ,$i \in \{2, 3, 4\}$ in (36)).

V. Conclusion

In this correspondance, we have derived the Statistical Resolution Limit (SRL) for two closely spaced near-field time-varying narrowband known sources observed by a linear array (possibly lacunar/nonuniform). Toward this goal, we have conducted a first-order Taylor expansion of the observation model and a Generalized Likelihood Ratio Test (GLRT) based on a Constrained Maximum Likelihood Estimator (CMLE) of the SRL. This analysis provides useful information concerning the behavior of the SRL and the minimum SNR required to resolve two closely spaced near-field sources for a given probability of false alarm and a given probability of detection. In this way, the SRL has been analyzed with respect to the power signal sources distribution and the array aperture.

Array type	Array configuration
Type 1	○ ● ● ○ ● ● ● ● ○
Type 2	● ○ ● ○ ● ○ ● ● ●
Type 3	● ○ ○ ○ ● ● ● ● ●
ULA	● ● ● ● ● ● ● ● ●

TABLE I

Different array geometries where ● and ○ denote the position of sensors and missing sensors, respectively. The inter-element distance is $d = \frac{\nu}{4}$.

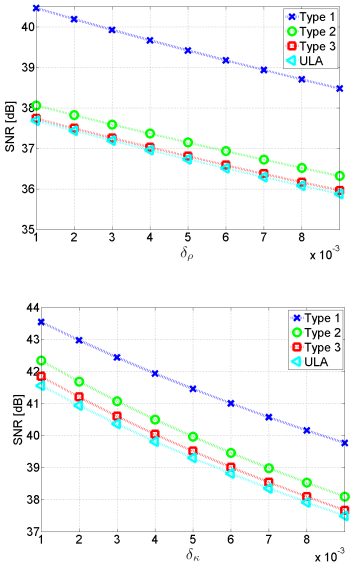

Fig. 3. The required SNR to resolve two known closely spaced near-field sources for different array geometries (see Table 1) with $L = 100$ snapshots, *(top)* for a fixed $\delta_\kappa = 0.001$, *(bottom)* for a fixed $\delta_\rho = 0.001$.

Appendix

The aim of this appendix is to find the distribution of $T(\mathbf{z})$ under $\mathcal{H}_0$ and $\mathcal{H}_1$. Toward this end, we first begin by deriving the covariance matrix of $\Re\left\{\mathbf{D}^H\mathbf{z}\right\}$ denoted by $\mathbf{C}_{\Re\left\{\mathbf{D}^H\mathbf{z}\right\}}$. Since

$$\Re\left\{\mathbf{D}^H\mathbf{z}\right\} \sim \mathcal{N}\left(E\left\{\Re\left\{\mathbf{D}^H\mathbf{z}\right\}\right\}, \mathbf{C}_{\Re\left\{\mathbf{D}^H\mathbf{z}\right\}}\right),$$

one has,

$$\mathbf{C}_{\Re\left\{\mathbf{D}^H\mathbf{z}\right\}} = E\left\{\Re\left\{\mathbf{D}^H\mathbf{v}\right\}\Re\left\{\mathbf{D}^H\mathbf{v}\right\}^T\right\} = E\left\{\boldsymbol{\alpha}\boldsymbol{\beta}^T\right\}, \quad (38)$$

where

$$\boldsymbol{\alpha} = \Re\left\{\mathbf{D}^H\right\}\Re\left\{\mathbf{v}\right\} - \Im\left\{\mathbf{D}^H\right\}\Im\left\{\mathbf{v}\right\} \quad (39)$$

and

$$\boldsymbol{\beta}^T = \Re\left\{\mathbf{v}^T\right\}\Re\left\{\mathbf{D}^*\right\} - \Im\left\{\mathbf{v}^T\right\}\Im\left\{\mathbf{D}^*\right\}. \quad (40)$$

Since $\mathbf{v}$ is a complex white Gaussian circular noise, thus

$$E\left\{\Re\left\{\mathbf{v}\right\}\Re\left\{\mathbf{v}\right\}^T\right\} = E\left\{\Im\left\{\mathbf{v}\right\}\Im\left\{\mathbf{v}\right\}^T\right\} = \frac{\sigma^2}{2}\boldsymbol{I} \quad (41)$$

and

$$E\left\{\Re\left\{\mathbf{v}\right\}\Im\left\{\mathbf{v}\right\}^T\right\} = E\left\{\Im\left\{\mathbf{v}\right\}\Re\left\{\mathbf{v}\right\}^T\right\} = \mathbf{0}. \quad (42)$$

Thus, (38) becomes

$$\mathbf{C}_{\Re\{\mathbf{D}^H\mathbf{z}\}} = \frac{\sigma^2}{2} \times \left(\Re\left\{\mathbf{D}^H\right\}\Re\left\{\mathbf{D}^*\right\} + \Im\left\{\mathbf{D}^H\right\}\Im\left\{\mathbf{D}^*\right\}\right) \tag{43}$$

$$= \frac{\sigma^2}{2}\mathbf{D}^H\mathbf{D}. \tag{44}$$

Consequently, $T(\mathbf{z})$ can be written as

$$T(\mathbf{z}) = \acute{\mathbf{z}}^T\mathbf{C}_{\acute{\mathbf{z}}}^{-1}\acute{\mathbf{z}}. \tag{45}$$

where the Gaussian random variable $\acute{\mathbf{z}}$ is given by $\acute{\mathbf{z}} = \Re\left\{\mathbf{D}^H\mathbf{z}\right\}$ and $\mathbf{C}_{\acute{\mathbf{z}}}$ denotes the covariance matrix of the random variable $\acute{\mathbf{z}}$. Thus, from (45), one can notice that

$$T(\mathbf{z}) \sim \chi_2^2(\lambda(P_{fa}, P_d)), \tag{46}$$

where $\chi_2^2(\lambda(P_{fa}, P_d))$ denotes the non-central distribution of two degree of freedom in which the non-centrality parameter is given by

$$\lambda(P_{fa}, P_d) = E\left\{\acute{\mathbf{z}}\right\}^T\mathbf{C}_{\acute{\mathbf{z}}}^{-1}E\left\{\acute{\mathbf{z}}\right\} = \frac{2\left\|\boldsymbol{s}_-\right\|^2}{\sigma^2}\boldsymbol{\delta}^T\mathbf{F}\boldsymbol{\delta}. \tag{47}$$

Finally, one obtains

$$T(\mathbf{z}) \sim \begin{cases} \chi_2^2(0) = \chi_2^2 & \text{under } \mathcal{H}_0, \\ \chi_2^2\left(\lambda(P_{fa}, P_d)\right) & \text{under } \mathcal{H}_1, \end{cases}$$

which concludes the proof.

REFERENCES

[1] Y. D. Huang and M. Barkat, "Near-field multiple source localization by passive sensor array," *IEEE Trans. Antennas Propagat.*, vol. 39, pp. 968–975, 1991.

[2] J. Lee, Y. Chen, and C. Yeh, "A covariance approximation method for near-field direction-finding using a uniform linear array," *IEEE Trans. Signal Processing*, vol. 43, pp. 1293–1298, May 1995.

[3] N. Yuen and B. Friedlander, "Performance analysis of higher order ESPRIT for localization of near-field sources," *IEEE Trans. Signal Processing*, vol. 46, pp. 709–719, 1998.

[4] E. Grosicki, K. Abed-Meraim, and Y. Hua, "A weighted linear prediction method for near-field source localization," *IEEE Trans. Signal Processing*, vol. 53, pp. 3651–3660, 2005.

[5] M. N. El Korso, G. Bouleux, R. Boyer, and S. Marcos, "Sequential estimation of the range and the bearing using the zero-forcing MUSIC approach," in *Proc. EUSIPCO*, Glasgow, Scotland, Aug. 2009, pp. 1404–1408.

[6] H. B. Lee, "The Cramér-Rao bound on frequency estimates of signals closely spaced in frequency," *IEEE Trans. Signal Processing*, vol. 40, no. 6, pp. 1507–1517, 1992.

[7] S. T. Smith, "Statistical resolution limits and the complexified Cramér Rao bound," *IEEE Trans. Signal Processing*, vol. 53, pp. 1597–1609, May 2005.

[8] M. N. El Korso, R. Boyer, A. Renaux, and S. Marcos, "Statistical resolution limit for multiple signals and parameters of interest," in *Proc. of IEEE Int. Conf. Acoust., Speech, Signal Processing*, Dallas, TX, 2010.

[9] M. Shahram and P. Milanfar, "On the resolvability of sinusoids with nearby frequencies in the presence of noise," *IEEE Trans. Signal Processing*, vol. 53, no. 7, pp. 2579–2585, July 2005.

[10] J.-P. Delmas and H. Abeida, "Statistical resolution limits of DOA for discrete sources," in *Proc. of IEEE Int. Conf. Acoust., Speech, Signal Processing*, vol. 4, Toulouse, France, 2006, pp. 889–892.

[11] Z. Liu and A. Nehorai, "Statistical angular resolution limit for point sources," *IEEE Trans. Signal Processing*, vol. 55, no. 11, pp. 5521–5527, Nov. 2007.

[12] A. Amar and A. Weiss, "Fundamental limitations on the resolution of deterministic signals," *IEEE Trans. Signal Processing*, vol. 56, no. 11, pp. 5309–5318, Nov. 2008.

[13] L. L. Scharf, *Statistical Signal Processing: Detection, Estimation, and Time Series Analysis*. Reading: Addison Wesley, 1991.

[14] S. M. Kay, *Fundamentals of Statistical Signal Processing : Detection Theory*. NJ: Prentice Hall, 1998, vol. 2.

[15] F. Gini, F. Bordoni, and A. Farina, "Multiple radar targets detection by exploiting induced amplitude modulation," *IEEE Trans. Signal Processing*, vol. 52, pp. 903–913, Apr. 2004.

[16] M. N. El Korso, R. Boyer, A. Renaux, and S. Marcos, "Conditional and unconditional Cramér-Rao bounds for near-field source localization," *IEEE Trans. Signal Processing*, vol. 58, no. 5, pp. 2901–2907, May 2010.

[17] B. Ottersten, M. Viberg, P. Stoica, and A. Nehorai, "Exact and large sample maximum likelihood techniques for parameter estimation and detection in array processing," in *Radar Array Processing*, S. Haykin, J. Litva, and T. J. Shepherd, Eds. Berlin: Springer-Verlag, 1993, ch. 4, pp. 99–151.

[18] H. L. VanTrees, *Detection, Estimation and Modulation theory: Optimum Array Processing*. New York: Wiley, 2002, vol. 4.

[19] J. Proakis and M. Salehi, *Digital communications*. New York: McGraw-hill, 2001.

C.5 IEEE-SP-S

M. N. El Korso, R. Boyer, A. Renaux and S. Marcos, "Statistical Resolution Limit for Source Localization With Clutter Interference in a MIMO radar Context", soumis à *IEEE Transactions on Signal Processing*.

Statistical Resolution Limit for Source Localization With Clutter Interference in a MIMO radar Context

Mohammed Nabil EL KORSO, *Student Member, IEEE,* Rémy BOYER, *Member, IEEE,* Alexandre RENAUX, *Member, IEEE* and Sylvie MARCOS

***Abstract*—During the last decade, Multi-Input Multi-Ouput (MIMO) radar has received an increasing interest. One can find several estimation schemes in the literature related to the direction of arrivals and/or direction of departures, but their ultimate performance in terms of the Statistical Resolution Limit (SRL) have not been fully investigated. In this correspondence, we fill this lack. Particulary, we derive the SRL to resolve two closely spaced targets in clutter interference using a MIMO radar with widely separated antennas. Toward this end, we use a hypothesis test formulation based on the Generalized Likelihood Ratio Test (GLRT). Furthermore, we investigate the link between the SRL and the minimum Signal-to-Noise Ratio (SNR) required to resolve two closely spaced targets for a given probability of false alarm and for a given probability of detection. Finally, theoretical and numerical analysis of the SRL are given for several scenarios (with/without clutter interference, known/unknown parameters of interest and known/unknown noise variance).**

INDEX TERMS

Statistical resolution limit, MIMO radar, performance analysis, clutter interference.

I. INTRODUCTION

Based on the attractive Multi-Input Multi-Ouput (MIMO) communication theory, the MIMO radar has received an increasing interest [1]. The advantage of the MIMO radar is to use multiple antennas to simultaneously transmit several non-coherent known waveforms and to exploit multiple antennas to receive the reflected signals (echoes).

One can find a plethora of algorithms for target localization using a MIMO radar and some related lower bounds (see [1]–[4] and references therein). However their ultimate performance in terms of the Statistical Resolution Limit (SRL) has not been fully investigated. The SRL [5]–[8], defined as the minimal separation between two signals in terms of the parameter of interest allowing a correct source resolvability, is an essential tool to quantify the estimator performance.

Among all the different approaches to characterize the SRL, one can find three families. i) The first one is based on the null spectrum [9], [10]. However, this criterion is only relevant to a specific high-resolution algorithm. ii) The second one is based on the estimation accuracy [5], [11], [12]. Indeed, since the Cramér-Rao Bound (CRB) expresses a lower bound on the covariance matrix of any unbiased estimator, then it expresses also the ultimate estimation accuracy. Consequently, it could be used to describe/obtain the SRL. For example, in this context, the Smith criterion states that two signals are resolvable if the separation (between the parameters of interest), is less than the standard deviation of the separation estimation [5]. iii) The last one is based on detection theory using a hypothesis test formulation [7], [8], [13]. The main idea is to decide if one or two closely spaced signals are present in the set of the observations. Consequently, in this context, the challenge is to link the minimum separation, between two targets, that is detectable at a given SNR (for a given probability of false alarm and a given probability of detection).

Several works have been done on the SRL and most of them in the context of spectral analysis and/or far field source localization ([5], [7]–[13] and the references therein). However, in the MIMO radar context, to the best of our knowledge, no results are available (expcet in [14] where one can find the asymptotic SRL, using the Smith criterion, for the co-located MIMO radar without clutter interference and with a prior knowledge on the target and the radar cross-section). The goal of this paper is to derive the SRL for two targets imbedded in clutter interference. We consider a MIMO radar with widely separated arrays (*i.e.,* where the transmitter and the receiver are far enough so that they do not share the same angle variable [2], [4]). The cases of known/unknown parameters of interest and known/unknown nuisance parameters with/without clutter interference are studied. The strategy adopted in this correspondence is the use of the hypothesis test formulation (more precisely, the Generalized Likelihood Ratio Test (GLRT)). This choice is motivated by the nice property of the GLRT (*i.e.,* it is an asymptotically Uniformly Most Powerful (UMP) test among all the invariant statistical tests [15], which is the strongest statement of optimality that one could expect to obtain). Furthermore, in this work, it is shown that the proposed test has the same behavior compared to the (ideal) clairvoyant detector in the Neyman-Pearson sense.

Consequently, in this paper, we derive closed form expressions of the SRL in known/unknown parameters of interest and known/unknown nuisance parameters. Finally, theoretical and numerical analysis of the SRL are given for several scenarios.

II. PROBLEM SETUP

A. Observation model

The output of a MIMO radar with widely spaced arrays where M targets are present is modelled for the ℓ-th pulse as follows [4]:

$$\boldsymbol{X}_\ell = \sum_{m=1}^{M} \rho_m e^{2i\pi f_m \ell} \boldsymbol{a}_{\mathcal{R}}(\omega_m^{(\mathcal{R})}) \boldsymbol{a}_{\mathcal{T}}(\omega_m^{(\mathcal{T})})^T \boldsymbol{S} + \boldsymbol{W}_\ell,$$

$\ell \in [0 : L-1]$ where L, ρ_m and f_m denote the number of samples per pulse period, a complex coefficient proportional to the Radar Cross-Section (RCS) and the normalized Doppler frequency of the m-th target, respectively. Let T, $N_{\mathcal{T}}$ and $N_{\mathcal{R}}$ denote the number of snapshots, the number of sensors at the transmitter and the receiver, respectively[1]. Then, the

The authors are with Laboratoire des Signaux et Systèmes (L2S), Université Paris-Sud XI (UPS), CNRS, SUPELEC, 3 rue Joliot Curie, Gif-Sur-Yvette, 91192, France, phone: +331 6985 1763, fax: +331 6985 1765, {elkorso, remy.boyer, alexandre.renaux, marcos}@lss.supelec.fr. This project is funded by region Île de France and Digeteo Research Park. This work was partially presented during the *ICASSP'11* Conference.

[1]In the following, the upper/sub-script calligraphic letters $\mathcal{T}$ and $\mathcal{R}$ denote the transmitter and the receiver part, respectively.

known $N_{\mathcal{T}} \times T$ signal source matrix is defined by $\boldsymbol{S} = \begin{bmatrix}\boldsymbol{s}_0 & \dots & \boldsymbol{s}_{N_{\mathcal{T}}-1}\end{bmatrix}^T$ where $\boldsymbol{s}_{N_t} = \begin{bmatrix}s_{N_t}(1) & \dots & s_{N_t}(T)\end{bmatrix}^T$, $N_t \in \{0, \dots, N_{\mathcal{T}} - 1\}$, whereas, the $N_{\mathcal{R}} \times T$ noise matrix for the ℓ-th pulse is denoted $\boldsymbol{W}_\ell$. The transmitter steering and receiver steering vectors are denoted $\boldsymbol{a}_{\mathcal{T}}(.)$ and $\boldsymbol{a}_{\mathcal{R}}(.)$. The i-th elements of these steering vectors are given by $[\boldsymbol{a}_{\mathcal{T}}(\omega_m^{(\mathcal{T})})]_i = e^{j\omega_m^{(\mathcal{T})} d_i^{(\mathcal{T})}}$ and $[\boldsymbol{a}_R(\omega_m^{(\mathcal{R})})]_i = e^{j\omega_m^{(\mathcal{R})} d_i^{(\mathcal{R})}}$ where $\omega_m^{(\mathcal{T})} = \frac{2\pi}{\nu}\sin(\psi_m)$ and $\omega_m^{(\mathcal{R})} = \frac{2\pi}{\nu}\sin(\theta_m)$ in which ψ_m is the angle of the target with respect to the transmit array (*i.e.*, Direction Of Departures (DOD)), where θ_m is the angle of the target with respect to the reception array (*i.e.*, Direction Of Arrivals (DOA)), and where ν is the wavelength. The distance between a reference sensors (the first sensor herein) and the i-th sensor is denoted by $d_i^{(\mathcal{T})}$ and $d_i^{(\mathcal{R})}$ for the transmission and the reception arrays, respectively[2].

The diversity of the MIMO radar in terms of waveform coding allows to transmit orthogonal waveforms [2], such that, $\boldsymbol{S}\boldsymbol{S}^H = \boldsymbol{S}^*\boldsymbol{S}^T = T\boldsymbol{I}_{N_{\mathcal{T}}}$. After matched filtering [16], one obtains

$$\begin{aligned}\boldsymbol{Y}_\ell &= \frac{1}{\sqrt{T}}\boldsymbol{X}_\ell \boldsymbol{S}^H \\ &= \sum_{m=1}^{M} \alpha_m e^{2i\pi f_m \ell} \boldsymbol{a}_{\mathcal{R}}(\omega_m^{(\mathcal{R})}) \boldsymbol{a}_{\mathcal{T}}(\omega_m^{(\mathcal{T})})^T + \boldsymbol{Z}_\ell,\end{aligned}$$

where $\alpha_m = \sqrt{T}\rho_m$ and where $\boldsymbol{Z}_\ell = \frac{1}{\sqrt{T}}\boldsymbol{W}_\ell \boldsymbol{S}^H$ denotes the noise matrix after the matched filtering. It is straightforward to rewrite the above matrix-based expression as a vectorized CanDecomp/Parafac [17], [18] model of dimension $P = 3$ according to $\boldsymbol{y} = [\text{vec}(\boldsymbol{Y}_0)^T \dots \text{vec}(\boldsymbol{Y}_{L-1})^T]^T = \boldsymbol{x} + \boldsymbol{z}$, where *vec* denotes the *vectorization* operator, $\boldsymbol{z} = [\boldsymbol{z}_0^T \dots \boldsymbol{z}_{L-1}^T]^T$ with $\boldsymbol{z}_\ell = \text{vec}(\boldsymbol{Z}_\ell)$ and

$$\boldsymbol{x} = \sum_{m=1}^{M} \alpha_m \boldsymbol{g}_m, \tag{1}$$

in which $\boldsymbol{c}(f_m) = [1 \;\; e^{2i\pi f_m} \;\; \dots \;\; e^{2i\pi f_m (L-1)}]^T$, $\boldsymbol{g}_m = \left(\boldsymbol{c}(f_m) \otimes \boldsymbol{a}_{\mathcal{T}}(\omega_m^{(\mathcal{T})}) \otimes \boldsymbol{a}_{\mathcal{R}}(\omega_m^{(\mathcal{R})})\right)$ and where $\otimes$ denotes the Kronecker product.

B. Statistic of the observations

Assuming that the noise interferences (before the matched filtering) are complex circular Gaussian independent and identically distributed samples with zero-mean and a covariance matrix $\sigma^2\boldsymbol{I}$ [1] and, thanks to the waveforms orthogonality, one can notice that $E(\boldsymbol{z}_\ell \boldsymbol{z}_\ell^H) = \frac{1}{T}(\boldsymbol{S}^* \otimes \boldsymbol{I}_{N_{\mathcal{R}}}) E(\text{vec}(\boldsymbol{W}_\ell)\text{vec}(\boldsymbol{W}_{\ell'})^H)(\boldsymbol{S}^T \otimes \boldsymbol{I}_{N_{\mathcal{R}}}) = \sigma^2 \boldsymbol{I}_{N_{\mathcal{T}} N_{\mathcal{R}}}$ and that $E(\boldsymbol{z}_\ell \boldsymbol{z}_{\ell'}^H) = \boldsymbol{0}$ for $\ell \neq \ell'$. Thus, $E(\boldsymbol{z}\boldsymbol{z}^H) = \sigma^2 \boldsymbol{I}_{LN_{\mathcal{T}} N_{\mathcal{R}}}$. Consequently, the observation follows a complex circular Gaussian distribution $\boldsymbol{y} \sim \mathcal{CN}(\boldsymbol{x}, \sigma^2 \boldsymbol{I}_{LN_{\mathcal{T}} N_{\mathcal{R}}})$.

III. Detection approach

Without loss of generality, in the remain of the paper, we consider that the targets of interest are the first and the second one. The $M-2$ remaining targets consist of the clutter interference.

[2] *e.g.,* in the case of Uniform Linear Transmission Array (ULTA), $d_i^{(\mathcal{T})} = (i-1)d_{\mathcal{T}}$ where $d_{\mathcal{T}}$ is the inter-element space between two successive transmission sensors

A. Hypothesis test formulation

Resolving two closely spaced sources, with respect to their parameter of interest $\omega_m^{(\mathcal{T})}$ and $\omega_m^{(\mathcal{R})}$, can be formulated as a binary hypothesis test (see [7], [8], [13], [19] and references therein). The hypothesis $\mathcal{H}_0$ represents the case where the two emitted signal sources are combined into one signal, whereas the hypothesis $\mathcal{H}_1$ embodies the situation where the two signals are resolvable. Thus, one obtains the following binary hypothesis test:

$$\begin{cases}\mathcal{H}_0 : & (\delta_{\mathcal{R}}, \delta_{\mathcal{T}}) = (0,0), \\ \mathcal{H}_1 : & (\delta_{\mathcal{R}}, \delta_{\mathcal{T}}) \neq (0,0),\end{cases} \tag{2}$$

where the so-called Local SRLs (LSRL) are given by $\delta_{\mathcal{T}} \triangleq \omega_2^{(\mathcal{T})} - \omega_1^{(\mathcal{T})}$ and $\delta_{\mathcal{R}} \triangleq \omega_2^{(\mathcal{R})} - \omega_1^{(\mathcal{R})}$. Since the LSRLs are unknown, it is impossible to design an optimal detector in the Neyman-Pearson sense. Alternatively, the Generalized Likelihood Ratio Test (GLRT) [15] is a well known approach appropriate to solve such a problem. The GLRT statistic is expressed as $G(\mathbf{y}) = \frac{p(\mathbf{y}; \hat{\delta}_{\mathcal{R}}, \hat{\delta}_{\mathcal{T}}, \hat{\boldsymbol{\rho}}_1, \mathcal{H}_1)}{p(\mathbf{y}; \hat{\boldsymbol{\rho}}_0, \mathcal{H}_0)} \underset{\mathcal{H}_0}{\overset{\mathcal{H}_1}{\gtrless}} \eta'$, in which $p(\mathbf{y}; \hat{\boldsymbol{\rho}}_0, \mathcal{H}_0)$ and $p(\mathbf{y}; \hat{\delta}_{\mathcal{R}}, \hat{\delta}_{\mathcal{T}}, \hat{\boldsymbol{\rho}}_1, \mathcal{H}_1)$ denote the probability density functions of the observation under $\mathcal{H}_0$ and $\mathcal{H}_1$, respectively. η', $\hat{\delta}_{\mathcal{R}}$, $\hat{\delta}_{\mathcal{T}}$ and $\hat{\boldsymbol{\rho}}_i$ denote the detection threshold, the Maximum Likelihood Estimate (MLE) of $\delta_{\mathcal{R}}$ and $\delta_{\mathcal{T}}$ under $\mathcal{H}_1$ and the MLE of the parameter vector $\boldsymbol{\rho}_i$ (containing all the unknown nuisance and/or unwanted parameters) under $\mathcal{H}_i, i = 0, 1$, respectively.

One can easily see that the derivation of $\hat{\delta}_{\mathcal{R}}$ and $\hat{\delta}_{\mathcal{T}}$ is a nonlinear optimization problem which is analytically intractable. Using the fact that the separation is small [7], [8], [13], [19], [20] (this assumption can be argued by the fact that the high resolution algorithms have asymptotically an infinite resolution power), one can approximate the model (1) into a model which is linear w.r.t. the unknown parameters.

B. Linear form of the MIMO model

First, let us introduce the so-called center parameters $\omega_c^{(\mathcal{T})} \triangleq \frac{\omega_1^{(\mathcal{T})} + \omega_2^{(\mathcal{T})}}{2}$ and $\omega_c^{(\mathcal{R})} \triangleq \frac{\omega_1^{(\mathcal{R})} + \omega_2^{(\mathcal{R})}}{2}$. Second, as in [7], [13], [19] we use the first order Taylor expansion of (1) around $\delta_{\mathcal{T}} = 0$ and $\delta_{\mathcal{R}} = 0$, thus, one obtains $\boldsymbol{a}_{\mathcal{T}}(\omega_1^{(\mathcal{T})}) = \boldsymbol{a}_{\mathcal{T}}(\omega_c^{(\mathcal{T})}) - \frac{j}{2}\delta_{\mathcal{T}}\dot{\boldsymbol{a}}_{\mathcal{T}}(\omega_c^{(\mathcal{T})})$, $\boldsymbol{a}_{\mathcal{R}}(\omega_1^{(\mathcal{R})}) = \boldsymbol{a}_{\mathcal{R}}(\omega_c^{(\mathcal{R})}) - \frac{j}{2}\delta_{\mathcal{R}}\dot{\boldsymbol{a}}_{\mathcal{R}}(\omega_c^{(\mathcal{R})})$, $\boldsymbol{a}_{\mathcal{T}}(\omega_2^{(\mathcal{T})}) = \boldsymbol{a}_{\mathcal{T}}(\omega_c^{(\mathcal{T})}) + \frac{j}{2}\delta_{\mathcal{T}}\dot{\boldsymbol{a}}_T(\omega_c^{(\mathcal{T})})$ and $\boldsymbol{a}_{\mathcal{R}}(\omega_2^{(\mathcal{R})}) = \boldsymbol{a}_{\mathcal{R}}(\omega_c^{(\mathcal{R})}) + \frac{j}{2}\delta_{\mathcal{R}}\dot{\boldsymbol{a}}_{\mathcal{R}}(\omega_c^{(\mathcal{R})})$, where $\dot{\boldsymbol{a}}_{\mathcal{T}}(.) \triangleq \boldsymbol{a}_{\mathcal{T}}(.) \odot \boldsymbol{d}_{\mathcal{T}}$, and $\dot{\boldsymbol{a}}_{\mathcal{R}}(.) \triangleq \boldsymbol{a}_{\mathcal{R}}(.) \odot \boldsymbol{d}_{\mathcal{R}}$ and where $\odot$ denotes the Hadamard product, $\boldsymbol{d}_T = [d_0^{(\mathcal{T})} \; d_1^{(\mathcal{T})} \; \dots \; d_{N-1}^{(\mathcal{T})}]^T$ and where $\boldsymbol{d}_R = [d_0^{(\mathcal{R})} \; d_1^{(\mathcal{R})} \; \dots \; d_{N-1}^{(\mathcal{R})}]^T$. Thus, one can rewrite the observation model as

$$\boldsymbol{y} = \check{\boldsymbol{G}}\check{\boldsymbol{\zeta}} + \check{\boldsymbol{D}}\check{\boldsymbol{\alpha}} + \boldsymbol{z}, \tag{3}$$

where the $(LN_{\mathcal{T}}N_{\mathcal{R}}) \times 4$ matrix $\check{\boldsymbol{G}}$ is defined as $\check{\boldsymbol{G}} = \begin{bmatrix}\boldsymbol{\varrho}_1 & \boldsymbol{\varrho}_2 & \boldsymbol{\varrho}_3 & \boldsymbol{\varrho}_4\end{bmatrix}$, in which $\boldsymbol{\varrho}_1 = \boldsymbol{c}(f) \otimes \boldsymbol{a}_{\mathcal{T}}(\omega_c^{(\mathcal{T})}) \otimes \boldsymbol{a}_{\mathcal{R}}(\omega_c^{(\mathcal{R})})$, $\boldsymbol{\varrho}_2 = \boldsymbol{c}(f) \otimes \boldsymbol{a}_{\mathcal{T}}(\omega_c^{(\mathcal{T})}) \otimes \dot{\boldsymbol{a}}_{\mathcal{R}}(\omega_c^{(\mathcal{R})})$, $\boldsymbol{\varrho}_3 =$

$\boldsymbol{c}(f) \otimes \dot{\boldsymbol{a}}_{\mathcal{T}}(\omega_c^{(\mathcal{T})}) \otimes \boldsymbol{a}_{\mathcal{R}}(\omega_c^{(\mathcal{R})})$, and $\boldsymbol{\varrho}_4 = \boldsymbol{c}(f) \otimes \dot{\boldsymbol{a}}_{\mathcal{T}}(\omega_c^{(\mathcal{T})}) \otimes \dot{\boldsymbol{a}}_{\mathcal{R}}(\omega_c^{(\mathcal{R})})$. The unknown 4×1 parameter vector is given by

$$\breve{\boldsymbol{\zeta}} = \begin{bmatrix} \alpha_1 + \alpha_2 \\ \frac{j}{2}\delta_{\mathcal{R}}(\alpha_2 - \alpha_1) \\ \frac{j}{2}\delta_{\mathcal{T}}(\alpha_2 - \alpha_1) \\ \frac{-1}{4}\delta_{\mathcal{R}}\delta_{\mathcal{T}}(\alpha_1 + \alpha_2) \end{bmatrix},$$

whereas $\breve{\boldsymbol{D}} = \begin{bmatrix} \boldsymbol{g}_3 & \dots & \boldsymbol{g}_M \end{bmatrix}$ and $\breve{\boldsymbol{\alpha}} = \begin{bmatrix} \alpha_3 & \dots & \alpha_M \end{bmatrix}^T$. Rearranging (3), one obtains

$$\boldsymbol{y} = \boldsymbol{G}\boldsymbol{\zeta} + \boldsymbol{D}\boldsymbol{\alpha} + \boldsymbol{z}, \tag{4}$$

where $\boldsymbol{G} = \begin{bmatrix} \boldsymbol{\varrho}_2 & \boldsymbol{\varrho}_3 & \boldsymbol{\varrho}_4 \end{bmatrix}$, the clutter interference $\boldsymbol{D} = \begin{bmatrix} \boldsymbol{\varrho}_1 & \boldsymbol{g}_3 & \dots & \boldsymbol{g}_M \end{bmatrix}$, $\boldsymbol{\alpha} = \begin{bmatrix} \alpha_1 + \alpha_2 & \alpha_3 & \dots & \alpha_M \end{bmatrix}^T$ and $\boldsymbol{\zeta} = \frac{j}{2}\begin{bmatrix} \delta_{\mathcal{R}}(\alpha_2 - \alpha_1) & \delta_{\mathcal{T}}(\alpha_2 - \alpha_1) & \frac{j}{2}\delta_{\mathcal{R}}\delta_{\mathcal{T}}(\alpha_1 + \alpha_2) \end{bmatrix}$.

C. Assumptions

Throughout the rest of the paper, the following assumptions are assumed to hold:

$\boldsymbol{\mathcal{A}1}$) The parameters $\omega_c^{(\mathcal{T})}$ and $\omega_c^{(\mathcal{R})}$ (which represent the center parameters) are assumed to be known [8] or previously estimated [7].

$\boldsymbol{\mathcal{A}2}$) For sake of simplicity the Doppler frequency f_1 and f_2 are assumed to be equal to f (possibly equal to zero). Nevertheless, numerical simulations will show that the derived SRL (with equal Doppler frequency assumption) has the same behavior compared to the clairvoyant detector.

$\boldsymbol{\mathcal{A}3}$) Finally, the clutter interference $\boldsymbol{D}$ is known or previously estimated [21]. However, one should note that α_m, $i = 1 \dots M$ are considered as unknown unequal deterministic complex parameters.

One should note that the case of $f_1 \neq f_2$, the case of unknown $\omega_c^{(\mathcal{T})}$, the case of unknown $\omega_c^{(\mathcal{R})}$ and the case of unknown clutter interference $\boldsymbol{D}$ leads to an untractable solution of the GLRT and, consequently, is beyond the scope of this paper.

In the following, we use the linear form of the signal model (4). Both cases of known and unknown noise variance will be considered.

IV. Derivations and analysis of the SRL

A. Case of a known noise variance

1) Case of two targets with interference clutter: We consider the case where two closely spaced targets are imbedded into clutter interference. The noise variance is assumed to be known. Consequently, using the linear form in (4), the binary hypothesis test in (2) can be re-formulated as follows

$$\begin{cases} \mathcal{H}_0: & \boldsymbol{y} = \boldsymbol{D}\boldsymbol{\alpha} + \boldsymbol{z} \sim \mathcal{CN}(\boldsymbol{D}\boldsymbol{\alpha}, \sigma^2\boldsymbol{I}), \\ \mathcal{H}_1: & \boldsymbol{y} = \boldsymbol{G}\boldsymbol{\zeta} + \boldsymbol{D}\boldsymbol{\alpha} + \boldsymbol{z} \sim \mathcal{CN}(\boldsymbol{G}\boldsymbol{\zeta} + \boldsymbol{D}\boldsymbol{\alpha}, \sigma^2\boldsymbol{I}). \end{cases} \tag{5}$$

Based on (5), the unconstrained MLEs of the unknown parameters are given by [22]:

$$\hat{\boldsymbol{\zeta}} = (\boldsymbol{G}^H\boldsymbol{P}_{\boldsymbol{D}}^{\perp}\boldsymbol{G})^{-1}\boldsymbol{G}^H\boldsymbol{P}_{\boldsymbol{D}}^{\perp}\boldsymbol{y}, \tag{6}$$

$$\hat{\boldsymbol{\alpha}}_{\mathcal{H}_0} = (\boldsymbol{D}^H\boldsymbol{D})^{-1}\boldsymbol{D}^H\boldsymbol{y}, \tag{7}$$

$$\hat{\boldsymbol{\alpha}}_{\mathcal{H}_1} = (\boldsymbol{D}^H\boldsymbol{P}_{\boldsymbol{G}}^{\perp}\boldsymbol{D})^{-1}\boldsymbol{D}^H\boldsymbol{P}_{\boldsymbol{G}}^{\perp}\boldsymbol{y}, \tag{8}$$

where $\boldsymbol{P}_{\boldsymbol{D}}^{\perp} \triangleq \boldsymbol{I} - \boldsymbol{P}_{\boldsymbol{D}}$, in which $\boldsymbol{P}_{\boldsymbol{D}}$ denotes the orthogonal projector onto the subspace spanned by the columns of the matrix $\boldsymbol{D}$.

Consequently, the MLEs of the noise vector are given by

$$\begin{cases} \hat{\boldsymbol{z}}_{\mathcal{H}_0} = \boldsymbol{y} - \boldsymbol{D}\hat{\boldsymbol{\alpha}} = \boldsymbol{P}_{\boldsymbol{D}}^{\perp}\boldsymbol{y} & \text{under } \mathcal{H}_0, \\ \hat{\boldsymbol{z}}_{\mathcal{H}_1} == \boldsymbol{P}_{[\boldsymbol{G}\boldsymbol{D}]}^{\perp}\boldsymbol{y} & \text{under } \mathcal{H}_1, \end{cases} \tag{9}$$

where the oblique projectors $\boldsymbol{E}_{\boldsymbol{G}\boldsymbol{D}}$ and $\boldsymbol{E}_{\boldsymbol{D}\boldsymbol{G}}$ are defined as $\boldsymbol{E}_{\boldsymbol{G}\boldsymbol{D}} = \boldsymbol{G}(\boldsymbol{G}^H\boldsymbol{P}_{\boldsymbol{D}}^{\perp}\boldsymbol{G})^{-1}\boldsymbol{G}^H\boldsymbol{P}_{\boldsymbol{D}}^{\perp}$ and $\boldsymbol{E}_{\boldsymbol{D}\boldsymbol{G}} = \boldsymbol{D}(\boldsymbol{D}^H\boldsymbol{P}_{\boldsymbol{G}}^{\perp}\boldsymbol{D})^{-1}\boldsymbol{D}^H\boldsymbol{P}_{\boldsymbol{G}}^{\perp}$ [23]. Now, we are ready to use the statistic $T'(\boldsymbol{y})$ of the GLRT which is defined as follows

$$T'(\boldsymbol{y}) \triangleq 2\ln G(\boldsymbol{y}) = \frac{2}{\sigma^2}\left(\|\hat{\boldsymbol{z}}_{\mathcal{H}_0}\|^2 - \|\hat{\boldsymbol{z}}_{\mathcal{H}_1}\|^2\right) \tag{10}$$

$$= \frac{2}{\sigma^2}\boldsymbol{y}^H\left(\boldsymbol{P}_{\boldsymbol{D}}^{\perp} - \boldsymbol{P}_{[\boldsymbol{G}\boldsymbol{D}]}^{\perp}\right)\boldsymbol{y}. \tag{11}$$

Using [24, eq (3.7)] and [22, eq (19)], one has $\boldsymbol{P}_{\boldsymbol{D}}^{\perp} - \boldsymbol{P}_{[\boldsymbol{G}\boldsymbol{D}]}^{\perp} = \boldsymbol{P}_{\boldsymbol{D}}^{\perp}\boldsymbol{E}_{\boldsymbol{G}\boldsymbol{D}}\boldsymbol{P}_{\boldsymbol{D}}^{\perp} = \boldsymbol{P}_{\boldsymbol{P}_{\boldsymbol{D}}^{\perp}\boldsymbol{G}}$. Thus,

$$T'(\boldsymbol{y}) = \frac{2}{\sigma^2}\boldsymbol{y}^H\boldsymbol{P}_{\boldsymbol{P}_{\boldsymbol{D}}^{\perp}\boldsymbol{G}}\boldsymbol{y}. \tag{12}$$

Let $\boldsymbol{P}_{\boldsymbol{P}_{\boldsymbol{D}}^{\perp}\boldsymbol{G}} = \boldsymbol{U}\boldsymbol{U}^H$ be any orthogonal decomposition [25] of the projector $\boldsymbol{P}_{\boldsymbol{P}_{\boldsymbol{D}}^{\perp}\boldsymbol{G}}$ such that $\boldsymbol{U}^H\boldsymbol{U} = \boldsymbol{I}$ and define an auxiliary random variable $\tilde{\boldsymbol{y}} = \boldsymbol{U}^H\boldsymbol{y}$. One should note that

$$\begin{cases} \tilde{\boldsymbol{y}} = \boldsymbol{U}^H\boldsymbol{z} \sim \mathcal{CN}(\boldsymbol{0}, \sigma^2\boldsymbol{I}) & \text{under } \mathcal{H}_0, \\ \tilde{\boldsymbol{y}} = \boldsymbol{U}^H\boldsymbol{G}\boldsymbol{\zeta} + \boldsymbol{U}^H\boldsymbol{z} \sim \mathcal{CN}(\boldsymbol{U}^H\boldsymbol{G}\boldsymbol{\zeta}, \sigma^2\boldsymbol{I}) & \text{under } \mathcal{H}_1. \end{cases} \tag{13}$$

Consequently,

$$T'(\boldsymbol{y}) \sim \begin{cases} \chi_{2r}^2 & \text{under } \mathcal{H}_0, \\ \chi_{2r}^2(\lambda_{\mathrm{K}}(P_{fa}, P_d)) & \text{under } \mathcal{H}_1, \end{cases} \tag{14}$$

in which P_{fa} and P_d denote the probability of false alarm and the probability of detection, respectively, where the subscript K stands for the case of Known noise variance, χ_{2r}^2 and $\chi_{2r}^2(\lambda_{\mathrm{K}}(P_{fa}, P_d))$ denote the central and the non-central chi-square distribution with $2r$ degrees of freedom, respectively, in which $r = \mathrm{trace}(\boldsymbol{P}_{\boldsymbol{P}_{\boldsymbol{D}}^{\perp}\boldsymbol{G}}) = \mathrm{rank}(\boldsymbol{P}_{\boldsymbol{P}_{\boldsymbol{D}}^{\perp}\boldsymbol{G}}) = LN_{\mathcal{T}}N_{\mathcal{R}} - M + 1$ [26]. The non-centrality parameter is given by

$$\lambda_{\mathrm{K}}(P_{fa}, P_d) = \frac{\boldsymbol{\zeta}^H\boldsymbol{G}^H\boldsymbol{U}\boldsymbol{U}^H\boldsymbol{G}\boldsymbol{\zeta}}{\sigma^2/2} = \frac{2\boldsymbol{\zeta}^H\boldsymbol{G}^H\boldsymbol{P}_{\boldsymbol{P}_{\boldsymbol{D}}^{\perp}\boldsymbol{G}}\boldsymbol{G}\boldsymbol{\zeta}}{\sigma^2}. \tag{15}$$

Note that $\lambda_{\mathrm{K}}(P_{fa}, P_d)$ can be numerically computed as the solution of $\mathcal{Q}_{\chi_{2r}^2}^{-1}(P_{fa}) = \mathcal{Q}_{\chi_{2r}^2(\lambda_{\mathrm{K}}(P_{fa},P_d))}^{-1}(P_d)$, where $\mathcal{Q}_{\chi_{2r}^2}(.)$ and $\mathcal{Q}_{\chi_{2r}^2(\lambda_{\mathrm{K}}(P_{fa},P_d))}(.)$ denote the right tails of the pdf χ_{2r}^2 and the pdf $\chi_{2r}^2(\lambda_{\mathrm{K}}(P_{fa}, P_d))$, respectively.

Result 1: The minimum SNR required to resolve two closely spaced targets in clutter interference in the known noise variance case is given by

$$\mathrm{SNR}_{\mathrm{K}} \triangleq \frac{\mathrm{trace}\left\{\boldsymbol{S}\boldsymbol{S}^H\right\}}{T\sigma^2} = \frac{N_{\mathcal{T}}\lambda_{\mathrm{K}}(P_{fa}, P_d)}{2\boldsymbol{\zeta}^H\boldsymbol{G}^H\boldsymbol{P}_{\boldsymbol{P}_{\boldsymbol{D}}^{\perp}\boldsymbol{G}}\boldsymbol{G}\boldsymbol{\zeta}} = \frac{N_{\mathcal{T}}\lambda_{\mathrm{K}}(P_{fa}, P_d)}{2\left\|\boldsymbol{U}^H\boldsymbol{G}\boldsymbol{\zeta}\right\|^2}. \tag{16}$$

2) Case of two targets without interference: The case of two targets without interference can be deduced from the previous result. First, note that without interference the matrix $\boldsymbol{D}$ becomes a column vector equal to $\boldsymbol{\varrho}_1$. Second, using [22, eq (19)], one has

$$\boldsymbol{G}^H \boldsymbol{P}^{\perp}_{\boldsymbol{P}_{\boldsymbol{\varrho}_1}\boldsymbol{G}} \boldsymbol{G} = \boldsymbol{G}^H \left(\boldsymbol{P}^{\perp}_{\boldsymbol{\varrho}_1} - \boldsymbol{P}^{\perp}_{[\boldsymbol{\varrho}_1 \boldsymbol{G}]} \right) \boldsymbol{G} \tag{17}$$

$$= \boldsymbol{G}^H \left(\boldsymbol{P}_{[\boldsymbol{\varrho}_1 \boldsymbol{G}]} - \frac{\boldsymbol{\varrho}_1 \boldsymbol{\varrho}_1^H}{L \mathcal{N}_T \mathcal{N}_R} \right) \boldsymbol{G} = L \left(\boldsymbol{\Phi} - \frac{1}{N_{\mathcal{T}} N_{\mathcal{R}}} \boldsymbol{\kappa} \boldsymbol{\kappa}^T \right), \tag{18}$$

where $\boldsymbol{\Phi} = \begin{bmatrix} f_{0,2} & f_{1,1} & f_{1,2} \\ f_{1,1} & f_{2,0} & f_{2,1} \\ f_{1,2} & f_{2,1} & f_{2,2} \end{bmatrix}$, $\boldsymbol{\kappa} = \begin{bmatrix} f_{0,1} & f_{1,0} & f_{1,1} \end{bmatrix}^H$, in which $f_{p,q} = \sum_{n_t=1}^{N_{\mathcal{T}}} \left(d_{n_t}^{(\mathcal{T})} \right)^p \sum_{n_r=1}^{N_{\mathcal{R}}} \left(d_{n_r}^{(\mathcal{R})} \right)^q$. By denoting $\boldsymbol{K} \triangleq \frac{1}{N_{\mathcal{T}}} \left(\boldsymbol{\Phi} - \frac{1}{N_{\mathcal{T}} N_{\mathcal{R}}} \boldsymbol{\kappa} \boldsymbol{\kappa}^T \right)$ and by plugging (18) into (16), one obtains:

Result 2: The relationship between the SRL ($\delta_{\mathcal{T}}$ and $\delta_{\mathcal{R}}$) and the minimum SNR, required to resolve two closely spaced sources, is then given by

$$\mathrm{SNR}_{\mathrm{K}} = \frac{\lambda_{\mathrm{K}}\left(P_{fa}, P_d\right)}{2L \boldsymbol{\zeta}^H \boldsymbol{K} \boldsymbol{\zeta}}. \tag{19}$$

3) Case of two targets without interference and with symmetric arrays: By symmetric arrays we mean $f_{p,1} = f_{1,p} = 0, \forall p$. The expression of the minimum SNR (required to resolve two closely spaced targets) becomes more compact as follows:

Result 3: The relationship between the SRL ($\delta_{\mathcal{T}}$ and $\delta_{\mathcal{R}}$) and the minimum SNR, required to resolve two closely spaced targets, for symmetric arrays is then given by

$$\mathrm{SNR}_{\mathrm{K}_{\mathrm{sym}}} = \frac{2 N_{\mathcal{T}} \lambda_{\mathrm{K}}\left(P_{fa}, P_d\right)}{L \left(\left(\delta_{\mathcal{R}}^2 + \delta_{\mathcal{T}}^2\right) \left(\alpha_2 - \alpha_1\right)^2 + \delta_{\mathcal{R}}^2 \delta_{\mathcal{T}}^2 \left(\alpha_2 + \alpha_1\right)^2 \right)}.$$

B. Case of unknown noise variance

1) Case of two targets with interference clutter: One can extend the latter analysis to the case of unknown noise variance σ^2. The observations under each hypothesis are given by

$$\begin{cases} \mathcal{H}_0: & \boldsymbol{y} = \boldsymbol{D}\boldsymbol{\alpha} + \boldsymbol{z} \sim \mathcal{CN}(\boldsymbol{D}\boldsymbol{\alpha}, \sigma^2 \boldsymbol{I}), \quad \sigma^2 > 0 \\ \mathcal{H}_1: & \boldsymbol{y} = \boldsymbol{G}\boldsymbol{\zeta} + \boldsymbol{D}\boldsymbol{\alpha} + \boldsymbol{z} \sim \mathcal{CN}(\boldsymbol{G}\boldsymbol{\zeta} + \boldsymbol{D}\boldsymbol{\alpha}, \sigma^2 \boldsymbol{I}), \sigma^2 > 0. \end{cases} \tag{20}$$

Consequently, from (20), the GLRT is given by

$$G(\boldsymbol{y}) = \frac{\hat{\sigma}_0^2}{\hat{\sigma}_1^2} = \frac{||\hat{\boldsymbol{z}}_{\mathcal{H}_0}||^2}{||\hat{\boldsymbol{z}}_{\mathcal{H}_1}||^2}, \tag{21}$$

where the MLE of the noise variance under each hypothesis is given by [27]

$$\hat{\sigma}_i^2 = \frac{1}{NL} ||\hat{\boldsymbol{z}}_{\mathcal{H}_i}||^2, \quad i = 0, 1. \tag{22}$$

After some straightforward derivations, one obtains

$$\begin{cases} \hat{\boldsymbol{z}}_{\mathcal{H}_0} = \boldsymbol{y} - \boldsymbol{D}\hat{\boldsymbol{\alpha}}_{\mathcal{H}_0} = \boldsymbol{P}^{\perp}_{\boldsymbol{D}} \boldsymbol{y} & \text{under } \mathcal{H}_0, \\ \hat{\boldsymbol{z}}_{\mathcal{H}_1} == \boldsymbol{P}^{\perp}_{[\boldsymbol{G}\boldsymbol{D}]} \boldsymbol{y} & \text{under } \mathcal{H}_1, \end{cases} \tag{23}$$

where $\hat{\boldsymbol{\zeta}}$, $\hat{\boldsymbol{\alpha}}_{\mathcal{H}_0}$ and $\hat{\boldsymbol{\alpha}}_{\mathcal{H}_1}$ are given by (6), respectively. In this case it is more convenient to define the statistic $T''(\boldsymbol{y})$ as follows

$$T''(\boldsymbol{y}) \triangleq \left(\ln G(\boldsymbol{y})\right)^{\frac{1}{NL}} - 1 = \frac{T'(\boldsymbol{y})}{N(\boldsymbol{y})} \tag{24}$$

where $N(\boldsymbol{y}) = \frac{2}{\sigma^2} \boldsymbol{y}^H \boldsymbol{P}^{\perp}_{[\boldsymbol{G}\boldsymbol{D}]} \boldsymbol{y}$. In addition, using any orthogonal decomposition [25], one has $\boldsymbol{P}^{\perp}_{[\boldsymbol{G}\boldsymbol{D}]} = \boldsymbol{U}' \boldsymbol{U}'^H$. Consequently, $N(\boldsymbol{y}) = \frac{1}{\sigma^2} ||\bar{\boldsymbol{y}}||^2$, in which $\bar{\boldsymbol{y}} = \boldsymbol{U}'^H \boldsymbol{y}$. Thus,

$$T''(\boldsymbol{y}) = \frac{||\tilde{\boldsymbol{y}}||^2}{||\bar{\boldsymbol{y}}||^2}, \tag{25}$$

and

$$\begin{cases} \bar{\boldsymbol{y}} = \boldsymbol{U}'^H \boldsymbol{z} \sim \mathcal{CN}(\boldsymbol{0}, \sigma^2 \boldsymbol{I}) & \text{under } \mathcal{H}_0, \\ \bar{\boldsymbol{y}} = \boldsymbol{U}'^H \boldsymbol{z} \sim \mathcal{CN}(\boldsymbol{0}, \sigma^2 \boldsymbol{I}) & \text{under } \mathcal{H}_1, \end{cases}$$

then,

$$\begin{cases} N(\boldsymbol{y}) \sim \chi^2_{2r'} & \text{under } \mathcal{H}_0, \\ N(\boldsymbol{y}) \sim \chi^2_{2r'}(0) & \text{under } \mathcal{H}_1, \end{cases}$$

where $r' = \mathrm{trace}(\boldsymbol{P}^{\perp}_{[\boldsymbol{G}\boldsymbol{D}]}) = \mathrm{rank}(\boldsymbol{P}_{[\boldsymbol{G}\boldsymbol{D}]}) = LN_{\mathcal{T}}N_{\mathcal{R}} - (M + 2)$.

Furthermore, one can notice that the random variables $||\bar{\boldsymbol{y}}||^2$ and $||\tilde{\boldsymbol{y}}||^2$ are independent[3]. Consequently, a new statistic $V(\boldsymbol{y})$ can be introduced as follows

$$V(\boldsymbol{y}) \triangleq \frac{r'}{r} T''(\boldsymbol{y}) \sim \begin{cases} F_{2r,2r'} & \text{under } \mathcal{H}_0, \\ F_{2r,2r'}\left(\lambda_{\mathrm{U}}\left(P_{fa}, P_d\right)\right) & \text{under } \mathcal{H}_1, \end{cases} \tag{26}$$

where $F_{2r,2r'}$ and $F_{2r,2r'}\left(\lambda_{\mathrm{U}}\left(P_{fa}, P_d\right)\right)$ denote the F central and non-central distributions [15], respectively, with $2r$ and $2r'$ degrees of freedom, in which the non-centrality parameter is given by

$$\lambda_{\mathrm{U}}(P_{fa}, P_d) = \frac{2 \boldsymbol{\zeta}^H \boldsymbol{G}^H \boldsymbol{P}_{\boldsymbol{P}^{\perp}_{\boldsymbol{D}} \boldsymbol{G}} \boldsymbol{G} \boldsymbol{\zeta}}{\sigma^2}. \tag{27}$$

Once again, note that the non-centrality parameter $\lambda_{\mathrm{U}}(P_{fa}, P_d)$ can be computed numerically as the solution of $\mathcal{Q}^{-1}_{F_{2r,2r'}}(P_{fa}) = \mathcal{Q}^{-1}_{F_{2r,2r'}(\lambda_{\mathrm{U}}(P_{fa},P_d))}(P_d)$, where $\mathcal{Q}^{-1}_{F_{2r,2r'}}(.)$ and $\mathcal{Q}^{-1}_{F_{2r,2r'}(\lambda_{\mathrm{U}}(P_{fa},P_d))}(.)$ denote the right tails of the pdf $F_{2r,2r'}$ and $F_{2r,2r'}(\lambda_{\mathrm{U}}(P_{fa}, P_d))$, respectively.

Result 4: The SNR threshold with respect to the SRL ($\delta_{\mathcal{T}}$ and $\delta_{\mathcal{R}}$) required to resolve two closely spaced targets in the presence of clutter interference and with unknown noise variance, is given by

$$\mathrm{SNR}_{\mathrm{U}} = \frac{N_{\mathcal{T}} \lambda_{\mathrm{U}}\left(P_{fa}, P_d\right)}{2 \left\| \boldsymbol{U}^H \boldsymbol{G} \boldsymbol{\zeta} \right\|^2}. \tag{28}$$

[3]Since $E(\bar{\boldsymbol{y}}) = \boldsymbol{0}$ under $\mathcal{H}_0$ and $\mathcal{H}_1$, one has $\mathrm{Cov}(\bar{\boldsymbol{y}}, \bar{\boldsymbol{y}}) = E(\bar{\boldsymbol{y}}\bar{\boldsymbol{y}}^H) = \boldsymbol{U}'^H E(\boldsymbol{y}\boldsymbol{y}^H)\boldsymbol{U} = \boldsymbol{U}'^H \boldsymbol{U}' \boldsymbol{U}'^H E(\boldsymbol{y}\boldsymbol{y}^H) \boldsymbol{U}\boldsymbol{U}^H \boldsymbol{U} = \boldsymbol{U}'^H \boldsymbol{P}^{\perp}_{[\boldsymbol{G}\boldsymbol{D}]} E(\boldsymbol{y}\boldsymbol{y}^H) \boldsymbol{P}_{\boldsymbol{P}^{\perp}_{\boldsymbol{D}}\boldsymbol{G}} \boldsymbol{U} = \boldsymbol{U}'^H \left(\sigma^2 \boldsymbol{P}^{\perp}_{[\boldsymbol{G}\boldsymbol{D}]} \boldsymbol{P}_{\boldsymbol{P}^{\perp}_{\boldsymbol{D}}\boldsymbol{G}} + \left(\boldsymbol{P}^{\perp}_{[\boldsymbol{G}\boldsymbol{D}]} \boldsymbol{e} \right) \left(\boldsymbol{P}_{\boldsymbol{P}^{\perp}_{\boldsymbol{D}}\boldsymbol{G}} \boldsymbol{e} \right)^H \right) \boldsymbol{U}$ where $\boldsymbol{e} = \boldsymbol{G}\boldsymbol{\zeta} + \boldsymbol{D}\boldsymbol{\alpha}$ under $\mathcal{H}_1$ and $\boldsymbol{e} = \boldsymbol{D}\boldsymbol{\alpha}$ under $\mathcal{H}_0$. Noting that $\boldsymbol{P}^{\perp}_{[\boldsymbol{G}\boldsymbol{D}]} \boldsymbol{e} = \boldsymbol{0}$, and $\boldsymbol{P}^{\perp}_{[\boldsymbol{B}\boldsymbol{D}]} \boldsymbol{P}_{\boldsymbol{P}^{\perp}_{\boldsymbol{D}}\boldsymbol{B}} = \boldsymbol{P}^{\perp}_{\boldsymbol{D}} (\boldsymbol{P}^{\perp}_{\boldsymbol{D}} \boldsymbol{E}_{\boldsymbol{B}\boldsymbol{D}} - \boldsymbol{E}_{\boldsymbol{B}\boldsymbol{D}} \boldsymbol{P}^{\perp}_{\boldsymbol{D}} \boldsymbol{E}_{\boldsymbol{B}\boldsymbol{D}}) \boldsymbol{P}^{\perp}_{\boldsymbol{D}} = (\boldsymbol{P}^{\perp}_{\boldsymbol{D}} \boldsymbol{E}_{\boldsymbol{B}\boldsymbol{D}} - \boldsymbol{P}^{\perp}_{\boldsymbol{D}} \boldsymbol{E}_{\boldsymbol{B}\boldsymbol{D}} \boldsymbol{P}^{\perp}_{\boldsymbol{D}} \boldsymbol{E}_{\boldsymbol{B}\boldsymbol{D}}) \boldsymbol{P}^{\perp}_{\boldsymbol{D}} = (\boldsymbol{P}^{\perp}_{\boldsymbol{D}} \boldsymbol{E}_{\boldsymbol{B}\boldsymbol{D}} - \boldsymbol{P}^{\perp}_{\boldsymbol{D}} \boldsymbol{E}_{\boldsymbol{B}\boldsymbol{D}}) \boldsymbol{P}^{\perp}_{\boldsymbol{D}} = \boldsymbol{0}$. Consequently, $\mathrm{Cov}(\bar{\boldsymbol{y}}, \tilde{\boldsymbol{y}}) = \boldsymbol{0}$. Meaning that $\bar{\boldsymbol{y}}$ and $\tilde{\boldsymbol{y}}$ are uncorrelated. Thus, they are independent in the normal distribution case. Consequently, it is straightforward to conclude that $\|\bar{\boldsymbol{y}}\|^2$ and $\|\tilde{\boldsymbol{y}}\|^2$ are also independent.

2) Case of two targets without interference: The case of two targets without interference can be deduced from the previous result. Using the same steps as in subsection A.2, one obtains

Result 5: The relationship between the SRL ($\delta_{\mathcal{T}}$ and $\delta_{\mathcal{R}}$) and the minimum SNR, required to resolve two closely spaced targets with unknown noise variance, is then given by

$$\text{SNR}_{\text{U}} = \frac{\lambda_{\text{U}}\left(P_{fa}, P_d\right)}{2L\boldsymbol{\zeta}^H \boldsymbol{K}\boldsymbol{\zeta}}. \tag{29}$$

3) Case of two targets without interference and with symmetric arrays: Once again, since $f_{p,1} = f_{1,p} = 0, \forall p$, for symmetric arrays, one has:

Result 6: The relationship between the SRL ($\delta_{\mathcal{T}}$ and $\delta_{\mathcal{R}}$) and the minimum SNR, required to resolve two closely spaced targets with unknown noise variance and for symmetric arrays is given by

$$\text{SNR}_{\text{U}_{\text{sym}}} = \frac{2N_{\mathcal{T}}\lambda_{\text{U}}\left(P_{fa}, P_d\right)}{L\left(\left(\delta_{\mathcal{R}}^2+\delta_{\mathcal{T}}^2\right)\left(\alpha_2-\alpha_1\right)^2+\delta_{\mathcal{R}}^2\delta_{\mathcal{T}}^2\left(\alpha_2+\alpha_1\right)^2\right)}.$$

C. The ideal (clairvoyant) detector

In the previous results we have derived the SRL using the GLRT because the Neyman-Pearson test cannot be conducted due to the fact that $\boldsymbol{\delta}$ is an unknown parameter. Thus, it is interesting to compare SNR_{K} and SNR_{U} with the SNR associated to the clairvoyant Neyman-Pearson test (where all the parameter are known, *i.e.,* α_m, $m = 1 \ldots M$ and even $\delta_{\mathcal{T}}$ and $\delta_{\mathcal{R}}$). Toward this aim, one can consider the new observation vector $\boldsymbol{y}' \triangleq \boldsymbol{y} - (\alpha_1+\alpha_2)\boldsymbol{c}(f) \otimes \boldsymbol{a}_{\mathcal{T}}(\omega_c^{(\mathcal{T})}) \otimes \boldsymbol{a}_{\mathcal{R}}(\omega_c^{(\mathcal{R})})$. Thus, it can be shown that $\boldsymbol{y}' = \boldsymbol{G}\boldsymbol{P}^T\boldsymbol{P}\boldsymbol{\zeta} + \boldsymbol{z}$, where $\boldsymbol{P} = [\boldsymbol{0}\ \boldsymbol{I}_3]$ leading to the following binary hypothesis test $\begin{cases}\mathcal{H}_0: & \boldsymbol{y}' = \boldsymbol{z}, \\ \mathcal{H}_1: & \boldsymbol{y}' = \boldsymbol{G}\boldsymbol{P}^T\boldsymbol{\zeta} + \boldsymbol{z},\end{cases}$.The latter hypothesis test is a detection problem of a known deterministic signal imbedded in a complex white Gaussian noise with known variance. This is the so-called mean-shifted Gauss-Gauss detection problem such that $T_{\text{C}}(\boldsymbol{y}') \sim \begin{cases}\mathcal{H}_0 : \mathcal{CN}(0, \frac{\sigma^2\mathcal{E}}{2}) \\ \mathcal{H}_1 : \mathcal{CN}(\mathcal{E}, \frac{\sigma^2\mathcal{E}}{2})\end{cases}$ [15], where the subscript C stands for the Clairvoyant case, and where $\mathcal{E} = \boldsymbol{\zeta}^H\boldsymbol{P}\boldsymbol{G}^H\boldsymbol{G}\boldsymbol{P}^T\boldsymbol{\zeta} = \boldsymbol{\zeta}^H\boldsymbol{\Phi}\boldsymbol{\zeta}$. On the other hand, the detection performance are given by $\lambda_{\text{C}}(P_{fa}, P_d) = \left(Q^{-1}\left(P_{fa}\right) - Q^{-1}\left(P_d\right)\right)^2$, in which λ_{C} denotes the so-called deflection coefficient, whereas $Q^{-1}(.)$ is the inverse of the right tail of the probability function for a Gaussian random variable with zero mean and unit variance, whereas $\lambda_{\text{C}}(P_{fa}, P_d) = \frac{2\mathcal{E}}{\sigma^2}$ [15, p. 103]. Consequently, denoting $\boldsymbol{K}' = \frac{1}{N_{\mathcal{T}}}\boldsymbol{\Phi}$, one has

Result 7: The relationship between $\boldsymbol{\zeta}$ and the minimum SNR, required to resolve two closely spaced sources in the optimal (clairvoyant) case, is then given by

$$\text{SNR}_{\text{C}} = \frac{\lambda_{\text{C}}\left(P_{fa}, P_d\right)}{2L\boldsymbol{\zeta}^H\boldsymbol{K}'\boldsymbol{\zeta}}. \tag{30}$$

The next section is devoted to the theoretical and numerical analysis of the SRL (or equivalently their corresponding minimal SNRs, *i.e.,* SNR_{K}, SNR_{U} and SNR_{C}).

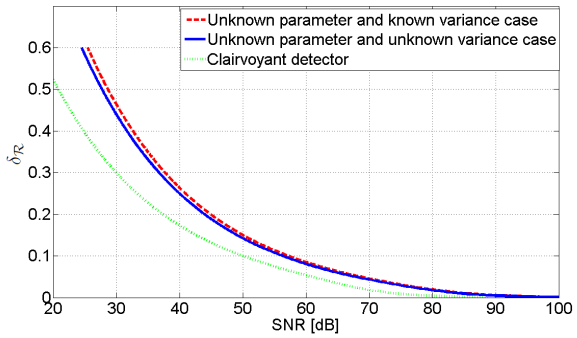

Fig. 1. The LSRL versus the required SNR to resolve two closely spaced targets for $L = 4$ samples per pulse period, ULA at the transmitter and at the receiver with $N_{\mathcal{T}} = N_{\mathcal{R}} = 4$ and $T = 100$ snapshots.

V. Analysis of the SRL and simulations results

A. Effect of the prior on the noise variance and/or the SRL

Let us compare the derived SNR i) in the clairvoyant case, ii) in the unknown parameters with known noise variance case and iii) and in the unknown parameters with unknown noise variance case. On one hand, from (19), (29) and (30) one obtains

$$\frac{\text{SNR}_{\text{C}}}{\text{SNR}_{\text{K}}} = \rho\frac{\lambda_{\text{C}}(P_{fa}, P_d)}{\lambda_{\text{K}}(P_{fa}, P_d)} \text{ where } \rho = \frac{\boldsymbol{\zeta}^H\boldsymbol{K}\boldsymbol{\zeta}}{\boldsymbol{\zeta}^H\boldsymbol{K}'\boldsymbol{\zeta}} \tag{31}$$

$$\text{and} \quad \frac{\text{SNR}_{\text{K}}}{\text{SNR}_{\text{U}}} = \frac{\lambda_{\text{K}}(P_{fa}, P_d)}{\lambda_{\text{U}}(P_{fa}, P_d)}. \tag{32}$$

On the other hand, note that: $\boldsymbol{\mathcal{P}1}$) for any $P_d > P_{fa}$ one has $\lambda_{\text{C}}(P_{fa}, P_d) < \lambda_{\text{K}}(P_{fa}, P_d) < \lambda_{\text{U}}(P_{fa}, P_d)$ [7]. $\boldsymbol{\mathcal{P}2}$) let us set $\boldsymbol{\kappa}_0 = \boldsymbol{Q}^*\boldsymbol{\kappa}/\sqrt{N_{\mathcal{T}}N_{\mathcal{R}}}$, in which $\boldsymbol{Q} = diag\left\{\frac{j}{2}(\alpha_2-\alpha_1), \frac{j}{2}(\alpha_2-\alpha_1), \frac{1}{4}(\alpha_1+\alpha_2)\right\}$. Then the Hermitian matrix $\boldsymbol{\Omega} = \boldsymbol{K}'-\boldsymbol{K} = \boldsymbol{\kappa}_0\boldsymbol{\kappa}_0^H$ is a positive semi-definite matrix. Thus, $\rho \leq 1$. Consequently, from (31), (32), $\boldsymbol{\mathcal{P}1}$ and $\boldsymbol{\mathcal{P}2}$ one deduces, as expected, that for fixed P_{fa} and P_d (such that $P_d > P_{fa}$) one has $\text{SNR}_{\text{C}} < \text{SNR}_{\text{K}} < \text{SNR}_{\text{U}}$. In Fig. 1 we have reported the LSRL $\delta_{\mathcal{R}}$ in the clairvoyant, the known noise variance and the unknown noise variance cases versus the SNR (the same conclusion are done also for the LSRL $\delta_{\mathcal{T}}$). One can notice that the LSRLs derived in the cases of known and unknown noise variance have the same behavior as the one in the clairvoyant case. For the same SRL (*i.e.,* for a fixed $\delta_{\mathcal{T}}$ and $\delta_{\mathcal{R}}$), the gap between SNR_{K} and SNR_{U} is exclusively due to the non-centrality parameters $\lambda_{\text{K}}(P_{fa}, P_d)$ and $\lambda_{\text{U}}(P_{fa}, P_d)$. This gap is approximatively equal to 1dB. Whereas, the gap between SNR_{C} and SNR_{K} is due to both: i) the ratio of the deflection coefficient $\lambda_{\text{C}}(P_{fa}, P_d)$ over the non-centrality parameter $\lambda_{\text{K}}(P_{fa}, P_d)$, and, ii) the norm of $\boldsymbol{\Omega}$ which reflects the value of ρ. This latter gap, is evaluated to 9 dB.

B. Effect of the clutter interference

In the following we consider that the targets of interest (*i.e.,* the first one and the second one) are spaced by $\delta_{\mathcal{T}}$ and $\delta_{\mathcal{R}}$,

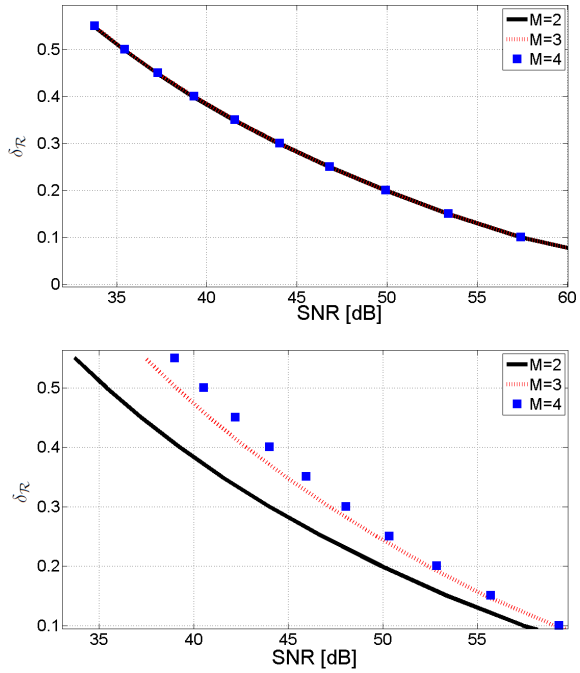

Fig. 2. *(left)* The minimum SNR to resolve two closely spaced targets with known noise variance for different values of M in which $\Delta_{\mathcal{R}} = \Delta_{\mathcal{T}} = 1.5$. *(right)* The minimum SNR to resolve two closely targets with known noise variance for different values of M in which $\Delta_{\mathcal{R}} = \Delta_{\mathcal{T}} = 0.7$.

whereas, the $M-2$ remain targets are equally spaced by $\Delta_{\mathcal{T}}$ and $\Delta_{\mathcal{R}}$.

In Fig. 2, we have reported the effect of additional sources (considered as a clutter interference) on the SNR threshold (*i.e.,* the required SNR to resolve two closely spaced targets) *w.r.t.* $\delta_{\mathcal{R}}$ (the same conclusion are done also for $\delta_{\mathcal{T}}$). One can distinguish two cases:

1) The first one represents the scenario where $\Delta_{\mathcal{T}} \gg \delta_{\mathcal{T}}$ and $\Delta_{\mathcal{R}} \gg \delta_{\mathcal{R}}$. In this case, one can notice that the additional sources do not affect the minimal SNR (Fig.2 (*left*)). This can be explained by the fact that the high resolution algorithms have asymptotically an infinite resolving power [1], [20].
2) The second scenario is for $\Delta_{\mathcal{T}} > \delta_{\mathcal{T}}$ and $\Delta_{\mathcal{R}} > \delta_{\mathcal{R}}$. In this case, one can notice the drastic effect of the interfering sources (Fig.2 (*right*)). For example, the SNR gap between $M = 2$ targets and $M = 4$ targets is evaluated around 6 dB.

C. Effect of missing sensors

The effect of missing sensors is considered herein. Let us consider different scenarios. In each scenario we have the same ULA at the transmitter with $N_{\mathcal{T}} = 10$ sensors but different receiver arrays (from a scenario to another) having the same array aperture. Let us denote these receiver arrays by $A_{N_{\mathcal{R}}}$ where $N_{\mathcal{R}}$ represents the number of sensors in the receiver arrays. In Fig. 3 we plot the LSRL for the receiver (*i.e.,* we focus only on $\delta_{\mathcal{R}}$, the case of $\delta_{\mathcal{T}}$ has the same behavior) for different $A_{N_{\mathcal{R}}}$ with $N_{\mathcal{R}} \in \{5, 7, 8, 9, 10\}$. This figure

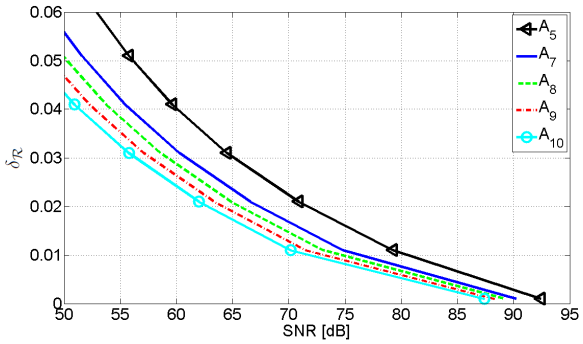

Fig. 3. The LSRL versus the required SNR to resolve two closely spaced targets for $T = 100$, $L = 10$, a ULA transmitter with $N_{\mathcal{T}} = 10$ sensors and for different $A_{N_{\mathcal{R}}}$ of $N_{\mathcal{R}} \in \{5, 7, 8, 9, 10\}$.

represents qualitatively the loss due to missing sensors (but for the same array aperture) which is, *e.g.,* evaluated to 3dB between A_5 and A_7.

VI. Conclusion

In this paper, we have derived the Statistical Resolution Limit (SRL) for two closely spaced targets using a MIMO radar with widely separated arrays (made from possibly nonuniform transmitter and receiver arrays) in the presence of clutter interference. Toward this goal, we have conducted a hypothesis test approach. Based on the Generalized Likelihood Ratio Test (GLRT). This analysis provides useful information concerning the behavior of the SRL and the minimum SNR required to resolve two closely spaced targets for a given probability of false alarm and a given probability of detection. Finally, numerical simulations shows that the derived SRL has the same behavior compared to the clairvoyant (ideal) detector.

References

[1] J. Li and P. Stoica, *MIMO radar Signal Processing*. Wiley-Interscience, 2008.
[2] A. Haimovich, R. Blum, and L. Cimini, "MIMO radar with widely separated antennas," *IEEE Signal Processing Magazine*, vol. 25, pp. 116–129, Jan. 2008.
[3] R. Boyer, "Co-Located MIMO radar with orthogonal waveform coding: Cramér-Rao lower bound," in *Proc. of IEEE Int. Workshop on Computational Advances in Multi-Sensor Adaptive Processing*, Aruba, Dutch Antilles, 2009.
[4] M. Jin, G. Liao, and J. Li, "Joint DOD and DOA estimation for bistatic MIMO radar," *Elsevier Signal Processing*, vol. 2, pp. 244–251, Feb. 2009.
[5] S. T. Smith, "Statistical resolution limits and the complexified Cramér Rao bound," *IEEE Trans. Signal Processing*, vol. 53, pp. 1597–1609, May 2005.
[6] M. N. El Korso, R. Boyer, A. Renaux, and S. Marcos, "Statistical resolution limit for multiple signals and parameters of interest," in *Proc. of IEEE Int. Conf. Acoust., Speech, Signal Processing*, Dallas, TX, 2010.
[7] M. Shahram and P. Milanfar, "Imaging below the diffraction limit: A statistical analysis," *IEEE Trans. Image Processing*, vol. 13, no. 5, pp. 677–689, May 2004.
[8] Z. Liu and A. Nehorai, "Statistical angular resolution limit for point sources," *IEEE Trans. Signal Processing*, vol. 55, no. 11, pp. 5521–5527, Nov. 2007.
[9] H. Cox, "Resolving power and sensitivity to mismatch of optimum array processors," *J. Acoust. Soc.*, vol. 54, no. 3, pp. 771–785, 1973.
[10] K. Sharman and T. Durrani, "Resolving power of signal subspace methods for fnite data lengths," in *Proc. of IEEE Int. Conf. Acoust., Speech, Signal Processing*, Florida, USA, 1995, pp. 1501–1504.

[11] H. B. Lee, "The Cramér-Rao bound on frequency estimates of signals closely spaced in frequency," *IEEE Trans. Signal Processing*, vol. 40, no. 6, pp. 1507–1517, 1992.

[12] ——, "The Cramér-Rao bound on frequency estimates of signals closely spaced in frequency (unconditional case)," *IEEE Trans. Signal Processing*, vol. 42, no. 6, pp. 1569–1572, 1994.

[13] A. Amar and A. Weiss, "Fundamental limitations on the resolution of deterministic signals," *IEEE Trans. Signal Processing*, vol. 56, no. 11, pp. 5309–5318, Nov. 2008.

[14] R. Boyer, "Performance bounds and angular resolution limit for the moving co-located mimo radar," *to appear in IEEE Transactions on Signal Processing*, 2011.

[15] S. M. Kay, *Fundamentals of Statistical Signal Processing : Detection Theory*. NJ: Prentice Hall, 1998, vol. 2.

[16] P. Woodward, *Probability and Information Theory with Applications to Radar*. MA : Artech House: Norwood, 1980.

[17] D. Nion and N. Sidiropoulos, "A PARAFAC-based technique for detection and localization of multiple targets in a MIMO radar system," in *Proc. of IEEE Int. Conf. Acoust., Speech, Signal Processing*, Taipei, Taiwan, 2009.

[18] R. Harshman, *Foundations of the PARAFAC procedure: Models and conditions for an "explanatory" multi-modal factor analysis*. UCLA Working Papers in Phonetics, 1970.

[19] M. Shahram and P. Milanfar, "On the resolvability of sinusoids with nearby frequencies in the presence of noise," *IEEE Trans. Signal Processing*, vol. 53, no. 7, pp. 2579–2585, Jul. 2005.

[20] H. L. VanTrees, *Detection, Estimation and Modulation theory: Optimum Array Processing*. New York: Wiley, 2002, vol. 4.

[21] R. Behrens, "Subspace signal processing in structured noise," Ph.D. dissertation, University of Colorado, Boulder, US-CO, 1990.

[22] R. T. Behrens and L. L. Scharf, "Signal processing applications of oblique projection operators," *IEEE Trans. Signal Processing*, vol. 42, no. 6, pp. 1413–1424, Jun. 1994.

[23] G. H. Golub and C. F. V. Loan, *Matrix Computations*. London: Johns Hopkins, 1989.

[24] L. L. Scharf and B. Friedlander, "Matched subspace detectors," *IEEE Trans. Signal Processing*, vol. 42, no. 8, pp. 2146–2157, Aug. 1994.

[25] P. Stoica and R. Moses, *Spectral Analysis of Signals*. NJ: Prentice Hall, 2005.

[26] L. L. Scharf, *Statistical Signal Processing: Detection, Estimation, and Time Series Analysis*. Reading: Addison Wesley, 1991.

[27] S. M. Kay, *Fundamentals of Statistical Signal Processing : Estimation Theory*. NJ: Prentice Hall, 1993, vol. 1.

Bibliographie

[Abe06] H. Abeida. *Imagerie d'antenne pour signaux non circulaires : bornes de performance et algorithmes.* PhD thesis, université Paris 6, France, November 2006.

[AD08] H. Abeida and J.-P. Delmas. Statistical performance of MUSIC-like algorithms in resolving noncircular sources. *IEEE Trans. Signal Processing*, 56(6) :4317–4329, September 2008.

[AGGS96] Y. Abramovich, D.A. Gray, A.Y. Gorokhov, and N.K. Spencer. Comparaison of DOA estimation performance for various types of sparse antenna array geometries. In *EUSIPCO*, pages 1968–1972, Trieste, Italy, September 1996.

[ASG99] Y. I. Abramovich, N. K. Spencer, and A. Y. Gorokhov. Positive-definite toeplitz completion in DOA estimation for nonuniform linear antenna arrays. II : Partially augmentable arrays. *IEEE Trans. Signal Processing*, 47(6) :1502–1521, June 1999.

[Ath05] F. Athley. Threshold region performance of Maximum Likelihood direction of arrival estimators. *IEEE Trans. Signal Processing*, 53 :1359–1373, April 2005.

[AW08] A. Amar and A.J. Weiss. Fundamental limitations on the resolution of deterministic signals. *IEEE Trans. Signal Processing*, 56(11) :5309–5318, November 2008.

[Beh90] R.T. Behrens. *Subspace signal processing in structured noise.* PhD thesis, University of Colorado, Boulder, US-CO, 1990.

[Bel95] K. Bell. *Performance bounds in parameter estimation with application to bearing estimation.* PhD thesis, George Mason University, Fairfax, VA, 1995.

[BFL04] E. Boyer, P. Forster, and P. Larzabal. Non asymptotic statistical performances of beamforming for deterministic signals. *IEEE Signal Processing Lett.*, 11(1) :20–22, January 2004.

[BK83] G. Bienvenu and L. Kopp. Optimaly of high resolution array processing using the eigensystem approach. *IEEE Trans. Acoust., Speech, Signal Processing*, 31(5) :1235–1247, October 1983.

[Böh86] J. F. Böhme. Estimation of spectral parameters of correlated signals in wavefields. *Signal Processing*, 10 :329–337, 1986.

[Boy08] R. Boyer. Deterministic asymptotic Cramér-Rao bound for the multidimensional harmonic model. *Signal Processing*, 88 :2869–2877, 2008.

[BP08] R. Boyer and J. Picheral. Second-order near-field localization with automatic paring operation. In *Proc. of IEEE Int. Conf. Acoust., Speech, Signal Processing*, Las Vegas, 2008.

[BS94] R. T. Behrens and L. L. Scharf. Signal processing applications of oblique projection operators. *IEEE Trans. Signal Processing*, 42(6) :1413–1424, June 1994.

[BT06] I. Bekkerman and J. Tabrikian. Target detection and localization using MIMO radars and sonars. *IEEE Trans. Signal Processing*, 54 :3873–3883, October 2006.

[Cap69] J. Capon. High resolution frequency wavenumber spectrum analysis. *Proc. IEEE*, 57 :1408–1418, August 1969.

[CGQL08] E. Chaumette, J. Galy, A. Quinlan, and P. Larzabal. A new Barankin bound approximation for the prediction of the threshold region performance of maximum likelihood estimators. *IEEE Trans. Signal Processing*, 56(11) :5319–5333, November 2008.

[CM97] M. Cedervall and R. L. Moses. Efficient maximum likelihood DOA estimation for signals with known waveforms in presence of multipath. *IEEE Trans. Signal Processing*, 45 :808–811, March 1997.

[Cox73] H. Cox. Resolving power and sensitivity to mismatch of optimum array processors. *J. Acoust. Soc. Am*, 54(3) :771–785, 1973.

[Cra46] H. Cramér. *Mathematical Methods of Statistics*. Princeton University, Press, New York, 1946.

[DA06] J.-P. Delmas and H. Abeida. Statistical resolution limits of DOA for discrete sources. In *Proc. of IEEE Int. Conf. Acoust., Speech, Signal Processing*, volume 4, pages 889–892, Toulouse, France, 2006.

[Dil98] E. Dilaveroglu. Nonmatrix Cramér-Rao bound expressions for high-resolution frequency estimators. *IEEE Trans. Signal Processing*, 46(2) :463–474, February 1998.

[Dug37] D. Dugué. Application des propriétés de la limite au sens du calcul des probabilités à l'étude des diverses questions d'estimation. *Ecol. Poly.*, 3 :305–372, 1937.

[EBBM09] M. N. El Korso, G. Bouleux, R. Boyer, and S. Marcos. Sequential estimation of the range and the bearing using the zero-forcing MUSIC approach. In *Proc. EUSIPCO*, pages 1404–1408, Glasgow, Scotland, August 2009.

[EBM09] M. N. El Korso, R. Boyer, and S. Marcos. Fast sequential source localization using the projected companion matrix approach. In *Proc. of IEEE Workshop on Computational Advances in Multi-Sensor Adaptive Processing, CAMSAP-09*, Aruba, Dutch Antilles, December 2009.

[EBRM09] M. N. El Korso, R. Boyer, A. Renaux, and S. Marcos. Nonmatrix closed-form expressions of the Cramér-Rao bounds for near-field localization parameters. In *Proc. of IEEE Int. Conf. Acoust., Speech, Signal Processing*, Taipei, Taiwan, 2009.

[EBRM10a] M. N. El Korso, R. Boyer, A. Renaux, and S. Marcos. Conditional and unconditional Cramér-Rao bounds for near-field source localization. *IEEE Trans. Signal Processing*, 58(5) :2901–2907, May 2010.

[EBRM10b] M. N. El Korso, R. Boyer, A. Renaux, and S. Marcos. Statistical resolution limit for multiple signals and parameters of interest. In *Proc. of IEEE Int. Conf. Acoust., Speech, Signal Processing*, Dallas, TX, 2010.

[EBRM11a] M. N. El Korso, R. Boyer, A. Renaux, and S. Marcos. A GLRT-based framework for the multidimensional statistical resolution limit. In *Proc. of IEEE Workshop on Satistical Signal Processing*, Nice, France, June 2011.

[EBRM11b] M. N. El Korso, R. Boyer, A. Renaux, and S. Marcos. Statistical resolution limit for source localization in a MIMO context. In *Proc. of IEEE Int. Conf. Acoust., Speech, Signal Processing*, Prague, Czeh, May 2011.

[Fis22] R. A. Fisher. On the mathematical foundations of theoretical statistics. *Phil. Trans. Royal Soc.*, 222 :309, 1922.

[FL02] Ph. Forster and P. Larzabal. On lower bounds for deterministic parameter estimation. In *Proc. of IEEE Int. Conf. Acoust., Speech, Signal Processing*, Orlando, Fl, 2002.

[FLV08] A. Ferreol, P. Larzabal, and M. Viberg. On the resolution probability of MUSIC in presence of modeling errors. *IEEE Trans. Signal Processing*, 56(5) :1945–1953, May 2008.

[Fre43] M. Frechet. Sur l'extension de certaines evaluations statistiques au cas de petit echantillons. *Rev. Inst. Int. Statist.*, 11 :182–205, 1943.

[GAMH05] E. Grosicki, K. Abed-Meraim, and Y. Hua. A weighted linear prediction method for near-field source localization. *IEEE Trans. Signal Processing*, 53 :3651–3660, 2005.

[GL89] G. H. Golub and C. F. Van Loan. *Matrix Computations*. Johns Hopkins, London, 1989.

[Gla72] F. E. Glave. A new look at the Barankin lower bound. *IEEE Trans. Inform. Theory*, 18(3) :349–356, May 1972.

[God97] L.C. Godara. Applications of antenna arrays to mobile communications : II. Beamforming and direction of arrival considerations. *IEEE Trans. Antennas Propagat.*, 85(8) :1195–1245, August 1997.

[GS05] A.B. Gershman and N.D. Sidiropoulos. *Space-time processing for MIMO communications*. Wiley, New York, 2005.

[GSPL02] A.B. Gershman, P. Stoica, M. Pesavento, and E.G. Larsson. Stochastic Cramér-Rao bound for direction estimation in unknown noise fields. *IEE Proceedings-Radar, Sonar and Navigation*, 149 :2–8, January 2002.

[Ham50] J. M. Hammersley. On estimating restricted parametrers. *J. R. Soc. Ser. B*, 12 :192–240, 1950.

[Hay85] S. Haykin. *Array signal processing*. Englewood Cliffs, NJ, Prentice-Hall, 1985.

[HB91] Y. D. Huang and M. Barkat. Near-field multiple source localization by passive sensor array. *IEEE Trans. Antennas Propagat.*, 39 :968–975, 1991.

[HN98] M. Haardt and J.A. Nossek. Simultaneous schur decomposition of several nonsymmetric matrices to achieve automatic pairing in multidimensional harmonic retrieval problems. *IEEE Trans. Signal Processing*, 46(1) :161–169, January 1998.

[JF05] Y. Jin and B. Friedlander. A CFAR adaptive subspace detector for second-order Gaussian signals. *IEEE Trans. Signal Processing*, 53(3) :871–884, March 2005.

[JLL09] M. Jin, G. Liao, and J. Li. Joint DOD and DOA estimation for bistatic MIMO radar. *Elsevier Signal Processing*, 2 :244–251, February 2009.

[JStB01] T. Jiang, N.D. Sidiropoulos, and J.M.F. ten Berge. Almost-sure identifiability of multidimensional harmonic retrieval. *IEEE Trans. Signal Processing*, 49(9) :1849–1859, September 2001.

[Kay93] S. M. Kay. *Fundamentals of Statistical Signal Processing : Estimation Theory*, volume 1. Prentice Hall, NJ, 1993.

[Kay98] S. M. Kay. *Fundamentals of Statistical Signal Processing : Detection Theory*, volume 2. Prentice Hall, NJ, 1998.

[KB86] M. Kaveh and A. Barabell. The statistical performance of the MUSIC and the minimum-norm algorithms in resolving plane waves in noise. In *Proc. ASSP Workshop on Spectrum Estimation and Modeling*, volume 34, pages 331–341, 1986.

[KBRM11a] M. N. El Korso, R. Boyer, A. Renaux, and S. Marcos. Statistical resolution limit for the multidimensional harmonic retrieval model : Hypothesis test and cramér-rao bound approaches. *EURASIP Journal on Advances in Signal Processing, special issue on Advances in Angle-of-Arrival and Multidimensional Signal Processing for Localization and Communications*, (5), May 2011.

[KBRM11b] M. N. El Korso, R. Boyer, A. Renaux, and S. Marcos. Statistical resolution limit of the uniform linear cocentered orthogonal loop and dipole array. *IEEE Trans. Signal Processing*, 59(1) :425–431, January 2011.

[KG09] J. Kusuma and V.K. Goyal. On the accuracy and resolution of powersum-based sampling methods. *IEEE Trans. Signal Processing*, 57(1) :182–193, January 2009.

[Kie52] J. Kiefer. On minimum variance estimators. *Ann. Math. Stat.*, 23 :627–629, 1952.

[KS99] S. Kraut and L.L. Scharf. The CFAR adaptive subspace detector is a scale-invariant GLRT. *IEEE Trans. Signal Processing*, 47(9) :2538–2541, September 1999.

[KSM01] S. Kraut, L.L. Scharf, and L.T. McWhorter. Adaptive subspace detectors. *IEEE Trans. Signal Processing*, 49(1) :1–16, January 2001.

[KT83] R. Kumaresan and D. W. Tufts. Estimating the angles of arrival of multiple plane waves. *IEEE Trans. Aerosp. Electron. Syst.*, 19(1) :134–138, 1983.

[KV96] H. Krim and M. Viberg. Two decades of array signal processing research : The parametric approach. *IEEE Signal Processing Mag.*, 13(4) :67–94, 1996.

[LC91] J. Li and R. Compton. Angle and polarization estimation using esprit with a polarizationsensitive array. *IEEE Trans. Antennas Propagat.*, 39(9) :1376–1383, September 1991.

[LC93] J. Li and R. T. Compton. Maximum likelihood angle estimation for signals with known waveforms. *IEEE Trans. Signal Processing*, 41 :2850–2862, September 1993.

[LC03] J. Lebrun and P. Comon. An algebraic approach to blind identification of communication channels. In *Seventh International Symposium on Signal Processing and Its Applications.*, 2003.

[Lee92] H. B. Lee. The Cramér-Rao bound on frequency estimates of signals closely spaced in frequency. *IEEE Trans. Signal Processing*, 40(6) :1507–1517, 1992.

[Lee94] H. B. Lee. The Cramér-Rao bound on frequency estimates of signals closely spaced in frequency (unconditional case). *IEEE Trans. Signal Processing*, 42(6) :1569–1572, 1994.

[Leh83] E. L. Lehmann. *Theory of Point Estimation.* Wiley, New York, 1983.

[LHSV95] J. Li, B. Halder, P. Stoica, and M. Viberg. Computationally efficient angle estimation for signals with known waveforms. *IEEE Trans. Signal Processing*, 43 :2154–2163, September 1995.

[LL93] H. B. Lee and F. Li. Quantification of the difference between detection and resolution thresholds for multiple closely spaced emitters. *IEEE Trans. Signal Processing*, 41(6) :2274–2277, 1993.

[LN07] Z. Liu and A. Nehorai. Statistical angular resolution limit for point sources. *IEEE Trans. Signal Processing*, 55(11) :5521–5527, November 2007.

[LSZ96] J. Li, P. Stoica, and D. Zheng. Efficient direction and polarization estimation with a cold array. *IEEE Trans. Antennas Propagat.*, 44(4) :539–547, April 1996.

[LVT89] F. Li, J. Vaccaro, and D. W. Tuft. Min-Norm linear prediction for arbitrary sensor arrays. In *Proc. of IEEE Int. Conf. Acoust., Speech, Signal Processing*, pages 2613–2616, Glasgow, GB, May 1989.

[LW90] H.B. Lee and M.S. Wengrovitz. Resolution threshold of beamspace MUSIC for two closely spaced emitters. *IEEE Trans. Acoust., Speech, Signal Processing*, 38(9) :1545–1559, September 1990.

[Mar98] S. Marcos. *Les Méthodes à Haute Résolution : Traitement d'Antenne et Analyse Spectrale*. Hermes, Paris, 1998.

[MD01] Y. Meurisse and J.P. Delmas. Bounds for sparse planar and volume arrays. *IEEE Trans. Signal Processing*, 47 :464–468, January 2001.

[MH71] R. J. McAulay and E. M. Hofstetter. Barankin bounds on parameter estimation. *IEEE Trans. Inform. Theory*, 17 :669–676, November 1971.

[ML99] J.C. Mosher and R.M. Leahy. Source localization using recursivaly applied and projected (rap) music. *IEEE Trans. Signal Processing*, 47 :332–340, February 1999.

[Mof68] A. Moffet. Minimum-redundancy linear arrays. *IEEE Antennas Propagat. Mag.*, 16(2) :172–175, June 1968.

[MS69] R. J. McAulay and L. P. Seidman. A useful form of the Barankin lower bound and its application to ppm threshold analysis. *IEEE Trans. Inform. Theory*, 15 :273–279, March 1969.

[MSPM04] K.N. Mokios, N.D. Sidiropoulos, M. Pesavento, and C.F. Mecklenbrauker. On 3-D harmonic retrieval for wireless channel sounding. In *Proc. of IEEE Int. Conf. Acoust., Speech, Signal Processing*, volume 2, pages 89–92, Philadelphia, U.S.A., 2004.

[NS09] D. Nion and N.D. Sidiropoulos. A PARAFAC-based technique for detection and localization of multiple targets in a MIMO radar system. In *Proc. of IEEE Int. Conf. Acoust., Speech, Signal Processing*, Taipei, Taiwan, 2009.

[NS10] D. Nion and D. Sidiropoulos. Tensor algebra and multi-dimensional harmonic retrieval in signal processing for MIMO radar. *IEEE Trans. Signal Processing*, 58 :5693–5705, November 2010.

[OVSN93] B. Ottersten, M. Viberg, P. Stoica, and A. Nehorai. Exact and large sample maximum likelihood techniques for parameter estimation and detection in array processing. In S. Haykin, J. Litva, and T. J. Shepherd, editors, *Radar Array Processing*, chapter 4, pages 99–151. Springer-Verlag, Berlin, 1993.

[PG01] M. Pesavento and A.B. Gershman. Maximum-likelihood direction-of-arrival estimation in the presence of unknown nonuniform noise. *IEEE Trans. Signal Processing*, 49 :1310–1324, July 2001.

[PMB04] M. Pesavento, C.F. Mecklenbrauker, and J.F. Bohme. Multidimensional rank reduction estimator for parametric MIMO channel models. *EURASIP Journal on Applied Signal Processing*, 9 :1354–1363, 2004.

[PP06] K.B. Petersen and M.S. Pedersen. The matrix cookbook. *Citeseer*, 2006.

[RAFL07] A. Renaux, L. N. Atallah, Ph. Forster, and P. Larzabal. A useful form of the Abel bound and its application to estimator threshold prediction. *IEEE Trans. Signal Processing*, 55(5) :2365–2369, May 2007.

[Rao45] C. R. Rao. Information and accuracy attainable in the estimation of statistical parameters. *Bull. Calcutta Math. Soc.*, 37 :81–91, 1945.

[RB74] D. C. Rife and R. R. Boorstyn. Single tone parameter estimation from discrete time observations. *IEEE Trans. Inform. Theory*, 20 :591–598, 1974.

[Ren07] A. Renaux. Weiss-Weinstein bound for data aided carrier estimation. *IEEE Signal Processing Lett.*, 14(4) :283–286, April 2007.

[Rendf] A. Renaux. *Contribution à l'analyse des performances d'estimation en traitement statistique du signal.* PhD thesis, Ecole Normale Supérieure de Cachan, Cachan, FR., July 2006. http ://www.satie.ens-cachan.fr/ts/These_Alex.pdf.

[RFCL06] A. Renaux, Ph. Forster, E. Chaumette, and P. Larzabal. On the high SNR conditional maximum-likelihood estimator full statistical characterization. *IEEE Trans. Signal Processing*, 12(54) :4840–4843, December 2006.

[RH89] B.D. Rao and K.V.S. Hari. Performance analysis of root-MUSIC. *IEEE Trans. Acoust., Speech, Signal Processing*, 37(12) :1939–1949, December 1989.

[RHG07] F. Roemer, M. Haardt, and G. Del Galdo. Higher order SVD based subspace estimation to improve multi-dimensional parameter estimation algorithms. 2007.

[RM95] I. Reuven and H. Messer. The use of the Barankin bound for determining the threshold SNR in estimating the bearing of a source in the presence of another. In *Proc. of IEEE Int. Conf. Acoust., Speech, Signal Processing*, volume 3, pages 1645–1648, Detroit, USA, May 1995.

[RM97] I. Reuven and H. Messer. A Barankin-type lower bound on the estimation error of a hybrid parameter vector. *IEEE Trans. Inform. Theory*, 43(3) :1084–1093, May 1997.

[RPK86] R. Roy, A. Paulraj, and T. Kailath. ESPRIT a subspace rotation approach to estimation of parameters of cisoids in noise. *IEEE Trans. Acoust., Speech, Signal Processing*, 34 :1340–1342, 1986.

[Sch81] R. O. Schmidt. *A signal subspace approach to multiple emitter location and spectral estimation.* PhD thesis, Stanford University, Stanford, CA, November 1981.

[Sch91] L. L. Scharf. *Statistical Signal Processing : Detection, Estimation, and Time Series Analysis.* Addison Wesley, Reading, 1991.

[SD95] K. Sharman and T. Durrani. Resolving power of signal subspace methods for fnite data lengths. In *Proc. of IEEE Int. Conf. Acoust., Speech, Signal Processing*, pages 1501–1504, Florida, USA, 1995.

[SF94] L. L. Scharf and B. Friedlander. Matched subspace detectors. *IEEE Trans. Signal Processing*, 42(8) :2146–2157, August 1994.

[SLG01] P. Stoica, E.G. Larsson, and A.B. Gershman. The stochastic CRB for array processing : a textbook derivation. *IEEE Signal Processing Lett.*, 8 :148–150, May 2001.

[SM04] M. Shahram and P. Milanfar. Imaging below the diffraction limit : A statistical analysis. *IEEE Trans. Image Processing*, 13(5) :677–689, May 2004.

[SM05a] M. Shahram and P. Milanfar. On the resolvability of sinusoids with nearby frequencies in the presence of noise. *IEEE Trans. Signal Processing*, 53(7) :2579–2585, July 2005.

[SM05b] P. Stoica and R.L. Moses. *Spectral Analysis of Signals.* Prentice Hall, NJ, 2005.

[Smi98] S. T. Smith. Accuracy and resolution bounds for adaptive sensor array processing. In *Proceedings in the ninth IEEE SP Workshop on Statistical Signal and Array Processing*, pages 37–40, 1998.

[Smi05] S. T. Smith. Statistical resolution limits and the complexified Cramér-Rao bound. *IEEE Trans. Signal Processing*, 53 :1597–1609, May 2005.

[SN89] P. Stoica and A. Nehorai. MUSIC, maximum likelihood and the Cramér Rao bound. *IEEE Trans. Acoust., Speech, Signal Processing*, 37 :720–741, May 1989.

[SN90a] P. Stoica and A. Nehorai. MUSIC, maximum likelihood and the Cramér Rao bound : further results and comparisons. *IEEE Trans. Acoust., Speech, Signal Processing*, 38 :2140–2150, 1990.

[SN90b] P. Stoica and A. Nehorai. Performances study of conditional and unconditional direction of arrival estimation. *IEEE Trans. Acoust., Speech, Signal Processing*, 38 :1783–1795, October 1990.

[SSS95] P. Stoica, V. Simonyte, and T. Soderstrom. On the resolution performance of spectral analysis. *Elsevier Signal Processing*, 44 :153–161, January 1995.

[Ste76] B.D. Steinberg. Principles of aperture and array system design : Including random and adaptive arrays. *New York, Wiley-Interscience*, vol. 1 :p. 374, 1976.

[STWT06] C. Schneider, U. Trautwein, W. Wirnitzer, and R.S. Thoma. Performance verification of MIMO concepts using multi-dimensional channel sounding. In *Proc. EUSIPCO*, Florence, Italy, September 2006.

[THL+01] R.S. Thoma, D. Hampicke, M. Landmann, G. Sommerkorn, and A. Richter. MIMO measurement for double-directional channel modelling. In *COLLOQUIUM DIGEST-IEE*, pages 1–7, 2001.

[TK99] J. Tabrikian and J.L. Krolik. Barankin bounds for source localization in an uncertain ocean environment. *IEEE Trans. Signal Processing*, 47 :2917–2927, November 1999.

[TT10] K. Todros and J. Tabrikian. General classes of performance lower bounds for parameter estimation Part I : Non-bayesian bounds for unbiased estimators. *IEEE Trans. Inform. Theory*, 56 :5045–5063, October 2010.

[Van68] H. L. VanTrees. *Detection, Estimation and Modulation Theory*, volume 1. Wiley, New York, 1968.

[Van95] F. Vanpoucke. *Algorithms and Architectures for Adaptive Array Signal Processing.* Ph. D. dissertation, Universiteit Leuven, Leuven, Belgium, 1995.

[Van01] H. L. VanTrees. *Detection, Estimation and Modulation Theory : Radar-Sonar Signal Processing and Gaussian Signals in Noise*, volume 3. Wiley, New York, 2001.

[Van02] H. L. VanTrees. *Detection, Estimation and Modulation theory : Optimum Array Processing*, volume 4. Wiley, New York, 2002.

[VEB+11] D. T. Vu, M. N. El Korso, R. Boyer, A. Renaux, and S. Marcos. Angular resolution limit for vector sensor arrays : Detection and information theory approaches. In *Proc. of IEEE Workshop on Satistical Signal Processing*, Nice, France, June 2011.

[VH86] E. Vertatschitsch and S. Haykin. Nonredundant arrays. *IEEE Trans. Signal Processing*, 74(1) :217–217, June 1986.

[VO91] M. Viberg and B. Ottersten. Sensor array processing based on subspace fitting. *IEEE Trans. Signal Processing*, 39 :1110–1121, May 1991.

[VOK91] M. Viberg, B. Ottersten, and T. Kailath. Detection and estimation in sensor array processing using Weighted Subspace Fitting. *IEEE Trans. Signal Processing*, 39(11) :2436–2449, November 1991.

[VON95] M. Viberg, B. Ottersten, and A. Nehorai. Performance analysis of direction finding with large arrays and finite data. *IEEE Trans. Signal Processing*, 43(2) :469–477, February 1995.

[VSO97] M. Viberg, P. Stoica, and B. Ottersten. Maximum likelihood array processing in spatially correlated noise fields using parameterized signals. *IEEE Trans. Signal Processing*, 45(4) :996–1004, April 1997.

[WF93] A. J. Weiss and B. Friedlander. Range and bearing estimation using polynomial rooting. *IEEE J. Oceanic Eng.*, 18 :130–137, July 1993.

[WZ97] K.T. Wong and M.D. Zoltowski. Uni-vector-sensor ESPRIT for multisource azimuth, elevation, andpolarization estimation. *IEEE Trans. Antennas Propagat.*, 45(10) :1467–1474, October 1997.

[XBR04] W. Xu, A. B. Baggeroer, and C. D. Richmond. Bayesian bounds for matched-field parameter estimation. *IEEE Trans. Signal Processing*, 52 :3293–3305, December 2004.

[Xu01] W. Xu. *Performances bounds on matched-field methods for source localization and estimation of ocean environmental parameters.* PhD thesis, Massachusetts Institute of Technology, Cambridge, MA, June 2001.

[YF98] N. Yuen and B. Friedlander. Performance analysis of higher order ESPRIT for localization of near-field sources. *IEEE Trans. Signal Processing*, 46 :709–719, 1998.

[ZC07] W. Zhi and M.Y.W. Chia. Near-field source localization via symmetric subarrays. *IEEE Signal Processing Lett.*, 14(6) :409–412, 2007.